EVALUATION OF FLOW AND IN-PLACE STRENGTH CHARACTERISTICS OF FLY ASH COMPOSITE MATERIALS

Hrushikesh Naik

Department of Mining Engineering
National Institute of Technology, Rourkela

EVALUATION OF FLOW AND IN-PLACE STRENGTH CHARACTERISTICS OF FLY ASH COMPOSITE MATERIALS

*A thesis submitted in partial fulfilment of the requirements
for the degree of*

Doctor of Philosophy

in

Mining Engineering

by

Hrushikesh Naik

Under the supervision of

**Dr. M.K. Mishra (N.I.T Rourkela)
&
Dr. K.U.M. Rao (I.I.T Kharagpur)**

**Department of Mining Engineering
National Institute of Technology
Rourkela - 769 008, India**
September, 2013

CERTIFICATE

This is to certify that the thesis entitled *"Evaluation of flow and in-place strength characteristics of fly ash composite materials"*, being submitted by **Hrushikesh Naik**, Roll No. 50605001 to the National Institute of Technology, Rourkela for the award of the degree of ***Doctor of Philosophy*** in Mining Engineering, is a bona fide record of research work carried out by him under our supervision and guidance.

The candidate has fulfilled all the prescribed requirements for award of the degree.

The thesis, which is based on candidate's own work, has not been submitted elsewhere for the award of a degree.

In our opinion, the thesis is of the standard required for the award of Doctor of Philosophy in Mining Engineering.

To the best of our knowledge, he bears a good moral character and decent behaviour.

Supervisors

Dr. M.K. Mishra	**Dr. K.U.M.Rao**
(Supervisor)	**(Co-supervisor)**
Department of Mining Engineering	*Department of Mining Engineering*
NATIONAL INSTITUTE OF TECHNOLOGY	**INDIAN INSTITUTE OF TECHNOLOGY**
Rourkela-769 008 (INDIA)	Kharagpur-721302 (INDIA)

Acknowledgement

This report is a result of my efforts as a research scholar towards my Ph. D. at Geomechanics Laboratory of the Department of Mining Engineering, National Institute of Technology Rourkela. During this time, I have been supported by various people to whom I wish to express my gratitude.

I would first like to express my deep sense of respect and gratitude towards my supervisors Prof. M.K. Mishra and Prof. K.U.M. Rao, for their inspiration, motivation, guidance, and generous support throughout this research work. I am greatly indebted to them for their constant encouragement and valuable advice at every phase of the doctoral programme. The dissertation work would not have been possible without their elaborate guidance and full encouragement. What I learned from them will be an invaluable asset for the rest of my life.

I would like to extend my special thanks to the Management of Thermal Power Plants from where the fly ash samples were collected for carrying out this research work especially to the Head, Ennore Thermal Power Plant and Captive Thermal Power Plant II of Rourkela Steel Plant and all other power plants for providing fly ash which is used in this research.

My special thanks go to Prof. B.K. Pal, Prof. D.P. Tripathy, and Prof. S. Jayanthu (former Heads of the Department of Mining Engineering) and all other faculty and staff members of the department for their help in completion of this work.

ABSTRACT

Of the seven hundred and fifty millions of metric tons of fly ash that are produced annually worldwide, only a small portion e.g., 20% to 50% of the fly ash is used for productive purposes, such as an additive or stabilizer in cement, bricks, embankments, etc. The remaining amount of fly ash produced annually must either be disposed off in controlled landfills/ mine fills or waste containment facilities, or stockpiled for future use or disposal. As a result of the cost associated with disposing these vast quantities of fly ash, a significant economical incentive exists for developing new and innovative, yet environmentally safe applications for the utilization of fly ash. The main aim of the present investigation was designed to develop an engineered backfill material to be placed in mine voids using fly ash as the major component. Experimental set up was designed and fly ash samples from seven numbers of thermal power plants situated at different parts of the country were collected. Investigation into detail physical, chemical, morphological, and mineralogical characterizations have been carried out to choose the most favorable fly ash source for slurry transportation.

Flow parameters such as viscosity, shear stress, shear rate ($25s^{-1}$ to $1000s^{-1}$), temperature (20^0C to 40^0C), and solid concentration (20% to 60%), etc. were determined. Flow behavior was influenced with addition of additives as cationic surfactant cetyltrimethyl ammonium bromide (CTAB) and a counter-ion sodium salicylate (NaSal). As the fly ash concentration in the slurry increased an increase in viscosity was observed. Addition of surfactants (0.1% to 0.5%) modified the flowing attributes from shear thickening to shear thinning/Newtonian pattern and eliminated yield stress completely/partially compared to that of untreated fly ash slurry. Temperature of the slurry environment was also observed to

influence the flowing behavior. An operating temperature varying from 30^0C to 40^0C was found to be ideal for improving the flowing attributes. Surfactants used in this study also reduced the surface tension of water by adsorbing at the solid-liquid interface. The addition of the surfactant resulted in reduced surface tension by 53 to 56% and facilitated floating of fly ash particles for smooth flow in pipelines. The zeta potential value of the fly ash slurry was negative (-27mV) without any additive, but changed to positive value (> +30mV) when surfactant was added to the slurry. Addition of the surfactant modified the surface properties of the fly ash particles keeping the suspension in the stable condition. The settling characteristic of the slurry was studied to know the settling behavior of the fly ash particles. The treated fly ash slurry exhibited better suspension attributes as compared to that of untreated fly ash.

Lime was selected to enhance the strength characteristics of fly ash composite materials. Lime pH optimization study was carried out to find the optimum quantity of lime which was added to the fly ash to increase the in-place strength of fly ash composite materials. Unconfined compressive strength, Brazilian Tensile strength, and triaxial tests were conducted at varying curing periods i.e. at 0 day, 7 days, 14 days, 28 days, and 56 days. Ultrasonic pulse velocity was measured and microstructural analysis was carried out to examine the strength behavior of the developed composite materials. Fourier Transfom Infrared Spectroscopy (FTIR) study was carried out to find the effect of lime addition on strength parameters. The SEM images were also obtained to study the ettringite formation in the fly ash composite materials. From the results of this study it is inferred that there is substantial strength gain with curing period. Empirical equations are developed to predict the flow and strength behavior of the selected and optimized fly ash material.

CONTENTS

LIST OF FIGURES

LIST OF TABLES

CHAPTER 1

1.1. Introduction

This chapter gives backgrounds, motivations, and objectives for conducting research in the fields of fly ash utilization and management, a brief overview of the problem to be tackled, and its application domains. A brief summary of the structure of thesis in the form of a series of short chapter abstracts can be found at the end of this introductory chapter.

1.1.1. The background

The problem of fly ash generation and utilization has been extensively studied over the last three decades. With the increasing demand of coal consumption in turn generates huge amount of fly ash as a by-product of coal combustion. At present, approximately 290 million tons of coal is being consumed per annum and produces 170 million tons of fly ash per annum (Senapati and Mishra, 2012). The generation of fly ash is projected to exceed 300 million tons per annum by 2017 and 1000 million tons by 2032 A.D (Kumar, 2010). This large volume of fly ash would occupy huge land area (presently about 65,000 acres of valuable land is occupied by ash ponds in India) and will pose a serious threat to the environment. Therefore, there is an urgent need to adopt technologies for gainful utilization and safe management of fly ash on sustainable basis. Though efforts have been made to utilize the fly ash, yet it is very meagre as compared to its generation. Presently, India's fly ash utilization level is only about 85 million tons per year i.e. 50% (Kumar, 2010) and rest 50% is accumulating in the ash ponds every year. So there is a pressing need of finding higher utilization percentage of fly ash to address the ever decreasing availability of land area.

Fly ash finds its uses in applications such as in Cement/Concrete/Brick making, in highways, and embankments constructions, agriculture, hydro power, and irrigation, value added products like composites/wood substitutes/light weight aggregates/insulating, and abrasion resistant materials, and as effluent treatment agent etc. But none of these applications can consume huge volume that India produces. One area where large amount of fly ash can be used is mine void filling. Nearly one third of our thermal power plants are pit-head power

stations. Most of these mines cart sand for backfilling from river beds, which are normally 50-80 kms away from the mines. Apart from the royalty, huge amount of expenditure is also incurred on transportation of sand. In addition, sand is in great demand for many construction projects and is in short supply in many areas. The availability of river bed sand as a void filling material is decreasing. So finding an alternative to this is highly desirable. At the same time mine voids has strong potential to absorb fly ash in bulk without compromising the roof stability (Kumar, 2003). With the application of current level of technology the percentage of extraction in the underground coal mines is about 40-50% only, which can be increased significantly with change in implementation of higher level of technologies. Increased production through new technologies would also demand higher rates of restoration of mined out areas to ensure safety and ecological balance. The filling of mine cavities would also release millions of tons of coal blocked in support pillars.

Keeping the above fact in mind, an attempt is made in this investigation to develop an engineered backfill fly ash composite material which can replace river bed sand to be used for filling underground mine voids. However there exists no commercially established technology or mechanism to transport fly ash to underground void filling areas. The major impediment in fly ash transportation through water medium is its relative heavy particles. The efficiency of any transportation system would depend on the flow behaviour of the fly ash particles. In this investigation the flow characteristics of fly ash slurry was studied with and without an additive at varying temperature environment. There are many successful case histories of modifying the flow behavior of mineral slurries and liquids with additives. The problem with fly ash transportation is its specific gravity. Majority of the particles tend to settle down in water (sp. gr. 1) flow pipe lines due to its higher specific gravity (average > 2.0). In this investigation the influence of additives on flow behaviour has been evaluated.

1.1.2. Needs statement and motivation for the present work

The availability of land area to the growing population of India is becoming dearer day by day. It also adversely reflects in agricultural output. In India there are more than 85 coal based thermal power plants which are continuously producing fly ash and dumping the fly ash-water slurry in the ash ponds situated nearby the plant. Out of the 170 million tons of produced fly ash about 50% is utilized and 50% rest is dumped in the ash ponds. At present

about 65,000 acres of valuable cultivable land is occupied with fly ash. The problem is attributed to the fact that high concentration of fly ash or pond ash is difficult to be transported due to its higher specific gravity. In the lean slurry transportation system huge amount of water energy also goes to the ash pond area which not only occupies large area but also contaminates the surface and ground water regime. The other disadvantage of this system is that energy consumption to pump the slurry increases because of large volume of water involved in transportation of fly ash. This is because of the quick settling tendency of the fly ash particles in the pipe bottom during transportation which may lead to pipe jam if enough water is not flushed along with fly ash. Hence lean slurry transportation is adopted in all the power plants in India. Therefore to address the twin problem of quick settling nature of fly ash and to reduce the water requirement, the flow properties has been evaluated by selecting an additive which will modify the surface properties of the fly ash significantly as a result we can go for adopting high concentration slurry disposal system. The developed slurry can be transported in pipelines to mine void filling areas for stowing purposes to replace the ever depleting river bed sand.

The developed fly ash slurry can be constituted as a composite suspension of fly ash and chemical reagents in water. A number of available additives can be used to alter the chemical and physical properties of the fly ash slurry as required for better flowability and stability of the slurry. There is still a lack of information in the open literature regarding the effects of various chemical reagents such as surface active agents (surfactants) on the rheological properties of fly ash slurries at varying temperature environment. Hence, this research investigates the effects of chemical reagents on the rheology of fly ash slurries. Mineral and chemical reagents play an important role in controlling the physical and chemical properties of fly ash slurries. However, not all chemical reagents influence in the same way on the rheological properties, primarily because of their different physical and chemical properties. There is still a lack of information regarding the coupled effects of chemical reagents and temperature on the rheology of fly ash slurries. Therefore, in this investigation an attempt is made to develop a better understanding of the important mechanisms that controls the rheology of fly ash slurry subjected to varying temperature environment and to

investigate the performance of chemical reagents in controlling the rheological behavior of fly ash slurries.

The present study also undertakes in-place strength development investigation using another reagent i.e. lime to develop a backfill material to be placed in mine voids for filling purposes. The knowledge thus gained could ultimately allow the optimization of fly ash slurry rheology parameters to enhance flowing attributes and at the same time strength gain of the developed material would lead both to ecological and economic benefits. The details have been briefly described in the succeeding sections.

1.1.3. Objectives and scope of the work
1.1.3.1. Objectives

The primary objective of the present investigation was to develop an engineering material based on fly ash to be placed in underground coal mine voids. The specific objectives to meet the aim were the following:

 i. To characterize the typical fly ash from several sources
 ii. To select the most favourable fly ash for its potential to flow in hydraulic pipelines
 iii. To select and characterize the additives to modify the fly ash material
 iv. To determine the flow behavior with the selected additive and optimize the same
 v. To determine the strength characteristics of the in-place fly ash composite materials after mixing with lime.
 vi. Analysis of the experimental results to predict the behavior of fly ash composite material

1.1.3.2. Scope of the study

The investigation was undertaken with fly ash procured from seven number of thermal power plants located at various parts of the country listed elsewhere. The following works in addition to others were undertaken for all the seven fly ashes to determine their suitability for use as a stowing material.

 a. Mineralogical characterization such as
   - X-ray diffraction (XRD) analysis
   - Scanning Electron Microscopy (SEM) studies

b. Chemical Characterization such as :

- Energy-dispersive X-ray spectroscopy (EDX) studies
- Energy-dispersive X-ray Fluorescence (XRF) studies

c. Physical characterization such as:

- Specific surface area
- Particle size analysis
- Moisture content
- Specific gravity
- Bulk density
- Porosity
- pH

Out of the seven fly ashes studied only one fly ash was selected based on the above properties to further investigate the rheological behavior and in-place strength characteristics with and without an additive.

1.1.3.3. Approach/methodology

The objective of the investigation was to develop an alternate engineering material to be placed in underground coal mine voids. One of the major impediments in placing the fly ash in underground coal mines is its high specific gravity. It adversely affects the flowing behavior. So surface acting agents (surfactants) has been chosen and added to change the rheological parameters. Its in-place strength behavior was also tried to be enhanced with addition of another additive e.g. lime. The methodology followed is shown in the flow chart (Figure 1.1). The aim and objectives are achieved by:

i) Characterization of seven fly ashes and selection of the best one for further analysis

ii) Selection of additives and their characterization

iii) Development and characterization of fly ash based composite materials with additives

iv) Evaluation of rheological properties of the developed materials at varying conditions such as shear stress, shear rate, temperature, and concentration

v) Optimization of the fly ash composite material with respect to above for strength enhancement

vi)   Selection, characterization and optimization of strength enhancing materials

vii)   Determination of the mechanical behaviour of the developed fly ash composite materials

viii)   Analysis of results to assist in deciding the influence of different parametric variations.
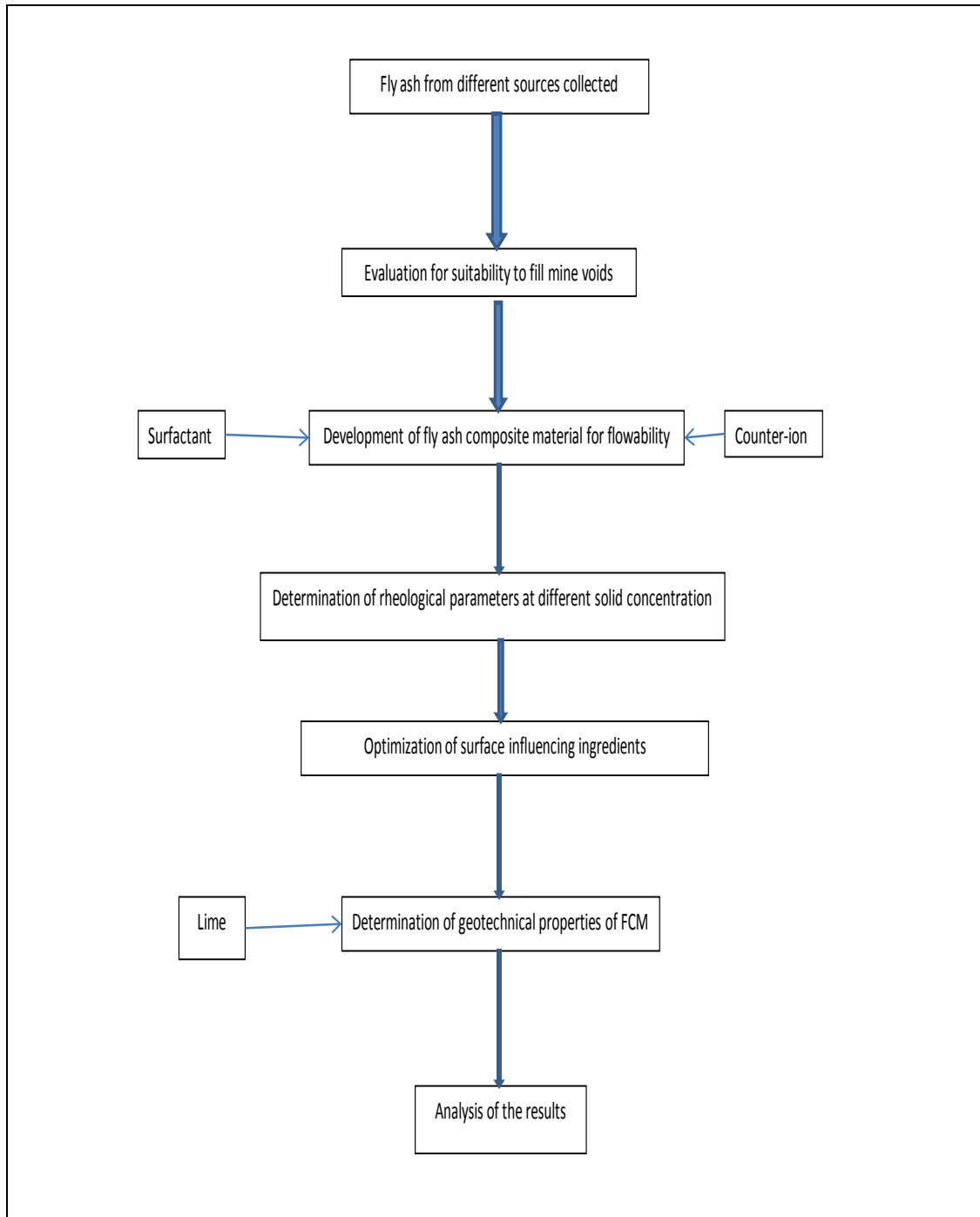
Figure 1.1: Schematic diagram showing the detailed scheme of the investigation

1.1.4. Outline and organization of thesis

The aim and specific objectives have been addressed through well designed and regulated approaches. The details of the investigation carried out as well as the results are reported in different sections. The thesis is structured as follows:

- **Chapter 1** introduced problem statement, background of the work, goal to reflect the long term objectives and specific objectives to meet the goal. It also introduced the methodology adoted with a flow chart to show the different steps involved in carrying out the research and parametric variations that were experimented.

- **Chapter 2** is devoted to a detailed literature survey on fly ash utilization trends in mining sector and its economical and environment friendly transportation to mine filling site. Also the basic concepts involved in fly ash slurry transportation, the physical and chemical properties of fly ash and the role of chemical additives to reduce drag friction in pipelines are discussed. A brief introduction to rheology and constitutive rheological models are also reviewed.

- **Chapter 3** introduced the materials which were used to carry out the research, their sourcing and collection methods. In this chapter the material characterization and methods are discussed as per the National and International standards available in the literature. This chapter also discussed about sample preparation, testing process, machines used, and their brief specifications. I also highlight the sample size and number of tests carried out to meet the goal.

- **Chapter 4** described and presented the results of this investigation in three different sections. Section I deals with the material characterization results, section II deals with results of the rheology study, and section III deals with the results of strength characteristics study.

- **Chapter 5** deals with the summary of observations and important conclusions drawn on the basis of analysis and experimental results. A few recommendations for future research work have also been formulated here. Strength and weaknesses of the thesis is also highlighted.

<div align="right">

CHAPTER 2

</div>

2. Literature Review

This chapter provides information about the relevant work and the state-of-the-art related to the area of fly ash utilization and drag reduction phenomena in pipe line transportation system. The incremental development for rheology modification in slurry flow pipelines from past decades to the recent has been addressed here.

2.1. Introduction

There is a substantial amount of literature that focuses specifically on fly ash utilization and management. The ash ponds are typically near to the site of power plants as long distance transportation of large quantities is very uneconomical in terms of water consumption and power consumption. So, prospects of transporting increasing quantities of fly ash economically should be explored. Mine filling is one such option where large scale utilization is possible. But its transportation to mine filling site is not yet economically established. This investigation is an attempt to address a few aspects of this issue. A major problem in large scale transportation of fly ash is the high specific weight or settlement characteristics of the slurry.

The rheological behavior of the fly ash slurries must be optimized to achieve effective suspension properties for smooth flow in the pipe lines. Modification of surface properties of fly ash particles through additions of chemically active materials (additives) is one such option. A number of additives such as polymers and surfactants are available that alter the chemical and physical properties of the fly ash slurries as required for the flowability as well as stability of the slurry transportation. The various aspects such as rheology, additives, drag reduction; settlements etc. have been discussed in detail. The literature review part of the current investigation is divided into eight parts i.e.

i.   General properties of fly ash
ii.   Suitability of fly ash as a mine filling material

iii.   Hydraulic pipeline transportation with and without an additive

iv.   Drag reduction technology

v.   Drag reducing surfactants

vi.   Polymeric drag reduction research

vii.   Engineering uses of fly ash, specifically the strength development of fly ash composite materials.

viii.   Rheology and constitutive rheological models

2.2. General properties of fly ash

2.2.1. Physical Properties

Physical properties of fly ash help in classifying the fly ashes for engineering purposes. Rehsi and Garg (1988) have made a critical assessment of the different physical properties of Indian fly ashes. The particles of the fly ashes were angular as well as irregular in shape. The shape of particles were affected the different physical properties of fly ash. The specific gravity (sp. gr.) of fly ash is generally low compared to that of soil (Ghosh, 1996; Sridharan and Prakash, 2007). Pandian *et al.*, (1998) reported that the range of sp. gr. varies from 1.46 to 2.66 for Indian fly ashes. Sp. gr. of Indian fly ashes varies in the range of 1.66 to 2.55 as reported by Sridharan and Prakash (2007). Gray and Lin (1972) reported that the variation of sp. gr. of the fly ash is the result of a combination of many factors such as gradation, particle shape, and chemical composition. The low sp. gr. of the fly ash is mainly attributed due to the presence of large number of hollow cenospheres from which the entrapped air cannot be removed, or the variation in the chemical composition, in particular iron content, or both are attributable to these facts (Ghosh, 1996; Pandian *et al*., 1998; Pandian, 2004; Sridharan and Prakash, 2007).

Grain size distribution indicates if a material is well graded, poorly graded, fine or coarse, etc. and also helps in classifying the coal ashes. Coal ashes are predominantly silt sized with some sand-size fraction. Leonards and Bailey (1982) have reported the range of gradation for fly ashes and bottom ashes which can be classified as silty sands or sandy silts. The pond ashes consist of silt-size fraction with some sand-size fraction. The bottom ashes are coarser particles consisting predominantly of sand-size fraction with some silt-size fraction. Based on the grain-size distribution, the coal ashes can be classified as sandy silt to silty sand. They are poorly graded with coefficient of curvature ranging between 0.61 and 3.70. The

coefficient of uniformity is in the range of 1.59–14.0. Pandian *et al*., (1998) carried out experimental investigation on Indian coal ashes and reported that fly ashes are fine grained substances consisting of mainly silt-size particles with some clay-size particles of uniform gradation. Consistency limits namely liquid limit, plastic limit, and shrinkage limit are extensively used in the field of geotechnical engineering. Pandian (2004) reported that fly ashes have liquid limit ranging from 26 to 51%. He observed from the experimental study that fly ashes are non-plastic and hence plastic limit could not be determined. It was also not possible to carry out shrinkage limit tests since the ash pats crumbled upon drying. Free swell index has been developed in the field of geotechnical engineering to differentiate between the swelling and non-swelling soils (Sridharan and Prakash, 2007). Nearly 70% of Indian coal ashes exhibit negative free swell index which is due to flocculation, low sp. gr., and less quantity of clay size particles (Pandian, 2004; Sridharan and Prakash, 2007). Investigations carried out by Pandian *et al.,* (1998) show that the coal ash particles are generally cenospheres, leading to low values of specific gravity.

The classification of coal ashes from geotechnical engineering point of view is important for an effective and efficient use in geotechnical engineering practices (Pandian, 2004). The fly ashes are classified as fine grained ashes as they comprise of predominantly silt sized particles. They can belong to one of the five subgroups, namely MLN, MLN-MIN, MIN, MIN-MHN and MHN as reported by Sridharan and Prakash (2007). If more than 50% of fines belongs to either the coarse silt size (20 μm < particle size ≤ 75 μm) category, or the medium silt size (7.5 μm < particle size ≤ 20 μm) category or fine silt plus clay size (particle size ≤ 7.5 μm) category, then the ash is accordingly represented as MLN, MIN and MHN. If the coarse and medium silt size fractions comprise more than 50% fines and more than the percentage of combined medium silt and fine silt plus clay size fractions, then the ash is designated as MLN-MIN group. If the medium and fine silt plus clay silt size fractions comprise more than 50% fines and also more than the percentage of combined coarse silt and medium silt size fractions, then the ash is designated as MIN-MHN group.

2.2.2. Chemical Properties

Sridharan and Prakash (2007) stated that the chemical properties of fly ash depends upon many factors such as geological factors related with coal deposits deciding its quality,

the composition of the parent coal, the combustion conditions like the method of burning and control of combustion process, the additives used for flame stabilization, corrosion control additives used, hopper position, flow dynamics of the precipitators, and the removal efficiency of pollution control devices. In particular, fly ashes that are produced from the same source with similar chemical composition can have significantly different mineralogy depending upon the coal combustion technology used, which in turn affect the ash hydration properties. The mineral groups present in coal such as hydrated silicates, carbonates, silicates, sulphates, sulphides, phosphates, and their varying proportions normally play a dominant role in deciding the chemical composition of the fly ash. When the pulverized coal is subjected to combustion, the clay minerals undergo complex thermo-chemical transformations. During this process, sillimanite and mullite are crystallized as slender needles along with glass formation. Pyrites and other iron bearing minerals form iron oxides and calcite gets transformed into CaO. The glassy phase formed renders pozzolanity to the fly ash. In almost all geotechnical engineering applications, the pozzolanic property of fly ash plays an important role.

Krishna, (2001) stated that the term pozzolana is used to designate a siliceous or a siliceous and aluminous material which by itself, possesses no cementitious value but in the presence of water, chemically reacts with calcium hydroxide to form the compounds possessing cementitious properties. Based on pozzolanic property, fly ashes can be classified as self pozzolanic, pozzolanic, and non-pozzolanic. Fly ashes can also be classified as reactive and non reactive fly ashes. Reactive fly ashes are those, which react with lime to give sufficient amount of strength. Non-reactive fly ashes are those, which do not give sufficient strength even on addition of lime. Self pozzolanic and pozzolanic fly ashes are reactive fly ashes where as non-pozzolanic fly ashes are nothing but non reactive fly ashes.

According to the American Society for Testing Materials (ASTM C618 – 08) the ash containing more than 70 wt% $SiO_2 + Al_2O_3 + Fe_2O_3$ and being low in lime are defined as class F, while those with a $SiO_2 + Al_2O_3 + Fe_2O_3$ content between 50 and 70 wt% and high in lime are defined as class C. The low-calcium Class F fly ash is commonly produced from the burning of higher-rank coals (bituminous or anthracite coals) that are pozzolanic in nature. The high-calcium Class C fly ash is normally produced from the burning of low-rank coals

(lignite or sub-bituminous coals) and is self pozzolanic in nature. Ahmaruzzaman (2010) stated that the chief difference between Class F and Class C fly ash is in the amount of calcium and the silica, alumina, and iron content in the ash. In Class F fly ash, total calcium typically ranges from 1 to 12%, mostly in the form of calcium hydroxide, calcium sulphate, and glassy components, in combination with silica and alumina. In contrast, Class C fly ash may have reported calcium oxide contents as high as 30 - 40%. Another difference between Class F and Class C fly ash is that the amount of alkalis (combined sodium and potassium), and sulphates (SO_4), are generally higher in the Class C fly ash than in the Class F fly ash. The range of chemical composition of Indian coal ashes together with that for soil (for comparison purposes) is reported in Table 2.0.

Table 2.0.Range of chemical composition of Indian coal ashes and soils (Pandian, 2004)

Compounds	Fly ash	Soils
SiO_2	38–63	43–61
Al_2O_3	27–44	12–39
TiO_2	0.4–1.8	0.2–2
Fe_2O_3	3.3–6.4	1–14
MnO	0–0.5	0–0.1
MgO	0.01–0.5	0.2–3.0
CaO	0.2–8	0–7
K_2O	0.04–0.9	0.3–2
Na_2O	0.07–0.43	0.2–3
LOI	0.2–3.4	5–16

Roode (1987) reported that loss on ignition is generally equal to the carbon content. Throne and Watt (1965) observed that the amount of SiO_2 or SiO_2 + Al_2O_3 in fly ash influences the pozzolanic activity. Minnick (1959) reported that a relatively high percentage of carbon content decreases the pozzolanic activity. The silica content in fly ashes ranges between 38 to 63%, the alumina content ranges between 27 and 44%, the calcium oxide content is in the range of 0 to 8%. It has been found that all the Indian coal ashes satisfy the chemical requirements for use as a pozzolana. According to ASTM 618 classification, typically fly ash originated from lignite coal as from Neyveli lignite mines can be termed as Class 'C' and the rest can be termed as Class 'F'. Torrey (1978) reported that fly ash collected by electrostatic precipitators (ESP) has 38% more CaO and 58% less carbon content than ash collected by mechanical collectors. Moreover the former is finer than the latter.

Davis (1949) has stated that finer the fly ash, higher is its pozzolanic reactivity.The investigations carried out on Indian fly ashes show that all the fly ashes contain silica, alumina, iron oxide, and calcium oxide (Pandian and Balasubramonian, 2000). The mineralogical composition of fly ash, which depends on the geological factors related to the formation and deposition of coal, its combustion conditions, can be established by X-ray diffraction (XRD) analysis. Quartz and mullite are the major crystalline constituents of low-calcium fly ash (CaO < 5%), whereas high-calcium fly ash (CaO > 15%) consists of quartz, C_3A, CS, and C_4AS (Sengupta, 1991; Erol *et al*., 2000; Singh and Kolay, 2002; Pandian, 2004; Sridharan and Prakash, 2007; Ahmaruzzaman, 2010). The morphological studies through Scanning Electron Microscope (SEM) indicate that the coal ash contains glassy solid spheres (plerospheres), hollow spheres called cenospheres, sub rounded porous grains, irregular agglomerates, and irregular porous grains of unburned carbon (Senol *et al*., 2003; Sridharan and Prakash, 2007).

When water or any aqueous medium comes in contact with fly ash iron, aluminum, and manganese oxides sink which determines the release of the trace elements associated with them into the aqueous medium. The degree of solubility of these oxides in turn depends upon the pH of the aqueous medium (Sridharan and Prakash, 2007). The fly ash with higher free lime and alkaline oxides exhibits higher pH values (Pandian, 2004; Sridharan and Prakash, 2007). Sridharan and Prakash (2007) reported that about 50% of Indian fly ashes are alkaline in nature.

Formation of cementitious materials by the reaction of lime with the pozzolans in presence of water is called hydration. The hydrated calcium silicate or calcium aluminate, join the inert materials together to give strength to fly ash material. The pozzolanic reactions for stabilisation are given by the following equations.

$CaO + H_2O \rightarrow Ca (OH)_2 + Heat$

$Ca (OH)_2 \rightarrow Ca^{++} + 2(OH)$

$Ca^{++} + 2(OH) + SiO_2 \rightarrow CSH$ (Calcium Silicate Hydrate)
$\qquad\qquad$ (Gel)

$Ca^{++} + 2(OH) + Al_2O_3 \rightarrow CAH$ (Calcium Aluminate Hydrate)
$\qquad\qquad$ (Fibrous)
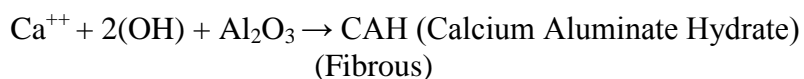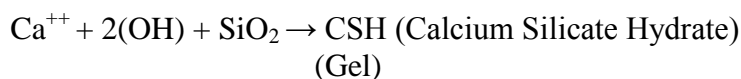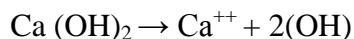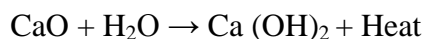
Class C type fly ash does not need addition of lime where as class F does (Senol *et al*., 2002).

2.3. Fly ash as mine void filling material

This section provides information about the relevant work and the state-of-the-art related to the area of fly ash utilization in mining sector focusing its suitability and detailed review of fly ash utilization trends in underground and opencast coal mining sectors. More literature on this topic can be found elsewhere (Chugh *et al.,* 2001; Kumar, *et al.*, 2003; Kumar and Mathur, 2005; Rao *et al.,* 2005; Paul *et al.,* 1994; Rahman, 2005; Ram *et al.,* 2007; Arora and Aydilek, 2005).

2.3.1. Suitability of fly ash as mine filling material

Recently Ahmaruzzaman (2010) published a critical review article on the utilization of fly ash. In his paper he discussed about current and potential applications of coal fly ash, including its utilization in cement and concrete, adsorbent for the removal of organic compounds, waste water treatment, light weight aggregates, zeolite synthesis, mine backfill, and road construction. However, no reference is given to its rheological parameters to transport fly ash hydraulically to mine filling areas.

Jirina and Jan (2010) studied the possibility of filling empty underground void spaces with fly ash and cement fly ash mixes, for the purpose of reducing the impact of deep mining activities on the surface. The method of physical modelling was used to study the behaviour of fly ash mixes deposited in extracted mine spaces. The physical model experiment proved that fly ash mixes could be used as a filling material in underground cavities that was created as a result of deep mining, without serious difficulties of strata movement. Due to its small angle of slope ($30\text{-}35^0$), fly ash material spread out to the sides. The fly ash settled not only in the lower parts of the mine working, but also penetrated beyond the caving falls created, e.g. due to seismic events. Due to its higher cohesion (C=9.5 KPa for dry fly ash), the fly ash did not behave as loose material, but blocks are formed that gradually become submerged in water.

Bulusu *et al*., (2005 & 2007) investigated the success of coal combustion by-product based grout mixtures in reducing acid mine drainage problems in mines. Laboratory experiments conducted for grouts with different proportions of class F fly ash, flue gas desulfurization by-product, and quicklime, for slump, modified flow, bleed, and strength. The

selected optimal grout mixture was injected into the Frazee mine, located in Western Maryland. Pre- and post-injection water quality data were collected to assess the long-term success of the grouting operation by analysing mine water, surface water, and ground water. The tests indicated that the four mechanical properties of grout mixtures, slump, modified flow, bleed, and strength, are related to the fly ash and free lime content of the mixture. Eight years of post-injection water quality monitoring showed that there was significant decrease in acidity, concentration of major ions, and trace elements in the mine water. The grout cores showed that the hardened grout retained its strength and low hydraulic conductivity with no evidence of in-situ weathering.

Mishra and Das (2010) examined the suitability of Talcher coal fly ash for stowing in the nearby underground coal mines based on their physico-chemical and mineralogical properties. The SEM images revealed spherical particle morphology of the ash samples which would create lubricating action due to the well known "ball-bearing" effect which would result in frictionless flow in the stowing range causing less wear and tear on the pipelines. Due to improved rheology, it would also help in reducing the energy cost in pipeline transportation during hydraulic stowing operations. The presence of SiO_2 in abundance would increase the strength and the presence of CaO would give cementing properties after stowing. The ash samples also contain very negligible amount of unburned carbon and hence there is no risk of spontaneous heating if utilized as a stowing material in underground coal mines.

Ozerskii and Ozerskii (2003) reported the results of a study of the mineral, chemical, and radionuclide compositions of coal ash and slag waste of the Berezovsk state regional power plant and the capping of the Berezovskii-1 coal mine suggested disposal of the waste into the mined-out space. The use of the ash for reclamation of refuse soils have a positive ecological effect due to the chemical amelioration, strengthening, and lower settlement of the refuse soils and compensation of the rock mass deficit in the mined-out space.

Ward *et al*., (1999) described a power station fly ash transportation system, from a bag house to a mine rehabilitation site, at a distance of 12 Km. Ash was mixed with water and pumped to the mine rehabilitation site. The concentration of the ash / water mixture was kept at $C_w \approx 70\%$. Physical tests demonstrated that it is possible to leave the pipeline full of slurry

at $C_w = 65\%$ for up to 24 hours and still successfully restart the plant. The deposited ash also exhibited a relative fast strength gain which allowed rehabilitation to be commenced in 1-2 weeks of cessation of ash deposition.

Kumar (2000) studied the leaching behaviour of trace elements of the ashes of a Captive Thermal Power Station and the following conclusions were drawn from his study:

- ➢ In the study period of 274 days there was practically no leaching of elements namely chromium, selenium, aluminium, silver, arsenic, boron, barium, vanadium, antimony, and molybdenum from all the fly ash samples reported.
- ➢ Out of the nine elements found in the leachates only calcium and magnesium were found to be leaching in the entire period. The other seven elements namely iron, lead, copper, zinc, manganese, sodium, and potassium leaching was sometimes intermittent. The leaching of sodium and potassium practically stopped after 35 days and 40 days respectively.
- ➢ The concentration of elements in the leachates was below the permissible limits for discharge of effluents as per IS: 2490 and also for drinking water standards IS: 10500.

On the basis of the above observations it is found that fly ash is environmentally benign material and can be engineered for their bulk utilization for reclamation of mined out areas and for soil amendment for good vegetation.

Jain and Sastry (2001) reported that the acid mine drainage (AMD) problem can be mitigated in the coal mining areas with the use of fly ash and slurry transportation system can be conveniently adopted. Size modification can improve its flow properties. Pelletization of fly ash is one such option to improve size and shape of fly ash.

Vories (2003) reported that the placement of fly ash materials on the mine site resulted in a beneficial impact to human health and the environment. He opined that the beneficial uses of fly ash in mining sector include:

a. A seal to contain acid forming materials and prevent the formation of AMD;

b. An agricultural supplement to create productive artificial soils on abandoned surface mine lands where native soils are not available;

c. A flowable fill that seals and stabilizes abandoned underground coal mines to prevent from subsidence and strata movement;

d. A non-toxic, earth like filling material for final pits ad within the spoil area.

Kumar & Mathur (2005) reported that about 10,000 m^3 of pond ash was stowed in an underground coal mine successfully. About 13,000 m^3 pond ashes were also stowed in Durgapur Rayatwari Colliery of Western Coalfields Ltd. (Singh & Goel, 2006). The results of both the demonstration were quite encouraging and it is observed that fly ash stowed bed has good stability. The leachate was also found to have no adverse impact due to the use of these additives (Kumar *et al.,* 2003).

Ghosh (2005) demonstrated through laboratory tests that pond ash with additives could be safely used as a stowing material for underground coal mines. He reported that the water percolation rate was 16.235 cm/h without any additive and 18.97 cm/h with additive. This shows that use of an additive has a positive impact on the percolation rate. The results of spontaneous heating tests showed that the proportion of total combustible material is very low, i.e. 2.244%. So the ash sample did not attain crossing point and ignition point temperature even at a bath temperature of 200^{0}C.

Panday and Kumar (2005) reported the feasibility of filling about 150 lakh MT of fly ash in 10 years time in one of the underground coal mine by adopting lean slurry transportation system. Prashant (2005) reported that the present share of mine filling application is about 3% only which can increase many folds by proper utilization in filling of abandoned and active coal mines.

Rao *et al.,* (2005) reported that the overall cost of stowing was less than that of sand stowing. They also observed that the system of ash stowing was advantageous over sand stowing and estimated that the overall ash stowing cost was nearly Rs.24 less than that of sand stowing.

Roy Choudhry (2005) reported successful dumping of 100 lac m^3 of ash in underground collieries which were very close to thermal power plants. The attributes of fly ash such as silt-size particles, low bulk density, high water holding capacity, favourable pH,

presence of many nutrients such as N, P, S, etc. are favourable properties for mine spoil reclamation as well (Ram amd Masto, 2010).

Ghosh *et al.,* (2006) reported that fly ash has no affinity towards spontaneous heating and hence can be safely used as underground filling material for stowing purposes. They also reported that the sp. gr. of the ash was 2.0, about 25% lighter than river bed sand (average sp. gr. 2.65). These characteristics favour hydraulic transportation during filling as it would cause less head loss during transportation through pipelines reducing energy cost and cost of hydraulic transportation as compared to sand. The ash was also having low bulk density i.e. 1.08 t/m^3, which is 37% less than that of sand (with average bulk density of 1.67 t/m^3).

2.3.2. Settling characteristics, leachates, and heavy metals in fly ash

Colloidal solids normally carry charges on their surface which lead to the stabilization of the suspension by addition of some chemical reagents. The surface property of such colloidal particles can be changed or the dissolved material can be precipitated to facilitate the separation by gravity or by filtration.

Dutta *et al.,* (2009) reported the leaching of ten elements-namely, Fe, Mn, Ca, Na, K, Cu, Cr, Zn, Arsenic, and Pb. The leaching conditions were selected to broadly simulate that of surface coal mines in order to estimate the usefulness of the materials for back-filling of abandoned coal mines and assess the possibility of contamination of the sites by release of heavy metal ions. A much higher mobility of the elements had been observed at a low pH. Less leaching was found at a high pH except for arsenic. The mobility of toxic elements from fly ash was negligible where the final pH of the leachate was alkaline or nearly neutral.

Prasad *et al.,* (2003) found that pond ash and weathered ash leach heavy metals in alarming concentration when pH value was beyond 6.0.

Hwang and Lattore (2011) conducted a statistical screening test to obtain information on the factors governing groundwater quality after open pit restoration using manufactured coal ash aggregates (MAs) as a sub-soil substitute. MA application rate was (2:1 or 1:2 topsoil/MA volume ratio), rainfall intensity (high or low), and aggregate size (2.36-4.75 mm or 4.75- 9.53 mm). Among the water quality parameters examined (pH, turbidity, heavy metal

content, conductivity, and hardness), the last two parameters were significantly higher ($p <$ 0.05) in soil amended with MAs than in a control reactor using sand. Based on the statistical analysis, the results depicted that the pH, turbidity, and heavy metal (Pb and Cd) concentration were not a problem in mine restoration operation.

Kumar *et al.,* (2006) reported that faster rate of settlement is desirable for quicker drainage of water during hydraulic stowing with fly ash. Faster settlement of solids avoids clogging of pores of barricades and also it would not cause building up of any hydrostatic pressure inside the barricades leading to its damage. On the other hand if the solids are left in suspension for a longer period of time, there is a likelihood of escape of fines through the barricades. It is found that the settlement rate can be increased by increasing the slurry concentration by using a suitable additive (Jain and Sastry 2003).

Jain *et al.,* (2006) observed that elements from acidic ash leach readily than from alkaline ash. Fly ashes are generally disposed at pH 7.0-8.5. They confirmed that the leaching in alkaline medium was much lower as compared to acidic medium and opined that fly ash can be used safely for mine filling purposes in alkaline medium without having any adverse impact on the environment.

2.3.3. Paste backfill system

It is basically high solids concentration slurry. The term "paste" generally implies mixes containing over 70% solids concentration with less than 4% bleed.

Bunn (1989) observed that at a concentration of less than 60% with a maximum flow rate of 0.03 m^3/s resulted in 1.7 m/s velocity, enough to facilitate pipe line transportation smoothly. Approximately 900 tonnes of fly ash paste with $C_w<64\%$ was transferred to the disposal site in a period of 21 pumping days with an average of paste mass flow rate of 30 t/h. The angle of inclination of the deposited material was 2 to 3 degrees. Even the heavy rainfall during monsoon has produced no erosion at the observed site.

Bunn *et al*., (1990) examined the maximum amount of water that is available for recycling from a range of dense phase fly ash slurries. It was found that in a dense phase slurry system that disposed 1000 tons of slurry, with a C_w of 73% required 730 tons of fly ash

with 270 tons of water. When this 1000 tons of slurry was deposited at the disposal site 120 tons of water was available for recycling. Therefore, 150 tons of water was captured in the deposited ash. From this study it was found that the percentage of water available for recycling varied depending on the concentration C_w and the particle size distribution of the fly ash. The volume of return water varied from 12.4% to 59.8%. It was also observed that the deposited slurry placement density showed an increase when the slurry pumped was above C_w of 65%.

Bunn *et al*., (1991) examined the relationship between the packing density of slurry obtained by assisted compaction and the pumpability as determined by rheology testing. The results indicated that the differences between the C_w's from the rheology tests and the compacted fly ash slurries varied from 12.5% to 14.94%. The variation in the d_{50} of the fly ash samples tested ranged from 8µm to 45µm.

Rudzinski (2005) described a study of the behaviour of fresh cement pastes under shear in a rotational viscometer. It was observed that an addition of fly ash to Portland chinker influenced the change of flow behaviour of cement pastes from thixotropic flow to thixotropic-dilatant flow. Addition of fly ashes without decreasing the amount of cement brought about an increase in the basic rheological characteristics of cement pastes, growth intensity being dependent on volume fraction of solid and percentage of addition.

Chugh *et al.,* (1999) developed paste backfill mixes consisting of 70% Coal Combustion By-products (CCBs) to reduce movement and acid mine drainage (AMD) and opined that the mix could increase production by 5-8% more. They also successfully demonstrated that backfill material with 65-70% CCBs, gob and fine coal processing waste provided lateral containment and strengthened coal pillars.

Jorgenson and Crooke (2001) indicated that placement of fly ash paste under saturated and unsaturated conditions would not impact ambient water quality. The fly ash paste exhibited good engineering characteristics when compared to the native soils and mine spoils currently used for reclamation. Strengths obtained from the fly ash and water mixtures were generally higher than those found in the natural soils.

Nagataki *et al*., (1984) found that the rate of adsorption of superplasticizer on fly ash was higher than that in cement. It was also observed that amount of superplasticizer had positive influence on coefficient of viscosity of fly ash and there was a correlation between bulk sp. gr. of fly ash and fluidity of paste. The higher the bulk sp. gr., the lower is the coefficient of viscosity.

Mahlaba *et al*., (2011) compared the behaviour of pastes by varying brine composition mixed with two types of fly ashes. The results showed that fly ash played a more prominent role in the behavior of pastes than brines. Therefore they concluded that the constituent of paste play a major role in the development of an environmentally sound paste backfill practice.

Turkel (2007) studied a mixture of high volume fly ash, crushed limestone powder, and low percentage of pozzolana cement in different compositions. The amount of pozzolana cement was kept constant as 5% of fly ash weight. The amount of mixing water was chosen in order to provide optimum pumpability by determining the spreading ratio of the mixture using flow table method. The test results indicated that the mixtures had superior shear strength properties compared to that of compacted soils.

Corners (2001) reported that cement was the largest cost component in the backfill system and recommended that partial replacement of cement with type "C" fly ash as 50%. It was observed that compressive strengths equal or greater than the compressive strengths of type "F" fly ash mixture at only 20% cement replacement.

McLoren *et al.,* (2001) evaluated the use of admixtures in reducing backfill binder concentrations and demonstrated a 20% reduction of cement is possible while maintaining critical strength and flowability criteria. The addition of an admixture (in two variations i.e. 0.25g per kg and 0.50g per kg) - a foaming agent, had several effects on the backfill including slower water drainage from the backfill resulting in a reduction of total bleed water, reduced sensitivity of the flow properties to variations in the moisture content, increased compaction rate of the backfill at high solids contents, a higher dispersion with the addition of the cement than that of the tailings alone, enhanced flowability of the backfill material, and an overall reduction in the compressive strength of the backfill. The treated mixture had better

flow properties and hold particles in suspension more effectively than untreated backfill. The reduced shrinkage of the material allowed better adhesion of the mass to the stope walls. The reduction in uniaxial compressive strength in three-day tests made it impractical for use in backfill. The addition of other alternative admixtures resulted in an increase in compressive strength and substantial binder content reduction. Additionally, the admixture enhanced flowability of the backfill to an extent that further strength gains may be possible by reducing the water content of the backfill while still maintaining minimum flowability criteria.

Deb and Chugh (2005) developed eco-friendly paste backfill mixes using coarse coal processing wastes (gob) and CCBs and placed 9,293 tons in an abandoned underground panel. The developed grouts flowed laterally to a distance greater than the depth of the mine.

Prashant *et al.,* (2005) observed in laboratory testing that pond ash could be used as a paste backfill material up to a concentration of 58% by wt.

2.4. High concentration hydraulic slurry pipeline system

Conventionally fly ash is mixed with large amount of water and transported by pipelines to nearby ash ponds which involve little economic evaluation and other aspects. But for long distance transportation of high volume fly ash, there exist no established criteria. Problems faced in this system are friction loss, head loss, high energy consumption, high settlement rate at the pipeline itself, very less volume/concentration etc. There have been many attempts by researchers for high concentration slurry transportation world over. But the mechanism has not yet been commercially established. In this literature review details of flow behavior of fly ash and high concentration slurry with and without an additive have been presented. There are many published articles or literatures on pipeline transportation with addition of polymers and surfactants to alter the rheological behavior (Durand, 1951; Horsely, 1982; Wasp *et al*., 1977). One of the major impediments in pipeline transportation is the velocity of flow that depends on many factors (Wood and Kao, 1966). Some of the important parameters are:

(i)   Carrier fluid properties like viscosity, density, etc.
(ii)   Properties of solid particles like sp. gr., size, shape, terminal settling velocity etc.

 (iii) Properties of the slurry, solid concentration, viscosity, and particle size distribution, percentage of sub-sieve particles etc.

 (iv) Pipe diameter, pipe surface condition etc.

The presence of fine particles increases the viscosity of the slurry and they offer increased resistance to settling behaviour of larger particles. The various design parameters that are required to be established for the design of the pipeline system can be classified under the following three categories:

 (i) Hydraulic parameters

 (ii) Parameters affecting corrosion-erosion characteristics

 (iii) Parameters affecting the operational stability of the system.

Newtonian state of motion is preferable to non-Newtonian state as the former uses less energy due to reduced head loss (Hanks, 1982).

 Panda *et al.,* (1996) have established the pressure loss in horizontal pipes for transportation of fly ash up to 60% solid concentration (by weight) by correlating it with the rheological behaviour of the slurry. They estimated pressure loss using pressure loss models developed for Newtonian fluids in the range of 20-25% concentration by weight.

 Chandel *et al*., (2010) evaluated the performance of fly ash slurry in terms of pressure drop, specific energy consumption etc. for C_w of 50-70%. They observed that with increase in flow velocity, the pressure drop in the pipeline increased with minimum value for 60% solid concentration and maximum value for 70.2%. The relative pressure drop decreased for increase in flow velocity for a flow velocity range of 1 to 2m/s and specific energy consumption increased steeply when the concentration value was more than 65%. They found the flow behavior to be non-Newtonian for fly ash and bottom ash slurry. Gahlot *et al.,* (1992) investigated the performance of centrifugal slurry pumps with coal and zinc tailings slurries in the concentration ranges of 0-57 % by weight. They observed that the head and the efficiency of the pump decreased with increase in solid concentration, particle size, and sp. gr. of solids, but independent of the pump flow rate. They observed higher reduction in the head compared to the efficiency and had shown linear decrease in the head and the efficiency ratios with increase in solid concentration up to 50% by weight.

Seshadri and Singh (2000) found that relative viscosity of fly ash slurry increased sharply as the solid concentration exceeded 40% by weight. For bottom ash slurry the relative viscosity increased sharply beyond 30% by weight. The yield stress of the fly ash slurry also increased sharply beyond 40% by weight. Total head of slurry column decreased almost linearly as the discharge rate increased from 3 lps to 18 lps and pump input power increased linearly as the discharge rate increased from 3 lps to 18 lps. The pump efficiency increased from 10% to 45% as the discharge rate increased from 2 lps to 18 lps. The specific energy consumption decreased from 1.4 kWh to almost 0.2 kWh as the solid concentration is increased from 15% to 53% by weight. From the above results it was concluded that it is possible to subsequently increase the concentration of solids and affect savings in water and energy consumption.

Knezevic and Kolonja (2008) conducted experiments at a concentration of solid and liquid components: 1:1.92 (mass concentration C_w = 34.2%, Volume concentration C_v = 19.8%), 1:1.485 (C_w = 40.2%, C_v = 24.2%), 1:1.015 (C_w = 49.6%, C_v = 31.9%) and 1:0.9 (C_w = 54.6%, C_v = 36.4%). The authors accomplished the transport of ash and bottom ash slurry at mass concentrations between 40% and 50%. The test of the pressure decrease showed that the energy losses were the highest when the concentration was more than 50% solids.

Verkerk (1982) concluded that the mass concentration of 45% was the boundary value for the substitution of the centrifugal slurry pumps with the piston pumps. The test ascertained that the slurry with lower ash and bottom ash concentration acted as fluid, while as the concentration increased it became more like a 'sliding panel'. The boundary value for this change was set at 69±1% of mass concentration.

Sive and Lazarus (1986) have concluded that the centrifugal slurry pumps were applicable when the mass concentration was kept below 48%, based on their tests in the closed test circuit with varying flow rate (up to 100 dm^3/s) and with different velocities (up to 6.4 m/s).

Vlasak and Chara (2007) presented the results of an experimental study of flow behavior of fine-grained highly concentrated slurries consisting of a mixture of water, kaolin, and fly ash in horizontal straight pipes. Kaolin slurry showed time-independent, yield pseudo-

plastic response for volume concentrations higher than about 60%. However the fluidic fly ash- gypsum water mixture showed time dependent and substantial decrease of flow resistance due to the effect of shearing during the initial period of pumping. An intensive shearing of concentrated fluidic fly ash-gypsum slurry resulted in a substantial reduction of the hydraulic gradient in the laminar region and in a marked shift of the laminar/ turbulent transition point towards a lower velocity value. After shearing in a turbulent regime a reduction in the hydraulic gradient at the transition point reached about 50% of its original value.

Sadisun *et al*., (2006) observed that unconfined compressive strength (UCS) increased with curing time as well as fly ash content. The higher the fly ash content the more was the strength. Slaking index also decreased with increase in fly ash content as well as cement content in the mixture. They opined that fly ash content had a direct bearing on viscosity of mixture, its stability, reduced clogging, etc. They proposed optimum constituents of 8% cement with 42% fly ash for lining materials.

Bournonville and Nzihou (2002) investigated two different water-washed municipal solid waste incinerator fly ashes at 23°C with concentration 35% to 50%. The rheological behavior of these fly ashes in aqueous suspensions was studied using a parallel plate rheometer. Shear-thinning behavior was observed in one sample whereas thixotropic behavior was found in the other. The viscosity is found to be dependent on both the volume fraction of solids in the suspension and on the yield stress. Viscosity decreased with increase in concentration as well as the shear rate which was due to breakdown of the structures of the suspension.

Senapati *et al.*, (2010) investigated the rheological behavior of 5 different fly ash slurry samples with varying median particle size. Shear thinning behavior was observed for all the samples at higher solids volume fractions in the range of 0.32-0.49. It was also found from the study that the relative viscosity is very much sensitive to the concentration of solids, particle size, and particle size distribution.

Revati *et al*., (2009) experimented with different composition of fly ash, gypsum and quarry waste for both flow behavior as well as UCS value. It was found that quarry waste

content influenced the water requirement more than that due to fly ash. It was also found that 150±50mm flow was not readily flowable as compared to other flow ranges.

Tsai and Knell (1986) found that the rheological behavior of coal water slurry followed the Ostwald-de Waele power law model for the entire shear rate range (0-10000 s^{-1}). The flow behavior index was found to increase from 0.6 to 1.0 (i.e. from pseudoplastic to Newtonian), as shear rate exceeded a threshold value (i.e. 400s^{-1}) that depended on coal content and coal particle size and size distribution. The 70 wt% utility grind coal water slurry (average particle diameter of 38 μm) became less pseudoplastic with flow behavior index increasing from 0.70 to 0.82 at shear rates above 400s^{-1}.

Chen *et al*., (2009) obsreved that 65.3 wt% exhibited a Newtonian fluid behavior and the slurry flow was free from wall-slip effects. But at 67.1 wt % and 68.2 wt% solid contents, the slurry flows were strongly affected by wall-slip and with the increase of wall shear stress, the slurries exhibited their true rheological behaviors firstly as a shear-thinning fluid and then as a shear thickening fluid. The existence of a minimum value of slippage contribution indicated the transition of flow behavior from shear thinning to shear thickening.

Lu *et al.,* (1998) discussed the flow pattern and pressure drop in highly concentrated slurry transportation pipelines. They observed that the particles tend to settle down to the bottom of pipes due to the action of gravity force forming different flow patterns which can be indicated by particle concentration profile. Three distinct flow patterns were observed for different particle size distribution at different velocities; such as fully stratified, partially stratified, and fully suspended flow patterns. Pressure drop in slurry flows are strongly dependent on the flow pattern developed in pipelines. Fine particles suspended in water make the water more viscous, and increase the friction. The mixture of particles of different sizes is helpful to reduce pressure drop in pipeline flow slurries.

Chandel *et al.,* (2011) observed that for a fly ash slurry concentration C_w = 60% at 25°C with relative slurry viscosity of 16.27, the centrifugal pump efficiency was 32% at a discharge rate of 40m^3/hr. It was also observed that as the relative slurry viscosity increased the pump efficiency decreased.

Fly ash slurries exhibited time dependent and non-Newtonian flow behavior for $C_w >$ 60% (Bunn *et al.*, 1990). They observed that Bingham model fitted well for $C_w < 0.6\%$ and Bingham plastic model for $C_w > 60\%$. It was also found that C_w is sensitive to source of ash, temperature, pH, and the total mass flow rate of slurry, pipe diameter, and pump pressure and power requirement.

Hellsten and Harwigsson (1999) found out that a combination of Betaine surfactant and an anionic surfactant reduced the flow resistance between a flowing water-based liquid system and a solid surface.

Bunn *et al.,* (1999) conducted experiments on fly ash slurries in the concentration range of 65% to 74 % in a 120mm diameter pipe loop having a length of 125m. Rise in pressure loss was accompanied by a change in the flow properties of slurry which changed from a liquid like mixture to one that tends to form sliding paste at the concentration of around 69% ± 1% by weight.

Kuganathan (2001) developed the tailings paste fill composition from blended tailings paste fill using 3-3.5% port land cement and found out that the cost of paste fill was much lower than the total tailings paste fill that could be produced from the same tailings. He observed that there was an optimum range of particle size distribution associated with any particular tailings, which would result in the most economical paste fill for those tailings.

Usui *et al.,* (2001) carried out experimental studies on rheology and pipeline transportation of dense fly ash slurry. Simha's model was used to predict the maximum packing volume fraction for non-spherical particles suspension and successfully used to predict the slurry viscosity under completely dispersed conditions. The model resulted in the estimation of inter particle bonding force between primary particles in a cluster and the power consumption and flow rate relationship in hydraulic slurry pipeline transportation system. A possible way to reduce the cost of slurry pipeline system by means of periodical addition of a stabilizer was proposed. Vlasak *et al.,* (2002) highlighted the use of peptizing agent to decrease the viscosity and yield stress depressing the strong non-Newtonian flow behaviour of the slurry due to the presence of colloidal particles.

Lei *et al.,* (2002) studied rheological characteristics and sedimentation stability of the slurry with the addition of four kinds of stabilizing additives. Additives used in their study were rhamsan gums, carboxymethyl cellulose, xanthan gum, and naphthalene-sulfonate formaldehyde condensate (NSF). They observed that viscosity of the fly ash-water slurry increased as the concentration of stabilizer increased. Therefore NSF was used as a dispersing additive to reduce the viscosity of the fly ash water slurry. The concentration of dispersing additive (NSF) was 0.3 weight % /slurry. The long molecular branches of the additive were effective for building up network structures necessary to prevent the sedimentation of fly ash particles. They suggested the use of an additive as a stabilizing agent at a concentration of 0.2 weight % for preparation of stable fly ash-water slurry.

Parida *et al.,* (1996) reported that ash slurry consisting of fly ash or fly ash-bottom ash mixture exhibit non-Newtonian pseudo-plastic flow behaviour at high concentrations in the range of 60-65% by weight. Presence of bottom ash having larger particles in the ash slurry affected slurry rheology and head loss in pipeline flow positively.

Singh and Singh (2003) reported that when filling material is sent through pipelines in the form of slurry, frictional head loss was an important factor to be computed. Jain and Sastry (2004) found that more the concentration of fly ash more the loss in pressure. Simultaneously higher the velocity of slurry flow higher the pressure loss. The pressure loss was minimized by adding an additive to the slurry. They also observed the maximum fly ash concentration possible for slurry transportation was 50%.

Thissen and Kuy (2005) found out to dispose 1000 ton of fly ash about 5667 m^3 of water was required at 15% solid concentration whereas only 667 m^3 of water was required to dispose same amount of fly ash at 65% solid concentration saving about 88% of water energy which in turn reduced the pumping cost. From this study it was concluded that the conventional lean slurry disposal system is plagued with transporting large quantities of water with only small amount of ash loading.

The rheological behaviour of fly ash slurry having particle size 0.3mm - 75μm was studied by Seshadri *et al.,* (2005) at different concentrations with and without an additive i.e. sodium hexametaphosphate of 0.1 % concentration. The computations of pressure drop

showed substantial saving in energy consumption when the additive was added into the fly ash slurry at higher concentrations as it modified the rheological properties of the fly ash slurry significantly. They reported that slurries above solid concentration of 60% by weight were non-Newtonian and Bigham plastic model fitted the data over the range of shear rates investigated. Sodium hexametaphosphate at 0.1 % concentration as an additive reduced both Bigham viscosity and yield stress of the fly ash slurry significantly.

Addition of certain kinds of surfactants, as well as polymers, to a Newtonian fluid causes considerable drag reduction in the turbulent pipe flow. Surfactants used by Aguilar *et al.,* (2006) were Tris (2-hydroxys-ethyl) tallowalkyl ammonium acetate (tallowalkyl N-(C_2H_4) OH)$_3$ AC, from AKZO Chemicals. This solution consists of 2,000 ppm of surfactant, plus 1740 ppm of sodium salicylate (NaSal) used as counterion, and 3.75 mM/l of copper hydroxide (Cu (OH)$_2$), which is a compound that helps reduce the fluid viscosity to a water – like value, without diminishing its drag-reducing ability.

Knezevic *et al.,* (2008) observed marginal drop in flow rate and pressure when the ash concentration was beyond 40 to 50% compared to quantity of fly ash and bottom ash transported during the time limit. Senapati *et al.,* (2008) studied the modelling of viscosity for power plant ash slurry at higher concentrations and effect of solid volume fraction, particle size, and hydrodynamic forces in a non-Newtonian laminar flow regime. A model incorporating maximum solids fraction, power law index, median particle size, co-efficient of uniformity, shear rate is developed to predict the viscosity.

Chandel *et al.,* (2009) described the effect of additives on pressure drop and rheological characteristics of fly ash slurry at high concentration (above C_w = 60% by weight). There was reduction in pressure drop when soap solution (0.1 to 1.5%) was added to the fly ash slurry at higher concentrations. Slurries of fly ash at these concentrations showed a Bingham fluid behaviour. The Bingham viscosity and yield shear stress values increased with increase in concentrations, the increase being more pronounced at higher concentrations. The addition of soap solution as an additive to the fly ash slurry reduced the rheological parameters and resulted in substantial decrease in energy consumption. Steward and Slatter (2009) tested the pipe flow behaviour of fly ash and water mixtures in a closed loop pipe

system at solids concentrations ranging from 51% to 74% by mass. They used the Herschel-Bulkley rheological model to evaluate pipe flow.

Nigle and Neil (2003) observed that friction reduction in non-settling pipe flow occurred when viscosity was changed with chemical reagents and additives. They studied the effects of different chemical reagents on drilling mud slurries (using sodium acid pyrophosphate and sodium hexametaphosphate), phosphate rock slurries (using caustic soda), and limestone cement feed slurries (using a combination of sodium tripolyphosphate and sodium carbonates).

Slaczka and Piszczynski (2008) tested four nonionic surfactants as additives to enhance flowability of coal-water slurries. The flow properties were measured by means of a coaxial rotating rheometer for 55 wt% coal concentration. From the study it was found that such a mixture without any additive has a consistency of dense pulp and not indicated any flowability. The addition of the surfactant made the mixture flowable. Increasing the hydrophobicity of coal grains improved flowability of coal-water slurry and allowed to get slurries of higher concentrations. It was also observed that removing the air from the surface of coal grains, by heating slurries up to the boiling point, exposed the larger part of their surface and consequently increased the adsorption of surfactant, that led to increase in hydrophobicity of the coal grains surface and finally decreased the viscosity of the slurry. For the most effective additive, after heating slurry to boiling point before introducing the chemical agent (surfactant), for the lowest tested shear rates the apparent viscosities were decreased by 11.8%, 9.7% and 0% for the additive dosages of 250g/t, 500g/t, and 750 g/t, respectively in comparison with those not degassed. Vlasak *et al.*, (2010) tested three different kaolin-water mixtures with an overpressure capillary viscometer, rotational viscometer, and experimental pipeline loop. The effect of peptizing agents and their concentration was investigated. It was demonstrated that even very low concentration of peptizing agent resulted in a significant reduction in the apparent viscosity and in the yield stress. Sodium carbonate and soda water-glass were used as peptizing agent in the mass concentration varying from C_a=0.02 to 2%. The original value of yield stress of the kaolin slurry with concentration C_m = 0.55 could be reduced from τ_y= 134 Pa to 6 Pa for C_a = 0.15% and from τ_y=34.1 Pa to 0.5 Pa for C_a = 0.1% respectively.

Boylu *et al.,* (2005) studied the effect of caboxymethyl cellulose (CMC) on the stability of coal-water slurry. The results depicted that polymeric anionic CMC agent had higher effect on the stability of coal-water slurry.

Shimada *et al*., (2008) concluded that addition of 3% surfactant controlled the bleeding of fly ash-water slurry that also improved its fluidity.

Cassasa *et al.,* (1984), studying the rheological behaviour, sedimentation stability, and electrophoretic mobility of four bituminous coals in water and in solutions of simple well-characterized surfactants, observed that slurry rheology and stability depended on coal particle surface charge and recommended the use of the additives to improve rheological parameters.

Huynh *et al.,* (2000) measured the rheological properties of chalcopyrite slurry with chemical treatments, showing that there was an increase in repulsive electrostatic forces between particles which, in turn, reduced the slurry viscosity and the solid content of the slurry was increased by over 10 wt. % for the same pumping energy input. He *et al.,* (2004), using a cationic surfactant selected to modify fly ash particle behaviour recommended that the dispersing agents influence viscosity, pH, and be non-toxic, and biodegradable.

Elizabet *et al*., (2011) treated fly ash under variety of conditions with an anionic surfactant. The properties of the modified products were compared to those of the untreated samples. The surfactant dosage was 0.1%, 05% and 0.2% wt and temperature varied from 50°C to 80°C. It was found from the study that the surface of the modified fly ash became more hydrophobic in comparison to that of the untreated fly ash. The degree of agglomeration reduced significantly in the modified samples.

Chandel *et al*., (2009) reported the effect of a mixture of sodium carbonate and Henko detergent in the ratio of 5:1 (0.2% by wt) as an additive on pressure drop and rheological characteristics of fly ash slurry at high concentration (above $C_w \approx 60\%$ by weight). They found a reduction in pressure drop when the above additive was added to the fly ash slurry at higher concentrations. They observed a marked decrease in viscosity of the fly ash slurry from 14.50 Pa.s to 7.75 Pa.s at $C_w = 60\%$ and at 70% solid concentration, plastic viscosity reduced

from 245.30 Pa.s to 150.2 Pa.s. Data also showed that the additive decreased the yield shear stress of fly ash slurry from 0.36 Pa to 0.1 Pa at C_w =60% and at 70% solid concentration yield stress reduced from 1.945 Pa to 1.20Pa.

Vlasak and Chara (2009) investigated the effect of slurry composition and volumetric concentration on the flow behaviour of fluidic fly and bottom ash and sand slurries containing fine-grained and coarse-grained particles. Kaolin slurries with and without a peptizing agent were used as the carrier liquid for the sand slurries to compare the effect of Newtonian and non-Newtonian carriers. The study revealed a time-dependent yield pseudo-plastic behavior of fluidic fly and bottom ash slurries. The highly concentrated sand-kaolin slurries showed non-Newtonian behavior. When the carrier kaolin slurry is peptized, the hydraulic gradient in the laminar region markedly lowered and the addition of small amounts of kaolin favorably affected the flow behavior of the sand slurry. To compare the effect of Newtonian and non-Newtonian carriers on the slurry flow behavior, a chemical agent with a peptizing effect (a sodium carbonate, which supplied the slurry with Na^+ ions for the compensation of the Kaolin particle surface charge) was used to change the physical- chemical environment of the slurry and to depress the attractive interparticle forces, which evoke non-Newtonian behavior of the slurry. Due to the peptizing agent the slurry flow behavior changed from non-Newtonian to nearly Newtonian.

Tsutsumi and Yoshida (1987) found that at a constant shear rate the apparent viscosity of the suspension with agglomerates decreased with temperature while the relative viscosity increased. The change was caused by the growth of agglomeration, because hydrodynamic forces decrease with temperature.

Lee and Sakai (2003) investigated the influence of the character of fly ash on the fluidity of cement paste with a polycarboxylic acid type superplasticizer in connection with the particle size distribution, unburned carbon content, specific surface area and shape of the fly ash. The fluidity of the fly ash cement paste with an added 20 vol% fly ash increased with an increasing roundness of the fly ash and they also found that there was a linear correlation between the roundness and the fluidity of fly ash cement paste. It was also reported that the

improvement of fluidity from mixing with fly ash typically came from the ball bearing effect of fly ash that have spherical particles.

Mosa *et al*., (2008) investigated the effect of chemical additives on rheological characteristics of coal water slurry. The power-law model was applied to determine the non-Newtonian properties of coal slurries. Three types of dispersants, namely sulphonic acid, sodium tri-polyphosphate, and sodium carbonate were studied and tested at different concentrations ranging from 0.5 to 1.5% by weight from total solids, out of which sulphonic acid was recorded the best performance in modification and reducing slurry viscosity. Sodium salt of carboxymethyl cellulose and xanthan gum were tested as stabilizers at concentrations in the range of 0.05 to 0.25 % by weight from total solids. It was found that apparent viscosity and flow properties of coal water slurries are sensitive to the use of chemical additives. The best dosage of all tested dispersants was found to be as 0.75% by wt of solids and the best dosage of stabilizers was found to be 0.1% by weight of total solids.

Karmakar *et al*., (2011) studied the effectiveness of flocculants as anioninc, non-ionic, and cationic and observed that settling rate was fastest with anionic polymers (39.8 cm/min), and slowest with cationic polymers (3.8 cm/min). It was also observed that for cationic polymers the residual turbidity was very less (46 NTU) as compared to anionic (262 NTU) and non-ionic (716 NTU). The size of flocs was very small in case of cationic, moderate in case of non-ionic and much larger in case of anionic. The interface appeared very late in case of cationic but it appeared instantly in case of anionic polymers.

Seshadri *et al*., (2008) used sodium hexametaphosphate at 0.1% concentration (by weight) as an additive to study the rheological behaviour of fly ash slurries and observed that Bingham plastic model represented the variation of shear stress with shear rate reasonably well. For sample number 1 at 60% solid concentration the slurry yield stress was 0.3541 Pa which is reduced to 0.0194 Pa by addition of the additive. Similarly the slurry viscosity was 13.1 Pa without any additive and it is reduced to 8.6 Pa by addition of the additive. This trend was observed for all the five samples tested.

Mishra *et al*., (2002) investigated the rheological behavior of some Indian coal-water slurries using a HAAKE RV30 viscometer. It was found that coal-water slurry exhibited

pseudoplastic flow behavior. The apparent viscosity varied with the amount of coal in the slurry, pH, and temperature, which was the highest around pH 6 and the lowest near pH 8. Coal – water slurries showed non-Newtonian behavior at low pH. The change in apparent viscosity with the temperature of coal-water slurry could be described by a simple Arrhenius-type equation. The values of apparent activation energy were found to be relatively independent of the rate of shear and solid concentration.

Huynh *et al*., (2000) found that the magnitude of the yield stress reduced when either hydrochloric, nitric or sulfuric acid was used to decrease the pH of chalcopyrite slurry. With hydrochloric and nitric acids, the viscosity of the slurry also reduced with decreasing pH- a behavior which was attributed to changes in the surface chemistry of the particles with pH. Addition of phosphates to the slurry also reduced the yield stress as well as the viscosity as absorbed phosphate produced an enhanced repulsive force between particles due to the presence of long-range electrostatic and short-range steric interactions. The use of either acids or phosphates permitted the solid content of the slurry to be increased by over 10 wt. % for the same pumping energy input. It was also observed that the yield stress of the chalcopyrite slurry decreased from a value of 75 Pa to 10 Pa as the pH of the slurry was decreased from 11 to 3.5. The magnitude of the yield stress decreased as the pH is reduced for all the acids used. Viscosity is decreased when pH of the slurry is increased with addition of H_2SO_4 but the trend was reversed in the case of HCl and HNO_3 as pH modifiers. It will support the addition of lime for our case. The influence of phosphates on slurry rheology revealed that the yield stress decreased from a value of 70 Pa to 25 Pa as the concentration of polyphosphate increased from 0 to 9mg/kg for slurry concentration of 69 wt%. The pumping energy requirement for the chalcopyrite slurry reduced from a value of 175000 kWh to 45000 kWh when the pH was reduced from a value of 11.5 to 7.5. Similarly the pumping energy requirement was found to increase as the solid concentration of the slurry was increased from 50 wt% to 70 wt% for various doses phosphate addition.

2.5. Drag reduction technology

Drag reduction is a phenomenon in which the friction of a fluid flowing in a pipeline in turbulent flow is decreased by using a small amount of an additive. Drag reduction occurs

when a small amount of an additive such as a surfactant or polymer causes a reduction in the turbulent friction. This reduction in friction causes the pressure drop in the pipe flow to be less than that of the pure fluid leading to decrease in the pumping energy requirements of such systems. Several types of additives have been studied which cause this drag reduction phenomenon to occur. These include:

    i.   Surfactants

    ii.   Polymers

    iii. Aluminium disoaps and

    iv. Fibres

Surfactants are very useful due to its ability to self- repair upon mechanical degradation due to high shear. Degradation occurs when a molecule undergoes a region of high shear in hydraulic pipeline transport systems because these systems use multiple pumps. Surfactants are efficient drag reducers. Surfactants are able to repair themselves in a matter of few seconds upon degradation from shear. This characteristic makes surfactants a good additive for pipeline transport system. Now-a-days biodegradable surfactants are available as drag reducing additives. These surfactants are less susceptible to mechanical degradation. The influence of these surfactants on turbulent flow characteristics is appreciable with only few parts per million of surfactant solution, added to the solvent (Ohlendorf *et al.*, 1986). The effect of surfactants to reduce drag has been studied and reported in many literatures (e.g. Lumley, 1969; Virk, 1971; Sellin *et al.,* 1982; Hoyt, 1986; Morgan & McCormick, 1994; Tiederman, 1985; Matthys, 1991; Gyr and Bewersdorf, 1995).

The main purpose of drag reduction is to delay the onset of turbulent flows. In other words, a drag reducer will shift the transition from a laminar flow to a turbulent flow to higher flow velocity. Guar gum, a natural polymer (polysaccharide) also showed effective influence on drag reduction. Hoyt (1990) used 10 ppm polymer concentration in the pipeline transportation system which not only reduced the drag, but also reduced the heat transfer that maintained low oil viscosity. Similar observations were also reported by Beaty *et al.,* (1984). Also, in sewerage pipes and storm-water drains polymers have been used to increase the flow rates so that the peak loads do not result in over flowing; if only relatively infrequent use is required, this can be much cheaper than constructing new pipelines (Sellin, 1982).

2.5.1. Drag reduction by using surfactants

Surfactants are molecules which contain a hydrophobic tail and a hydrophilic head groups. Surfactants can be further classified by their hydrophilic group. The different types of surfactants are anionic, nonionic, zwitterionic, and cationic. Surfactants behave in a characteristic manner in aqueous solution. In these solutions the hydrophobic groups avoid contact with water by forming micelles. In micelles the hydrophilic parts, which are polar, contacts the water allowing the non-polar, hydrophobic, parts to concentrate in the centre of the micelle. The micelles form different structures in aqueous solutions including spherical, rod-like, lamellar, and vesicles. The types of surfactant as well as the structure of the micelle both contribute to the drag reducing properties of the molecule.The principal uses of surfactants and related compounds are the dispersion of fly ash particles in water for smooth flow in hydraulic pipelines. Hydrophilic fly ash particles can be rendered more hydrophobic, which is a necessary requirement for the floatability of fly ash particles, by addition of surfactants. The use of aqueous surfactant solutions to improve wetting properties of fly ash particles has important practical consequences for its transportation in pipelines. Cationic surfactants and others are used in this application.

Chandel *el al*., (2011) investigated the effect of drag reducing additives on the characteristics of two different types of pumps with fly ash slurries and found that the head and efficiency of the centrifugal slurry pump decreased with increase in solid concentration and slurry viscosity whereas pump input power increased with increased solid concentration. The addition of drag reducing additive improved the performance of the centrifugal slurry pump in terms of head and efficiency.

Roh *et al.*, (1995) observed that surfactants improved the slurriability of coal with shear thinning behavior. The addition of surfactants also enhanced the resistance of coal-water slurry to sedimentation. It was also found that the slurriability at a constant apparent viscosity of 2000 mPa.s could be increased by ~11 wt% when an anionic surfactant (CWM 1002) was added together with a small amount of electrolyte (NaOH). The amounts of CWM 1002 and electrolyte (NaOH) as the dispersing materials were 0.4 and 0.1% wt% on the dry coal basis respectively.

Granville *et al.,* (1977) observed that molecular structure of surfactant had profound effect on the wetting rates of fly ash particles. Wetting rates increased in roughly linear fashion in the temperature range from 20^0C to 40^0C.

Dodge and Metzner (1959), and Shaver and Merrill (1959) noticed unusually low friction factors for certain non-Newtonian solutions like those of sodium carboxy methylcellulose in water. Drag reduction has also been reported for several suspensions of insoluble particles such as fine grains or fibres and for micro bubbles. Ohlendorf *et al.* 1986; Rose and Foster, 1989; and Chou, 1991 investigated a number of alkyltrimethyl ammonium cationic surfactants with excess sodium salicylate drag reducers with alkyl groups ranging from C_{12} to C_{22} (even – numbered carbon atoms).

Shikata *et al.,* (1988, 1997) indicated that counterions played a role as break down and reformation of the entanglement points. They also pointed out that, there were three kinds of motions in a rod-like surfactant solution. The first and second motions are the entanglement release motion and the motion of bending parts of rod-like micelles, respectively. These kinds of motions strongly affect the rheological properties of the surfactant solution. The last one is the rotational and translational motion of surfactants and counterions in rod like micelle. This kind of motion does not strongly affect the rheological properties of the rod like surfactant solution.

Barret *et al.,* (1993) showed a steep increase of viscosity of cetylpyridinium salt (CPy)-sodium salicylate mixture when the concentration increased, at a constant brine concentration. Surfactants: tris (2-hydroxyethyl) – tallow ammonium acetate (TTAA, Ethoquad T/13-50) (10 m mol/lit) with NaSal (10 m mol /litre) as counterion was investigated by Bottenhagen *et al.* (1997) in a couette cell under shear.

Stress-induced precipitation and microstructure change were studied by Lu *et al.,* (1998). They examined a solution of Arquad 16-50 (commercial cetyl trimethyl ammonium chloride, CTAC) (5m mol/l) with 3-chlorobenzoate (12.5 m mol /l) counterion under shear and extensional flow at 20^0C, shear rates of $1000s^{-1}$ and $1500s^{-1}$, and observed an abrupt decrease in shear viscosity after about 200s of shear.

Alkyltrimethyl ammonium surfactants were found to be effective drag reducers when combined with different counterions in the dilute concentration range (Zakin *et al.,* 1998). The experimental results conducted by various researchers showed that the drag reduction occurs only in turbulent flow when a certain wall shear stress is exceeded (Fontaine *et al*., 1999; Zakin *et al*., 1983).

Zwitterionic surfactants named SPE 98330 was added into the district heating system with the aim to decrease the flow resistance in the tubes and thus to decrease the energy consumption (Myska and Mik, 2003). Myska and Chara (2001) obtained the effectiveness in drag reduction as high as over 90% with this agent.

Roi Gurka *et al.,* (2004) used Agnique PG 264-U surfactant at 20ppm, biodegradable type, and found that the flow exhibited less floctuations. Munekata *et al.,* (2006) studied the surfactant solution with drag reduction in a swirling flow of vortex motion. The surfactant solution used 500 ppm of Cetyl-trimethyl Ammonium Bromide (CTAB) with water containing Sodium Salicylate (NaSal) at the same molar concentration as CTAB. They found that the maximum drag reduction reached up to 80% when the inclination angle of the vane was 45^0.

Feng-Chen *et al.,* (2008) tested cationic surfactant, Cetyltrimethyl Ammonium Chloride (CTAC) in a closed circuit water flow. Local tap water was used as the solvent. Sodium Salicylate (NaSal) was added to the solution with the same weight concentration as that of CTAC for providing counterions. 25 ppm and 75 ppm CTAC solutions at 30^0 C were used as the drag-reducing fluid. The rheology measurement indicated that only 75 ppm CTAC solution showed distinct rheological properties whereas the measured properties of 25 ppm CTAC solution were almost the same as those of water at the same temperature.

Piotrowski (2008) studied the polymer surfactant complex formation and its effect on drag reduction. For a mixture the following substrates were used: poly (ethylene oxide) (PEO) and cetyl trimethyl ammonium bromide (CTAB) with sodium salicylate (NaSal). The drag reduction behaviours of PEO, CTAB with salt and their mixtures in dilute aqueous solution were compared.

Flow regimes depend on many factors: such as the individual magnitudes of the liquid and gas flow rate; the physical properties such as density, viscosity, and surface tension. Very large pressure drops occur with the high viscosity fluids (Duangprasert *et al.*, 2008). Surfactants used by them was SDS ($C_{12} H_{25} NaO_4S$) solutions at 0.5,1, and 2 CMC (Critical micelle concentration), 1 CMC = 2.75 g/ liter (1 CMC $\approx$2750 ppm).

A type of cationic surfactant CTAC ($C_{16} H_{33} N (CH_3)_3 Cl$) cetyltrimethyl ammonium chloride mixed with same weight percent of counterion material NaSal ($HOC_6H_4 COONa$) was used (Kawaguchi and Feng, 2007) as a drag – reducing additive to water at a mass concentration of 40 ppm. The CTAC was dissolved in tap water. Cationic surfactants were less affected by calcium or sodium ions naturally found in tap water. This is the reason why cationic surfactants combined with a counterion such as sodium salicylate (NaSal) are frequently used in the basic studies or applications to district heating and cooling systems. At concentrations of 30 ppm and 100ppm, the shear viscosity of the solution at a shear rate of $200s^{-1}$ in 25^0C was 0.82 and 0.97 m Pa s respectively, showed no stress thinning in the range of $10s^{-1}$ to $300 s^{-1}$. For the surfactant drag-reducing additives, the rod-like micelle structures are thought to be the key to give complicated rheological fluid properties including viscoelasticity. NaSal acts to reduce ion radius of CTAC to deform micellar shape from globular to rod-like. In their experiment, same weight concentration of NaSal was always included in the CTAC solution.

Candau *et al.,* (1994) showed a constant viscosity of a solution of dodecyl methyl ammonium bromide but when NaCl was added, viscosity decreased. Ethoquad T/13-50 and Arquad 16-50, products of Akzo Chemie, in mixtures with sodium salicylate were tested in hydronic systems of buildings. Metaupon was used in 300 mm pipes of a cooling system in mines.

Cationic surfactants mostly create an effective drag reduction when used in combination with organic salts such as sodium salicylate. Sodium salicylate ions are known to bind strongly to the micelle surface and facilitate the formation of large semi-flexible wormlike aggregates, at very low concentration (around 1 mM), which form an entangled network. These solutions are characterized by a striking onset of viscoelasticity. In recent years, drag reducing aqueous surfactants has drawn much attention as a class of additives which are self-repairable after degradation. That feature makes them suitable for potential

applications in recirculation systems. Usually, as a drag reducer, poly (ethylene oxide) PEO is used. However, drag reducing polymers are sensitive to mechanical and thermal degradation.

Water-soluble polymers like PEO form complexes with cationic and anionic surfactants, in which polymer film was formed around micelle. The addition of salt facilitateed a formation of surfactant – polymer aggregates. The critical aggregation concentration (CAC), the concentration at which the surfactant started to bind to the polymer was lowered; the size of the surfactant micelles increased and the number of micellar aggregates attached to a polymer chain also increased with the ionic strength.

Certain surfactants, such as CTAB and CTAC, with addition of appropriate counterions such as sodium salicylate, form network microstructures at very low concentrations (a few hundred ppm to 4000 ppm) are very effective in reducing friction factors in turbulent flow. Cationic drag reducing surfactant solution have been the most extensively studied because of their broad drag reduction temperatures (unlike nonionic surfactants, which have narrow temperature ranges) and insensitive to the presence of calcium or magnesium ions in water, which cause the precipitation of some anionic surfactants. They are also much less expensive than zwitterionic surfactants. Many drag reducing cationic surfactants are quaternary ammonium salts with one long alkyl chain with typical chemical structures of the form $C_nH_{2n+1}N^+(CH_3)_3Cl$ (n=12-18) (Hu and Matthys, 1997).

Some aqueous solutions of cationic surfactants cause very effective drag reduction phenomena in turbulent flow even at very dilute concentration. These aqueous solutions can reduce 80% of the drag in a turbulent straight pipe flow in a wide range of temperature. Drag-reducing cationic surfactant molecules form rod-like micelles in an aqueous solution under the presence of a counterion. These rod-like micelles entangle together to make a certain network structure. Rod-like micelles are formed with not so strong intermolecular interaction, so two rod-like micelles can cross and pass through each other at the entangle point.

Polymers were initially used as drag reducing additives for turbulent water flow to reduce the frictional drag by up to 80%. However, polymer solutions are strongly affected by mechanical degradation, which may result in shorter life time of drag reduction effectiveness. Surfactants are emerging as approaches to reduce the frictional drag by 70% to 80% but to be

less affected by mechanical degradation. Therefore, surfactants are now being considered as practical drag reducing additives.

Hu and Matthys (1997) reported a shear thickening behavior of the system tetradecyl dimethyl aminoxide with sodium dodecylsulfate plus added NaCl with a peak of the viscosity curve around $60s^{-1}$ for a fixed concentration ratio of all three components.

Cates (1993) suggested that salt concentration and specific counterion effects are important in determining the dependence of average micellar size on concentration, and that the size of micelles influences the viscosity curve. They found that NaBr is able to promote a large increase of the size of micelles while NaCl has no noticeable effect.

2.5.2. Polymeric drag reduction research

In a number of practical situations of fluid flow, turbulence occurs near solid surfaces that results in high magnitude of energy losses due to turbulent friction. There are basically two types of additives which can alter the turbulent flow and cause a reduction in the pressure loss, namely macromolecules like polymers or surfactants, and simple solids like sand grains or fibres. The non-ionic surfactant Lubrol 17A10 in the presence of the electrolyte K_2SO_4 has been found to be an effective drag reducer at temperatures near its cloud point (ICI). Among the drag-reducers, poly oxyethylene alcohol non-ionic surfactants alone seem to be mechanically stable.

Polymer solutions are the most widely studied and most often employed for the drag reducing systems. Several typical polymer drag reducing solutions listed (Table 2.1).

Table 2.1: Drag reducing polymer solutions

Water – Soluble polymers	Solvent – soluble polymers
Poly (ethylene oxide)	Polyisobutylene
Polyacrylamide	Polystyrene
Guar gum	Poly (methyl methacrylate)
Xanthan gum	Polydimethylsiloxane
Carboxymethly cellulose	Poly (cis-isoprene)
Hydroxyethyl Cellulose	

The higher the molecular weight (MW) the more effective a given polymer as a drag reducer (Shenoy, 1976). Polymers with a MW below 1, 00,000 seem to be ineffective (Hoyt and Fabula 1963). As the average MW of poly (ethylene oxide) (PEO) is increased from $2x10^5$ to above $5x10^6$, the solution concentration to achieve about 70% drag reduction on a rotating disk is reduced from 600 to 100 ppm. The higher the MW the greater is the drag reduction for a given concentration and R_e number. The longer polymer chain provides more chance for entanglement and interaction with the flow. The extension of the polymer chain is critical for drag reduction. The most effective drag reducing polymers are essentially in linear structure, with maximum extensivity for a given molecular weight. Poly (ethylene oxide), Polyisobutylene and Polyacrylamide are typical examples of linear polymers. Polymers lacking linear structure, such as Gum Arabic and the Dextrans, are ineffective for drag reduction.

Phukan *et al.,* (2000) studied two types of polymers at various concentrations. The concentrations of 100, 250, 300 and 450 ppm of commercial guargum and 50, 100, and 150 ppm of purified guargum were used for homogeneous injection. The maximum power reduction of 28% was obtained in case of 300 ppm commercial guargum and approximately the same percentage was obtained in case of 100 ppm purified guargum. The maximum drag reduction was 35.5% at 300 ppm of commercial guargum and 38% at 100 ppm of purified guargum. The study revealed great potential of using drag reducing polymers for irrigation water management. There was reduction in power consumption, increase in radius of coverage and net drag reduction when polymer was added with the water used in sprinkler irrigation system.

A drag reduction occurs at very low concentrations in the ppm region. Increasing the concentration beyond 30-40 ppm lowers drag reduction for PEO in a small tube owing to increase of the viscosity with increasing concentration. Drag reduction was observed in concentration as low as 0.02 ppm (Oliver and Bakhtiyarov, 1983). Using a rotating disk apparatus (Choi and John, 1993) or a rotating cylinder (Bilgen and Boulos, 1972), drag reduction induced by water-soluble polymers (PEO and Guar gum) and solvent–soluble polymers (Polyisobutylene) showed similar results to the experiments performed with a small tube.

McCormick *et al.,* (1986) concluded that water soluble polymers as hydrophobically modified Polyacrylamide polymers, anionic, and cationic polyelectrolytes and polyampholytes were effective drag reducers. All copolymers were found to confirm a universal curve for drag reduction, when normalized for hydrodynamic volume fraction polymer in solution.

Biopolymers such as high molecular weight polysaccharides produced by living organisms can provide effective drag reduction (Shenoy, 1984). Polysaccharides of several fresh water and marine algae, fish slimes, sea water slime and other fresh water biological growths have been found to be good drag reducers also. Kim and Sirviente (2007) found out that Salt (Sodium chloride) enhanced the drag reduction efficiency of poly acrylic acid diluted solution because the salt molecules prevented the aggregation of PAA chains.

2.6. Surfactants

The term surfactant came from the contraction of "surface active agent". This contraction describes surfactants because a predominant characteristic of surfactants is their ability to lower the surface tension of liquids. Surfactants are amphiphilic compounds i.e. hydrophilic head group and a hydrophobic tail group. The hydrophilic head group is a polar group which usually ionizable and capable of forming hydrogen bonds. The hydrophobic tail group is a non-polar group which is typically a long chain alkyl group (Zakin *et al.,* 1998). Due to this unique structure, surfactants show characteristic behaviours when in an aqueous solution. The hydrophobic group repels water in solution while the hydrophilic group is attracted to the polar water molecules. This causes the hydrophobic groups to cluster together in hydrocarbon phase in order to avoid contact with the water while the hydrophilic polar groups surround them and are in contact with the water. The aggregates formed are called micelles.

2.6.1. Classification of surfactants

There are several types of surfactants which include anionic, cationic, zwitterionic, and nonionic surfactants. Anionic soap surfactants are water soluble and have a negative charge when in aqueous solutions. They exhibit good drag reduction results when the shear stress is not too high, i.e. lower flow rates. They are, however, very sensitive to hard water

metal ions such as Ca^{2+} and Mg^{2+} which make them insoluble in water. Anionic surfactants also form foam. This results in complications in many systems that do not have the ability to handle foam formation. Hence they have not been considered good surfactants to be drag reducing agents. Cationic surfacetants have a positive charge when immersed in aqueous solutions. These surfactants are not affected by the metal ions in tap water as the anionic surfactants. Cationic surfactants produce good drag reduction results over a wide temperature range, and are relatively stable and offer self-repairability.

Zwitterionic surfactants have both negative and positive charges on the head group of the molecule. Since these surfactants contain both types of charges, it may cause the surfactant molecule to be sensitive to the ions present in water or solutions which may decrease in the stability of these types of surfactants. One beneficial characteristic of zwitterionic surfactants is that they are readily biodegradable and less toxic than some other surfactants. This makes that environment friendly.

Nonionic surfactants have no charge on their head groups. These types of surfactants are stable and are able to self-repair quickly after degradation from high shear. Similar to zwitterionic surfactants, nonionic surfactants are also less toxic than most and are rapidly biodegradable. However, they are generally only effective as drag reducing agents over a relatively narrow temperature range near their upper consolute or cloud point temperature.

2.6.2. Micelles

Surfactants have the ability to group themselves in consistent patterns due to the hydrophobic and hydrophilic components of the molecules. The hydrophobic ends of the surfactants group themselves together when in aqueous solutions because these ends are non-polar and repel the polar water molecules. Conversely, the hydrophilic or polar ends of surfactants are attracted to the water molecules. This causes the surfactants to form clusters called micelles. Micelles form into several different shapes including spherical, rod-like, lamellar, and vesicles. Typically, at low concentrations micelles are spherical. When the concentration of the surfactant is increased or the temperature of the solution is decreased the micelles may form into rod-like micelles. Drag reducing surfactant systems are typically composed of long rod-like micelles. Surfactants are essentially "Schizophrenic" molecules

that have a distinct hydrophilic (water loving) head and a non-polar hydrophobic (water-avoiding) tail and can absorb at an interface to modify its properties (Figure 2.1).

| Tail | Figure 2.1: Structure of a surfactant | Head |
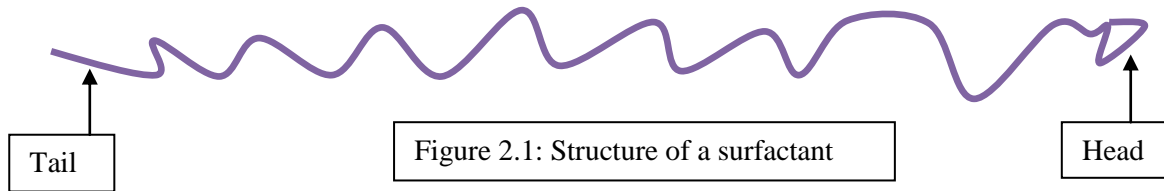
Surfactants are mostly complex mixtures of different variants generated during the manufacturing process, the commonest and simplest being the mix of oligomers that constitute a typical nonylphenol 9-mole ethoxylate. Interaction of various surfactants with solids and liquids can produce a wide range of effects such as wetting (lubrication), emulsifications, dispersions, anti-deposition, foaming, and anti-foaming. Surfactants reduce the surface tension of water by adsorbing at the solid-liquid interface. They also reduce the interfacial tension between solid and water by adsorbing at the solid-liquid interface. Some commonly encountered surfactants of each type are presented in Table 2.2.

Table 2.2: Some common types of surfactants

Types	Surfactants

Ionic	1) Anionic (based on sulphate, Sulfonate or Carboxylate anions)
	    a. Sodium dodecyl sulphate (SDS), ammonium lauryl sulphate, and other alkyl sulphate salts
	    b. Sodium laureth sulphate, also known as Sodium lauryl ether sulphate (SLES)
	    c. Alkyl benzene sulfonate
	    d. Soaps, or fatty acid salts
	2) Cationic (based on quaternary ammonium cations)
	    i) Cetyl trimethyl ammonium bromide (CTAB) a.k.a hexadecyl trimethyl ammonium bromide, and other alkyltrimethyl ammonium salts
	    ii) Cetylpyridinium chloride (CPC)
	    iii) Polyethoxylated tallow amine (POEA)

	iv) Benzalkonium chloride (BAC)
	v) Benzethonium chloride (BZT)
	3) Zwitterionic (Amphoteric)
	a. Dodecyl betaine
	b. Dodecyl dimethylamine oxide
	c. Cocamidopropyl betaine
	d. Coco ampho glycinate
Non-ionic	a) Alkyl Poly(ethylene oxide)
	b) Co-polymers of poly(ethylene oxide) and poly(propylene oxide)- commercially called Poloxamers or poloxamines
	c) Alkyl polyglucosides, including
	• Octyl glucoside
	• Decyl maltoside
	d) Fatty alcohols (such as Cetyl alcohol and Oleyl alcohol)
	e) Cocamide MEA, Cocamide DEA, Cocamide TEA

Surfactants which are used by different researchers are listed in Table 2.3. The advantage of incorporating a surfactant into the fly ash slurry is to reduce drag friction and improve upon flowing behaviour of the material. Different researchers have used different types of surfactants. Some of the commonly used surfactants are given in Table 2.4.

Table 2.3: List of commercially available surfactants which are already used by various researchers (Usui *et al.,* 2001, Lei *et al.,* 2002, and Seshadri *et al.,* 2005)

Sl.No.	Surfactants
1	Polystyrene sulphuric acid as dispersing additive
2	Sodium Hexametaphosphate of 0.1% concentration has been used as an additive
3	Rhamsan gums (S-194, S-130 obtained from Alcaligenes
4	Caboxymethyl Cellulose (CMC)
5	Xanthan gum (Vanzan)
6	Bio-polysaccharides
7	Naphthalene-sulfonate-formaldehyde condensate (NSF)
8	Pine oil

9	Glecerol (Natural oils & fats)
10	Any anionic detergent having good dispersing properties e.g. Sodium lauryl sulphate (SLS)
11	Polyelectrolites

Table 2.4: List of surfactants, counter ions and polymers used by different researchers

Name of the Surfactants	Researchers used for investigation
Cetyltrimethyl Ammonium Bromide (CTAB) It is a quaternary ammonium halide Chemical Formula: $C_{19}H_{42}BrN$ Type of surfactant: Cationic	Hu and Matthys, 1997, Munekata *et al*., (2006), Kaushal *et al*., (2005)
Cetyltrimethyl Ammonium Chloride (CTAC), Trade names: Arquad 16-50 & Ethoquad T/13-50, Arquad 18, Ethoquad O-12, $C_{16}H_{33}N(CH_3)_3Cl$ Habon G which is hexadecyl-dimethyl- hydroxyethyl ammonium, 3-hydroxy-2- naphtoate, Type of surfactant: Cationic	Qi and Zakin (2002), Kawaguchi *et al*., 1997, Rose *et al*., (1984), Myska and Stern, (1998), Lu *et al*., (1998)
Alkyltrimethylammonium Tris (2-hydroxyethyl)-tallow ammonium acetate, Type of surfactant: Cationic	Aguilar *et al.*, (2006), Boltenhagen *et al*., (1997)
SDS, Chemical formula: $C_{12}H_{25}NaO_4S$	Duangprasert *et al*., (2008)
SPE 98330, Type of surfactant: Zwitterionic SPE 9;8300 (It's basic components are Betaines) Oleyl Betaine Oleyl trimethylaminimide	Myska and Mik, (2003)
Dodecyl methyl ammonium Bromide	Candau *et al*., 1994
Lubrol 17A10- Condensate of Oleyl/ Cetyl Alcohol, Type of surfactant: Non-ionic Lubrol 12A9- Condensate of dodecyl alcohol Lubrol N13- Condensate of nonyl phenol with 13 mols of ethylene oxide	Shenoy, A.V. (1976)

Agnique PG 264-U (Alkyl Polyglycosides) also known as Agrimul PG 2062	Roi Gurka *et al*., (2004)
Sodium Oleate and Sodium Dodecyl Benzenesulfonate, Type of surfactant: An-ionic surfactant	Severson, K. (2005)
Aerosol OT	Fontaine, *et al*., (1999)
List of counter ions	
1. Sodium Salicylate (NaSal), HOC$_6$H$_4$COONa	Aguilar *et al*., (2006)
2. Sodium 2-hydroxy benzoate (Nasal)	Severson *et al*., (2005)
3. Sodium Bromide (NaBr)	Barret *et al*., (1993)
4. 3-Chlorobenzoate	Boltenhagen *et al*., (1997)
List of polymers	
1. Poly (ethylene oxide) (PEO) 2. Polyacrylamide 1822S and 1340S, MW=1.3X10^6 Da and 2.0X10^6 Da, Jayme Pinto *et al.*, (2006) 3. Guargum 4. Xanthan Gum 5. Carboxymethyl Cellulose 6. Hydroxyethyl Cellulose 7. Superfloc A110 (Hydrolysed Polyacrylamide), den Toonder *et al*., (1995)	

2.6.3. Drag reduction with surfactant solutions

When the concentration of a surfactant solution exceeds a critical value, the surfactant molecules start to form aggregates, i.e. micelles. The association of the molecules to micelles is reversible, i.e. when the concentration is below the critical value the micelles will dissociate into molecules again. The micelles are always in thermodynamic equilibrium with the molecules, and are of the size of about 20 to 1000 surfactant molecules. Depending on the molecular structure, concentration, type of solvent, three geometrical types of micelles can be distinguished: spheres, rods and discs. The drag reducing ability of a surfactant solution depends strongly on the shape of these micelles.

2.6.4. Anionic surfactants

Savins (1994) observed that the addition of an electrolyte (e.g. KCl) helped to increase the drag reduction. KCl helped in the enhancement of the association of the soap molecules and that the soap micelles, which were initially spherical in the aqueous solution, were rearranged under the influence of the electrolyte into cylindrical shapes, which in turn formed a network of interlaced rod-like elements. The soap concentrations involved were of the order of 0.1%, which are considerably higher than the polymer concentrations. The researcher also observed stress controlled drag reduction effect in the soap solutions. The drag reduction increased with increasing shear stress up to a critical value. Beyond the critical value, the drag reduction of the soap solution became indistinguishable from that of the soap-free solution. This indicates that the network of micelles collapses if the shear stress exceeds a critical shear stress. This occurs because of a temporary disentanglement of the network induced by turbulent vortices and eddies in fully developed flow. If the wall shear stress is reduced from above to below the critical value, then the network bond reform and the reducing ability of the solution is restored. In contrast, once the polymer chains are broken by high shear stress, the drag reducing ability of the polymer solution is permanently lost.

2.6.5. Cationic surfactants

Gadd (1966) suggested the possibility of using the CTAB-naphthol mixture to reduce turbulent friction, because the mixture showed shear-thinning characteristics. Similar to anionic surfactant solutions, the drag reducing ability of the CTAB-naphthol solution terminated at some upper Reynolds number corresponding to a critical shear stress where there was a scission of the micelles. One marked advantage of cationic surfactants over the anionic ones is that these complex soaps do not precipitate in the presence of calcium ions.

2.6.6. Non ionic surfactants

Zakin and Lui (1983) investigated the effect of temperature, electrolyte concentration, surfactant concentration and the effect of mechanical shear on three nonionic surfactants formed from linear alcohols and ethylene oxide moieties. They found that 1% solutions of the commercial surfactants like Alfonic 1214 were more effective than the 0.5% solutions. The critical shear stress for mechanical degradation in the case of nonionic surfactant was dependent on the surfactant concentration, electrolyte type and concentration, and on the

temperature. The molecular structure of the surfactant has an important effect on its micelle size and shape which in turn profoundly influence the drag reducing ability. Nonionic surfactants have an advantage over the anionic and cationic counter parts because they are both mechanically and chemically stable. They do not precipitate out in the presence of calcium ions and therefore can be used in impure waters, seawater or concentrated brine solutions.

2.7. Engineering uses of fly ash

There are numerous case histories available on the utilization of fly ash either alone or mixed with lime, gypsum or both. Typically fly ash has been used for soil stabilization (Chu *et al*., 1955), as embankment material (Rymond, 1961), Structural fill (Digioia and Nuzzo, 1972), for injection grouting (Joshi *et al.,* 1987), as a replacement to cement (Gopalan and Haque, 1986; Xu and Sarcar, 1994), in coastal land reclamation (Kim and Chun, 1994) and in roads and embankments (Kumar, 2003).

Many successful applications have involved mixing fly ash with additional lime and gypsum for strength gain purposes. Two types of reactions occur when lime, fly ash, and water are mixed. The first is the self-hardening of fly ash itself as it reacts with calcium ion in solution to form C-S-H gel. It is called pozzolanic reaction. The other reaction is due to presence of lime that produces various hydration products. Studies conducted by different researchers have concluded that the pozzolanic activity of the fly ash is influenced by its phase composition, chemical composition, fineness, morphology and loss on ignition. The reactions of fly ash with lime and/or gypsum are well documented and described in detail elsewhere (Sivapillaih *et al.,* 1995; Ramesh *et al.,* 1998; Ghosh and Subbarao, 2001; Sridharan *et al*., 1999).

Maser *et al.,* (1975) reported successful case studies on fly ash –cement mixture for subsidence control. Fauconnier and Kersten (1982) reported that the use of pulverized fly ash filling had effectively stabilized the coal pillars reducing the risk of pillar failure in areas of low safety factor.

Galvin and Waner (1982) opined that ash fill improved the model pillar strength significantly at 200 days. The strength increased by 50% and 40% for width to height ratio of

1.0 and 2.0 respectively. They also opined that the use of ash fill could improve extraction volume of 35%.

Yu and Counter (1988) reported the results of the use of class "C" type fly ash as a binder for consolidated backfill at a sulphide ore mine. The fly ash so used replaced about 60% of Portland cement with considerable cost savings. A mix proportion of 40% cement and 60% fly ash resulted in compressive strength of 2.4 MPa in 28 days.

Petulanans (1988) also reported the use of high volume fly ash for subsidence control. Palarski (1993) reported the use of fly ash, mill tailings, rock, and binding agents to make consolidated backfill material to improve extraction percentage in coal mines.

Ghosh (1996) achieved a tensile strength of 1.08 MPa and compressive strength of 1.32 MPa by adding lime of 10% and gypsum of 1% of fly ash to class F type fly ash.

Tannant and Kumar (2000) mixed fly ash, kiln dust, and mine spoil to obtain unconfined compressive strength of 1 MPa and moduli of 350 MPa in 28 days and found the composite suitable for haul road design.

Chugh *et al.,* (2001) successfully demonstrated that extraction ratio in a room- and-pillar mine can be increased by about 14% with paste backfill that included coal processing waste and coal combustion by products (fly ash). Sear (2001) identified the fill potential of fly ash with minimal adverse effect to environment.

Ziemkiewick and Bluck (2002) have reported that the use of grout consisting of 20% flue gas de-sulfurization (FGD) sludge, 20% class "F" type fly ash and 60% FBC ash. The final mixture showed an unconfined compressive strength of about 3.6 MPa in 28 days.

Kumar *et al.,* (2003) has reported the use of pond ash (a mixture of fly ash and bottom ash) of grain size between -75 to +20 meshes with equal percentage of water (by weight) for underground stowing of a coal mine. The pond ash water mixture with additives exhibited 100% settlement of solids within 30minutes of placement. The settlement time further reduced with an increase in additive concentration. The additives also improved the percolation rate of the mixture with little adverse effect on mine water. The barricades placed

to arrest the fill material showed negligible load due to the placement signifying self-standing behaviour of the mixture.

Narasimha *et al.,* (2003) in laboratory experiments have used gypsum to activate high calcium fly ash and obtained a compressive strength of about 6.9 MPa.

Mishra and Rao (2006) developed a fly ash composite material of uniaxial compressive strength of about 12 MPa over a curing period of 56 days with more than 85% fly ash mixed with lime and gypsum.

Another technique aimed at increasing or maintaining the stability of soil mass is chemical soil stabilization by adding some specific organic compounds such as surfactants. In a molecule of surfactant, one portion has great affinity for solvent, where as the remaining portion, with almost negligible affinity for the solvent, tends to concentrate on interface. This portion of surfactant rejected by solvent has a long hydrocarbon chain. The adsorption of this chain on the surfaces of soil particles helps in interlinking them. A relatively small quantity of these stabilizers may give optimum results in attaining better water proofing and strength properties.

Kaushal *et al.,* (2005) studied the different percentages of a cationic surfactant CTAB along with 0.2% non-woven geo-fibers and 1% lime by weight of dry fly ash with 0.095%, 0.190%, 0.285%, and 0.380% CTAB by dry weight of fly ash to treat and reinforce micro fine fly ash. The results showed that the CBR and shear strength values for fly ash mixed with 1% lime, 0.2% non-woven geo-fibers, and 0.19% of surfactant increased in comparison to that of untreated and un-reinforced fly ash by 3.36 and 2.04 times respectively.

Laboratory tests conducted by Raju *et al.,* (1996) have shown that at solid concentrations above 40% by weight, fly ash slurries more or less behave like pseudo homogenous suspensions. They opined that laminar flow can be obtained for concentration more than 50% when solid concentration approach static settled levels (maximum achievable concentration under gravity settling process). However, at these high concentrations, the fly ash slurries behave like non-Newtonian fluids with rheological equations showing either Bingham or yield pseudo-plastic behaviour.

The optimum transport concentration of slurry (Parida *et al.,* 2005) flow is determined with respect to the specific energy consumption (SEC) which is defined as the hydraulic energy in KWh, required to transport 1 ton of material through a distance of 1 km. Accordingly, SEC is given by the ratio P_h / W_s, Where P_h is the hydraulic power in Kw required to transport the slurry through 1 km at the minimum design velocity and W_s is the solids flow rate in tones / hr. Substituting the relevant terms for P_h and W_s, the equation for SEC in KWh / tone per km is given by:

$$SEC = 2.724 * 10^3 \, H / (\rho_m \, C_w) \qquad (2.1)$$

Where ρ_m=slurry density (kg/m^3), C_w=slurry concentration, and H is the hydraulic head.

It was observed by them that the SEC reaches the minimum value between concentrations 30-40 % by weight. From the point of commercial consideration, the higher limit of 40% by weight, where SEC value is reasonably low can be adopted as the optimum concentration for the mixture slurry. For a particular mass throughput there is an optimum pipeline diameter and density that will result in the lowest specific energy consumption. Alternatively, it is calculated from:

$$SEC \, (KWh/t/km) = g*i_m/3.6 \, S_s \, C_v \qquad (2.2)$$

Where, g = acceleration due to gravity (m/s^2), i_m = mixture head loss (m water/m), S_s = Solid's relative density, C_v = Solid's concentration by volume

The SEC is determined for a constant tonnage in a given pipe diameter as density or solid's concentration varies. For each pipeline diameter the minimum SEC occur at the transition, from laminar to turbulent flow. In this instance, it is not possible to operate at these velocities, as the solids will settle on the pipeline invert. The maximum density that can be achieved without significantly increasing the specific power consumption is approximately 1.75-1.80 t/m^3 in a 225mm pipeline. At higher densities, the flow becomes laminar and SEC increases dramatically.

While simplifying transport, the use of large amounts of water causes many problems. The fill must be dewatered after it is placed so that it will consolidate- a process which causes entrained fine material and cement to be flushed out along with the large volumes of excess water. This reduces the strength of the placed fill and deposits fines and cement in the lower

horizons, creating hazards for workers, and increasing the need for maintenance of workings and equipments. These factors limit the structural strength that can be obtained at low costs, since load-bearing capacity of the fill depends on cement content and void ratio (Landriault, *et al*., 2000 & 2001). The term course and fine are arbitrary and relative to the tailings grinds being compared. The percentage of material passing sizes of 0.074, 0.044, and 0.020mm (0.0029, 0.0017 and 0.00146 in.) is also used as a reference point, because materials of these sizes are missing from traditional classified sand-type tailings (Vickyery and Boltd, 1989). Materials of minus 0.074mm (200-mesh) are referred to as fines; materials of minus 0.044mm (325-mesh) are referred to as slimes.

There are also additional costs associated with pumping excess water to the surface, such as maintaining clogged bulkheads, ditches, and sumps; and repairing wear on pump components caused by the flushed cement. In recent years, low-water-content, high-concentration paste backfills have been developed to reduce the problems associated with high-water-content slurry backfills. This type of fill provides better support and a safer working environment than does slurry sand fill because the excess water is eliminated, which allows greater strength to be achieved and minimizes maintenance costs.

2.8. Colloidal stability

Most knowledge on the dense slurry flow in a pipe has been concerned with slurries consisting of either coarse particles with settling tendencies or very fine particles creating homogeneous, often non-Newtonian slurry. During the slurry flow, shear-induced translation and rotational motions of the particles cause hydrodynamic interactions, which result in particle-particle collisions and formation of temporary multiples. Such interactions lead to an increase in the rate of viscous energy dissipation and slurry bulk density. If the attractive forces acting in the slurry prevail, the process of coagulation and sedimentation is initiated. However, the simultaneous existence of the repulsive forces stabilizes the slurry and keeps individual particles separated. When the solid particles are mixed with water, attractive and repulsive forces between colloidal particles initiate the process of coagulation, and the particles tend to bunch into voluminous aggregates with a loose structure since coagulation decreases the total energy of the system. During the slurry flow a great deal of energy is consumed by the aggregates deformation. In the voluminous aggregates a great deal of water

is trapped, contributing to an increase in the yield stress and apparent viscosity of the slurry as well as decreasing the maximum slurry concentration.

Forces acting on particles: These arise from interaction between particles and result in the overall repulsion or attraction between particles.

Repulsive forces are:
- Electrostatic charges
- Entropic repulsion of polymeric or surfactant material on the surface of the particle.
- Net repulsive forces cause particles to remain separated.

Attractive forces are:
- London - Van der Walls attraction between particles
- Electrostatic attraction between unlike charges on different parts of a particle.
- Net attractive forces causes the particles to flocculate

Dispersion stability: There are generally two ways to modify the surface properties of a particle to maintain a stable dispersion. Those are Electrostatic forces and steric forces.

- Electro-statically: The existence of a net charge which causes particles to repel one another.
- Sterically: By absorption of polymer molecules on the particles and film of absorbed surfactant which prevents the particles from adhering to one another which may be sufficient to keep the dispersed particles in suspension.

2.8.1. Interparticle forces

When two colloidal particles approach each other, two types of interaction can occur: DLVO interactions and non-DLVO interactions (Verwey and Overbeek, 1947). The DLVO theory assumes that as two particles approach each other, repulsive and attractive forces act upon them. The total interaction energy between each pair of particles can be described by Equation 2.3.

$$V_{DLVO} = V_R + V_A \qquad (2.3)$$

Where V_{DLVO} is the total DLVO interaction potential, V_R is the total repulsive potential and V_A is the total attractive component.

The repulsive and attractive forces mainly involve the electrical forces, due to the overlap of the electrical double layers, and van der Waals forces, respectively. As two colloidal particles approach from a large separation to distances around 10 nm, the electrical repulsion rises to a maximum and the interaction energy is repulsive. While, at smaller separation distance the van der Waals attraction is dominant resulting in a deep minimum in the total interactions. At interparticle distances less than about 1 nm, repulsion exists due to the overlap of the electron clouds of the atoms; however, there are a number of other forces that come into play at such a short distance, such as solvent structural forces and electron overlap repulsion. Thus, a colloidal dispersion exhibiting DLVO interactions may be thermodynamically unstable due to the depth of the minimum, but kinetically stable due to the presence of the electrostatic barrier. Therefore, the ionic strength and pH of the medium, and consequently, the zeta potential of the particles are critical to particle stability if only DLVO interactions are considered. In colloidal suspensions that include either free or adsorbed or anchored polymer chains, an additional component to the interparticle interaction may be included, commonly referred to as non-DLVO interactions. Non-DLVO interactions can include hydrophobic, hydration, steric, and acid-base forces. Hydrophobic forces are long-range attractive forces having been shown to operate over distances of hundreds of nanometers, thus, they can dramatically affect interparticle forces. Hydration forces are the result of a gel-like layer formed around colloidal particles which is well known to be present on metal oxide surfaces (Hunter and Nicol, 1968).

2.9. Rheology, Fluid Behaviors, and Constitutive Models

It is appropriate to introduce the science of rheology at this point, since it does appear in various forms in a number of references visited in the literature review. Rheology is the discipline of fluid dynamics that studies the relationship between fluid deformation and stress. It is nothing but the science of deformation and flow of matter. It is also described as the study of flowing matter, such as liquids, slurries, emulsions, and melts. Rheology describes the deformation of such matter when it is subjected to external shear forces. Laboratory instruments called rheometers are available to experimentally investigate the deformation of such matter under measured rates of shears. Some fluids, such as water, exhibit Newtonian flow behavior, in which case the shear stress in the fluid is uniformly proportional to the applied rate of shear, Equation (2.4).

$$\tau = \eta \, \gamma \qquad\qquad (2.4)$$

Where τ is the shear stress, η is referred to as the Newtonian viscosity and γ is the applied shear rate. When the shear stress is plotted against the applied shear rate, the resultant graph is known as rheogram. In terms of fluid flow, materials may be classified as either Newtonian or Non-Newtonian fluids.

2.9.1. Newtonian Fluids

By definition Newtonian behavior is when the viscosity is independent of shear rate and does not depend on the shear history. Most simple liquids like water, acetone, or oils are Newtonian. Liquids showing any variation from this behavior are referred to as non-Newtonian. In pipeline transportation, concentrated suspensions showing non-Newtonian behavior are frequently encountered. Figure 2.2 illustrates the different types of rheological response by plots of shear stress vs. shear rate; these are also known as flow curves. In simple shear, the response of a Newtonian fluid is characterized by a linear relationship between the applied shear stress and the rate of shear. Newtonian fluids appear as straight lines that intersect the origin of a rheogram, the slope of which gives the viscosity of the fluid. Newtonian behavior is typically only observed in suspensions and slurries when the particles can be considered non-interacting or fully dispersed. Under these conditions particle collisions are assumed to occur in a relatively insignificant number of cases. Thus the movement of particles in the flow field results in only an increase in the viscous energy dissipation.

2.9.2. Non-Newtonian Fluids

Fluids for which the viscosity varies with shear rate are known as Non-Newtonian fluids. For non-Newtonian fluids the viscosity is often called the apparent viscosity to emphasize the distinction from Newtonian behavior. Non-Newtonian fluids will either exhibit a yield stress, non-linear viscosity characteristics, or both. The nature of the non-Newtonian behavior depends on the solids concentration, the particle shape, the particle size, the particle size distribution, and suspending liquid rheological properties. The suspension/slurry may develop a yield stress and/or become time dependent in nature as structures develop within the fluid at higher solids concentrations (Barnes, 1989).
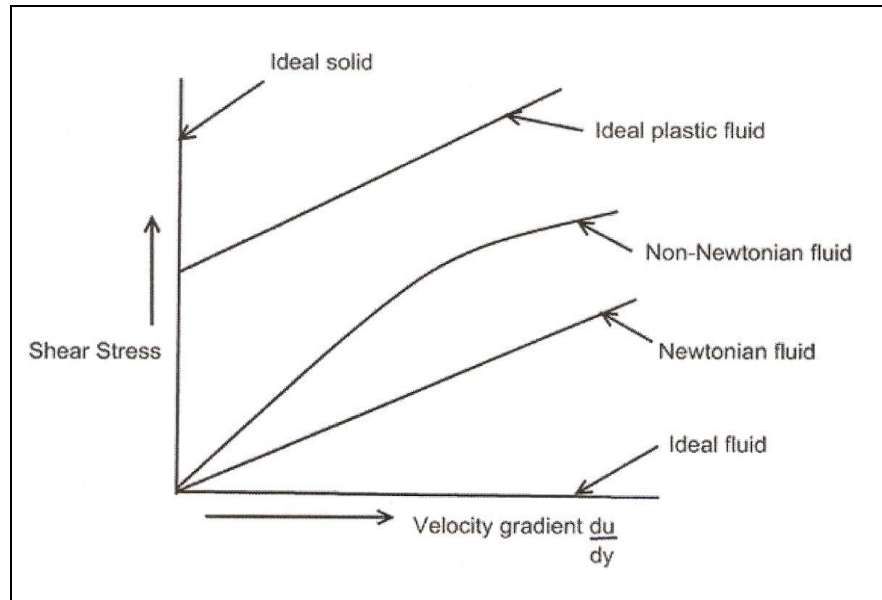
Figure 2.2: Different types of fluids

2.9.3. Time-Dependent Fluids

Two typical types of time-dependent fluid behaviors are possible i.e., thixotropy, where the fluid thins with shear and time and the opposite is the rheopexy, where the fluid thickens with shear and time.

2.9.3.1. Thixotropic Fluids

A fluid which exhibits a drop in viscosity with time under a constant shear strain rate is said to be thixotropic. The viscosity undergoes a gradual recovery when the shear stress is removed. A truly thixotropic fluid will exhibit a completely reversible behavior. If the flow curve of such a fluid is measured in a single experiment in which the value of shear rate is steadily increased at a constant rate from zero to some maximum value and then decreased at the same rate, a hysteresis loop is obtained. The larger the enclosed area in the loop, more severe is the time-dependent behavior of the material. The enclosed area would be zero for a purely viscous fluid, i.e. no hysteresis effect is expected for time-independent fluids. A pseudo thixotropic fluid does not completely return to its original state of yield stress.

2.9.3.2. Rheopectic Fluids

In this case an increase in apparent viscosity with time under constant shear rate or shear stress, followed by a gradual recovery when the stress or shear rate is removed. It is also called anti-thixotropy or negative thixotropy. Relatively few fluids which show the negative

thixotropy, i.e., their apparent viscosity increases with time of shearing. In this case, the hysteresis loop is obviously inverted. As opposed to thixotropic fluids, external shear fosters the buildup of structures in this case. It is not uncommon for the same fluid to display both thixotropy as well as rheopexy under appropriate combination of solid concentration and shear rate.

The present study however, is primarily focused on the measurement of the rheological properties of settling fly ash slurries where it is necessary to continuously shear the slurries to keep them water borne. Under these conditions it is assumed that the fluid will be fully sheared and that the rheological properties will be unlikely to change further with time. Thus time-dependent effects will not be investigated further and the discussion will focus only on time independent behavior.

2.9.4. Time-Independent Fluids
2.9.4.1. Pseudoplastic or Shear Thinning Fluids

Most common colloidal suspensions are shear thinning (also referred to as pseuodoplasticity) because the viscosity decreases as the shear rate increases (Figure 2.3). This is perhaps the most widely encountered type of time-independent non-Newtonian fluid behavior in engineering practices. Shear-thinning fluids are those for which the slope of the rheogram decreases with increasing shear rate (He *et al*., 2004). The shear thinning nature of industrial slurries is attributed to the alignment of particles and / or flocs in the flow field. An increase in the shear rate from rest results in instantaneous alignment of particles in the direction of shear, thus providing a lower resistance to flow. As such, the suspension will show a decreasing viscosity with increasing shear rate. Pseudoplastic fluids are typically suspensions of solids or dissolved long chain polymer strands. As the shear increases the structure of the fluid becomes more ordered, which steadily reduces the apparent viscosity.

2.9.4.2. Shear Thickening Fluids

Shear thickening behavior should not be confused with dilatancy, which is a change in volume on deformation, though dilatancy is often used to describe shear thickening behavior over certain ranges of shear rates. Such fluids exhibit an increase in viscosity with an increase in the shear strain rate (Figure 2.3). The degree of shear thickening and its onset is a function of the solids concentration, particle shape and size distribution. At rest the particles are

assumed to be situated in such a way that the void space between particles is at a minimum, but as the shear rate increases the particles become more disordered and there may be insufficient liquid to fill the space between the particles leading to direct particle-particle contact which causes an increase in the apparent viscosity of the fluid or shear thickening behavior. In the case of dilatancy the viscosity increases with shear rate. Although this behavior has received little attention in the test books on rheology, it has important consequences in pipeline transportation. For example, clay-based slips exhibit shear thickening behavior at high shear conditions ($>1000s^{-1}$), which is typical of mixing, pumping, spraying, bushing, and injection.
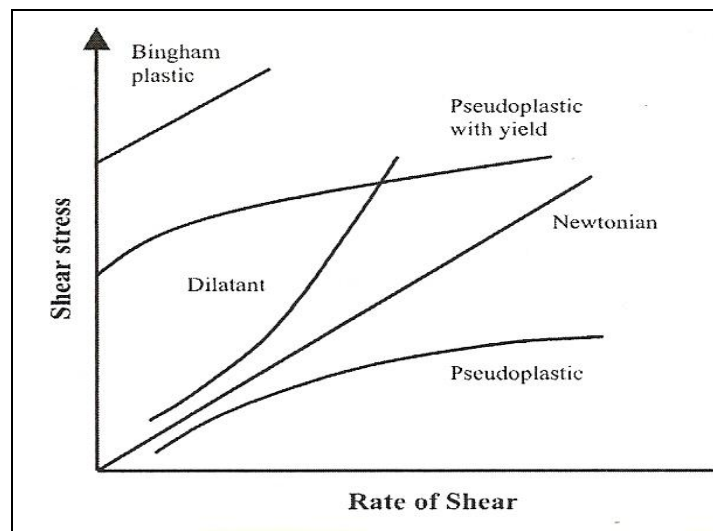
Figure 2.3: Rheograms of various continuum fluid models

2.9.4.3. Yield Shear Thickening

Yield shear thickening behavior is not common but over a certain range of shear rates, slurries and suspensions depending on the properties of the solid particles and the suspending liquid can exhibit shear thickening behavior (Figure 2.4). In the case of yield shear thickening behavior, Herschel-Bulkely model, Equation (2.11), outlined for yield-pseudoplastic fluids can be used to describe the fluids rheological behavior, except that pre-exponential parameter *n* must be greater than one.

2.9.4.4. Yield Stress

The yield stress of a fluid is commonly defined as the stress that is required to initiate flow of the material. It is an internal property that enables a fluid to resist deformation up to a

certain point, effectively enabling it to behave as a solid while it is subjected to stresses that are less than the yield stress. It is believed that the material responds similar to an elastic solid until the yield stress is reached, at which point the fluid starts to flow. The yield stress is usually explained as the fluid which contains an internal structure that is able to resist a certain amount of stress before flow commences. Yield stress has got its practical usefulness in engineering design and operation of processes where handling and transport of industrial suspensions are involved. The minimum pump pressure required to start a slurry pipeline and the entrapment of air in thick pastes are typical problems where the knowledge of the yield stress is essential. Some of the more simple types of flow curves associated with yield stress behavior in fluids are presented in Figure 2.4.
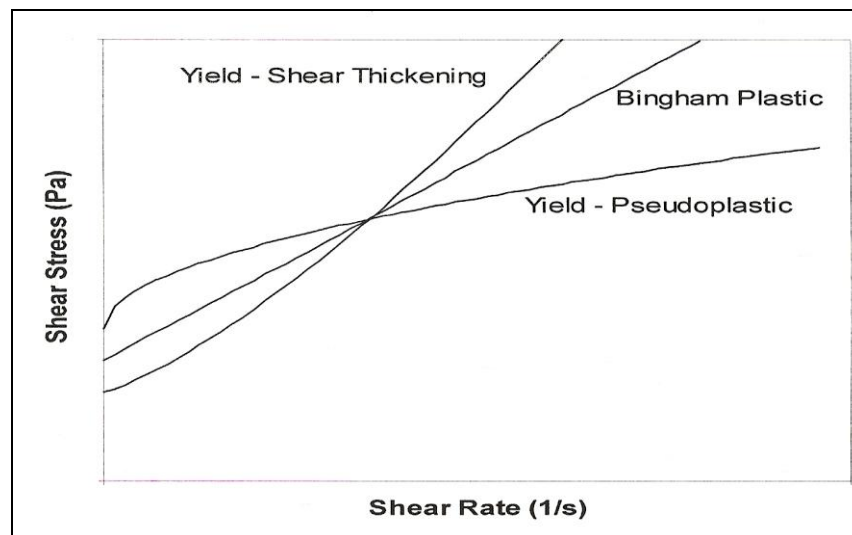
Figure 2.4: Flow curves for yield stress fluids

The two most common types of tests to determine the yield stress are direct measurement and extrapolation. Numerous techniques have been developed for the direct determination of the yield stress, but one of the more simple methods uses a generic rotational rheometer and vane geometry. If a direct measurement is not possible then rheological data must be obtained at shear rates as low as possible and then an extrapolation procedure must be used to obtain an estimated value for the yield stress. Indirect methods simply involve the extrapolation of shear stress-shear rate data to zero shear rate with or without the help of a rheological model. The value obtained by the extrapolation of a flow curve is known as "extrapolated" or "apparent" yield stress, whereas yield stress measured directly, usually under a near static condition, is termed "static" or "true" yield stress value. Direct measurements generally rely on some

independent assessment of yield stress as the critical shear stress at which the fluid yields or starts to flow. Indirect determination of the yield stress simply involves the extrapolation of experimental shear stress-shear rate data at zero shear rates.

2.10. Rheological Models

Numerous rheological models are available for the purpose of mathematically describing the rheological characteristics of a fluid (Table 2.5). Such models provide a means by which various aspects of a fluid's rheological behavior can be taken into account in the mathematical modeling of various fluid dynamics related processes, and many such examples can be found in the literature review.

Table 2.5.Different types of rheological fluid models

Newtonian	$\tau = \eta \, \dot{\gamma}$
Pseudoplastic	$\tau = K \, \dot{\gamma}^{n} \quad (n < 1)$
Dilatant	$\tau = K \, \dot{\gamma}^{n} \quad (n > 1)$
Bingham	$\tau = \tau_{y} + \eta \, \dot{\gamma}^{n}$
Casson	$\tau^{1/2} = \tau_{0}^{1/2} + \eta_{c}^{1/2} \, \dot{\gamma}^{1/2}$
Herschel-Bulkley	$\tau = \tau_{y} + K \, \dot{\gamma}^{n}$
Krieger-Dougherty equation	$\eta = \eta_{s} \, (1 - \Phi/\Phi_{m})^{-[\eta]\Phi m}$

Three commonly used rheological models are the Bingham plastic model, power law model, and Herschel-Bulkley models. Each of these three empirical rheological models along with Cross model and Casson model is presented below.

2.10.1. Bingham Plastic Model

Concentrated suspensions usually cannot flow until a minimum yield stress (τ_{y}) is exceeded. It corresponds to Bingham plastic flow which means the linear flow curve is

independent of the shear rate above τ_y. The simplest type of yield stress fluid model is the Bingham plastic model (Bingham, 1919), shown in Equation (2.5). This model is time-independent, two parameter rheological model.

$$\tau = \tau_y + \eta_p \, \dot{\gamma} \qquad (2.5)$$

Where τ is the shear stress (Pa), τ_y is the Bingham model yield parameter, η_p is the Bingham plastic viscosity (Pa.s) and $\dot{\gamma}$ is the shear rate applied to the fluid (1/s). This model suits a fluid with a yield stress and linear viscous behavior. For this model once the yield stress is exceeded it is assumed that the fluid behaves like a Newtonian fluid, where the shear stress increases proportionally with increases in shear rate. However, there are few suspensions and slurries for which the Bingham model can be used to describe the rheological behavior over a wide range of shear rates. But over a small range of low values of shear rate the Bingham model may be more applicable for a wider range of suspensions and slurries. This is illustrated by the flow curves in Figure 2.5 which depicts the various fluid models.
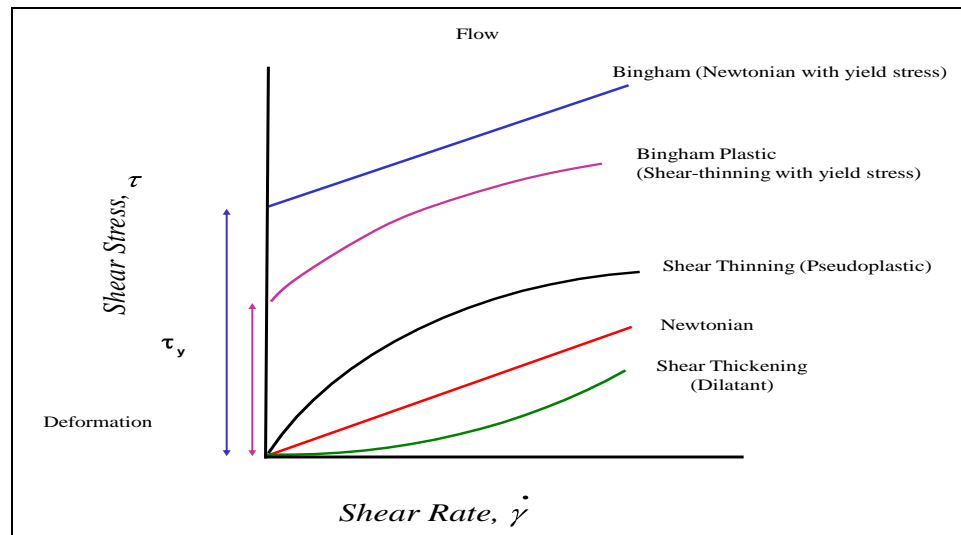
Figure 2.5.Plots of shear stress vs. shear rate (flow curves)

2.10.2. Cross Model

To predict the shape of the general flow curve it is necessary to differentiate well both the low and the high shear rate regions so that four parameter models are established. One such equation is given by the Cross model:

$$(\eta_o - \eta)/(\eta - \eta_\infty) = (K \, \dot{\gamma})^m \quad \text{or} \quad (\eta - \eta_\infty)/(\eta_o - \eta_\infty) = 1/(1 + K \, \dot{\gamma})^m \qquad (2.6)$$

Where η_o and η_∞ refers to asymptotic values of viscosity at very low and very high shear rates, K is a constant with dimensions of time and *m* is a dimensionless constant. It has essentially the same parameters, but can be broken down into sub-models to fit partial data.

2.10.3. Power Law Model

There are many rheological models available to study the flow behaviour of concentrated particulate slurries. Among them, the power law model is well accepted for various applications (Chhabra & Richardson, 1999; George *et al.,* 1984). Shear-thinning fluids without yield stress typically obey a power law model over a range of shear rates (Figure 2.5). The power law model also referred to as the Ostwald-de Waale model, Equation (2.7), may be used to model the rheological behavior of pseudoplastic fluids. The model is expressed as:

$$\tau = K\,\dot{\gamma}^n \tag{2.7}$$

Where, K is defined as the pre-exponential factor or consistency index or power law index (Pa.s^n) and *n* as the exponential factor or the flow-behavior index and also called power law exponent (dimensionless). The relative value of K refers to the viscous behavior of the fluid, while the value of *n* describes the deviation of the fluid behavior from Newtonian behavior. The power law describes three flow behaviours (Lester, 1994). For pseudoplastic fluids *n* must be less than unity. If *n* is equal to one then Equation (2.7) reduces to the Newtonian model and K becomes the Newtonian viscosity, η. A value of *n* greater than one is used to describe the behavior of a shear thickening fluid. The apparent viscosity (η_a) is estimated from the power-law model as:

$$\eta_a = \tau/\dot{\gamma} = K\,\dot{\gamma}^{n-1} \tag{2.8}$$

Which is also known as the power-law model, where η_a is known as the apparent viscosity (Pascal second), τ shear stress (Pascal), $\dot{\gamma}$ shear rate (s^{-1}), K consistency coefficient of fluid (Pa/s) (the higher the value of K the more viscous the fluid), and *n* is the flow behaviour index also called the power law index, which is a measure of the degree of departure from the Newtonian fluid flow. This model suits a fluid without yield stress that exhibits non-linear flow behavior. The power law model typically provides a good fit over a range of one to two orders of magnitude in shear rate.

The data generated from the present study were fitted to a linear equation using ordinary least squares regression to determine a slope (plastic viscosity) and an intercept (yield stress), according to Bingham model as below:

$$\tau = \tau_y + \eta_p \; \dot{\gamma} \tag{2.9}$$

Where τ is the measured shear stress at a shear rate of $\dot{\gamma}$, τ_y is the yield stress, and η_p is the plastic viscosity. The apparent viscosity, η_a, is typically reported as the ratio of the measured shear stress to the applied shear rate ($\tau/\dot{\gamma}$) at a specific shear rate (Hackley and Ferraris, 2001).

2.10.4. Casson Model

Generally most suspensions and slurries can be described as yield-pseudoplastic fluids; once the yield stress is exceeded the fluid can be expected to act similar to a non-yield stress shear thinning fluid. Two of the more simple models that exist for yield pseudoplastic fluids are the Casson and Herschel-Bulkely model. Initially developed to describe the properties of printing inks but latter shown to be suitable for some yield stress fluids, the Casson model is shown in Equation (2.10).

$$\sqrt{\tau} = \sqrt{\tau_y} + \sqrt{(\eta \; \dot{\gamma})} \tag{2.10}$$

This model is also time-independent two parameter rheological models can often be used to characterize non-settling fine particle slurries. These slurries are considered to be viscoplastic, which means that they behave like solids below a critical stress (the yield stress).

2.10.5. Herschel-Bulkley Model

Shear-thinning power law fluids with yield stress are sometimes called Herschel-Bulkley fluids. In most cases the flow curve above τ_y is shear dependent. Several models have been proposed to describe this behavior, one such model is called Herschel-Bulkley model. This model suits a fluid with a yield stress that exhibits non-linear viscous behavior. The Herschel-Bulkely model (Herschel and Bulkley, 1926) is a three parameter model that is quite similar to the power law model, with an additional yield stress term, τ_y, shown in Equation (2.11).

$$\tau = \tau_y + K \; \dot{\gamma}^{\,n} \tag{2.11}$$

Where τ is the shear stress (Pa), τ_y is the yield stress (Pa), K is the Herschel-Bulkley consistency index (Pa.s^n), $\dot{\gamma}$ is the shear rate applied to the fluid (1/s) and n is a power. This model is essentially the combination of the previous two. It carries an extra empirical parameter compared to each of the other two, but has the advantage of combining non-linear viscous behavior with a yield stress, which neither of the other two models can do. The Herschel-Bulkely model is more widely used than the Casson model because the extra term increases the range of fluid behavior that can be described by this model. In the case of either the Casson or Herschel-Bulkely model the fluids yield stress must either be obtained from an experimental measurement, such as vane method or by extrapolation from measured rheological data; shear stress and shear rate.

Typically fly ash slurry will exhibit both yield stress and varying viscosity at different shear rates, which firmly places it in the realms of a non-Newtonian fluid. Therefore, knowledge of rheological behavior is essential in numerous industrial operations that involve pipeline transportation of slurries or pastes, including (i) beneficiation (e.g., wet mixing and milling, atomization, and filtration), (ii) shape forming, and (iii) coating/deposition. Rheological properties are extremely useful in the structural characterization of particle-liquid systems, and the determination of how particle-particle interactions affect the stability of the slurry. A major objective in any slurry transportation system is to improve the homogeneity by reducing the number and size of defects. Accurate control of the slurry colloid chemistry leads to more uniform, denser, and favorable characteristics that result in engineered materials with the designed properties. The colloidal approach to slurry transportation allows control of the interaction forces between particles that determine the physical behavior at all stages of processing and transportation. The main goal of suspension transportation is to maintain stable particle dispersion since attractive forces (namely London-van der Waals forces) develop as particles approach each other. Colloid science offers different possibilities for maintaining a stable dispersion.

Repulsive forces between particles can be achieved by adding different kinds of deflocculants, which stabilize the suspension by electrostatic and/ or polymeric mechanisms. The flow properties of a suspension are influenced on the one hand by the quantity, shape, and size of particles, and on the other by the nature and strength of the inter-particle forces.

Particulate suspensions play key roles in hydraulic pipeline transportation systems. In general, suspended fly ash particles are smaller than approximately 100 microns in size. The most distinguishing feature of industrial suspensions is its polydispersity. The particle size distribution of industrial suspensions has a broad range, from several hundred micrometers to several nanometers, but, usually, the major part of the particles has a size range, approximately from 100-50 to 0.1-0.05 µm. Thus, the industrial suspensions are essentially the mixed colloidal-noncolloidal suspensions. Accordingly, rheology is a suitable tool to correlate the colloidal properties with the desired characteristics while the slurry is being transported.

2.11. Independent Characterization by Measuring Zeta Potential (ζ)

The indirect characterization of slurry rheology by measuring ζ is feasible because the relationship between ζ and apparent viscosity (η_a) is valid for a lot of solid/liquid systems (He *et al*., 2004). The state of dispersion in the slurry, namely, the rheological behaviour, is closely related to the ζ of the particles (Greenwood and Kendall, 1999), which represents the potential difference between the surface of the particles and the external plane of Helmholtz, illustrated by use of a model for the electric double layer as depicted in Figure 2.6. The ζ of a suspension is an indication of the magnitude of the repulsive force between the particles. The higher the ζ with the identical polarity is, the more predominant the electrostatic repulsion between the particles. On the contrary, when the ζ is close to the iso-electric point ($\zeta = 0$), the particles tend to flocculate, as illustrated in Figure 2.7 (He *et al*., 2004). The electric double layer develops when a particle is immersed in the continuous fluid (i.e. water). Once the immersion occurs, charged species will start to migrate across the solid/liquid interface until equilibrium is reached. Ions that directly increase the charge on the particle surface are called as potential determining ions which are unique to each type of the particle system. With many types of solid particle suspensions, especially oxides and sulfide mineral slurries, the potential determining ions are H^+ or OH^-. In this case, the change in the pH of a liquid can cause a change in the particle surface charge. Hence, for given mineral slurry, ζ is directly dependent on the pH value. The relationship between ζ and pH value in slurries can characterize rheological behaviours of slurries that confirms well to the results obtained using rheometers or viscometers.
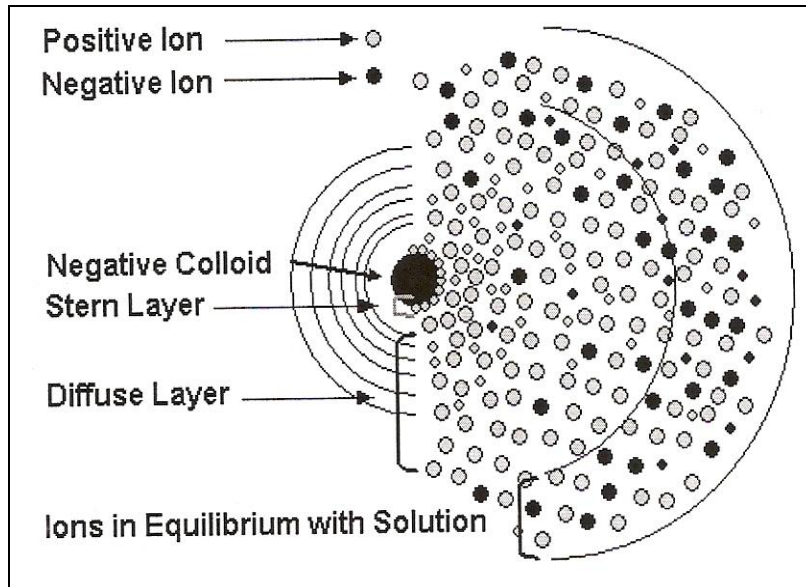
Figure 2.6: Schematic diagram of particle electric double layer
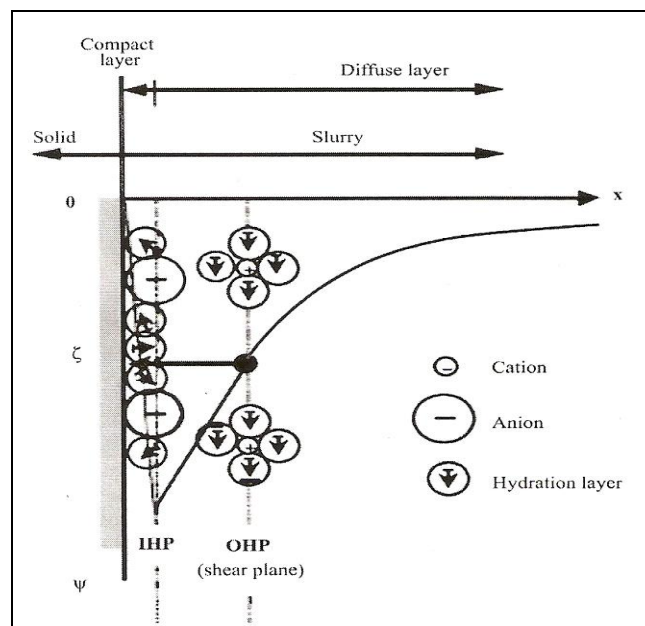
Figure 2.7: Mechanism of flocculation (He *et al*., 2004)

2.12. Viscosity and Viscosity-Temperature Models

When a stress (σ) is applied to a solid it deforms elastically according to Hooke's law:

$$\sigma = G \, \gamma \tag{2.12}$$

Where G is the elastic modulus (Young's modulus) and γ is the strain. When the strain falls to zero the sample recovers its original shape. This is commonly illustrated by a spring. If the

shear is large then the structure of the sample can break and hence it not only deforms but starts to flow. In the simplest case the response follows Newton's law:

$$\tau = \eta \, \dot{\gamma} \qquad (2.13)$$

Where τ is the shear stress, $\dot{\gamma}$ is the velocity gradient (also known as the shear rate) and η is a coefficient of viscosity (or simply the viscosity). Viscosity, also called internal friction, is one of the most important physical properties of a fluid system. Viscosity changes with shear rate, temperature, pressure, moisture, and solid concentration; all these changes can be modeled by using well known equations (Arrhenius and Frenkel). There are two kinds of viscosity: dynamic viscosity with a unit of Pa.s or P (poise) and kinematic viscosity expressed in m^2/s or S (stokes). The kinematic viscosity is a ratio of dynamic viscosity of a given liquid and its density at the same temperature. Plots of viscosity as a function of shear rate are known as viscosity curves.

2.12.1. Arrhenius Equation

The obtained viscosity values can be described by means of the most commonly applied Arrhenius equation. The effect of temperature is normally fitted with the Arrhenius-type relationship which is shown in Equation 2.14 (Choi *et al*., 2000). According to this equation, the viscosity values (η) obtained at a constant shear rate can be correlated with temperature:

$$\eta = A \exp^{E_a/TR} \qquad (2.14)$$

Where η is the dynamic viscosity (Pa.s), A is the pre-exponential factor (Pa.s) and a constant related to the molecular motion and the frequency of particle collisions in the collision theory, E_a is the exponential constant that is also known as flow activation energy for viscous flow at a constant shear rate (J/mol). It is referred by Arrhenius as representing the energy difference between the reactants and an activated species. The term E_a is therefore called the activation energy. The activation energy is the energy barrier that the reactants must surmount in order to react. Therefore, the activation energy is viewed as an energetic threshold for a fruitful reaction. R is the universal gas constant (J/mol/K) and T is the absolute temperature (Kelvin). According to this equation, viscosity decreases as temperature increases i.e. there is an inverse relationship between viscosity and temperature. The value of *A* can be approximated as the

infinite-temperature viscosity (η_∞), which is exact in the limit of infinite temperature. Hence, equation (2.14) can be rewritten in the following form:

$$\eta = \eta_\infty \exp^{Ea/RT} \tag{2.15}$$

Although equation (2.14) normally appears in the literature, equation (2.15) gives a more accurate representation of the fluid since the pre-exponential value is better defined here. It is widely accepted that natural logarithmic viscosity is directly proportional to the reciprocal value of the temperature. To increase the flexibility of this equation, constants *a* and *b* are introduced into equation (2.16) as shown below:

$$l_n (\eta) + a = b/T \tag{2.16}$$

By knowing that viscosity decreases with increasing temperature and has a curve concave upward when a viscosity vs. temperature graph is plotted, $\eta \approx \eta_{T\infty}$ when temperature is approximately infinity. Similarly, a decreasing temperature would increase the viscosity of a fluid body and thus, temperature at T_0 would give $\eta \approx \eta_{To}$ in which $\eta_{To} > \eta_{T\infty}$. Based on the above mentioned conditions, equation (2.16) can be rearranged into the following form:

$$\eta = \eta_{T\infty} (\eta_{To}/\eta_{T\infty})^{To/T} \tag{2.17}$$

The E_a can be obtained as the following after comparing equations (2.15) and (2.17):

$$E_a = T_0 R l_n (\eta_{To}/\eta_\infty) \tag{2.18}$$

R is the universal gas constant which is equal to 8.314 J/mol/K. η_{To} is the viscosity at temperature T_0 which, has been taken as the zero-temperature viscosity.

2.12.2. Frenkel Equation
The obtained viscosity values can also be described by means of the most commonly applied Frenkel Equation:

$$\eta = CT \exp^{D/T} \tag{2.19}$$

Where A, B, C, D are constants and T is the temperature.

2.13. Rheometry
The term "rheometry" is usually used to refer to a group of standard experimental techniques for investigating the rheological behavior of materials (fluid or solid). It is of great importance in determining the constitutive equation of a fluid or in assessing the relevance of

any proposed constitutive law. Rheometry aims at determining the fluid characteristics from measurements performed in simple and controlled flows. In these tests, the fluid is stressed in a simple manner, such that few components from its stress tensor differ from zero. Thus, from the components of shear stress and shear rate, one can obtain a characteristic equation. In practice, in order to measure a fluid's viscosity, the fluid should be confined between some devices, with determined conditions (one fixed and another with fixed speed). The fluid should be confined in a tube, between concentric cylinders. This device is defined as a rheometer. A rheometer is usually an engine, which can exert a torque / force on a material and accurately measures its response with time (or conversely, it can impose a strain and measure the resulting torque). The correct determination of the rheological properties of different fluids including suspensions and slurries is important to many research and industrial applications. To achieve this, the choice of the correct instrument for this application is essential, as many different methods and instruments exist for determining the rheological properties of fluids. Whatever the design of the instrument is two essential components are required to correctly measure the rheological flow properties of non-elastic fluids; these are an ability to apply a measured shear stress or shear rate to the fluid and to measure the fluids response to the applied shear stress or shear rate. All of those relying on a small gap between the shearing surfaces, like a cone and plate geometry or parallel plate geometry, generally are not used and are not applicable in the industry. The most common instrument used is that which relies on Couette flow, involving confinement of the sample between a rotating cup and a stationary bob, or (vice versa) a rotating bob and stationary cup. Here the torque is measured as a function of rotational speed and can be interpreted to determine the shear stress as a function of shear rate. Most common laboratory type instruments can be separated into two categories; rotational type and tube type.

2.13.1. Rotational Type Rheological Instruments

Of the two basic types of rheometers previously mentioned the rotational type is the most common and includes cones and plate, parallel plate, concentric cylinder, and vane geometries. In the rotational type rheological instruments, the fluid sample is sheared as a result of the rotation of a cylinder or cone. The shearing occurs in a narrow gap between two surfaces, usually one rotating and the other stationary. A significant advantage of the

rotational type rheometer is that only a small sample volume is usually required, which also means that control of temperature and pressure of the sample can be more readily achieved. Accuracy, reliability, and ease of use make these instruments extremely common, though they are more expensive compared to other types of rheometers.

2.13.1.1. Plate Type

2.13.1.1.1. Parallel Plate

The parallel plate geometry consists of two parallel disks separated by a defined distance, with the space between two disks filled with the sample liquid. One of the two disks rotates at a defined speed and the resistance of the fluid to the motion is recorded as a torque. Measurements of slurries and suspensions with the parallel plate geometry can be affected by slip and settling particles. As particles settle a concentration gradient will develop lending to incorrect values of measured torque and incorrectly determined rheological properties. A further problem with the parallel plate geometry is that there is often quite a low upper limit on the shear rates that can be examined, particularly with low viscosity fluids that can be ejected from the geometry due to centripetal forces at higher values of shear rate. The main disadvantage of parallel plates comes from the fact that the shear rate produced varies across the sample. In most cases the software takes an average value for the shear rate. Wider the gap, there is more chance of forming a temperature gradient across the sample and so it is important to surround the measuring system and sample with some form of thermal cover or oven.

2.13.1.1.2. Cone and Plate

The common feature of a cone-and-plate geometry is that the fluid is sheared between a flat plate and a cone with a low angle. In the case of cone and plate geometry either the cone or the plate can rotate at a set speed and the resistance of the fluid to motion, the torque, is measured. The calculations to determine the shear stress and shear rate require that the tip of the cone touch the plate, but because this is often impractical a truncated cone can be used instead. In a truncated cone a small portion of the tip of the cone is removed but the cone is positioned as if the cone was complete. The small clearance between the cone (whether truncated or not) and the stationary plate means that particles can become easily trapped. Trapped particles significantly increase the measured resistance (the torque) and this can lead

to significant errors in the calculated shear stress. Thus the size of particles in suspensions that can be measured with the cone and plate geometry is quite limited. Settling and slip may also affect the measurements from a cone and plate geometry, in same way that the parallel plate geometry is affected and test samples can also be ejected from this geometry at higher rotational speeds. For particulate material the cone and plate geometry is not recommended. Because, if the mean particle diameter is not some five to ten times smaller than the gap; the particles can jam at the cone apex resulting in noisy data. Materials with a high concentration of solids are also prone to being expelled from the gap under high shear rates, another reason to avoid the use of cone.

2.13.1.1.3. Concentric Cylinders (Cup and Bob)

The cup and bob type measuring systems come in various forms such as coaxial cylinder, double gap, Mooney cell, etc. The coaxial-concentric cylinder system consists of a bob or inner cylinder and a cup or outer cylinder, with the fluid placed in the annular region between the two cylinders. Usually the inner cylinder is rotated and the resistance of the fluid to the motion measured as a torque. Their advantage comes from being able to work with low viscosity materials and suspensions. Their large surface area gives them a greater sensitivity and so they will produce good data at low shear rates and viscosities. The shear rate is determined by geometrical dimensions and the speed of rotation. The shear stress is calculated from the torque and the geometrical dimensions. For concentric cylinder geometry, it is easier to calculate the shear stress compared to the shear rate, as the calculations are not dependent on the dimensions of the geometry or the rheological properties of the fluid being examined. Thus from the measured torque, the shear stress may be determined as shown in Equation (2.20).

$$\tau = M / [2\pi (\kappa R)^2 L] \tag{2.20}$$

Where, κ represents the ratio between the radius of the two cylinders (inner/outer), L the length of the cylinders and R the radius of the outer cylinder.

2.13.1.1.4. Vane Geometry

"Vane-in-a-cup" geometry can be used to eliminate the problem of slip. This configuration, which consists of four blades connected to a spindle, is simply used as an

attachment that can be made to fit an existing rheometer. However, the vane geometry cannot prevent particles settling and so it is generally restricted to those systems where particles either do not settle or settle very slowly. Another important use of the vane geometry is in the direct determination of the yield stress of a fluid.

2.13.2. Tube type rheometer

A tube rheometer primarily consists of a pressurized reservoir and a capillary tube. Fluid is filled in the reservoir and forced out through the tube under a certain pressure and the flow rate is recorded. Usually the tube is placed in a vertical position though measurements with horizontal tubes are possible. It is usual when determining the pressure drop across a tube rheometer to assume that the fluid has no (or a minimal) velocity when it exits the end of the tube. This assumption will not always be valid and under certain conditions can lead to significant errors that are referred to as "kinetic effects". End effects, which are the combination of entrance and exit effects, may influence the results from a tube rheometer.

2.14. Krieger-Dougherty model

This equation shows that there is an increase in the viscosity of the medium when particles are added. This increase depends on the concentration of the particles (Struble and Sun, 1995):

$$\eta = \eta_s \, (1 - \Phi/\Phi_m)^{-[\eta]\Phi_m} \qquad\qquad (2.21)$$

where $[\eta]$, the intrinsic viscosity, is equal to 2.5 for spheres, ϕ is the volume concentration of particles, ϕ_m the maximum packing, η the viscosity of the suspension and η_0 is the viscosity of the medium. Therefore, if the viscosity of the cement paste and the concentration of the aggregates are known, and the maximum packing of the particles is determined, then the viscosity of the concrete can be calculated.

Keeping the above literature in mind, it is decided to investigate the flow behaviour of surfactant admixtured fly ash slurry to reduce drag friction during hydraulic transportation in pipelines for filling mine voids, which constitutes the application I am most interested in.

CHAPTER 3

METHODOLOGY

3. Materials and methods

This chapter introduces the various materials used for this investigation and laboratory characterization techniques followed as per the prescribed standards and procedures in context of fly ash transportation and utilization.

3.1. Introduction

The objective of the investigation was to study the flow behavior of the fly ash slurry and to determine its in-place strength characteristics to achieve bulk utilization in filling mine voids. The major ingredients used were fly ash, surfactant, sodium salycilate, and lime. Sample preparation, various methods followed for characterization of ingredients, rheology study, strength study, and development of different composite materials are reported.

The coal ash, which includes both fly ash and the bottom ash (or boiler slag), and is better known as the pulverized fuel ash, is a by-product produced at thermal power plants due to the combustion of pulverized coal, with low calorific value and with high ash content. It is a pozzolana (a siliceous and aluminous material which in itself possesses little or no cementitious value but will, in finely divided form and in the presence of moisture, reacts chemically with calcium hydroxide, at normal temperatures, to form compounds possessing cementitious properties). The quality of the ash produced mainly depends on the quality of coal, its pulverization method, combustion technique, ash handling, and collection techniques. Physical properties help in classifying the coal ashes for various engineering purposes and some are related to engineering properties.

The properties investigated are specific gravity, grain size distribution, specific surface area, wet density, moisture content, porosity, chemical composition, morphological characteristics, turbidity, pH, rheology, settling characteristics, FTIR studies, optimum moisture content-maximum dry density relationships, unconfined compressive strength, Brazilian tensile strength, shear strength parameters, ultrasonic pulse velocity, poisson's ratio, Young's modulus, etc.

3.2. Materials

3.2.1. Fly ash

Fly ash samples used in the investigation were procured from seven numbers of coal-fired thermal power plants situated in India (Figure 3.1). They are class F fly ashes which were collected in dry state directly from hoppers attached to electrostatic precipitators in gunny bags made of strong poly-coated cotton with 50 kg capacity. The chute of hoppers was slowly opened and bags were filled. The mouth of each bag was sealed immediately after collection and the same was again inserted in another polypack to prevent atmospheric influences and transported with care from the plant to the place of experimentation and kept in a controlled environment. The sample ID and their source of collection are given in Table 3.1.

Table-3.1: Sample ID and their source of collection

Sample ID	Source of collection of samples	Sample Code	State
F_1	Ennore Thermal Power Plant, Ennore	(ETPS)	Tamilnadu
F_2	National Aluminium Company, Angul	(NALCO)	Odisha
F_3	IB Thermal Power Plant, Jharsuguda	(OPGC)	Odisha
F_4	Patratu Thermal Power Plant, Ranchi	(PTPS)	Jharkhand
F_5	Rourkela Steel Plant, CPP-II, Rourkela	(RSPII)	Odisha
F_6	Super Thermal Power Plant, NTPC, Angul	(STPP)	Odisha
F_7	Talcher Thermal Power Plant, Talcher	(TTPS)	Odisha

3.2.2. Additives
3.2.2.1. Surfactant

The surfactant used in this study was Cetyltrimethyl Ammonium Bromide (CTAB). Its chemical formula is $C_{19}H_{42}BrN$. This was chosen due to its relative inertness with calcium or sodium ions present in tap water. The surfactant was procured from LOBA Chemie Pvt. Ltd., Mumbai, India. The molecular weight of the surfactant is 364.46. CTAB is a cationic surfactant that is known to be very effective for drag reduction when accompanied with suitable counter-ions. The hydrophobic head group which is a long chain hydrocarbon with 19 carbons in the structure of the surfactant is attached to the fly ash particle, converting it from hydrophilic to hydrophobic property. The physical and chemical properties of the surfactant are shown in Table 3.2. The molecular structural diagram is shown in Figure 3.2.
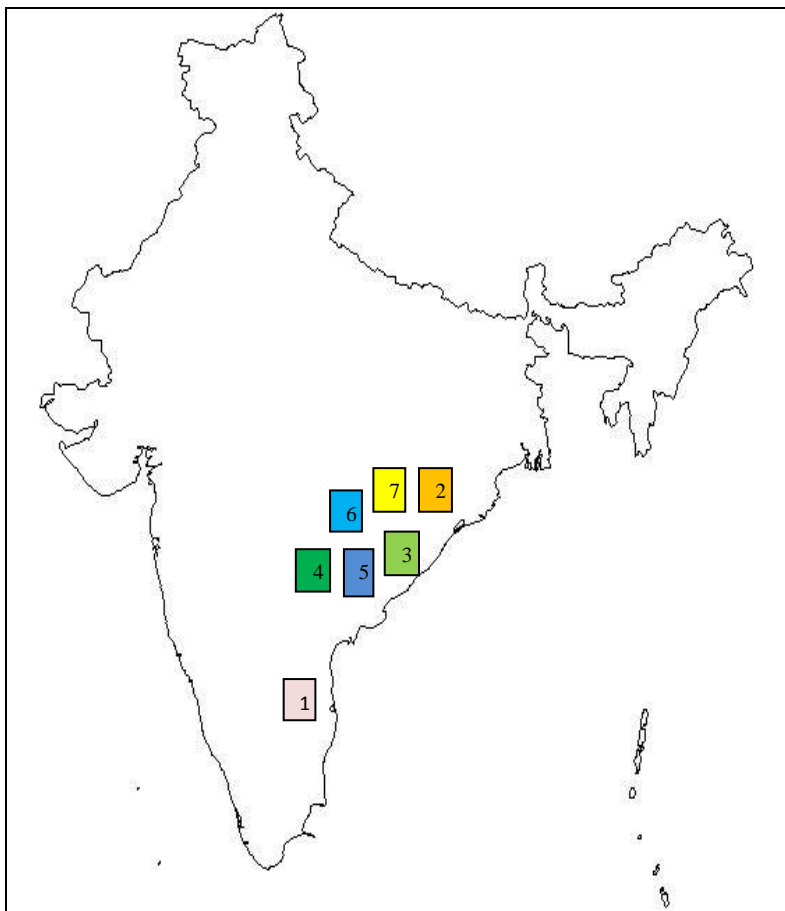
Figure 3.1: Location map of India from where the samples were collected

Table 3.2.Physical and chemical properties of the surfactant (CTAB)

Sl. No.	Parameters	% Value
1	Minimum Assay value	99
2	Heavy metals (as Pb)	0.001
3	Iron (Fe)	0.001
4	Sulphated ash	0.1
5	Loss on drying	1.0
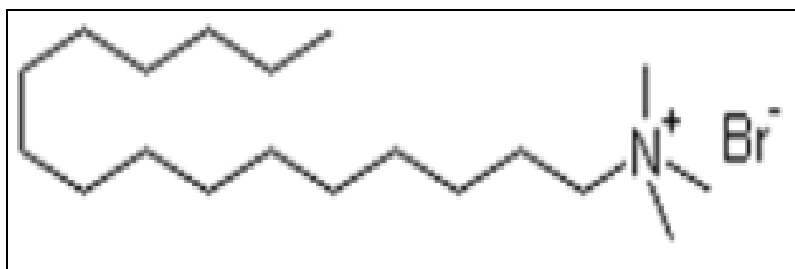
Figure 3.2.Molecular structural diagram of CTAB

3.2.2.2. Counter-ion

The counter-ion used was Sodium Salicylate (NaSal) (HOC_6H_4COONa). Its molecular weight is 160.10. This was added to the slurry at the same weight concentration as that of the surfactant. It was suggested that for the surfactant drag-reducing additives, the rod-like micelle structures are the key to give complicated rheological fluid properties including viscoelasticity. The counter-ion reduces ion radius of the surfactant to deform micellar shape from globular to rod-like micelles. These rod-like micelles entangle together to make a certain network structure (Rehage and Hoffmann, 1991). Nguyen *et al.* (2006) opined that counter-ions also play a role as catalysts for the breakdown and reformation of the entanglement points. The physical and chemical properties of the counter-ion used are given in Table 3.3. The molecular structural diagram of the counter-ion is presented in Figure 3.3.

Table 3.3.Physical and chemical properties of the counter-ion (NaSal)

Sl. No.	Parameters	% Value
1	Minimum assay (calculated to dried material)	99
	Maximum limits of impurities	
2	Loss on drying at 105^0 C	0.5
3	Chloride (Cl)	0.02
4	Sulphate (SO_4)	0.05
5	Heavy metals (as Pb)	0.002
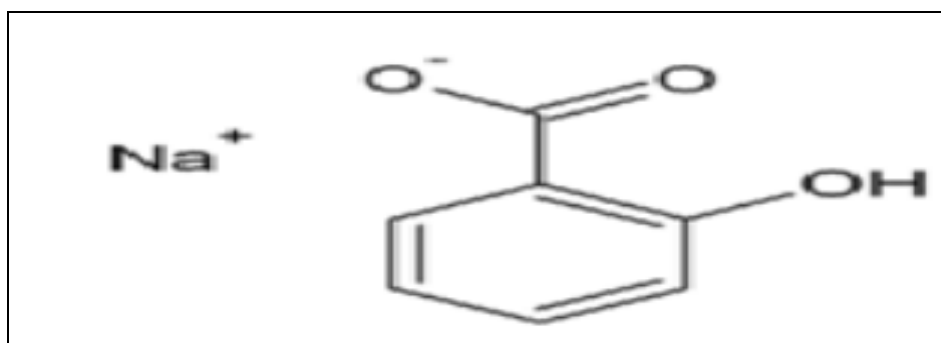
Figure 3.3.Molecular structural diagram of the counter-ion

3.2.2.3. Lime

Commercially available chemically pure lime ($CaCO_3$) (make: Merck Company Limited, Mumbai) has been used in this investigation. Table 3.4 gives the constituents of lime used.

3.2.3. Water

Since the fly ash is to be transported through ordinary water medium in pipelines, so ordinary tap water of pH 7.0 was chosen for preparation of the fly ash slurry in this study.

3.2.4. Millipore water

Millipore water was used for standardization of rheometer and surface tensiometer. It is ultra pure ion free water. Its electrical resistivity is 18.2MΩ, surface tension 71.5 mN/m and pH varies from 6.5 to 7.

3.2.5. Mobil oil (Tranself type B 85W140)

Elf Tranself type B 85 W 140 was used for standardization of rheometer readings. It is multi-grade transmission oil developed especially for the rear axles of many heavy earth moving machineries (HEMMs). It is known for its excellent thermal and oxidation stability (Net at 29.5^{0}C).

Table 3.4.Chemical composition of the lime

Minimum Assay (Acidimetric)	98.5 %
Maximum limits of impurities content expressed in percentages	
Substances insoluble in hydrochloric acid	0.050 %
Chloride (Cl) content	0.050 %
Sulphate (SO4) content	0.500 %
Heavy metals (as Pb) content	0.005 %
Iron (Fe) content	0.050 %

3.3. Laboratory investigation and characterization of materials

The following tests were conducted for the seven fly ash samples in the laboratory following the prescribed standards and procedures by using the various instruments discussed below:

3.3.1. X-ray diffraction (XRD) analysis

The raw materials after oven dried were taken for X-ray diffraction analysis. The X-ray diffraction was carried out by XRD Spectrometer (make: Philips Analytical X-ray B.V., UK) studies, using a graphite monochromator and Cu Kα radiation. The ash samples were

scanned for 2θ angle ranging from 5 to 80^0. These studies are carried out primarily to identify the mineral phases.

3.3.2. Scanning Electron Microscopy (SEM) studies

The raw materials after oven dried were also taken for Scanning Electron Microscope (SEM) study. SEM provides a means of imaging micro surfaces, particle size analysis, grain boundaries, etc. In this investigation a SEM (make: JEOL JSM 6480 LV, Japan) was used to conduct these studies. Figure 3.4 shows the Scanning Electron Microscope set up in the laboratory where the investigation was carried out.

Figure 3.4.Scanning Electron Microscope

3.3.3. Chemical characterization

The chemical properties of the coal ashes influence the environmental impacts that may arise out of their use/disposal. The adverse impacts include contamination of surface and subsurface water with toxic heavy metals present in the coal ashes, loss of soil fertility around the plant sites, etc. Thus a detailed study of the chemical composition, morphological studies, pH, total soluble solids etc. is necessary. Chemical composition also suggests the possible areas of application of coal ash.

3.3.3.1. Energy-dispersive X-ray spectroscopy (EDX) studies

The chemical composition, calculated as major oxides, of the ash samples are obtained with the help of an EDX set-up (make: JEOL JSM 6480 LV, Japan). EDX is a technique used

for identifying the elemental composition of the specimen. The EDX analysis system works as an integral feature of a SEM and cannot operate on its own without the latter. It is an analytical tool predominantly used for chemical characterization. Being a type of spectroscopy, it relies on the investigation of a sample through interactions between light and matter, analyzing X-rays in its particular case. Its characterization capabilities are due in large part to the fundamental principle that each element of the periodic table has a unique electronic structure and, thus, a unique response to electromagnetic waves. Spectroscopy data is often portrayed as a graph plotting counts vs. energy. The peaks correspond to characteristic elemental emissions. The release of X-rays creates spectral lines that are highly specific to individual elements; thus, the X-ray emission data can be analyzed to characterize the sample in question.

3.3.3.2. Energy dispersive X-ray fluorescence (ED-XRF) studies

XRF analysis (make: Philips PW2400 X-ray, Japan) was conducted to determine the chemical constituents of the samples. ED-XRF technology provides one of the simplest, most accurate and most economic analytical methods for the determination of the chemical composition of many types of materials. It is non-destructive and reliable, requires no, or very little, sample preparation and is suitable for solid, liquid and powdered samples. It can be used for a wide range of elements, from sodium (11) to uranium (92), and provides detection limits at the sub-ppm level; it can also measure concentrations of up to 100% easily and simultaneously.

3.3.4. Physical characterization

The physical properties such as grain size analysis, particle size distribution, specific gravity, and specific surface area were determined following the standard procedures.

3.3.4.1. Specific gravity (sp. gr.)

This is an important parameter and affects the flow characteristics of fly ash slurry. Sp. gr. is the density of a substance divided by the density of water. It is calculated as:

$$\text{Specific gravity, S} = \frac{(W_2 - W_1)}{(W_4 + W_2) - (W_3 + W_1)} \tag{3.1}$$

Where, W_1 = Weight of dry sp. gr. bottle with lid, W_2 = Weight of dry sp. gr. bottle with lid + 1/3rd vol. of ash sample, W_3 = W_2 + distilled water, W_4 = Weight of dry sp. gr. bottle with lid + Distilled water. The sp. gr. of the fly ash samples were determined in the laboratory by using a stoppered bottle having a capacity of 50 ml as per the guidelines provided by the American Society of Testing Materials (ASTM D 854).

3.3.4.2. Specific surface area

The specific surface area of the ash samples were determined by using a Blaine's apparatus (ASTM C 204) with Portland cement as a standard reference material. For calculating the specific surface area of the ash samples, the following equation given by Singh and Kolay (2002) was used: Specific surface area (cm^2/g),

$$A = \{S_s \, (1\text{-}e_s) \, \sqrt{e^3}\sqrt{T}\} \, / \, \{\sqrt{}\,e_s^3\sqrt{T_s}\,(1\text{-}e)\} \qquad (3.2)$$

Where A is the specific surface area of the ash sample, S_s the specific surface area of the Portland cement (3460 cm^2/g), e the void ratio of the ash sample, e_s the void ratio of the cement (=0.5), T_s the measured time interval of manometer drop, for cement (77.18s) and T is the measured time interval of manometer drop for ash sample.

3.3.4.3. Particle size analysis

The grain size analysis of the untreated fly ash sample was carried out by Malvern particle size analyzer (U.K) laser diffraction apparatus. In this investigation the gradational properties of the ash samples are obtained by using photo-sedimentation method, which measures the change of concentration by passing a beam of light through the suspension. Soft imaging system has also been used to determine the grain-size distribution characteristics of the ash samples by using Mastersizer 2000 version 5.22. A schematic layout of the instrument has been shown in Figure 3.5.

3.3.4.4. pH (ASTM D 4972)

The pH value was determined to identify the acidic or alkaline characteristic of fly ash samples. The pH value denotes the hydrogen ion concentration on the liquid and it is the measure of acidity and alkalinity of the liquid. According to the law of mass action, in any liquid, (Concentration of H^+ ions * concentration of OH^- ions) / (concentration of un-dissolved

HOH Molecules) = 10^{-14}. The pH is determined by the electrolysis and dissociation of H^+ and OH^- ions in a liquid and the milli volts generated gives the reading on scale either by movement of analog pointer or digital recording. In this study the measurement of pH was carried out using digital pH meter model 111 (make: Systronics, India) with accuracy up to ±0.02 units as per the procedure suggested by Jackson (1958). The instrument was standardized with three standard buffer solutions of pH 7.00, 4.00 and 10.00 at 25^0C. The suspension was stirred well and allowed to come to room temperature ($25\pm1°$C) before taking the pH measurement.
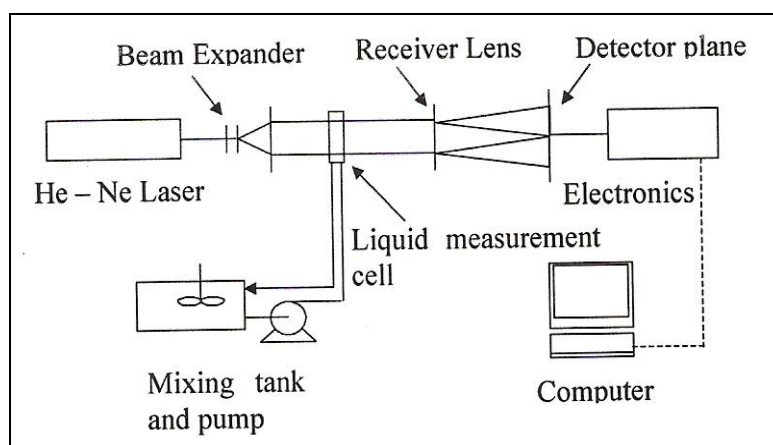
Figure 3.5 Shematic diagram of Malvern Particle Size Analyzer

3.3.5. Surface Tension

Surface tension is a property of the surface of a liquid that allows it to resist an external force. Surface tension of the fly ash slurry was measured by Surface Tensiometer (make: DCAT 11 EC, Dataphysics, Germany) a dynamic contact angle meter using the Wilhelmy plate with an accuracy of ±0.01 mNm^{-1} at room temperature 25^0C.

3.3.6. Zeta Potential (ζ)

The ζ of all the slurries was measured by using electrophoretic technique by zeta sizer (make: ZS Nano-Series, Malvern Instruments, U.K). This instrument automatically calculates the electrophoretic mobility of the colloidal fly ash particles and converts it into ζ. The ζ values are at least an average of five measurements. All measurements were made at the ambient temperature. Colloidal particles dispersed in a solution are electrically charged due to their ionic characteristics and dipolar attributes. Each particle dispersed in a solution is

surrounded by oppositely charged ions called the fixed layer. Outside the fixed layer, there are varying compositions of ions of opposite polarities, forming a cloud-like area. This area is called the diffuse double layer, and the whole area is electrically neutral. When a voltage is applied to the solution in which particles are dispersed, particles are attracted to the electrode of the opposite polarity, accompanied by the fixed layer and part of the diffuse double layer, or internal side of the "sliding surface".

The significance of ζ is that its value can be related to the stability of colloidal dispersions. The ζ indicates the degree of repulsion between adjacent, similarly charged particles in dispersion. For molecules and particles that are small enough, a high ζ will confer stability, i.e. the solution or dispersion will resist aggregation. When the potential is low, attraction exceeds repulsion and the dispersion will break and flocculate. So, colloids with high ζ (negative or positive) are electrically stabilized while colloids with low ζ tend to coagulate or flocculate as outlined in the Table 3.5 and Figure 3.6 (Vallar *et al.*, 1999).

Table 3.5: Relation between ζ and suspension stability

ζ [mV]	Stability behavior of the colloid
from 0 to ±5	Rapid coagulation or flocculation
from ±5 to ±10	Instable dispersion
from ±10 to ±30	Incipient instability
from ±30 to ±40	Moderate stability
from ±40 to ±60	Good stability
more than ±61	Excellent stability
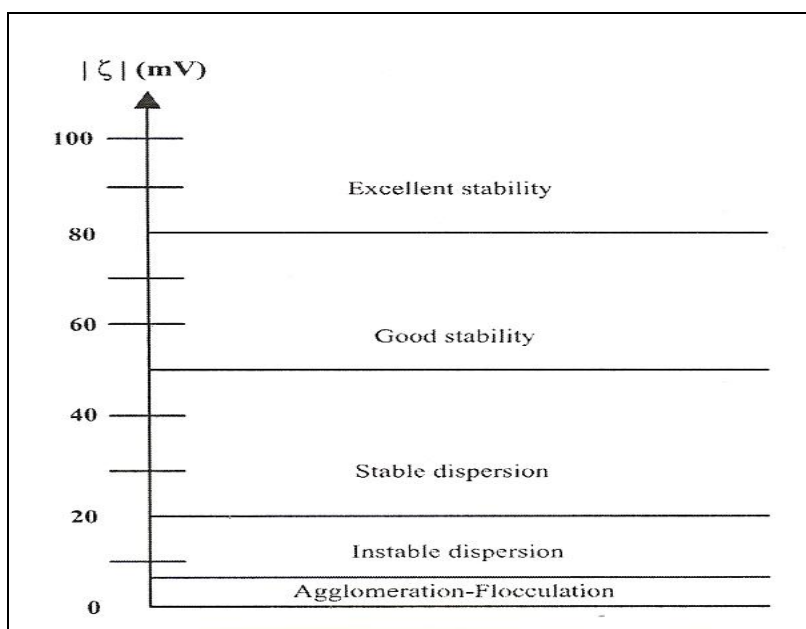
Figure 3.6: Relation between ζ and Suspension Stability

3.3.7. Settling study of fly ash slurry

3.3.7.1. Static settling tests

A series of experiments were conducted, which monitored the settling of fly ash slurry under static conditions for 24 hours (Figure 3.7). After this time, an obvious division between the settled material and the clear decant water could be seen. The depth of this section was measured and corresponding volume calculated. One of the objectives of this investigation was to provide a detailed study of the settling characteristics of fly ash slurry at different concentration levels. In this investigation settling study was carried out by using test tubes of 100 ml capacity as per prescribed standards. The maximum settled concentration of slurry is an indicator of the limiting concentration beyond which the flowability of fly ash slurry ceases to occur. The maximum settled concentration is found after allowing a slurry of given concentration to settle for a long period of time (>24 hours) until the equilibrium condition is reached. Studies were conducted by Senapati *et al.,* (2005) on fly ash slurry at weight concentrations varying from 50 – 67%. The slurry prepared at these concentrations settled in a graduated glass cylinder for 72 hours after which no further settling occurred. The maximum settled concentrations at different weight concentrations are determined from the readings of the settled volume and water volume using the following relationship.

$$C_{wmax} = W_s/ (W_s + W_w) \qquad (3.3)$$

Where W_s = weight of solids in the settled mass, W_w = weight of water present in the settled mass. The study conducted by them revealed that the maximum settled concentration of fly ash slurry is 58%.

Figure 3.7: Settling study of fly ash slurry

3.3.8. FTIR Spectroscopy study of fly ash

Fourier Transform Infrared (FTIR) IR Prestige-21 model was used for this investigation. FTIR spectroscopy bases its functionality on the principle that almost all molecules absorb infrared light. Most FTIR spectroscopy uses a Michelson interferometer to spread a sample with the infrared light spectrum and measure the intensity of the infrared light spectrum not absorbed by the sample. FTIR spectroscopy is a multiplexing technique, where all optical frequencies from the source are observed simultaneously over a period of time known as scan time. The spectrometer measures the intensity of a specially-encoded infrared beam after it has passed through a sample. The resulting signal, which is a time domain digital signal, is called an Interferogram and contains intensity information about all frequencies present in the infrared beam. This information can be extracted by switching this signal from a time domain digital signal to a frequency domain digital signal, which is accomplished by applying a Fourier transform over the interferogram and producing what is called a single beam spectrum. Fly ash samples both raw and modified by additives were analysed in the laboratory by preparing samples by using a hydraulic press. The results are reported and discussed in the respective sections.

3.4. Experimental apparatus used for rheology study

The various flow related properties as shear stress, shear rate, viscosity, torque, etc. were determined with a rheometer (make: Physica MCR 101, Germany). It employs concentric cylinder geometry with a rotating inner cylinder and a stationary outer cylinder. The torque developed on the inner cylinder due to a sample is directly related to the sample viscosity. In this study, all samples were measured by the use of CC 27 tool master system (as per DIN 6129 standard). A thermal jacket allows the use of an external fluid circulator to control or regulate the temperature of the sample measured. The laminar flow of a liquid in the space between coaxial cylinders is known as" Couette Flow". In this case, the outer cylinder, with a radius r_e remains stationary. The inner cylinder with a radius r_i and height L is rotated at constant speed (Ω rad/s). It is assumed that the flow of the fluid between the cylinders is steady and laminar and that the end effects are negligible. Consider a volume of fluid between the inner cylinder and an arbitrary radius r. Let ω be the angular velocity of the fluid at this radius r. The torque exerted on the fluid at this radius is:

$$M = \tau_r (2\pi rh) \, r \qquad (3.4)$$

Where τ_r is the shear stress: The torque M measured at the surface of the inner cylinder must be the same as the torque at any arbitrary radius r since the motion is steady. Rewriting in terms of the shear stress we get

$$\tau_r = \frac{M}{2\pi r^2 h} \qquad (3.5)$$

It can be observed from the equation 3.5 that the shearing stress is inversely proportional to the square of the distance from the axis of rotation. It is interesting to note that by using an annular gap that is small compared to the cylinder radii, the shearing stress on the fluid will be almost constant throughout the volume of the testing fluid. The tangential velocity of the fluid at the radius r is:

$$V = r \, \acute{\omega} \qquad (3.6)$$

The gradient of velocity is given by:

$$dv/dr = r \, (d\acute{\omega}/dr) + \acute{\omega} \qquad (3.7)$$

In equation 3.7, the first term represents the rate of shear and the second term represents the radial velocity gradient of rigid body rotation. For a Newtonian fluid, $\tau_r = \mu$, or

$$M/ (2\pi r^2 h) = \mu r \, (d\acute{\omega}/dr) \qquad (3.8)$$

Where, $\acute{\gamma} = r \, (d\acute{\omega}/dr)$, μ the viscosity and thus:

$$d\acute{\omega}/dr = M/ (2\pi h \mu r^3) \qquad (3.9)$$

Integrating the equation 3.9 with appropriate boundary conditions, results in the expression:

$$M = (4\pi \mu h R_1^2 R_2^2 \acute{\omega})/ (R_2^2 - R_1^2) \qquad (3.10)$$

or $M = c\mu \, \acute{\omega}$, where c is the instrument constant and R outer radius.

In Figure 3.8 the abbreviated numbers and legends may be read as: 1–inner cylinder connected with measuring scale; 2–fly ash slurry; 3–outer cylinder (measuring cup); 4–outer temperature controlling jacket connected to the circulator bath to control the temperature with an accuracy of $\pm$ 0.5^{0}C. Positioning length (DIN position) =72.5 mm; approximate sample volume = 19.0 ml, active length (check length) = 120.2 mm. The shear rate, for different rotating speed of the bob (1), is calculated using the equation:

$$\dot{\gamma} = (\pi*n/30)*[(1+\delta^2)/(\delta^2-1)]; \; \omega = (2\pi*n)/60 \qquad (3.11)$$

The shear strain γ is calculated using the equation:

$$\gamma = (1/10)*[(1+\delta^2)/(\delta^2-1)]*\varphi; \; \text{where } \delta = r_e/r_i \qquad (3.12)$$

Shear stress τ in fly ash slurry, are calculated using the equation:

$$\tau = [(1+\delta^2)/(200*\delta^2)]*[M/(2\pi L r_i^2 C_L] \qquad (3.13)$$

$\alpha_{cyl.\ cone} = 120^0; \; (r_{shaft}/r_i) \geq 0.3; \; L/r_i \geq 3$

Where, τ = shear stress (Pa), M = torque or moment (mNm), γ = strain or deformation (%), φ = deflection angle (m rad), $\dot{\gamma}$ = shear rate (s^{-1}), n= speed (min^{-1}), r_i/r_e = internal / external cylinder radius (m), ω = angular velocity (s^{-1}) = (2π/60)*n.

C_L = end effect correction factor = 1.10. Empirical values for: C_L=1.1 for Newtonian fluids, and up to 1.2 recommended for standard measurements according to ISO 3219 for shear thinning fluids. For pseudoplastic fluids at low shear rates C_L is up to 1.28.
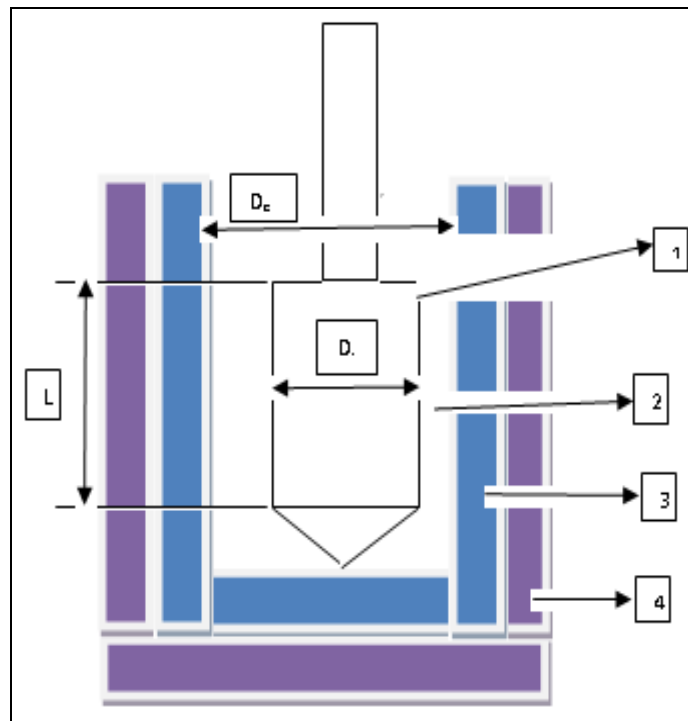
Figure 3.8: Schematic diagram of the rotational rheometer with coaxial concentric cylinder measuring system (Standard: ISO 3219) (δ≤1.2)

Rheological properties of tested slurries were obtained by measuring shear stress at specific shear rates ranging from 25-1000 s^{-1}. Physical parameters of the measuring tools and

sensor system are presented in Table 3.6. In this instrument, the stationary cup, which houses the slurry, and into which the rotating bob, mounted vertically, was inserted. The shear rate was linearly increased from 25-1000 s^{-1}. The temperature was varied from 20^{0}C to 40^{0}C by a water bath circulator. The above temperature range was selected based on the average temperature variation during the various seasons of a year in India during which the fly ash slurry is to be transported. Shear viscosity was measured by a shear rate sweep experiment. The minimum waiting time was set at 20 s at each shear rate. First, the equipment was tested for its reliability by use of standard Mobil oil (type B 85W140 multi-grade transmission oil meeting API GL-5, and MIL-L-2105D levels of specifications), distilled water, Millipore water (ultra pure and ion free water having pH 6.5 to 7, surface tension 71.5 mN/m) and ordinary tap water. The measured data matched favorably with their standard values. The rheological properties such as viscosity, shear stress, and torque were determined at a fixed shear rate for each sample and the reported values were the average of five measurements for each parameter.

Table 3.6: Physical parameters of the measuring tools and sensor system

Instrument Make	Anton Paar Rheometer, Germany
Model No.	Physica MCR 101 (air bearing system)
Sensor System	CC 27
Description	Co-axial cylinder measuring system
Standard	ISO 3219 ($\leq$ 1.2)
Cone angle	$\alpha_{\text{cyl. cone}} = 120^0$, L/r$_i \geq 3$
Measuring range	Shear rate 0-1000 s^{-1}
Physical Dimensions	Measuring Bob, Diameter, D$_i$ = 26.664 mm, Measuring Cup, Diameter, D$_e$ = 28.922 mm, Ratio of Radii, δ = 1.085; Gap Length = 40.014 mm Measuring Gap = 1.129 mm

3.4.1. Description of the Instrument

A temperature controlled couette rheometer with accurate independent temperature control device for measuring the viscosity of the fly ah slurry was used. The schematic diagram of the rheometer is presented in Figure 3.8. Both cup and bob are made up of 304 stainless steel coated with zirconia. The slurry was poured into the outer cylinder. When the

inner cylinder was placed concentrically, the slurry resided in the annular space between the cylinders. The inner cylinder was rotated by a drag cup motor which gives torque applied (M) to the inner cylinder (accuracy ~ 0.0001 µNm) and the outer cylinder is stationary. As the inner cylinder was rotated, the slurry was sheared continuously at the set temperature environment. Circulator bath was kept on all the time to maintain a constant set temperature of the slurry. During shearing, the rotational speed of the inner cylinder was measured by an inductive position sensor which gives the strain rate with accuracy ~ 0.008 µrad.
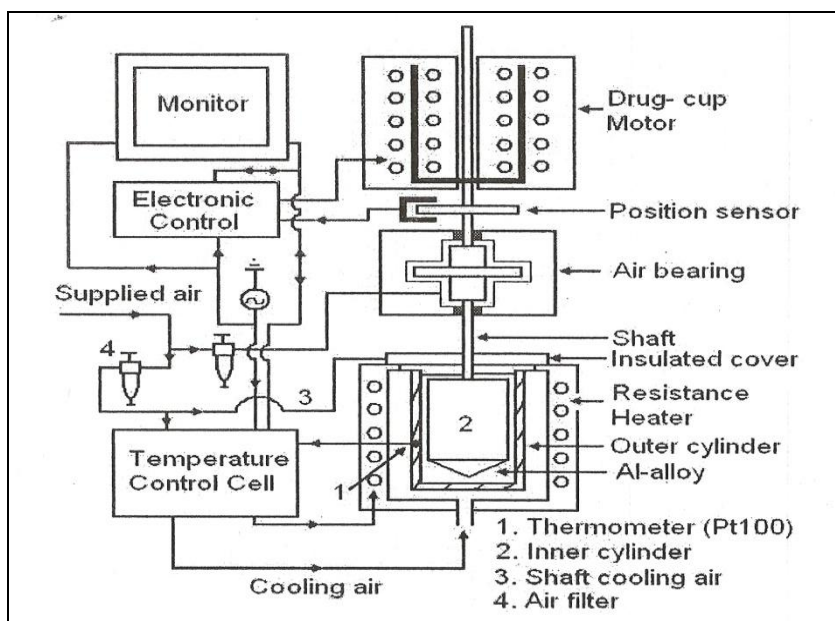
Figure 3.9: Schematic diagram of the Rheometer

3.4.2. Experimental steps for rheology measurement

For the rheometric test the F_1 fly ash sample was selected out of seven fly ash samples investigated due its favorable properties as a mine filling material (Table 4.1). The active dispersive agent used was CTAB. Couterion selected for this study was NaSal. The fly ash slurry was mixed thoroughly by a magnetic stirrer. The additive was mixed with water, used for slurry preparation. The simplified scheme of the rheometer is displayed on Figure 3.9. The fly ash slurry was poured into the container (3) i.e. the external cylinder which is fixed non-movably into the equipment stand. Inside the external cylinder the internal cylinder called the bob (1) can be rotated. Because of the intrinsic friction of the layers of the fly ash slurry (2) appearing between the rotating internal cylinder and the external cylinder torque developed is measured. The internal cylinder is connected to a measuring scale which makes a turn and the

data displayed on the measuring scale changes. The procedure followed in the rheometric tests was repetitive, and is summarized as follows:

i.   First, the entire apparatus was connected (Rheometer, circulator bath, computer and the air compressor) and power supply was made on.

ii. Next, the circulator bath temperature was set up. The working principle of this equipment was to maintain the temperature of the circulating fluid by means of heating and cooling fins. This fluid circulates through the "heat jacket" (accessory coupled to the rheometer in Figure 3.9), which envelops the spindle, maintaining the sample temperature constant. Depending on the temperature range at which it is working, a type of circulating fluid is to be used. For temperatures varying between 5^0C and 80^0C, the fluid is water.

iii. In the rheoplus software, the entire test procedure was configured: the option for shear stress or shear rate controlled test was made, the spindle used was indicated, the test time and shear rate or shear stress imposed was defined (for gathering shear stress or shear rate data, respectively).

iv. Next the rheometer was activated from the software, and the test started.

Test results were obtained by conducting close to 60 experimental tests for a particular concentration of solids.

3.5. Characterization of Fly Ash Slurry at 20% Solid Concentration

3.5.1. Experimental Procedure and Range of Parameters

The Rheometer confirms to ISO 3219 (DIN EN ISO 3219, 1993). It consists of a motor with attached gear box system for varying the speed in steps of equal ratio. The cylindrical measuring bob is attached to a torsion bar and the concentric measuring cup can be rotated at the desired speed. Temperature was controlled by a fluid bath circulator with an accuracy of $\pm 0.5^0$ C of the desired temperature. Shear viscosity was measured by the constant shear rate sweep test experiment. The minimum waiting time set is at 20 seconds at each shear rate to allow the viscosity value to reach equilibrium at each shear rate. Viscosity at each shear rate was calculated as the average of ten measurements.

3.5.2. Sample Preparation

The rheometric test needed 100ml of slurry suspension. It was prepared with 20 gram of fly ash and 80ml of ordinary tap water. Surfactant and counter-ion was added to water first and mixed thoroughly. Then the fly ash was added to it kept in a glass beaker. Stirring was done with a glass rod gently so as to avoid attrition of the particles. The container was then covered with aluminium foil tightly to avoid evaporation of water to the atmosphere as well as to enable uniform mixing of fly ash particles in the liquid medium. Tests were carried out after one hour of sample preparation. For rheometric tests, about 19 ml of the slurry sample was poured into the cup and the bob was lowered into the cup so that the free surface touches the top of the bob. The tests were conducted at shear rates varying from 100, 200, 300, 400, and 500 sec^{-1}. The recommended maximum shear stress is at a shear rate of about 511 sec^{-1} and exposing cement slurry to shear rates above 511 sec^{-1} has been reported to generate inconsistent results (Shah and Jeong, 2003).

3.5.3. Range of Parameters

Experiments were carried out for a total of six solid liquid mixtures at varying temperature environment. The concentration of additives used was 0, 0.1, 0.2, 0.3, 0.4, and 0.5% (by weight). This range of additive concentration was selected based on literature review (Seshadri *et al*., 2005 and Li *et al*., 2002). Table 3.7 shows the different fly ash composite slurries used in this investigation for 20% solid concentration.

Table 3.7.Sample ID, Parametric variations and suspension characteristic features at 20% solid conc

Sample No.	Fly ash (gram)	Surfactant (gm)	Counter-ion (gm)	Water (ml)	Solid Conc. C_w (by wt.)	Surface Tension (mNm)	Zeta Potential (mV)	pH at 27 ± 1^0C
20.1	19.0	0.5	0.5	80	20	31.636	+49.300	7.30
20.2	19.2	0.4	0.4	80	20	31.758	+37.500	7.59
20.3	19.4	0.3	0.3	80	20	31.224	+45.800	7.47
20.4	19.6	0.2	0.2	80	20	31.335	+36.900	7.97
20.5	19.8	0.1	0.1	80	20	32.897	+40.800	7.25
20.6	20.0	0.0	0.0	80	20	70.684	-27.000	7.74

The rates of shear during the measurements were varied from 100 to 500s^{-1} with a step of 100 each. These ranges correspond to the magnitudes of shear rates usually expected in low concentration fly ash slurry pipeline transportation systems. The lower shear rate range from 2 s^{-1} to 20 s^{-1} was used by Seshadri *et al.,* 2005 for highly concentrated slurries i.e. $C_w \approx 68\%$ (by weight). They also used shear rates ranging from 20 to 120 per second for high concentration slurry of C_w (60 to 65 %) for their rheological investigation.

3.6. Rheological characterization at 30% solid concentration

The cationic surfactant CTAB was selected for its eco-friendly nature. It is less susceptible to mechanical degradation (Zakin & Lui, 1983) and also known potential to positively influence turbulent flow with very small amount (Ohlendorf *et al*., 1986). It is also least affected by the presence of calcium and sodium ions in tap water (Kawaguchi *et al*., 1997; Feng-Chen *et al*., 2008). The counter-ion acts as a reagent to reduce ion radius of the surfactant to deform micellar shape from globular to rod-like micelles.

3.6.1. Sample preparation and measurement techniques followed

30% solids concentrations of slurries were prepared by using fly ash with ordinary tap water. For each temperature, the shear rates investigated varied from 25 to 500s^{-1}. On the basis of literature review, five different surfactant concentrations i.e. 0.1%, 0.2%, 0.3%, 0.4%, and 0.5% of the total weight of the slurry were selected (Seshadri *et al*., 2005; Verma *et al*., 2008; Biswas *et al*., 2000; Li *et al*., 2002; Usui *et al*., 2001). An equal amount of a counter-ion same as that of the surfactant concentration was also added to the slurry to take care of the calcium and sodium ions naturally present in tap water (Kawaguchi *et al*., 1997; Feng-Chen *et al*., 2008; Munekata *et al*., 2006). The samples were prepared by first adding the required amount of surfactant and the counter-ion to the required quantity of tap water. The prepared solution was mixed thoroughly using a magnetic stirrer, and fly ash was added to it. Table 3.8 presents the different composition of fly ash slurry and corresponding measured values of zeta potential and surface tension from the laboratory study for 30% solid concentration.

3.7. Characterization of fly ash slurries at 40% solid concentration

3.7.1. Parametric variations and sample preparation

Slurry samples were prepared with 40 wt. % of fly ash with ordinary tap water. The shear rates investigated varied from 25-1000 s^{-1} for each temperature. An equal amount of a

counter-ion equal to the surfactant concentration was also added to the slurry to prevent precipitation of surfactants due to the presence of Ca and Na ions in tap water (Munekata *et al.,* 2006; Li *et al.,* 2008). The counter-ion acts to reduce ion radius of the surfactant to deform micellar shape from globular to rod-like (Kawaguchi *et al.,* 1997). The samples were prepared by adding the required amount of surfactant and the counter-ion to the required quantity of tap water and mixing thoroughly by a magnetic stirrer. Measurements were carried out as per standards (DIN EN ISO: 3219, 1993). Table 3.9 presents the different composition of fly ash slurry and corresponding measured values of zeta potential and surface tension from the laboratory study for 40% solid concentration.

Table 3.8.Sample ID, Parametric variations and suspension characteristic features at 30% solid conc

Sample No.	Fly ash (gm)	Surfactant (gm)	Counter-ion (gm)	Water (ml)	Solid Conc. C_w (by wt.)	Surface Tension (mN/m)	Zeta Potential (mV)	pH at 25^0C
30.1	29.0	0.5	0.5	70	30	32.178	+35.200	7.73
30.2	29.2	0.4	0.4	70	30	32.249	+34.534	7.63
30.3	29.4	0.3	0.3	70	30	31.830	+33.800	7.24
30.4	29.6	0.2	0.2	70	30	31.902	+32.100	7.64
30.5	29.8	0.1	0.1	70	30	33.305	+31.700	7.66
30.6	30.0	0.0	0.0	70	30	57.900	-25.000	7.30

Table 3.9.Sample ID, Parametric variations and suspension characteristic features at 40% solid conc

Sample ID	Fly ash (gm)	Surfactant (gm)	Counter-ion (gm)	Water (ml)	Solid Conc. C_w (by wt.)	Surface Tension (mN/m)	Zeta Potential (mV)	pH at 25^0C
40.1	39.0	0.5	0.5	60	40	33.119	+36.511	7.23
40.2	39.2	0.4	0.4	60	40	32.225	+35.679	7.33
40.3	39.4	0.3	0.3	60	40	31.645	+33.796	7.14
40.4	39.6	0.2	0.2	60	40	31.231	+32.678	7.34
40.5	39.8	0.1	0.1	60	40	33.265	+31.689	7.56
40.6	40.0	0.0	0.0	60	40	58.543	-25.000	7.40

3.8. Rheological characterization at 50% solid concentration

Rheological characterization at 50% solid concentration was carried out at parametric variations listed in Table 3.10.

Table 3.10.Sample ID, Parametric variations and suspension characteristic features at 50% solid conc

Sample No.	Fly ash (gram)	Surfactant (gm)	Counter-ion (gm)	Water (ml)	Solid Conc. C_w (by wt.)
50.1	49.0	0.5	0.5	50	50
50.2	49.2	0.4	0.4	50	50
50.3	49.4	0.3	0.3	50	50
50.4	49.6	0.2	0.2	50	50
50.5	49.8	0.1	0.1	50	50
50.6	50.0	0.0	0.0	50	50

3.9. Rheological characterization at 60% solid concentration

Table 3.11 presents the different composition of fly ash slurry at 60% solid concentration.

Table 3.11.Sample ID, Parametric variations and suspension characteristic features at 60% solid conc

Sample No.	Fly ash (gram)	Surfactant (gm)	Counter-ion (gm)	Water (ml)	Solid Conc. C_w (by wt.)
60.1	59.0	0.5	0.5	40	60
60.2	59.2	0.4	0.4	40	60
60.3	59.4	0.3	0.3	40	60
60.4	59.6	0.2	0.2	40	60
60.5	59.8	0.1	0.1	40	60
60.6	60.0	0.0	0.0	40	60

3.10. Methods of sample preparation for strength study
3.10.1. Sample preparation

Availability of free lime enhances the pozzolanic reaction of materials. Silica lime reaction is pH dependent. The solubility of silica and its reaction with lime is directly related to the pH value. pH of the medium increases when the lime content exceeds the optimum lime content necessary for the silica to react. But pH reaches a constant value when the solution is saturated with lime (Sivapullaiah *et al.,* 1995). It reflects the saturation of the silica-lime reaction a pozzolanic activity. In this investigation quick lime - a commercially available additive was chosen for this study.

The pH of the raw fly ash and fly ash-surfactant-NaSal mixture were determined as suggested by IS: 2720-Part 26 (1987) at room temperature in a pH meter to identify the acidic or alkaline characteristic of fly ash. The suspension was stirred well and allowed to come to room temperature ($25\pm1°C$) before taking the pH measurement. The pH of raw fly ash and fly ash-surfactant-NaSal-lime were obtained, which varied within 6.67 to 12.5 (Table 3.12). The pH value increased by more than 50% at 5% lime content which remained almost constant after that (Figure 3.10). Therefore, on the basis of pH study (Figure 3.10), a fixed percentage of quick lime i.e. 5% was used in preparing the fly ash composites along with 0.2% CTAB and 0.2% NaSal (Table 3.13) for evaluation of strength properties.

3.10.2. OMC-MDD Study

Moisture content and dry unit weight have direct bearing on the compaction of particles. There exists an optimum quantity of moisture content at which the dry unit weight is maximum. Modified proctor compaction test was carried out as per IS: 2720 – Part (1983) to determine the maximum dry density and optimum moisture content of the fly ash- lime-

surfactant-NaSal mixes for preparation of specimen samples. The samples were prepared at their respective OMC and MDD. The ingredients such as fly ash, lime, surfactant, and NaSal were blended in the required proportion in dry condition. The dry mixed ingredients were put in a poly pack, covered, and left for about an hour for homogenization. Then required amount of water was added to the mixture and mixed thoroughly. The mixture was left in a closed container for uniform mixing and to prevent loss of moisture to atmosphere. The wet mixture was compacted in the proctor mould.

Table 3.12: Lime – pH relationship

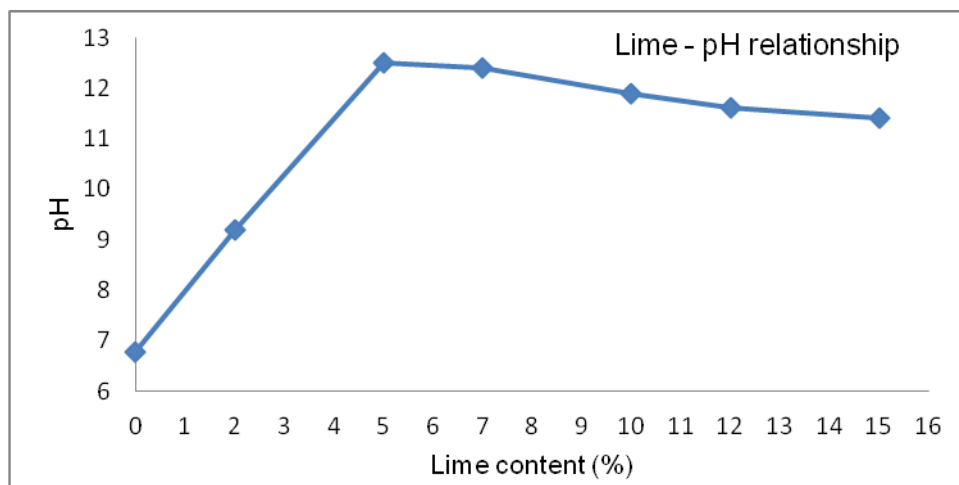| Lime %	pH
0	6.77
2	9.2
5	12.5
7	12.4
10	11.9
12	11.6
15	11.4

Figure 3.10: Lime-pH relationship diagram

Table 3.13: Various proportions of fly ash, surfactant (CTAB), NaSal, and Lime

Sl.No.	Ingredients	Percentage (%)
1.	Fly Ash	94.6%
2.	Lime	5.0%
3.	CTAB	0.2%
4.	NaSal	0.2%

3.10.3. Sample preparation for UCS test

A Mould of 38 mm diameter and 76 mm length was used for preparation of the unconfined compressive strength (UCS) test samples as per IS: 2720-part 10 (1991). Samples were prepared with uniform tamping. Two circular metal spacer discs of height 5 mm and diameter 37.5 mm each with base (7 mm height, 50 mm diameter) were used at top and bottom ends of the mould to compact the sample such that the length of the specimen was maintained at 76 mm (Figure 3.11). Then the discs were removed and another spacer disc of height 100 mm and diameter 37.5 mm with a base (height 7 mm, 50 mm diameter) was used to remove the sample from the mould. The final prepared specimen had length to diameter ratio of 2 (Figures 3.12 and 3.13).

Figure 3.11: UCS mould for sample preparation

3.10.4. Sample Preparation for Tensile Strength Test

The determination of direct tensile strength of soil or rock material is difficult. So, indirect way (Brazilian tensile strength) of its determination is practiced. The Brazilian tensile test make the sample fail under tension though the loading pattern is compressive in nature. The tensile strength was determined as per ASTM D 3967. The sample for Brazilian tensile strength test was prepared using the same mould of UCS test samples. For this purpose, two circular metal spacer discs of 5 mm and 62 mm heights and 37.5 mm diameters with base (height 7 mm, 50 mm diameter) were used. The final prepared specimen had length

to diameter ratio of 0.5. The specimens prepared for tensile strength test were of 38 mm diameter and 19 mm thick. The specimens were placed diametrically during test. The sample fails diametrically in tension by application of load.
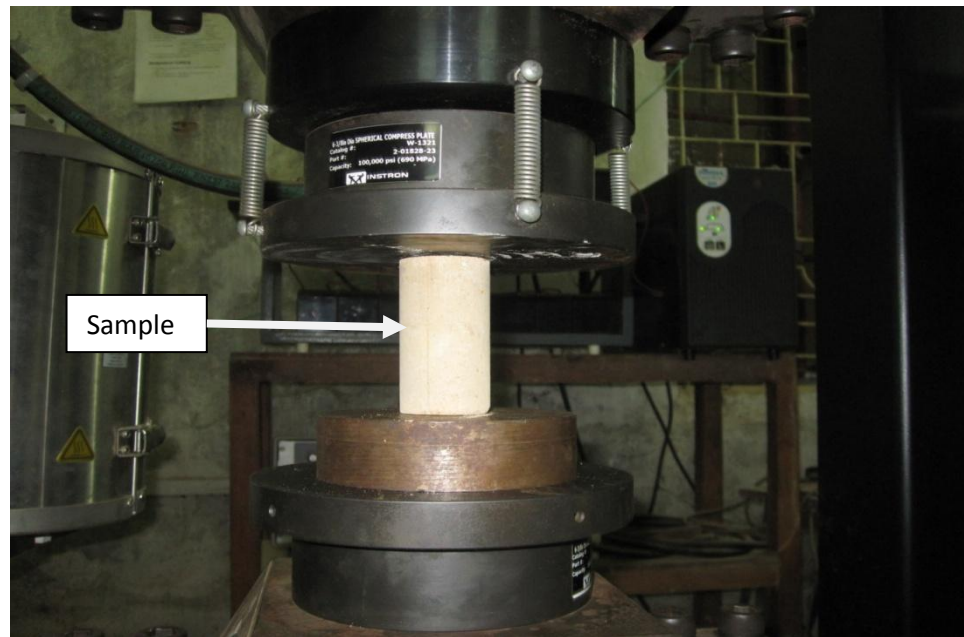
Figure 3.12: Sample inside mould for UCS test

Figure 3.13: Sample of UCS specimens prepared (undergoing curing)

3.10.5. Sample preparation for ultrasonic pulse velocity test

Ultrasonic pulse velocity test is a nondestructive testing technique typically used to determine the dynamic properties of materials. The accuracy of it is influenced by many factors such as direction, material composition, dampness, weaknesses present, travel

distance, and diameter of transducer. This test was carried out as per IS: 10782 (1983). The specimen used for the uniaxial compression tests were used for it. The ultrasonic pulse velocity test is a measurement of the transit time of a longitudinal vibration pulse through a sample of known path length. It is carried out with two transducers (transmitting and receiving) placed at the opposite ends of the samples (Figure 3.14).
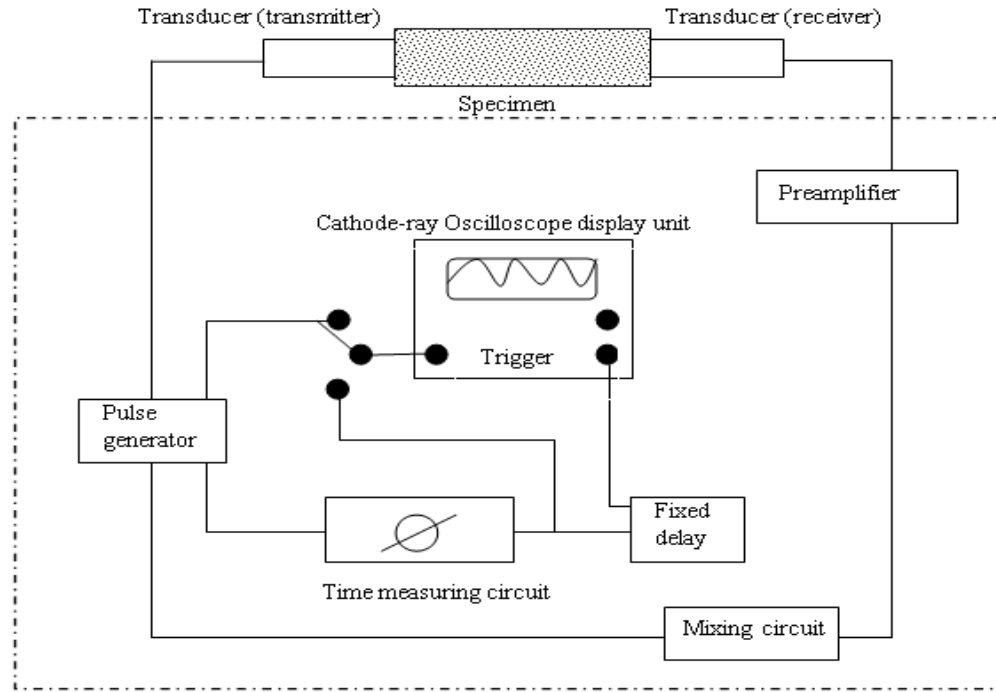
Figure 3.14: Schematic representation of ultrasonic velocity measurement

The electrical impulses of a specified frequency are generated by pulse generator that is converted into elastic waves which propagate through the sample by the transmitter. The mechanical energy of the propagating waves that propagate through the sample are received by the transducer (receiver) placed at the opposite end and then turns into electrical energy of the same frequency. The signal travel time through the specimen is registered in the oscilloscope.

The relationship between various parameters on pulse velocity, density, elastic constants, modulus values are given by the following equations.

$$v = \frac{V_p{}^2 - 2V_s{}^2}{2\left(V_p{}^2 - V_s{}^2\right)} \dots\dots\dots\dots\dots\dots\dots\dots\dots\dots\dots\dots\dots\dots\dots\dots \quad (3.14)$$

$$E = \frac{\rho\, V_s{}^2 \left(V_p{}^2 - 4V_s{}^2\right)}{V_p{}^2 - V_s{}^2} \dots\dots\dots\dots\dots\dots\dots\dots\dots\dots\dots\dots\dots\dots \quad (3.15)$$

$$K = \frac{\rho (V_p{}^2 - 4V_s{}^2)}{3} \quad \cdots\cdots\cdots\cdots\cdots\cdots\cdots\cdots\cdots\cdots\cdots\cdots \quad (3.16)$$

$$G = \rho V_s{}^2 \quad \cdots\cdots\cdots\cdots\cdots\cdots\cdots\cdots\cdots\cdots\cdots\cdots\cdots\cdots \quad (3.17)$$

Where, V_p= compression P wave velocity, m/s, V_s= shear S wave velocity, m/s, = density, kg/m³, v= Poisson's ratio, E= Young's Modulus, Pa, K= Bulk Modulus, Pa and G= Shear (Rigidity) Modulus, Pa.

3.10.6. Methods of Testing

3.10.6.1. Tri-axial Compression Test

Material properties as cohesion and angle of internal friction of the fly ash-Surfactant-NaSal-Lime composite material were determined from triaxial tests. The un-drained, tri-axial compression test was carried out as per IS: 2720 – Part 11 (1993). Three identical samples of 38 mm diameter and 76 mm length were prepared at optimum moisture content and maximum dry density of the materials obtained from the modified proctor compaction test. The samples were tested by giving confining pressures of 1 kg/cm², 2 kg/cm² and 3 kg/cm² respectively. Average values of three tests for each type were considered for analysis. Mohr-Coulomb relation between two normal stresses ($\tau = C + \sigma_n \tan\varphi$) was used to determine cohesion and angle of internal friction of the materials.

3.10.6.2. Compaction test

Modified proctor compaction test is typically used to give a higher standard of compaction. It was performed to determine the maximum dry density and optimum moisture content of the materials. The sample was compacted in the mould in five layers using a rammer of 4.9 kg mass with a fall of 450 mm by giving 25 blows per layer (Das and Yudhbir, 2006). The compacted energy value given was 2674 kJ/m³. Figure 3.15 depicts the arrangements made for sample preparation.

3.10.6.3. Unconfined Compressive Strength Test

Unconfined compressive strength test was carried out to determine the resistance of material to any external loading. The availability of free lime and reactive silica and aluminum etc. play a vital role in strength gain. Moisture content has direct effect on

reactivity. Hence it is preserved by curing the sample in a controlled chamber with > 95% humidity at 30 ± 2^0C. The unconfined compressive strength tests were conducted at a strain rate of 1.2 mm/min load and deformation data were recorded till failure of the specimen. The experimental set up and prepared samples for unconfined compression test are shown in Figure 3.16.

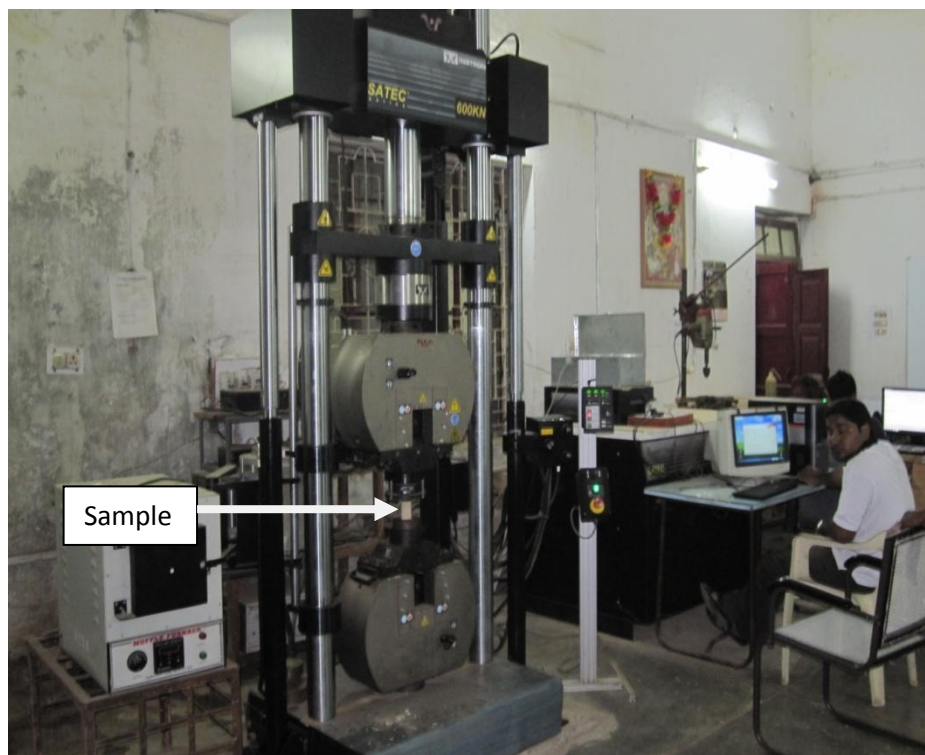Figure 3.15: Sample preparation for proctor compaction test

Figure 3.16: Unconfined Compressive Strength Test (make: Instron K600, UK)

3.10.6.4. Brazilian tensile strength test

Determination of direct tensile strength of soil or rock mass is difficult so indirect test i.e. Brazilian tensile test is practiced in real life situations. The Brazilian tensile test make the sample fail under tension though the loading pattern is compressive in nature. The samples were placed diametrically on the disc during testing (Figure 3.17). The sample fails diametrically in tension by application of load. The indirect tensile strength is calculated as:

$$\sigma_t = \frac{2P}{\pi D t} \qquad (3.18)$$

Where σ_t = Brazilian Tensile Strength, P = Failure load, D = Diameter of the sample, t =thickness of the sample.
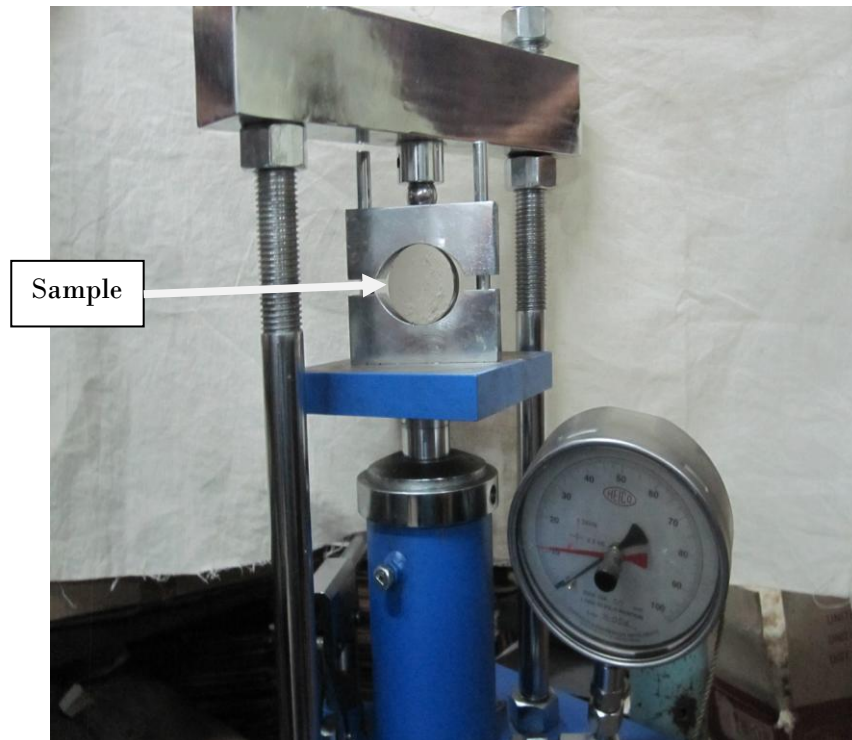
Figure 3.17: Test set up for Brazilian tensile strength test (make: HEICO, India)

3.10.6.5. Ultrasonic Pulse Velocity Test

P-wave velocity values of developed composites were determined using an ultrasonic velocity measurement system (make: GCTS, USA; Figure 3.14). This system includes 10 MHz bandwidth receiver with pulse raise time less than 5 nano-seconds, 20 MHz acquisition rate with 12 bit resolution digitizing board, transducer platens with 200 kHz compression mode and 20 kHz shears mode. The test was carried out by applying two sensors to opposite surface of the specimen. Sufficient surface contact between the sensors and the specimen was

maintained by a couplet such as honey. Figure 3.18 depicts the Ultrasonic pulse velocity test instrument and a view of test in progress. Figure 3.19 shows a typical P-wave velocity signal plot of fly ash composites.

Figure 3.18: Ultrasonic pulse velocity test instrument and view of test in progress

Figure 3.19: A typical P-wave velocity signal plot of fly ash composite

3.11. Experimental Size
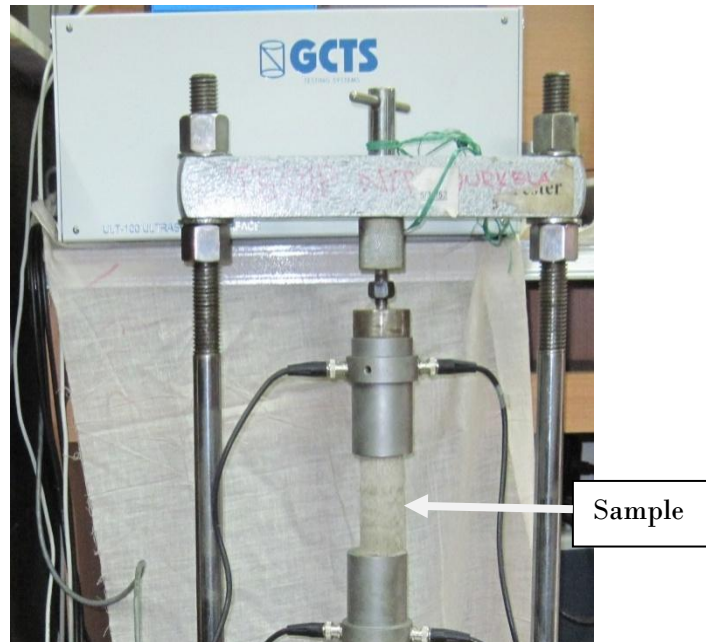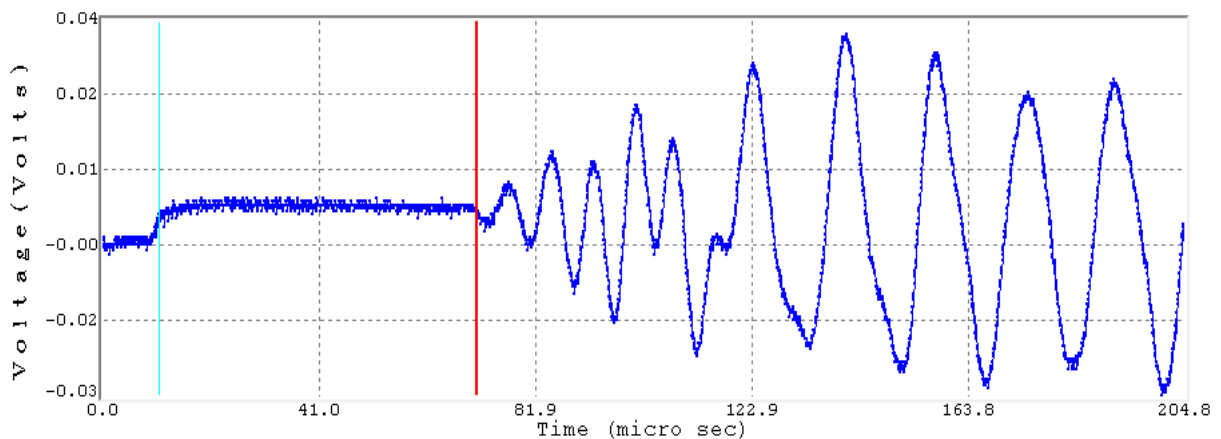
3.11.1. Characterization

Seven number of fly ash samples were characterized with a view to select the best material for flow and in-place strength study. The various tests conducted and number of samples tested is presented in Table 3.14.

Table 3.14: Experimental size for characterization study

Sl. No.	Type of test	No. of samples tested
1	XRD	21
2	SEM	21
3	EDX	21
4	XRF	7
5	Specific gravity	21
6	Specific surface area	21
7	Particle size analysis	21
8	Turbidity	21
9	pH	21
10	Surface tension	18
11	Zeta potential	18
12	Settling study	21
13	FTIR	21
		Total number of tests conducted= 253

3.11.2. Rheology

The surface nature of fly ash particles is an important factor in the high solid/ liquid ratio (fly ash-water) suspensions behavior. With a view to modify the surface properties of the fly ash particles in this investigation, a cationic surfactant CTAB was used along with a counter-ion NaSal to study the rheological properties of chemically treated fly ash slurry. Solid concentrations varying from 20% to 60% by weight of fly ash-water suspensions was treated with surfactant and counter-ion and analyzed experimentally at varying temperature environment (20^0C to 40^0C). Table 3.15 and Figure 3.20 present the detailed parametric variations and scheme of experimental studies designed for this investigation.

Table 3.15.Detailed parametric variations and scheme of experimental design for rheology study

FA (g)	CTAB (g)	NaSal (g)	WATER (ml)	TEMPERATURE (^{0}C)	SHEAR RATES (1/s)
20.0	0.0	0.0	80	20, 25, 30, 35, 40	100, 200, 300, 400, 500
19.8	0.1	0.1	80	20, 25, 30, 35, 40	100, 200, 300, 400, 500
19.6	0.2	0.2	80	20, 25, 30, 35, 40	100, 200, 300, 400, 500

| 19.4	0.3	0.3	80	20, 25, 30, 35, 40	100, 200, 300, 400, 500
19.2	0.4	0.4	80	20, 25, 30, 35, 40	100, 200, 300, 400, 500
19.0	0.5	0.5	80	20, 25, 30, 35, 40	100, 200, 300, 400, 500
30.0	0.0	0.0	70	20, 25, 30, 35, 40	25, 50, 100, 200, 300, 400, 500
29.8	0.1	0.1	70	20, 25, 30, 35, 40	25, 50, 100, 200, 300, 400, 500
29.6	0.2	0.2	70	20, 25, 30, 35, 40	25, 50, 100, 200, 300, 400, 500
29.4	0.3	0.3	70	20, 25, 30, 35, 40	25, 50, 100, 200, 300, 400, 500
29.2	0.4	0.4	70	20, 25, 30, 35, 40	25, 50, 100, 200, 300, 400, 500
29.0	0.5	0.5	70	20, 25, 30, 35, 40	25, 50, 100, 200, 300, 400, 500
40.0	0.0	0.0	60	20, 25, 30, 35, 40	25, 50, 100, 200, 300, 400, 500, 600, 700, 800, 900, 1000
39.8	0.1	0.1	60	20, 25, 30, 35, 40	25, 50, 100, 200, 300, 400, 500, 600, 700, 800, 900, 1000
39.6	0.2	0.2	60	20, 25, 30, 35, 40	25, 50, 100, 200, 300, 400, 500, 600, 700, 800, 900, 1000
39.4	0.3	0.3	60	20, 25, 30, 35, 40	25, 50, 100, 200, 300, 400, 500, 600, 700, 800, 900, 1000
39.2	0.4	0.4	60	20, 25, 30, 35, 40	25, 50, 100, 200, 300, 400, 500, 600, 700, 800, 900, 1000
39.0	0.5	0.5	60	20, 25, 30, 35, 40	25, 50, 100, 200, 300, 400, 500, 600, 700, 800, 900, 1000
50.0	0.0	0.0	50	20, 25, 30, 35, 40	25, 50, 100, 150, 200, 250, 300, 350, 400, 500, 600, 700, 800, 900, 1000
49.8	0.1	0.1	50	20, 25, 30, 35, 40	25, 50, 100, 150, 200, 250, 300, 350, 400, 500, 600, 700, 800, 900, 1000
49.6	0.2	0.2	50	20, 25, 30, 35, 40	25, 50, 100, 150, 200, 250, 300, 350, 400, 500, 600, 700, 800, 900, 1000
49.4	0.3	0.3	50	20, 25, 30, 35, 40	25, 50, 100, 150, 200, 250, 300, 350, 400, 500, 600, 700, 800, 900, 1000
49.2	0.4	0.4	50	20, 25, 30, 35, 40	25, 50, 100, 150, 200, 250, 300, 350, 400, 500, 600, 700, 800, 900, 1000
49.0	0.5	0.5	50	20, 25, 30, 35, 40	25, 50, 100, 150, 200, 250, 300, 350, 400, 500, 600, 700, 800, 900, 1000
60.0	0.0	0.0	40	20, 25, 30, 35, 40	10, 20, 25, 30, 40, 50, 60, 70, 80, 90, 100, 200
59.8	0.1	0.1	40	20, 25, 30, 35, 40	10, 20, 25, 30, 40, 50, 60, 70, 80, 90, 100, 200
59.6	0.2	0.2	40	20, 25, 30, 35, 40	10, 20, 25, 30, 40, 50, 60, 70, 80, 90, 100, 200
59.4	0.3	0.3	40	20, 25, 30, 35, 40	10, 20, 25, 30, 40, 50, 60, 70, 80, 90, 100, 200
59.2	0.4	0.4	40	20, 25, 30, 35, 40	10, 20, 25, 30, 40, 50, 60, 70, 80, 90, 100, 200
59.0	0.5	0.5	40	20, 25, 30, 35, 40	10, 20, 25, 30, 40, 50, 60, 70, 80, 90, 100, 200
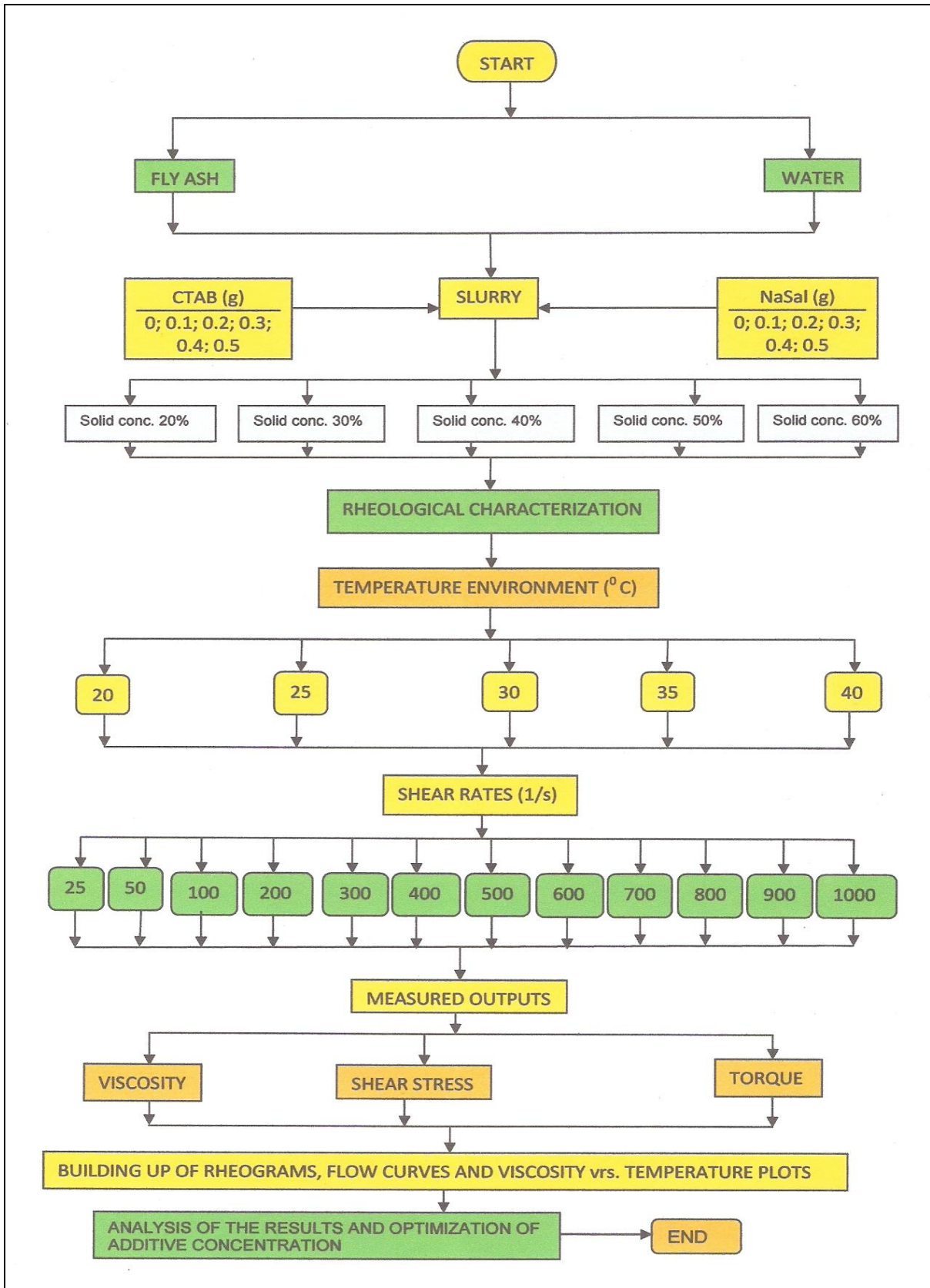
Figure 3.20: Parametric variations and scheme of experimental investigations for rheology study

3.11.3. Strength

The investigation included many characterization studies including major laboratory tests such as compaction, unconfined compressive strength (UCS), Brazilian tensile strength (BTS), Ultrasonic pulse velocity tests. The reported results represent average values of three to four samples for each test type except that for compaction to determine MDD and OMC. The test results that were not within 4% to 7% of each other were discarded and fresh samples were prepared and tested. The total numbers of tests conducted were 21 with about 65 samples (Tables 3.16 – 3.18).

Table 3.16: Various proportion of fly ash, CTAB, NaSal, Lime and Water for different curing periods

Sample No.	FA (g)	CTAB (g)	NaSal (g)	Lime (g)	Water (ml)	Curing Period (days)	Type of test	No. of samples tested
1	29.32	0.062	0.062	1.55	3.8	0	UTS	3
2	117.58	0.248	0.248	6.2	15.53	0	UCS	3
3	117.58	0.248	0.248	6.2	15.53	0	Triaxial	3
4	117.58	0.248	0.248	6.2	15.53	0	Ultrasonic	3
5	29.32	0.062	0.062	1.55	3.8	7	UTS	3
6	117.58	0.248	0.248	6.2	15.53	7	UCS	3
7	117.58	0.248	0.248	6.2	15.53	7	Triaxial	3
8	117.58	0.248	0.248	6.2	15.53	7	Ultrasonic	3
9	29.32	0.062	0.062	1.55	3.8	14	UTS	3
10	117.58	0.248	0.248	6.2	15.53	14	UCS	3
11	117.58	0.248	0.248	6.2	15.53	14	Triaxial	3
12	117.58	0.248	0.248	6.2	15.53	14	Ultrasonic	3
13	29.32	0.062	0.062	1.55	3.8	28	UTS	3
14	117.58	0.248	0.248	6.2	15.53	28	UCS	3
15	117.58	0.248	0.248	6.2	15.53	28	Triaxial	3
16	117.58	0.248	0.248	6.2	15.53	28	Ultrasonic	3
17	29.32	0.062	0.062	1.55	3.8	56	UTS	3
18	117.58	0.248	0.248	6.2	15.53	56	UCS	3
19	117.58	0.248	0.248	6.2	15.53	56	Triaxial	3
20	117.58	0.248	0.248	6.2	15.53	56	Ultrasonic	3
						Total number of samples tested =		60

Table 3.17: Total number of tests conducted

Proctor compaction	UCS	BTS	Triaxial	P-Wave velocity
1	5	5	5	5
			Total = 1+5+5+5+5 = 21	

Table 3.18: Total number of samples tested

Proctor compaction	UCS	BTS	Triaxial	P-Wave velocity
1x3	5x3=15	5x3=15	5x3=15	5x3=15
Total = 3+15+15+15+15=63				
(Excluding tests for material characterization and rheology = 200 samples)				

Table 3.19: Experimental Design Chart

Sl. No.	Compositions	Compaction	UCS				UTS				Triaxial				P-wave velocity			
	(FA+CTAB+NaSal+ Lime+Water)		7	14	28	56	7	14	28	56	7	14	28	56	7	14	28	56
1	(29.32+0.062+0.062+ 1.55+3.8)	☐	*	*	*	*	+	+	+	+	..	..	..	..	-	-	-	-
2	(117.58+0.248+0.248 +6.2+15.53)	☐	*	*	*	*	+	+	+	+	..	..	..	..	-	-	-	-
3	(117.58+0.248+0.248 +6.2+15.53)	☐	*	*	*	*	+	+	+	+	..	..	..	..	-	-	-	-

<div align="right">

CHAPTER 4

</div>

4. Results and Discussion

This chapter describes the results obtained from laboratory studies in three different sections. First section discusses the results obtained from material characterization study to select the best material out of seven different samples studied. Second section describes the results obtained from rheology tests for the selected best material at varying shear rates and temperature environment. Third section deals with the results obtained from strength study of the optimized fly ash slurry material at varying curing periods i.e., 0, 7, 14, 28, and 56 days.

4.1. Introduction

Slurries commonly refer to mixture of settling particles and some certain liquid such as water. The transport of slurries by hydraulic pipelines is widespread in the minerals, metallurgy, water, and some other industrial applications to carry the raw materials and their products to the designated places. Similarly, fly ash can be transported most economically over great distances using a hydraulic slurry pipeline. Notwithstanding the good technical results achieved by fly ash slurry technologies, technical areas, which deserve further development work, still exist. Design data for slurry pipeline systems are usually obtained using pilot plant studies. The high correlations obtained between pilot plant data and rheometer data suggests that it is possible to use a simple co-axial concentric rotational rheometer instead of a specially designed pilot plant in the design of slurry pipelines (Blissett and Rowson, 2013). The primary objective of this work was to investigate the rheological properties of concentrated fly ash slurries by using rheological instruments with a view to transport the material smoothly and economically (by reducing drag friction) to mine site area to fill worked out empty void spaces. Fine fly ash slurry may be described as a colloidal system in which the solids are dispersed through the liquid. Because of the high surface charge to mass ratio of fly ashes, van der Waals attractive forces and electrostatic repulsive forces dominate particle-particle interactions. It is the sum total of these two forces between

particles that determine the nature of the slurry rheology. The net particle interactions can be strongly repulsive, where the particles remain dispersed, so that the fluid exhibits Newtonian flow characteristics. The rheological properties of fine fly ash slurries can be manipulated by altering the concentration of solids and by controlling the electrostatic repulsive forces between the particles. The electrostatic repulsive forces can be increased or decreased by manipulating the pH and the ionic content in the suspending medium. Increasing the repulsive forces with the addition of a dispersing agent may break down the structure and reduce or eliminate non-Newtonian flow behaviour. Alternatively, the net interaction between particles can be strongly attractive so that a floc structure will be created. Flocs can form networks which cause the slurry to exhibit non-Newtonian flow characteristics. This structure can resist shear distortion giving the fluid a yield stress. With the addition of small amounts of specific chemical reagents it is possible to manipulate particle-particle interactions between fly ash particles in the slurry. Variations in flow behaviour including elimination of yield stress are associated with these changes. Almost all pipelines in the world today are transporting material in the turbulent flow regime using a critical velocity to keep the particles in suspension (Ihle and Tamburrino, 2012). Laminar flow attracts sedimentation and blockage of the pipelines. Therefore, rheological characterization is essential before designing any pipeline system. The engineering properties of a material are dependent to a large extent on the composition of material. There exists wide variation in the composition of fly ash depending on coal types, types of furnace, temperature, collection technique, etc. The geotechnical properties of the developed composite materials were also determined as per established methods. All the results of the current investigation and their corresponding analysis have been presented in different sections as mentioned below:

a.   Characterization of ingredients (fly ash) from seven different sources
b.   Selection of best fly ash material for rheology study
c.   Rheological investigation of the selected material
d.   Selection of best composite material with respect to its flow characteristics
e.   Geotechnical properties of developed composite materials
f.   Analysis of the results at different parametric variations

4.2. Section-I

4.2.1. Characterization of ingredients

The primary aim of this investigation was to develop fly ash based composite materials suitable for mine filling applications. So a detailed analysis of the constituent materials was first carried out to select the best material out of seven different sources for further study with respect to its flow and in-place strength characteristics. The results of the material characterization study are reported here as given below.

4.2.1.1. Physical properties

Physical properties help in classifying the coal ashes for engineering purposes and some are related to engineering properties. The fly ash was collected in dry state and was in loose stage. Its average water content was less than 1%. The fly ash used had a powdery structure with medium to dark grey colour indicating low lime content (Meyers *et al.*, 1976). The measured physical properties of seven fly ash samples are reported in Table 4.1.

4.2.1.1.1. Specific gravity (G)

Sp. gr. is an important physical property for evaluating geotechnical applications. A series of tests were conducted to determine the sp. gr. (G) values of the fly ash samples, and the average values of G are reported in Table 4.1. These values ranged from 2.20 to 2.27, indicating some variation among ash sources. The sp. gr. of F_1 is lower as compared to other ash sources i.e. 2.20 which are due to high percentage of fine particles. As reported by Kim and Chun (1994), the variation in G values is attributable to two factors: (1) chemical composition, and (2) presence of hollow fly ash particles or particles with porous or vesicular textures.

Different amounts of hollow particles present in fly ash caused a variation in apparent sp. gr. The apparent sp. gr. is also affected by the porosity of its particles. This variation may also be due to trapped micro bubbles of air in ash particles (Trivedi and Singh, 2004). Guo *et al.,* (1996) examined the chemical compositions of hollow and solid fly ash particles separately, and the data revealed that hollow-particle fly ash had significantly lower iron content (4.5%) than solid particle fly ash (25%).

4.2.1.1.2. Specific surface area and **bulk density**

The specific surface area of the fly ash samples varies between 0.187 m^2/g and 1.24 m^2/g and the bulk density of the fly ash samples ranged between 1.60 g/cm^3 and 1.99 g/cm^3 (Table 4.1). Though there is little difference in values, comparatively, the average sp. gr. and bulk density of fly ashes were found to be less than that of river bed sand. The F_1 fly ash is having less sp. gr. and more specific surface area compared to others which would also facilitate possible surface modification by chemical additives for smooth flow in the pipelines. A larger specific surface area of fly ash will make the fly ash particles more easily grafted by the surfactant, making it more suitable to be modified. The high specific surface area of fly ash will also result in a strong adsorptive capacity of fly ash to surfactant suspensions.

4.2.1.1.3. Porosity and moisture content

The porosity of the bulk fly ash samples varied between 9.135% and 34.2% and the moisture content varied between 0.15 % - 0.8% (Table 4.1). The presence of pores in fly ash may influence the eventual chemical state of the adsorbed vapour by shielding material contained in pores from photochemical degradation (Schure *et al.*, 1985).

Table 4.1.Physical properties of fly ash samples

Parameters	F_1	F_2	F_3	F_4	F_5	F_6	F_7
Colour	Grey	Grey	Grey	Dark grey	Light grey	Light grey	Light grey
Specific gravity (G)	2.20	2.23	2.27	2.25	2.26	2.24	2.21
Bulk density (ρ), g/cm^3	1.75	1.6	1.67	1.89	1.95	1.99	1.80
Porosity (φ), %	20.5	34.2	15.7	19.6	20.732	9.135	18.55
Moisture content, %	0.20	0.8	0.25	0.15	0.398	0.22	0.401
Specific surface area, m^2/g	1.24	0.185	0.458	0.187	0.408	0.428	0.395
Particle size analysis							
D(4,3), μm	171.61	14.27	48.204	91.26	48.214	59.79	65.608
D(3,2), μm	8.5	5.04	13.105	32.05	13.115	14.003	15.175
D_{90}	988.5	30.831	113.727	187.61	113.757	144.133	158.144
D_{50}	11.2	8.367	29.972	74.573	29.871	39.375	43.47
D_{10}	3.81	2.649	7.184	18.013	7.173	7.248	7.966
Coefficient of uniformity, C_u	6.3	1.15	1.12	0.70	1.13	1.09	1.07

4.2.1.1.4. Grain size analysis

The grain size distribution of fly ashes is very important factor for their use as pozzolans as it influences the strength behaviour. It provides information related to particle size- whether coarse grained or fine grained and their gradation, etc. The particle sizes of seven fly ash samples exhibit wide variations (Figures 4.1- 4.4), with F_4 being the coarsest and F_2 the finest fly ash. The results of particle size analysis of the fly ash samples are also summarized in Table 4.2. The grain size distributions for the fly ash samples indicated that the fly ash samples consist of sand-sized (<4.75 mm), silt-sized (0.075-0.002 mm), and clay-sized (<0.002 mm) particles. The sample from F_1 (ETPS) exhibits a near normal distribution of fines and coarse fractions. Almost 90% of the particles are less than 50 µm which confirms to the ASTM (D 2487-06, 2006). Fly ashes from other six sources though possess fine sizes; the percentage is less than that of F_1.

4.2.1.1.5. Coefficient of uniformity

The coefficientt of uniformity ($C_u=D_{60}/D_{10}$), defined as the ratio of the 60% passing size to 10% passing size affects the workability of the fly ash grains. Backfill materials with a C_u ranging from 4 to 6 would show improved packing density, reduced porosity, and generally high friction angle (Sargeant, 2008; Eromoto *et al*., 2006). The higher the coefficient of uniformity, the better is its adaptability to compaction and hence strength. The coefficient of uniformity of the seven samples varies from 0.70 to 6.3. The minimum value belongs to PTPS (F_4) which has highest fraction of coarsest particles. The maximum value 6.3 was exhibited by ETPS (F_1). This value is more than 6, thus the fly ash particles can be regarded as well graded (Sridharan and Prakash, 2007). Other fly ash specimens show C_u value less than 6. Hence the fly ash sample F_1 is well graded compared with the other fly ash samples as per the classification and gradation of soils (ASTM International D 2487-06, 2006).

Also, only the F_1 fly ash sample depicted bi-modal particle size distribution thought to be the sum of two normal distributions. These materials are known to favour high densities of the consolidated mass because of their enhanced packing characteristics (Oberacker *et al*., 2001).
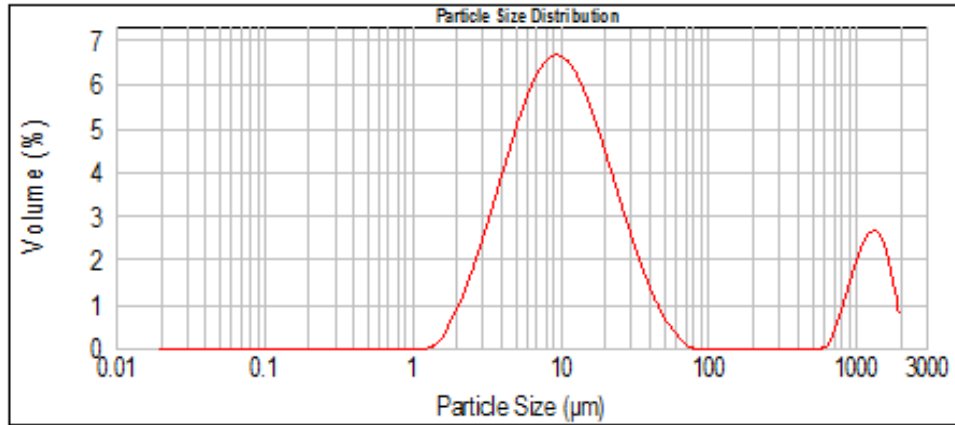
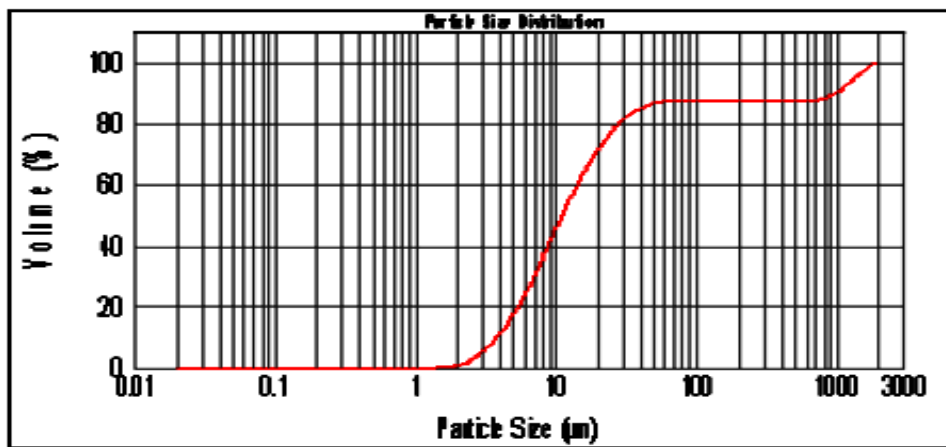Figure 4.1.Particle size distribution curve of fly ash sample F_1

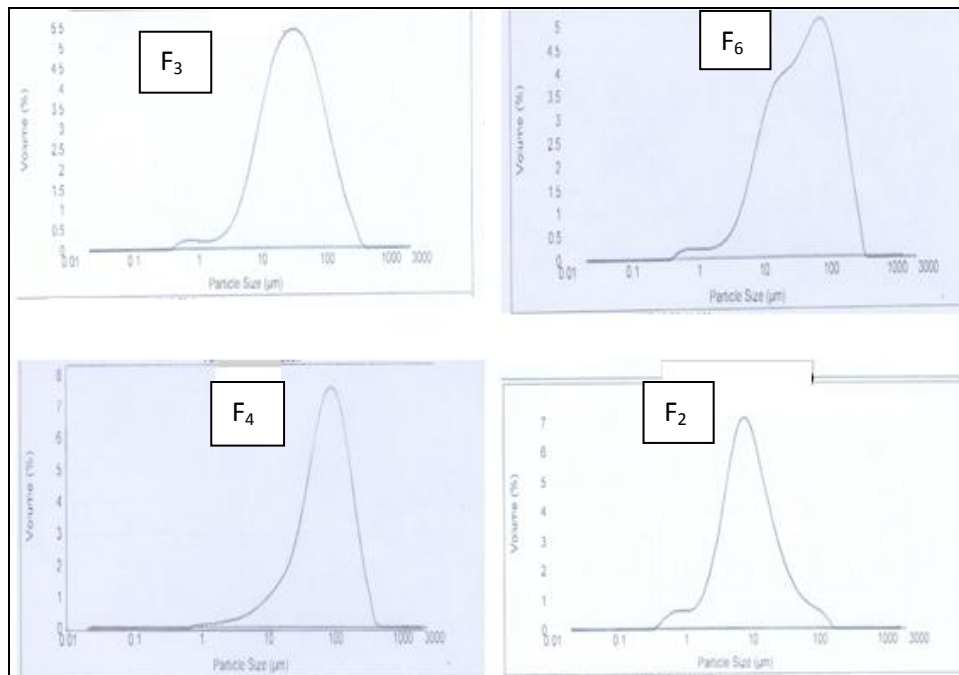Figure 4.2.Particle size distribution of F_1 fly ash sample

Figure 4.3.Particle size distribution curve of fly ash samples F_3, F_6, F_4 and F_2

4.2.1.2. Morphological properties

The SEM photomicrographs depicted the presence of particles with different shapes namely, glassy solid spheres, hollow sphere (cenospheres), broken, sphere within another sphere (plerosphere), tubular, smooth porous grains, and some other irregularly shaped particles (Figures 4.5 and 4.6). These particles affect the compaction behaviour (Leonards and Bailey, 1982). The micrographs depict without any formation of cementitious compounds. It confirms that the fly ash used in this investigation has low calcium content. It compares favourably well to those observed elsewhere (Baker and Laguros, 1984).

Table 4.2.Results of particle size analysis of fly ash samples

Sample ID	Size range (%)		
	‹ 1 µm	1 µm - 50 µm	› 50 µm
F_1	3.66	87.80	08.54
F_2	2.77	92.73	04.50
F_3	1.02	68.20	30.78
F_4	0.10	34.37	65.53
F_5	1.02	68.40	30.58
F_6	0.97	58.07	40.96
F_7	0.90	55.16	43.94

The fly ash investigated is predominantly fine grained and mostly composed of compact or hollow spheres of different sizes. Some other vitreous unshaped fragments also can be seen in the F_7 fly ash sample. SEMs also show that the spheres in the F_2 fly ash sample are more closely packed than those in the other samples; thus, F_2 exhibits the lowest surface area and pore volume. Unlike other samples, F_4 has many unshaped fragments that are ascribed to unburned char (Trivedi and Singh, 2004; Wang *et al.*, 2008). Spherical particles make up most of the fly ash, especially in the finer fractions. These spheres are glassy and mostly transparent (Figure 4.5: F_1, F_2; and Figure: 4.6, F_6), indicating complete melting of silicate minerals. The few opaque spheres (Figure 4.6, F_7) are mostly composed of magnetite or other iron oxide particles (Fisher *et al.*, 1978). The fly ash particles in F_1 sample are similar in shape and form- distinctly spherical shape which is considered to be ideal material for mine

filling purposes (Canty and Everett, 2001). It is apparent that F_1 fly ash has much superior particle morphology than the other fly ashes. Comparatively, it has more spherical particles compared with the other fly ash samples, and this feature would create a lubricating effect, known as the ball-bearing phenomena, resulting in a frictionless flow in stowing pipelines.
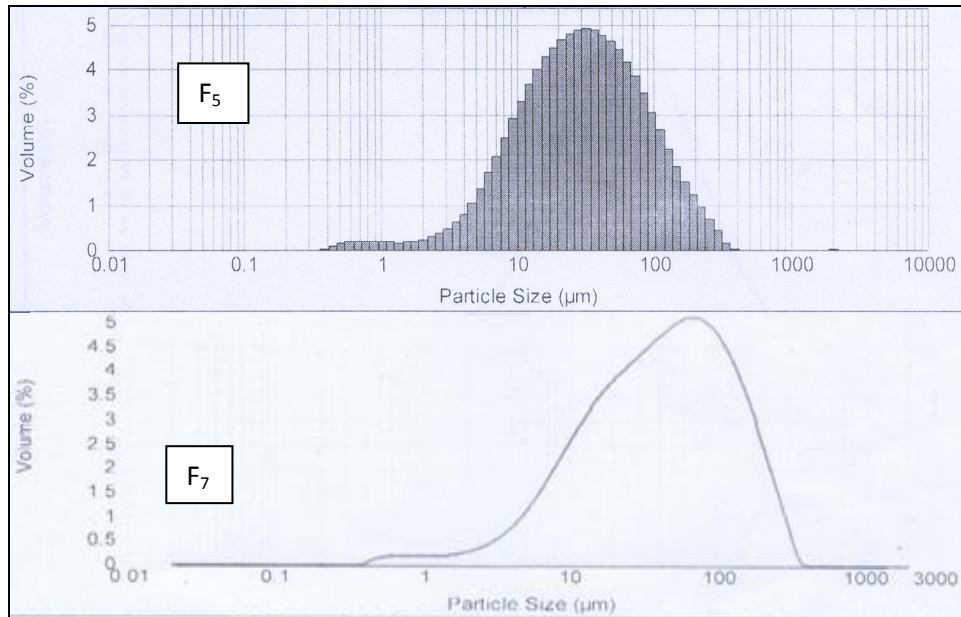

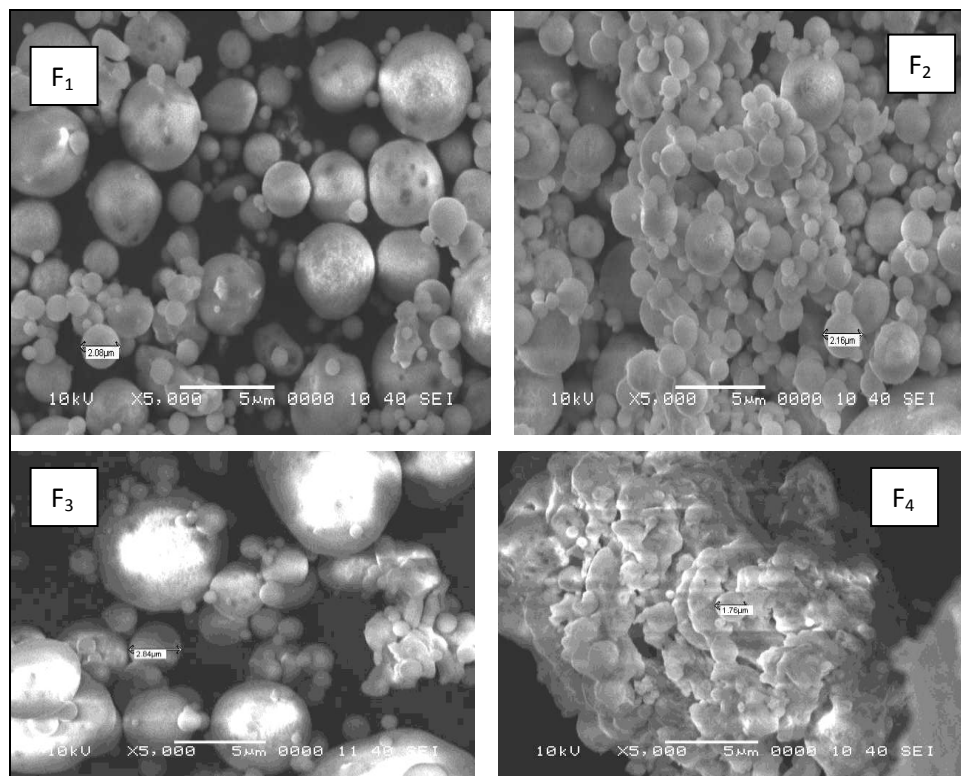Figure 4.4.Particle size distribution curve of fly ash samples F_5 and F_7

Figure 4.5.SEM Photomicrographs of F_1, F_2, F_3 and F_4 fly ash samples at 5000x
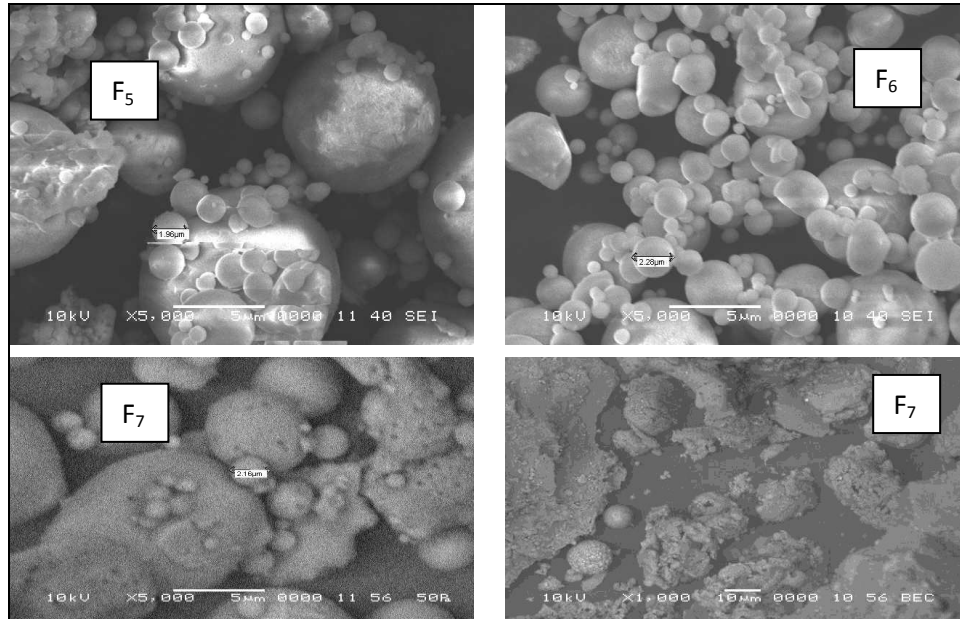
Figure 4.6.SEM Photomicrographs of F_5, F_6, and F_7 fly ash samples at 5000x and 1000x

4.2.1.3. Chemical and mineralogical properties

The chemical properties of the coal ashes greatly influence the environmental impacts that may arise out of their use/disposal as well as their engineering properties and also the chemical composition of fly ash is important indicators of suitability of a material for geotechnical applications. Hence, this calls for a detailed study of their chemical composition. The major constituents of these samples are silica (SiO_2), alumina (Al_2O_3), and iron oxide (Fe_2O_3). Minor quantities of calcium oxide (CaO), magnesium oxide (MgO), sodium oxide (Na_2O), potassium oxide (K_2O), titanium oxide (TiO_2), and other compounds are also observed to be present in lesser quantity (Table 4.3).

Table 4.3.Chemical composition of fly ashes obtained from EDX study

Sample ID	Elements (weight %)							
	SiO_2	Al_2O_3	Fe_2O_3	CaO	K_2O	TiO_2	Na_2O	MgO
F_1	56.77	31.83	1.82	0.98	1.96	2.77	0.68	2.39
F_2	59.15	34.80	3.52	0.76	2.62	1.14	0.05	0.05
F_3	59.64	35.60	2.86	0.85	1.86	0.91	0.06	0.67
F_4	68.48	22.90	3.15	0.36	0.91	1.46	0.03	0.06
F_5	62.41	31.65	3.17	0.89	2.63	0.00	3.42	0.08
F_6	62.25	30.47	2.48	0.92	1.39	0.58	0.02	1.90
F_7	61.46	36.95	2.59	0.82	2.01	0.31	0.07	0.26

The abundance of SiO_2 ($\approx$ 62% of the total composition) in all the fly ash samples would help in increasing the strength of the filling material and offer better load-bearing capacity in taking the load of the overlying strata after filling the mine voids. Because of a small amount of free lime (CaO) content (< 1%), the fly ash samples possess negligible pozzolanic or cementing properties. Because the sum total of SiO_2, Al_2O_3, and Fe_2O_3 is > 70% and CaO content is < 6% in all the fly ash samples tested, they are classified as class F fly ash (ASTM C 618-94, 1995). F_1 fly ash sample contains little higher calcium oxide content compared to other fly ash samples which would help in strength gain.

The elemental composition of fly ash samples is shown in Table 4.4, as obtained from XRF, a bulk technique that can determine average chemical composition of bulk fly ash and identify differences in matrix composition between individual particles (Hansen and Fisher, 1980). The results show that all the fly ash samples are abundant in Si and Al, and possess minor concentrations of Fe, Ca, Mg, K, Ti, and P. In the ash samples, the elements present in decreasing order of abundance are O, Si, Al, Fe, Ti, K, Ca, P, and Mg.

Table 4.4.Elemental composition of fly ashes obtained from XRF study

Elements/ Sample ID	Elements (weight %)							
	F_1	F_2	F_3	F_4	F_5	F_6	F_7	F_8
	ETPS	NALCO	OPGC	PTPS	RSPII	STPS	TTPS	ZPS
Ca	0.58	0.479	0.416	0.456	0.476	0.548	0.497	0.263
Fe	3.84	3.73	3.26	4.41	4.84	4.46	3.47	3.15
K	0.76	0.685	0.78	1.07	0.918	1.13	0.62	0.92
Mg	0.314	0.309	0.274	0.228	0.347	0.464	0.203	0.327
Na	0.086	0.070	0.056	0.064	0.075	0.082	0.058	0.067
P	0.157	0.142	0.062	0.116	0.137	0.210	0.123	0.112
S	0.044	0.072	0.025	0.033	0.124	0.040	0.029	0.055
Si	21.56	19.97	20.31	19.98	18.48	20.96	20.73	20.89
Ti	1.145	1.286	1.099	1.087	0.989	1.01	1.195	1.239
Al	16.14	17.70	15.29	13.95	13.418	15.79	15.58	17.516

Low calcium/class F fly ash has a relatively simple mineralogy consisting of aluminosilicate glass and varying amounts of the crystalline phase assemblage: quartz,

mullite, hematite, and ferrite spinel (McCarthy *et al*., 1981). The XRD patterns of the various fly ash samples are presented in Figures (4.7 - 4.9).
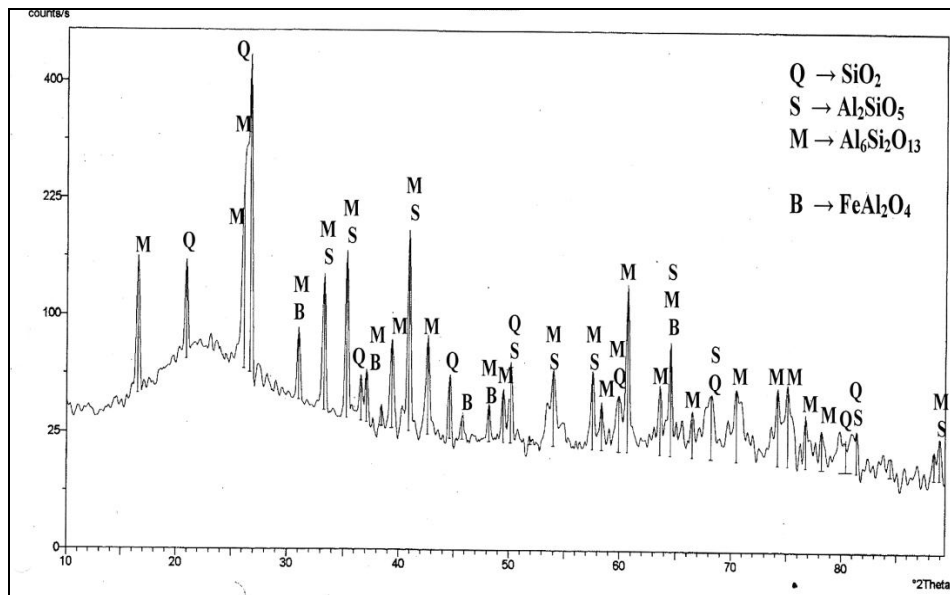
Figure 4.7.XRD Pattern of F_1 fly ash sample

The X-ray diffraction profiles of the fly ash samples indicate the presence of crystalline phases. The major mineral constituents of fly ashes are Quartz (SiO_2) and Mullite ($Al_6Si_2O_{13}$).
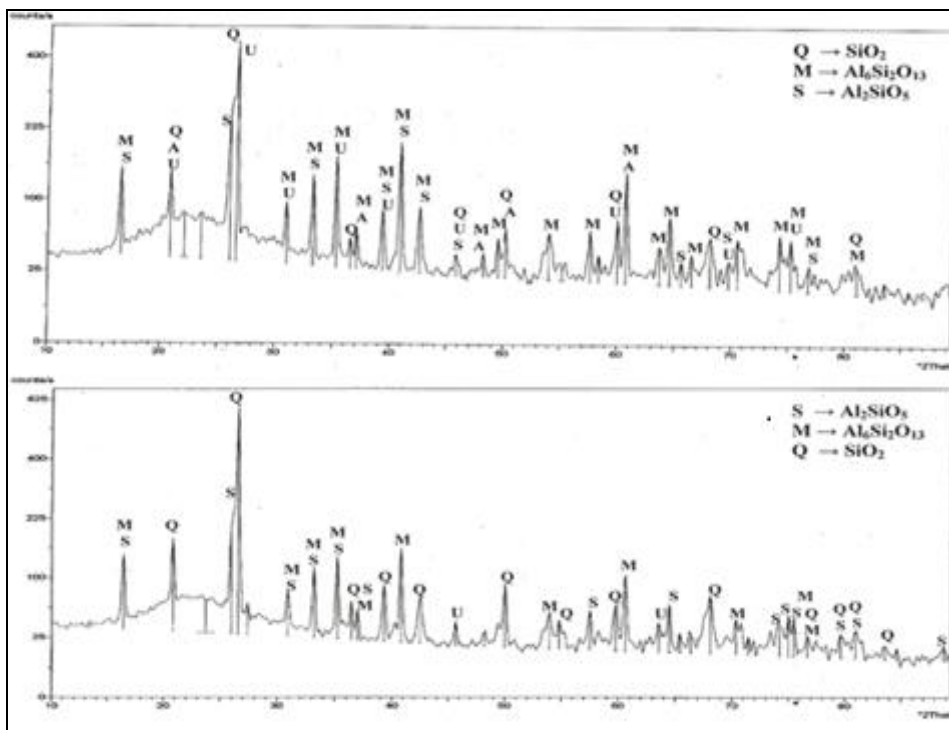

Figure 4.8.XRD Pattern of F_2 & F_3 fly ash samples

The other mineralogical fraction of the fly ash indicated the presence of hematite (Fe_2O_3), magnetite (Fe_3O_4), and rutile (TiO_2) (White & Case, 1990, Singh and Kolay, 2002). The diffractograms show that they have similar diffraction patterns. Crystalline phase quartz may be considered as the primary mineral present in all the fly ash samples, indicated by sharp peaks in the diffraction patterns (Trivedi and Singh, 2004). The peak near $2\theta=25.50^0$ are identified as mullite. The peaks which occur near $2\theta=16.5^0$ are identified as refractory mullite (Sarkar *et al.*, 2006). Along with the alumino-silicate mineral, the occurrence of strong peaks close to $2\theta=26.49^0$ indicates quartz. The presence of heavy minerals such as magnetite and hematite are identified by their respective peaks near $2\theta=21.4^0$ and $2\theta=26.2^0$.
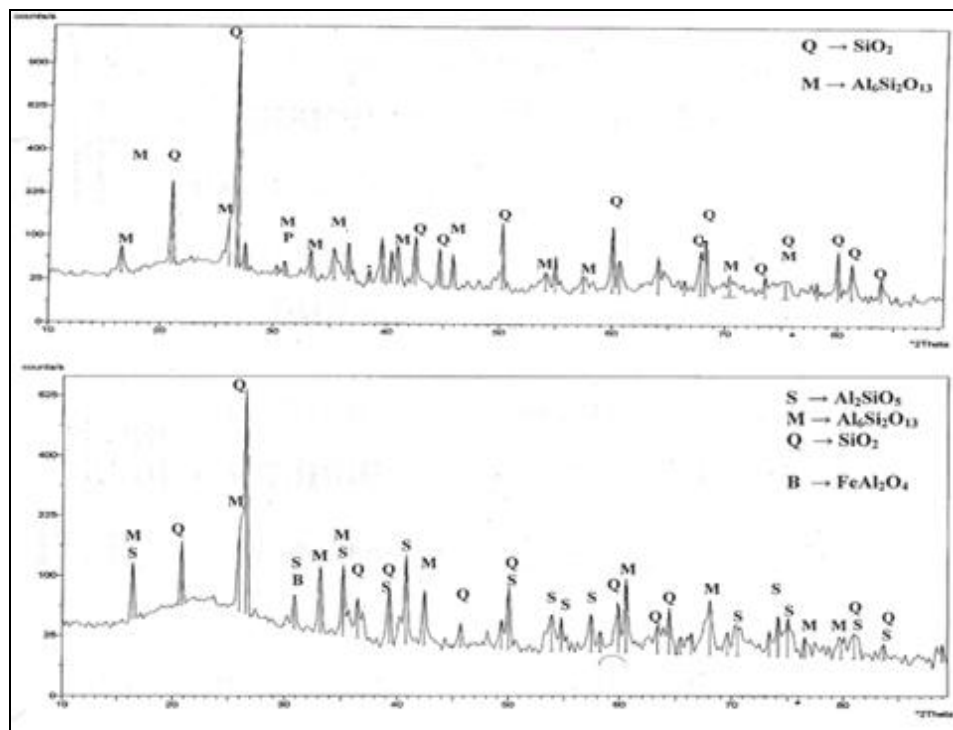
Figure 4.9.XRD Pattern of F_4 and F_5 fly ash sample

4.2.2. Summary

The primary objective of this study was to select the best mine filling material out of the seven fly ashes studied. On the basis of the results reported in this study, the following conclusions are made:

1. F_1 fly ash has good particle size distribution ($C_u > 6$) as compared to that of the other fly ashes, thereby fulfilling the requirements as a good grading material.

2. It has got greater amount of fine particles which favors for effective cover of surfactant on the surface of particles in the wet-modification process.

3. F_1 fly ash has a higher specific surface area compared with the other F class fly ashes, facilitating possible surface modification by chemical additives for smooth flow in the pipelines.

4. F_1 fly ash has much superior particle morphology compared with the other F class fly ashes. Comparatively, F_1 has more spherical particles, a feature that would create a lubricating effect due to the ball-bearing phenomena, resulting in a frictionless flow in stowing pipelines.

5. The F_1 sample has relatively high CaO content that would assist in strength enhancement without sacrificing its flow attributes.

6. The abundance of silica (SiO_2) would increase strength and CaO would enhance cementing properties.

7. F_1 fly ash sample has also lower sp. gr. value compared to other samples which would help in keeping the particles floated in pipelines during its hydraulic transportation.

Overall results have indicated that the F_1 fly ash have several superior desirable properties that would make it attractive to fill mine voids. Therefore, this fly ash material was selected for further study with respect to its flow and in-place strength characteristics.

4.3. Section II

The correct determination of the rheological properties of different fluids including suspensions and slurries is important to many research and industrial applications. To achieve this, the rheology investigation of the best fly ash material (F_1) was carried out at varying shear rates i.e. from 25 to 1000 1/s at varying temperature environment (20^0C to 40^0C). The study was carried out starting from 20% solid concentration (lean slurry) and went up to 60% solid concentration (high density slurry) at an incremental value of 10% each. The results of the study are presented in five different sub-sections i.e. for 20% solid concentration, for 30% solid concentration, for 40% solid concentration, for 50% solid concentration, and for 60% solid concentration and suitable conclusions are drawn at the end of each sub-section.

4.3.1. Results of 20% solid concentration (lean slurry concentration)

4.3.1.1. Effect of surfactants on fly ash slurry rheology

The aim of this investigation was to evaluate the rheological properties of fly ash composite materials after addition of surfactant and the counter-ion to reduce drag friction. The results are discussed with respect to varying temperature environment and additive concentration. It is observed that the variation of the shear stresses with shear rates at all slurry combinations for fly ash samples at varying temperature environment almost follows straight line behaviour with a zero yield stress (τ_y) (Figures 4.12 to 4.15). The slurry depicted shear thickening behaviour without any additive (Figure 4.10) that confirms to the observation made elsewhere (Whittingstall, 2001). The shear stress exhibited increasing trend as the shear rate increased from $100s^{-1}$ to $500s^{-1}$. The behavior did not change with higher temperature (Figure 4.10). This trend confirms to that of mineral suspended slurry (Boger, 2002). The governing relation for that slurry is given by Ostwald- De Waele model as below:

$$\tau = K\,\gamma^n \qquad\qquad (4.1)$$
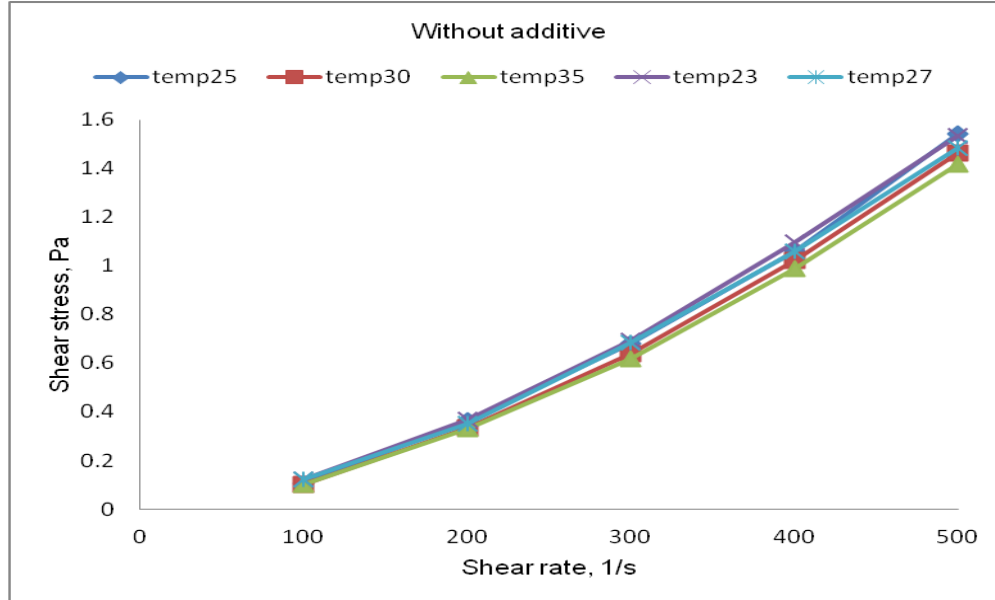
Figure 4.10.Rheogram of fly ash slurry without any additive

This shear thickening or dilatant behavior is an undesirable feature for any pipeline transportation system. Hence fly ash slurry flow behaviour was evaluated with additives. The additive was added at a concentration varying from 0.1%, 0.2%, 0.3%, 0.4%, and 0.5%. At

0.2% additive concentration, the shear stress value was minimum at 30^0 C at each shear rate. The trend was almost linear implying Newtonian flow behavior (Figure 4.12). Similar pattern were also observed for other additive concentration up to 0.5% with the shear stress values varied between 5 Pa to 12 Pa. The minimum shear stress observed was at 0.2% additive concentration at a temperature of 30^0 C at a shear rate value of $500s^{-1}$ reflecting the near Newtonian flow behaviour. However at a concentration of 0.4% at 31^0 C the slurry exhibited linear trend i.e. Newtonian behaviour. The slurry behaviour changed to non-Newtonian at 0.5% additive concentration. It reflects that addition of additive has positive impacts on slurry transportation system. The observation that the viscosity and shear stress decreased for all the cases with increase in temperature confirms that the slurry followed the fundamental properties of viscous materials. At 0.1% additive concentration the flow behaviour was erratic and uneven which is attributed to insufficient availability of additive concentration to modify the flow properties (Figure 4.11).
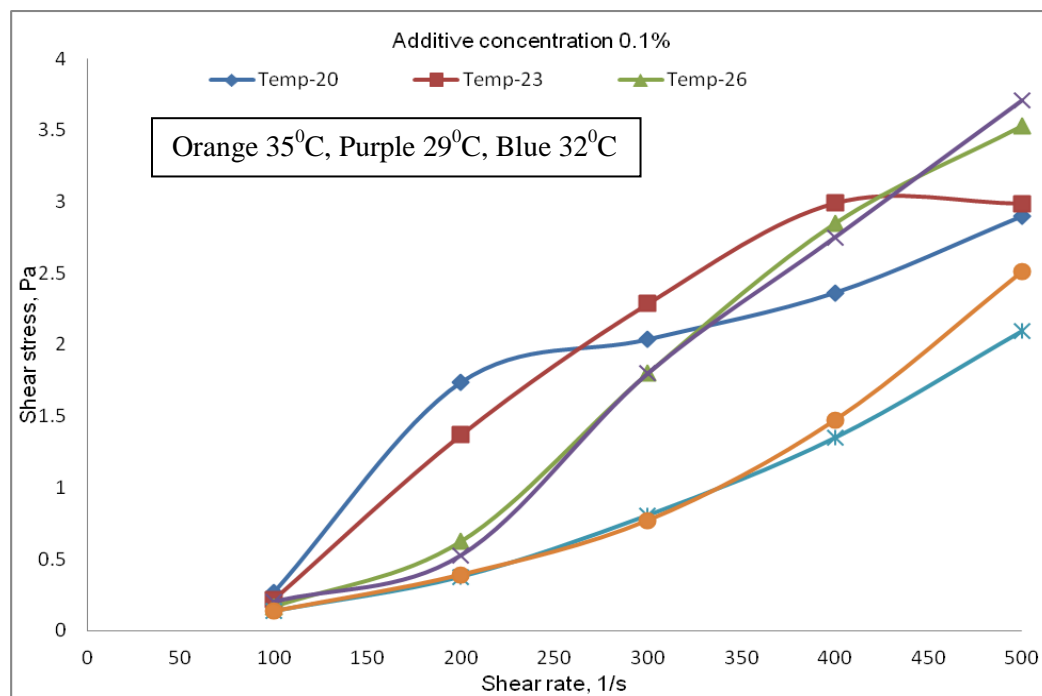
Figure 4.11.Rheogram of fly ash slurry with additive concentration 0.1%

The shear stress of the slurries decreased with increasing temperature (Figures 4.12 to 4.15). The slurry exhibited almost Newtonian flow pattern with a zero yield stress (Figures 4.12 to 4.15) when the concentration of the additive solution increased gradually with an incremental value of 0.1% (by weight).
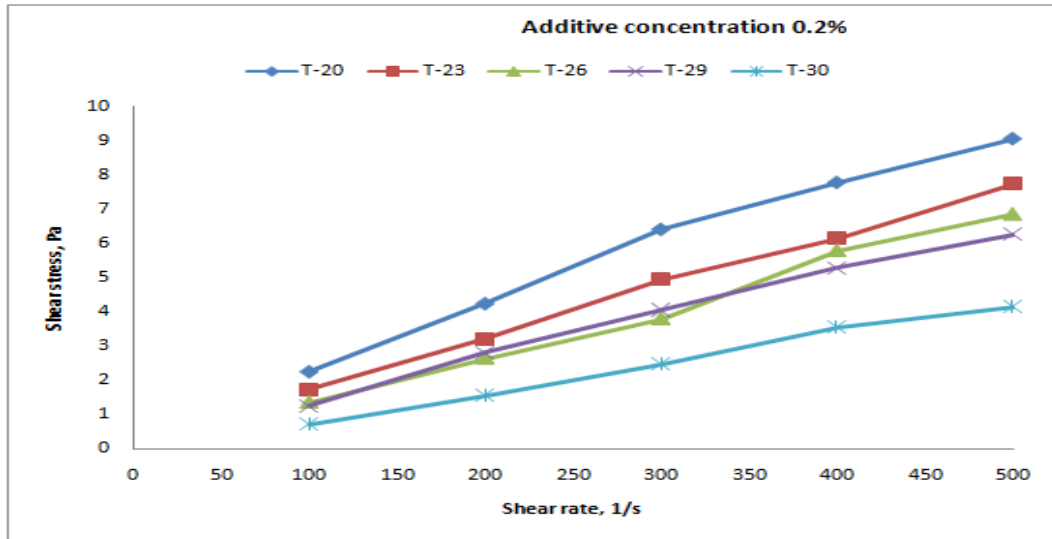
Figure 4.12.Rheogram of fly ash slurry with additive concentration 0.2%
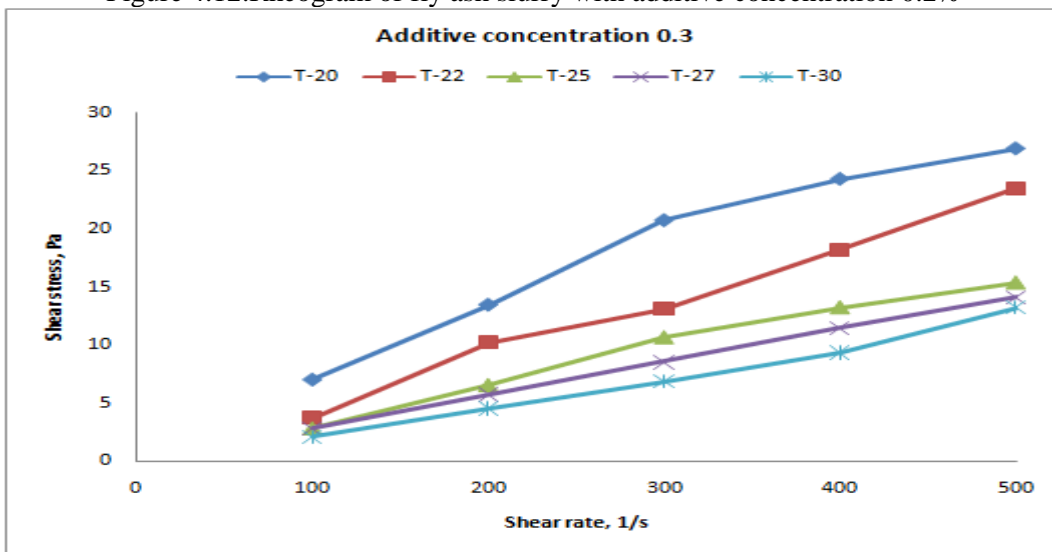
Figure 4.13.Rheogram of fly ash slurry with additive concentration 0.3%
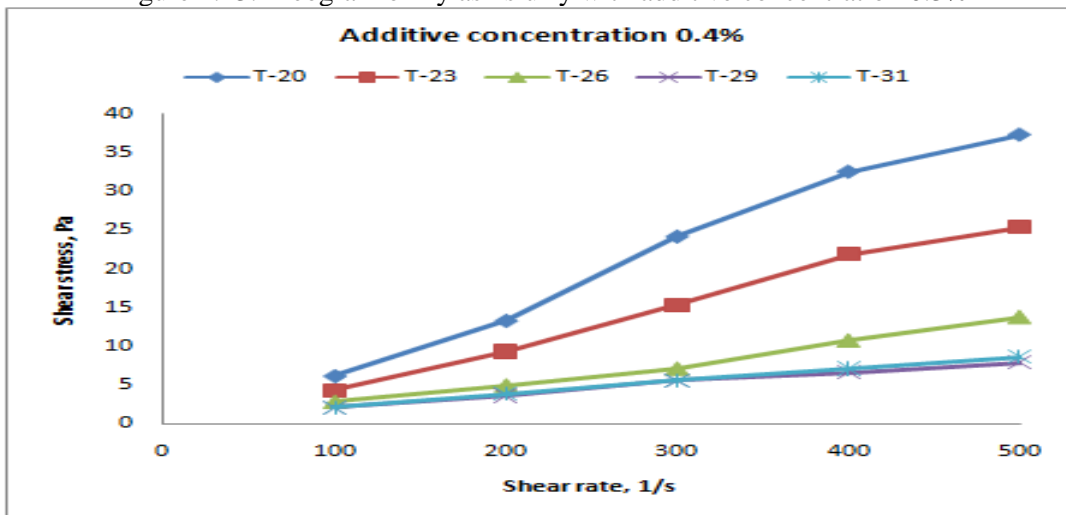
Figure 4.14.Rheogram of fly ash slurry with additive concentration 0.4%
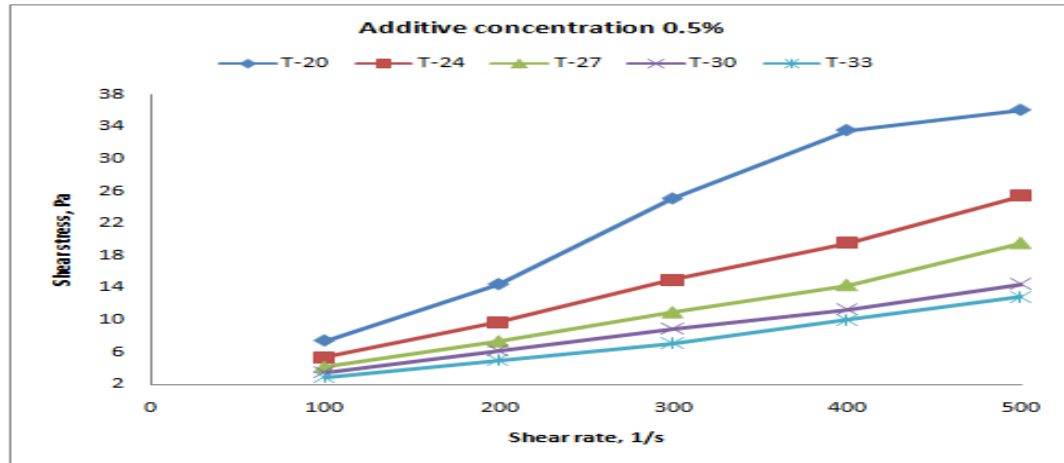
Figure 4.15.Rheogram of fly ash slurry with additive concentration 0.5%

4.3.1.2. Rheological behavior of fly ash slurry
4.3.1.2.1 Shear viscosity

Shear viscosity of fly ash slurries with and without an additive at varying temperature environment were also studied. The shear viscosity increased sharply from 1mPas to 3mPas with the shear rates varying from 100 to 500 per second for all the temperature ranges tested without any additive (Figure 4.16). This phenomenon confirms to that reported by Barnes *et al*., (1989). At additive concentration 0.1% the flow pattern was erratic and uneven depicting insufficient particle modification (Figure 4.17). When the temperature was maintained at 35^0C the flow behavior was shear thickening, but at 32^0C the viscosity increased linearly with shear rate. At additive concentration 0.2% and 0.3% (by weight) the slurry exhibited near Newtonian flow behaviour (Figure 4.18- 4.19). At 20^0C and 23^0C the slurry depicted shear thinning behavior. The shear thinning nature of the slurry is due to the alignment of particles in the flow field. The increasing rate of stress results in instantaneous alignment of particles in the direction of shear which in turn provides lower resistance to flow. This confirms to observations elsewhere (Boger, 2002).

Shear thinning behaviour was distinctly observed at 20^0 C at 0.3% additive concentration also (Figure 4.19). It is a desirable feature for any hydraulic pipeline transport system. Shear thinning pattern was observed from 29^0 C to 31^0 C though at a reduced rate at additive concentration of 0.4% (Figure 4.20). At concentration of 0.5% of the additive near Newtonian behaviour was observed except at 20^0 C (Figure 4.21). Addition of 0.5% (by weight) of additive concentration to the slurry has produced some undesirable results

compared to other additive concentrations, because of the high concentration of the additive which was added to the slurry. However at 0.2% and 0.3% (by weight) of additive concentration the slurry suspension showed good rheological behaviour at around 20^0 C. The effective additive concentration range was found to be from 0.2% to 0.3% (by weight).
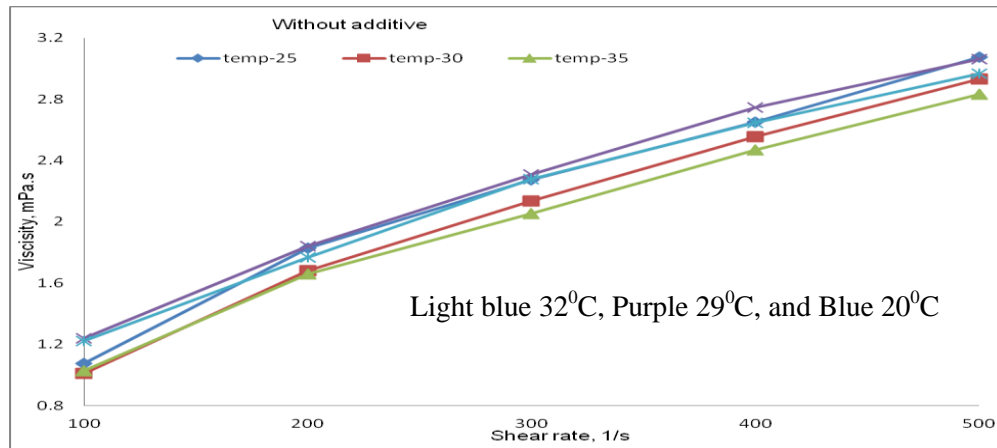
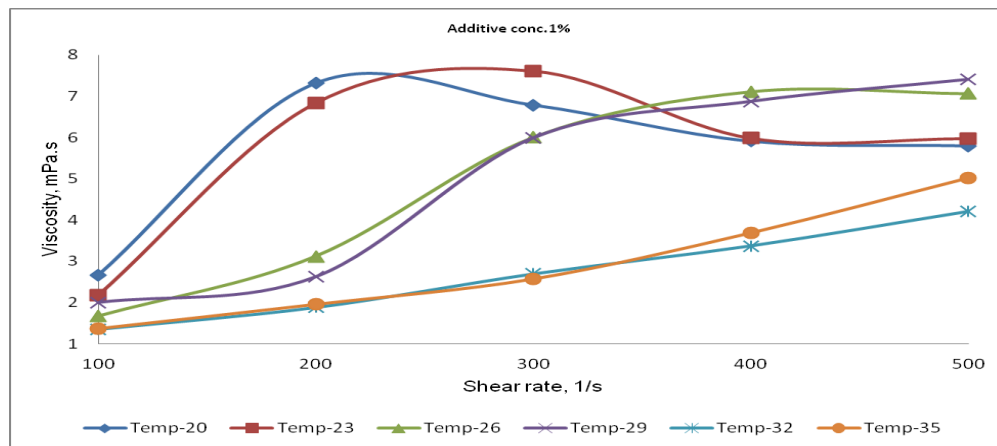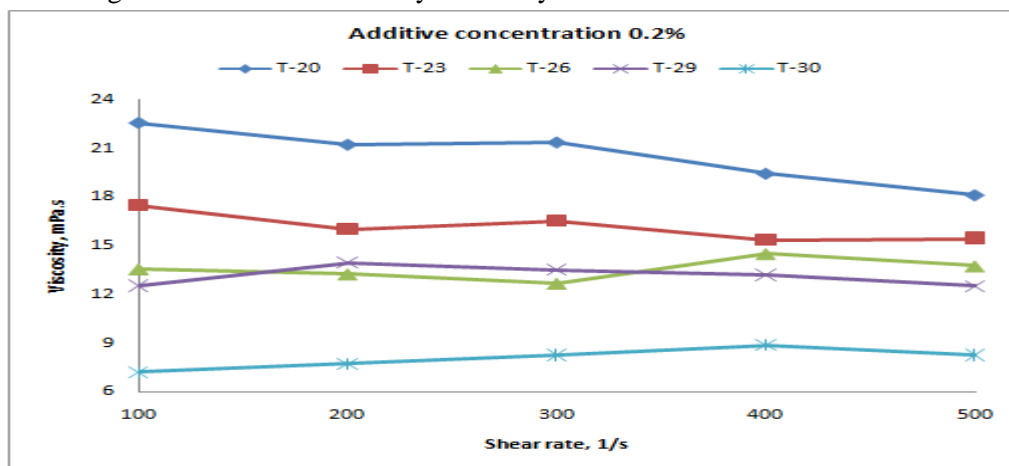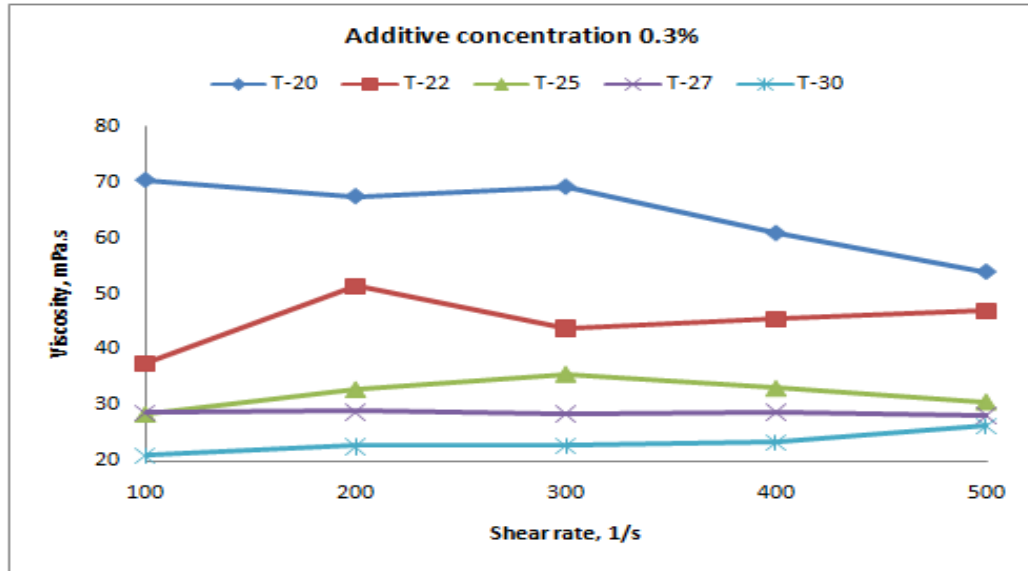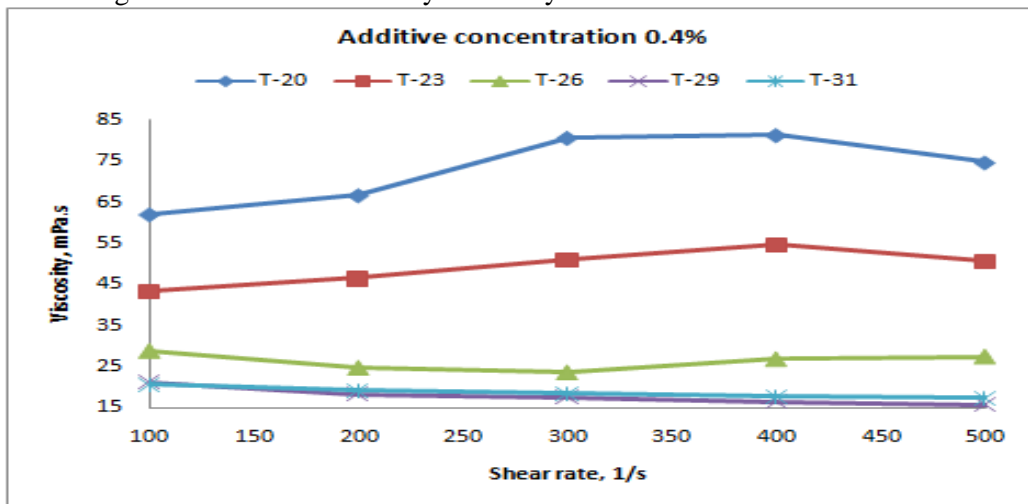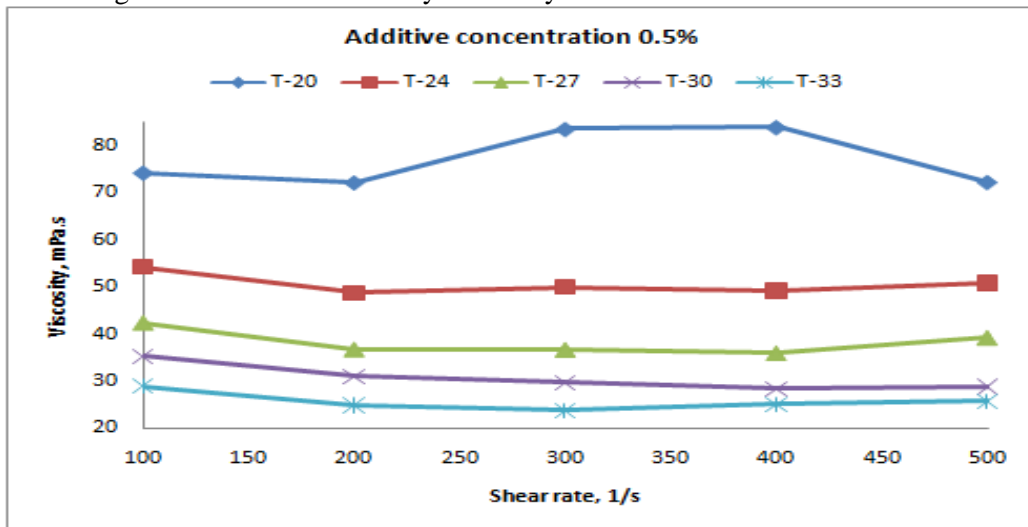Figure 4.16.Flow curve of fly ash slurry without any additive

Figure 4.17.Flow curve of fly ash slurry with additive concentration 0.1%

Figure 4.18.Flow curve of fly ash slurry with additive concentration 0.2%

Figure 4.19.Flow curve of fly ash slurry with additive concentration 0.3%

Figure 4.20.Flow curve of fly ash slurry with additive concentration 0.4%

Figure 4.21.Flow curve of fly ash slurry with additive concentration 0.5%

4.3.1.2.2. Effect of temperature on fly ash slurry rheology

Temperature affects the modification of the fly ash particles by decreasing the viscosities as the temperature rises. This is due to the enhanced dissolving activity of the surfactant at higher temperatures. However, an elevated temperature would weaken the surface grafting modification. The viscosity of untreated fly ash slurry did not show any variation with higher temperatures as well as shear rates. The viscosity values varied from 1.2 - 3 mPa.s at shear rates $100s^{-1}$ to $500s^{-1}$ respectively (Figure 4.22).
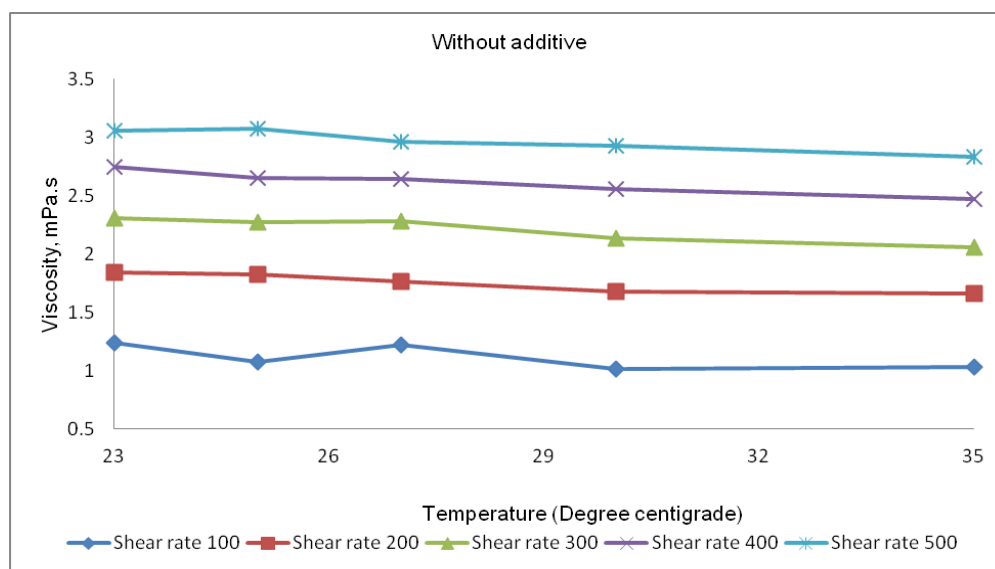
Figure 4.22.Viscosity vs. temperature plot of fly ash slurry without any additive

It shows the higher the shear rate the more is the viscosity. When surfactant additive at 0.1% was added, changes in viscosity values were observed without any established trend (Figure 4.23). This phenomenon is due to insufficient interaction between fly ash and surfactant at 0.1% additive concentration. At 0.2% additive concentration high slurry viscosity values were obtained at shear rate value of $100s^{-1}$. Minimum values between 6 to 9 mPa.s were obtained at 30^0C (Figure 4.24). When the surfactant concentration increased from 0.3 to 0.5% the slurry viscosity exhibited higher values i.e more than 15 mPa.s (Figures 4.25 to 4.27). The optimum modification temperatures for treated fly ash slurries were found to be 30^0C-35^0C.

The values of both shear stress and shear viscosity decreased with increase in temperature which confirms to the fundamental properties of any viscous material (Shenoy,

1976). It is attributed to the increase in the consistency of the slurries, which decreased the resistance to shear. A comparatively larger value of initial stress is required to start the process of shearing when relatively larger numbers of solid particles are present. The yield stress was almost zero as fly ash used in this investigation was very fine in nature. This decrease is due to decrease in the number of particles and the surface area of the solids per unit volume of the slurry with reduction in solid concentration. The viscosity of the fly ash slurry showed a decreasing trend with increase in temperature at 0.3%, 0.4% and 0.5% additive concentration (Figures 4.25 to 4.27). It confirms to the conclusion elsewhere (Shenoy, 1976).
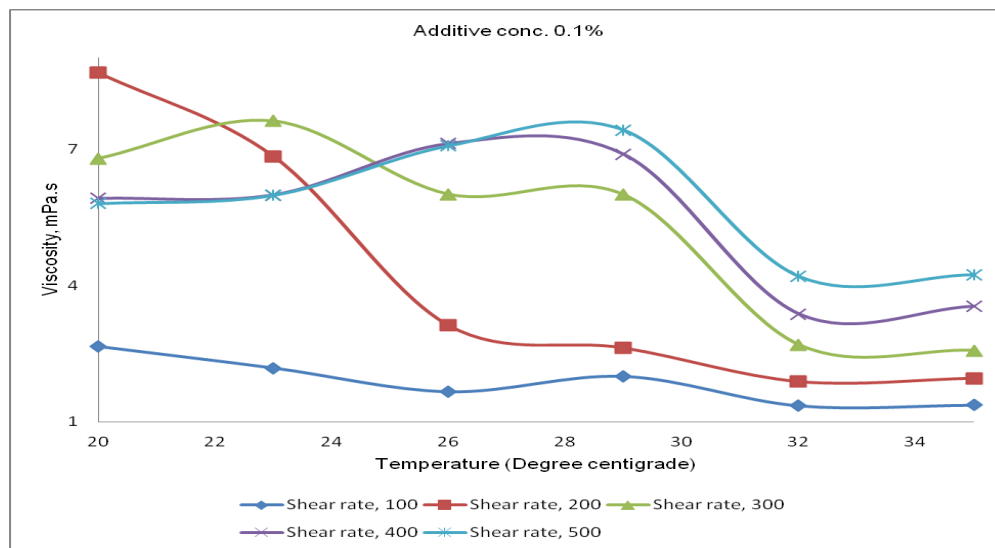
Figure 4.23.Viscosity vs. temperature plot of fly ash slurry with additive concentration 0.1%
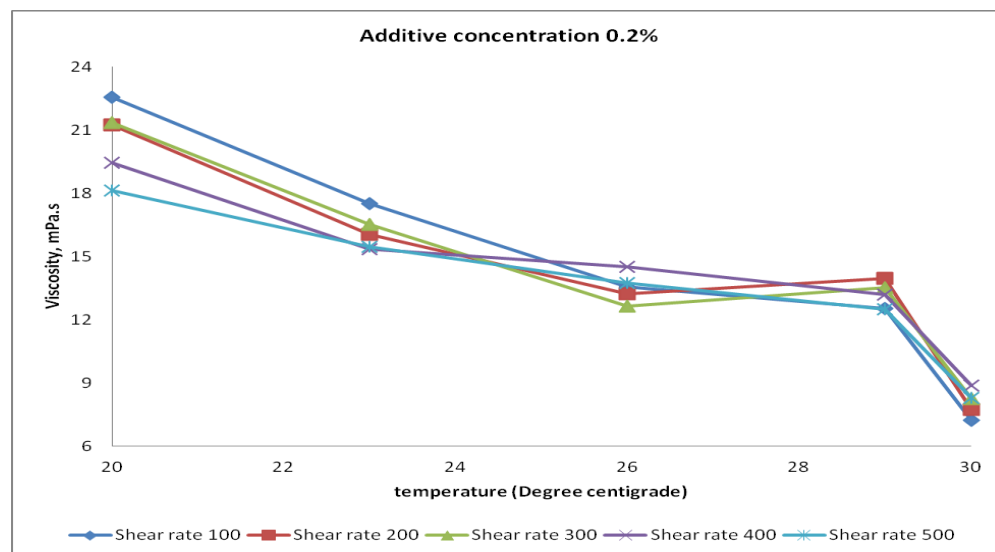
Figure 4.24.Viscosity vs. temperature plot of fly ash slurry with additive concentration 0.2%
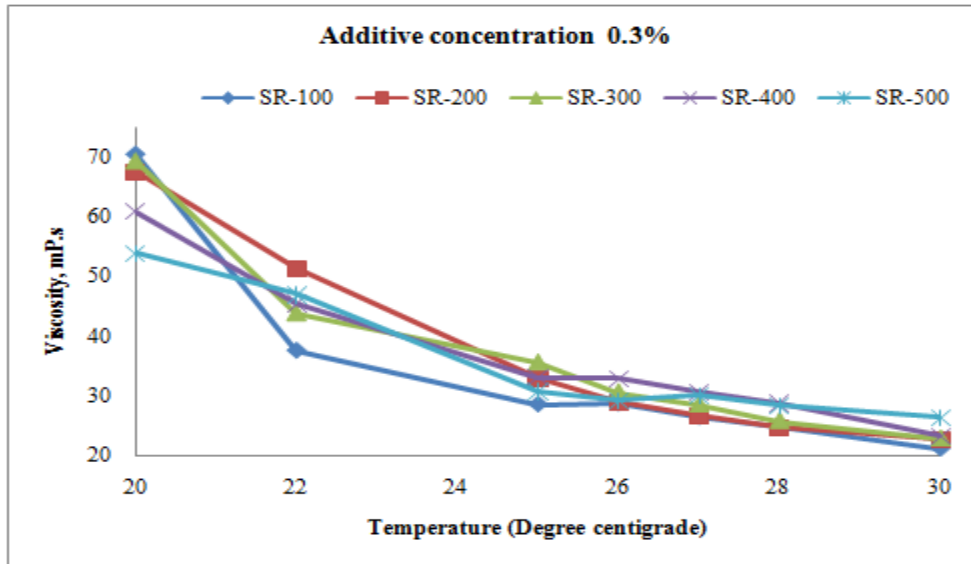
Figure 4.25.Viscosity vs. temperature plot of fly ash slurry with additive concentration 0.3%
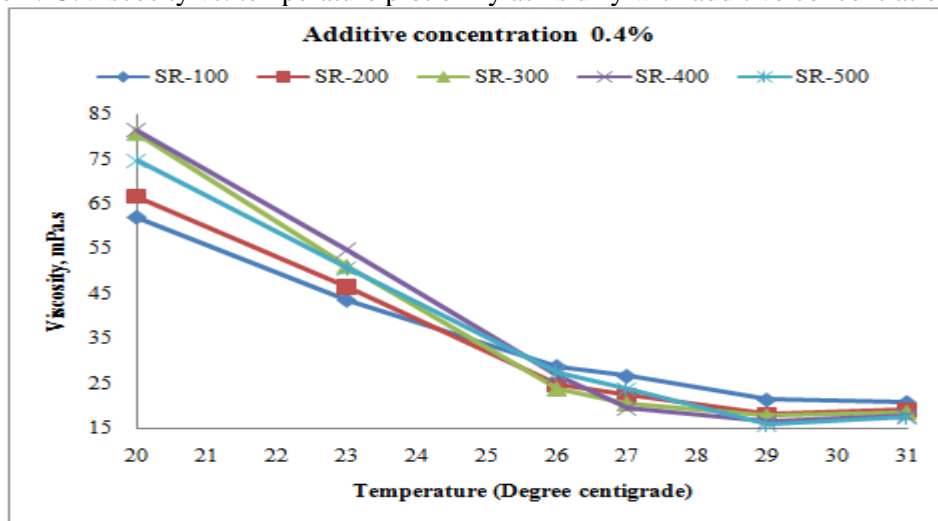
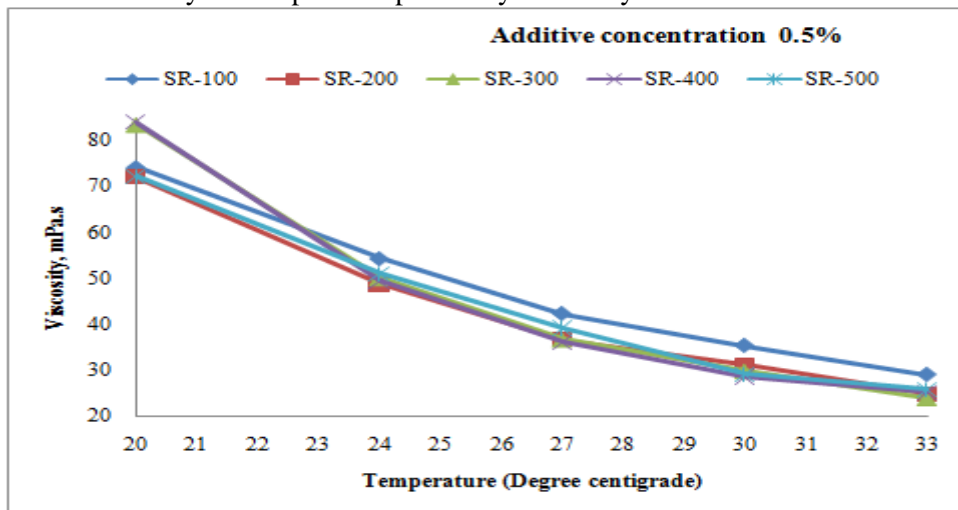Figure 4.26.Viscosity vs. temperature plot of fly ash slurry with additive concentration 0.4%

Figure 4.27.Viscosity vs. temperature plot of fly ash slurry with additive concentration 0.5%

4.3.1.3. Surface Tension

Surfactants are also known as tensides, which are wetting agents and can lower the surface tension of a liquid, allowing easier spreading leading to lower the interfacial tension between solid particles and the liquid. Surfactants reduced the surface tension of water by adsorbing at the solid-liquid interface. The addition of surfactant resulted in reduced surface tension by 53 to 56% as compared to that without any additive (Figure 4.28).
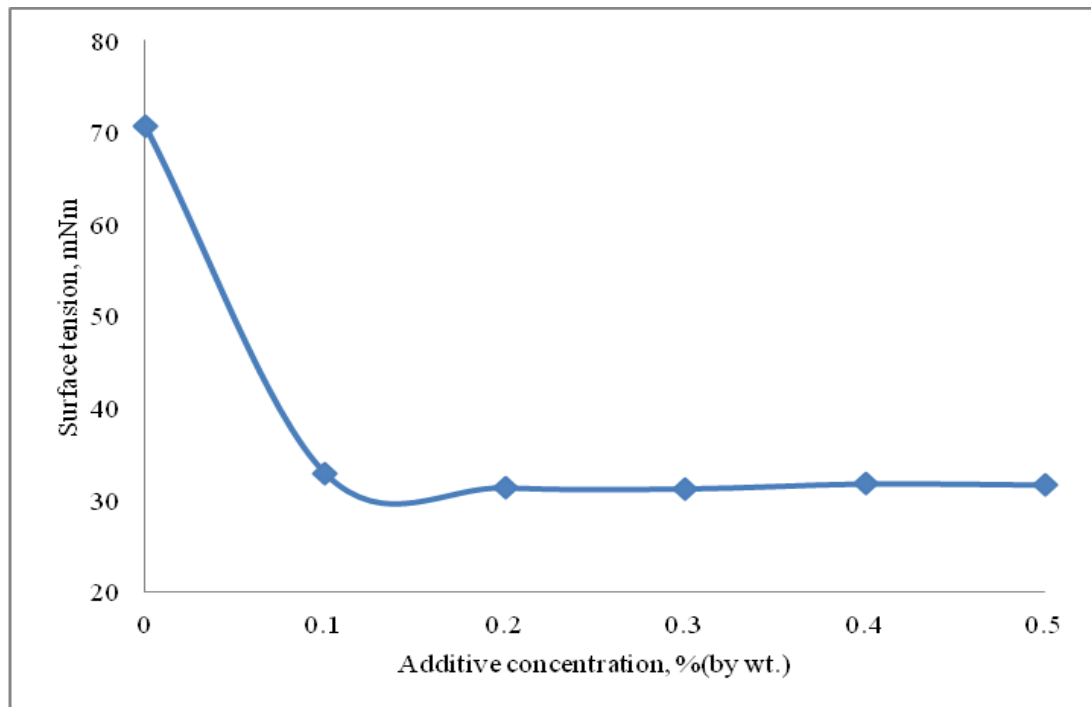
Figure 4.28.Plot of surface tension vs. additive concentration

4.3.1.4. Zeta Potential (ζ)

The ζ of fine powder fly ash particles and the amount adsorption of the slurry were investigated as well. The viscosity of the fly ash slurry without any additive was found to be varied from 1mPas to 3mPas during test measurements. This low value was because of the rapid settling tendencies of the fly ash particles at the bottom of the measuring cup during the test due to flocculation activity of the colloidal fly ash particles in the suspension. The ζ value of the fly ash slurry was negative (-27mV) without any additive, but changed to positive value (> +30mV) when surfactant was added to the slurry (Figure 4.29). This is due to electrostatic bonding between the negative sites of the fly ash particles and the cationic head groups of the surfactants. This mechanism is expected to result in higher positive ζ values. As a result, negatively charged fly ash particles would repel each other, and therefore, flocculation was

prevented and dispersion achieved. Addition of the surfactant modified the surface properties of the fly ash particles keeping the suspension in the stable condition. This observation is in agreement with the desirable features of any electrically stabilized colloids described elsewhere (Greenwood & Kendall. 1999).
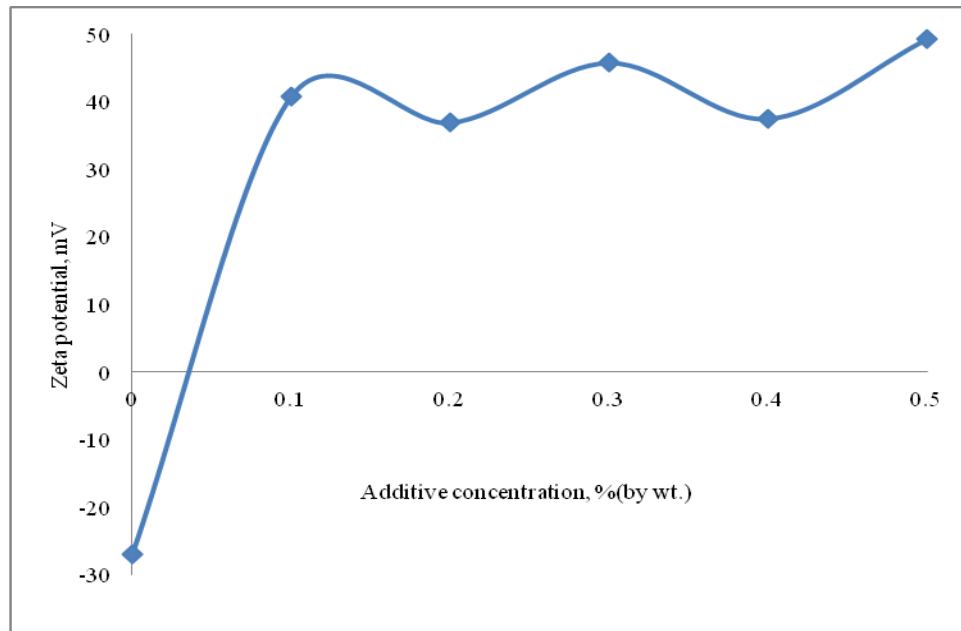

Figure 4.29.Plot of zeta potential vs. surfactant concentration

4.3.1.5. Summary of observations at 20% solid concentration

Rheological behaviour improved significantly when surfactant at 0.2% and 0.3% concentration were added to the fly ash slurry. It was also observed that the addition of the surfactant to the slurry suspension reduced the surface tension of the liquid considerably which would aid for better wetting of the fly ash particles and reduce the drag friction. The surfactant reduced the surface tension value of the liquid significantly from a value of 71 mNm^{-1} to 31 mNm^{-1} confirming better wetting properties. It would facilitate reduced resistance to flow. The zeta potential value for the fly ash slurry with addition of surfactant exceeded +30 mV. It confirms that the suspension was stable during the test measurements. It was also observed that the slurry suspension settled down leaving the water medium at the top after about three to four hours of the measurement (Figure 4.30). It would help in draining out excess water which is a desirable feature of the pipeline transport in any fly ash disposal system.

Figure 4.30: Settling results of fly ash slurry

4.3.2. Results of 30% solid concentration (low slurry concentration)

4.3.2.1. Rheology

Rheological parameters as viscosity, shear stress, surface tension, and zeta potential were studied for 30% concentration of fly ash with different percentage of surfactant and counter-ions. The results such as the rheograms and flow curves of fly ash slurries are presented in graphical form. The untreated suspensions of fly ash slurries exhibited heterogeneous flow behaviour (Seshadri and Singh, 2000) which is evident from Figures (4.31, 4.37, and 4.43) compared to the treated fly ash slurries. Addition of the surfactant to the fly ash slurries produced almost Newtonian behaviour and shear thinning effects. The majority of non-Newtonian fluids are infact shear-thinning, in that their viscosities decrease with increasing shear rate. As depicted by Whittingstall (2001), the structure of most fluids lends itself to this behavior because their components do one of the following: (1) Anisotropic particles align with the flow streamlines to reduce their hydrodynamic cross-section. (2) Aggregates of particles tend to break apart under shear forces, again minimizing hydrodynamic disturbance. (3) Surfactant molecules existing as random coils elongate in the streamlines. (4) Particles arrange themselves in formations to reduce energy, much like racing

cars line up behind each other to take advantage of the leading car. The effect of the additive is thus to reduce or eliminate the yield stress of the slurries rather than the viscosity which compares favourably well with the results obtained by Jones and Chandler (1989).

4.3.2.1.1. Effect of surfactants on fly ash slurry rheology

Figures (4.31 - 4.36) shows the rheograms of the fly ash slurries at different temperatures and effect of surfactant additive (0.1%, 0.2%, 0.3%, 0.4%, and 0.5% by weight) on the flow behaviour at varying shear rates. It is observed from the results that the untreated fly ash slurry showed turbulent flow behaviour (Figure 4.31) compared to treated fly ash slurries (Figures 4.32- 4.36). In the case of treated fly ash slurries shear stress decreased with increasing temperature at a fixed shear rate for all the surfactant dosages tested. The fly ash slurries showed shear thinning behaviour at 20^0C and 25^0C which is a desirable feature for any hydraulic transport system (Wei *et al*., 2009; Roh *et al*., 1995). At 30^0C, 35^0C, and 40^0C the slurries almost showed straight line (Newtonian) behaviour with a zero yield stress. At 0.1% additive concentration (Figure 4.32) the slurry followed Newtonian behaviour at 20^0 C, but changed to shear thickening behavior as temperature increased which is an undesirable property for pipeline transport system. Many of these rheograms exhibit a turbulent vortice artifact, where the measured shear stress was seen to climb dramatically from a certain shear rate value, in an apparent display of shear thickening. The rheogram presented at 30^0C, 35^0C and 40^0C (Figure 4.32) provides a good example of this artifact, where the shear stress data suddenly climbed away from the fitted curve at a shear rate of about $200s^{-1}$.
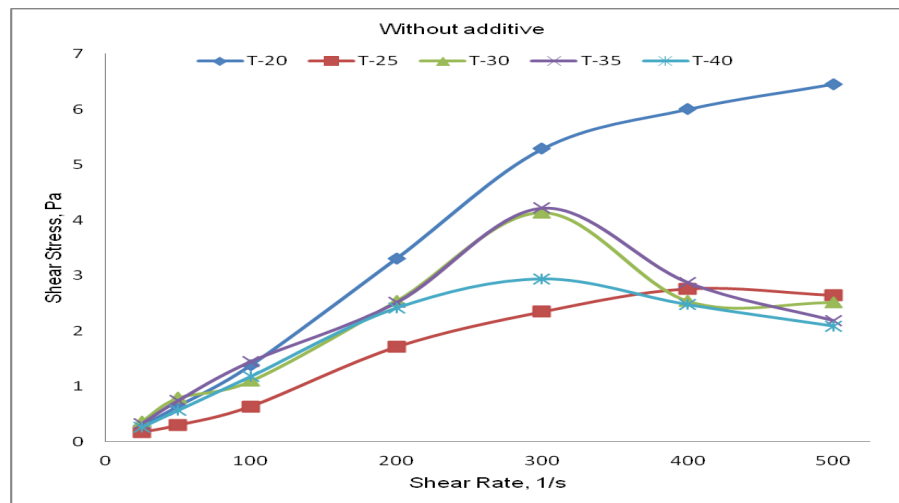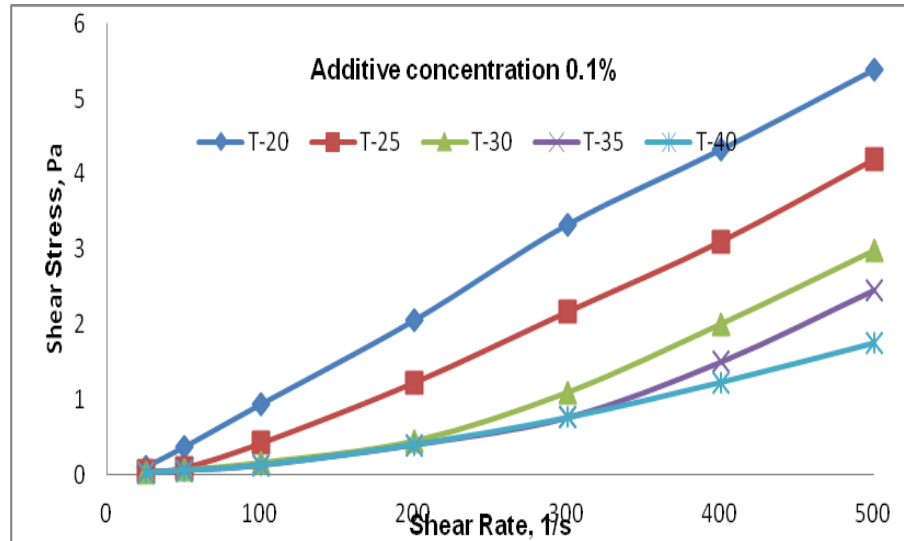

Figure 4.31.Rheogram of untreated fly ash slurry

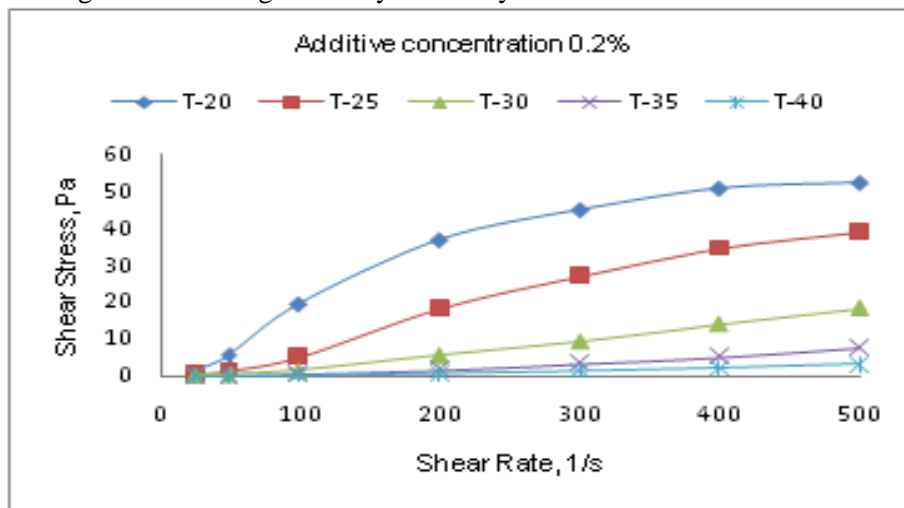Figure 4.32.Rheogram of fly ash slurry at additive concentration 0.1%

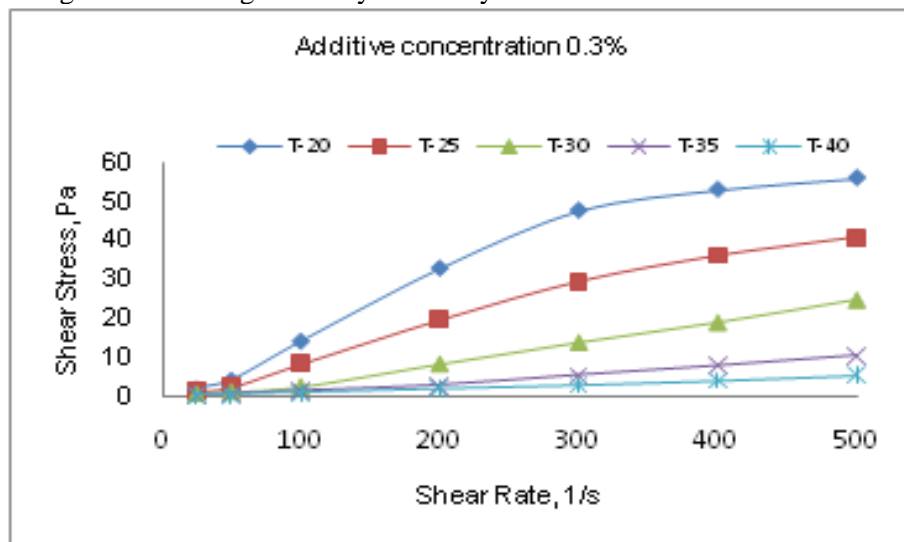Figure 4.33.Rheogram of fly ash slurry with additive concentration 0.2%

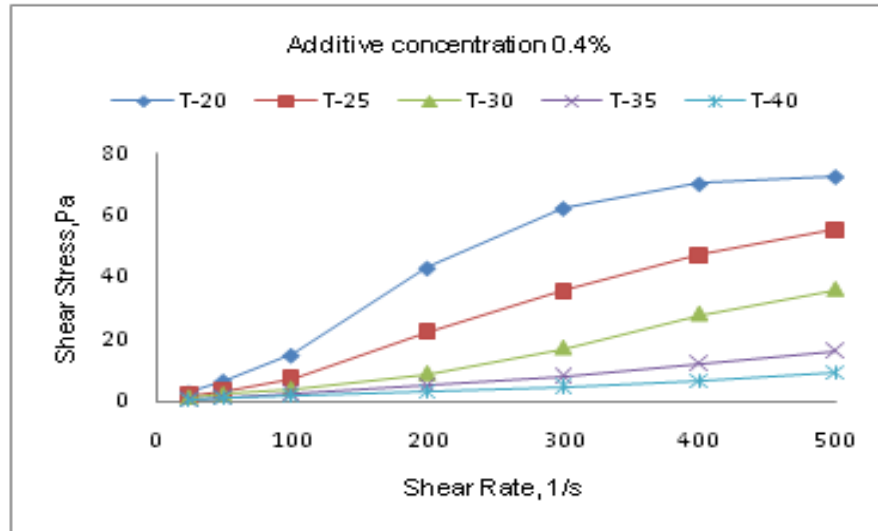Figure 4.34.Rheogram of fly ash slurry with additive concentration 0.3%

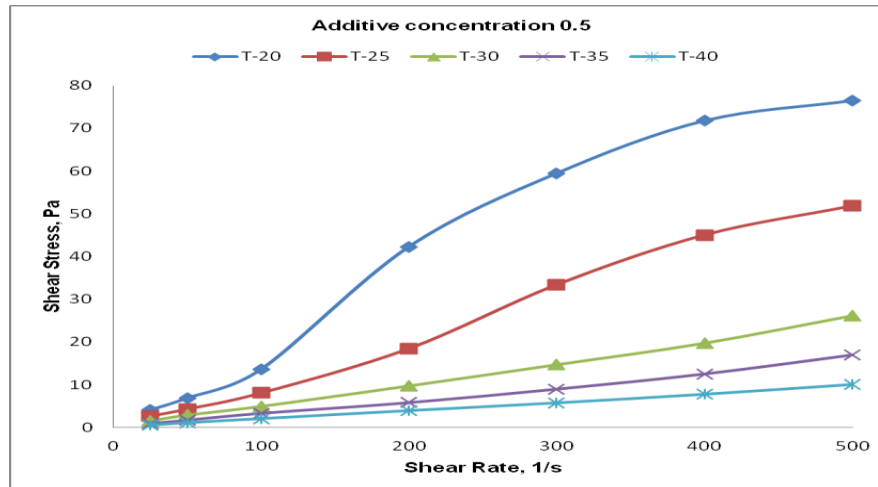Figure 4.35.Rheogram of fly ash slurry with additive concentration 0.4%

Figure 4.36.Rheogram of fly ash slurry at additive concentration 0.5%

4.3.2.1.2. Shear viscosity

Figures (4.37 - 4.42) shows the shear viscosity of fly ash slurries with additive concentration of 0.1%, 0.2%, 0.3%, 0.4%, and 0.5% (by weight) at varying temperatures. It is observed that the shear viscosity decreased sharply from 20^0C to 40^0C reaching a minimum value (4.8mPa.s) at 40^0C with the shear rates varying from $25s^{-1}$ to 500 s^{-1} for all the additive ranges tested (Figures 4.38 - 4.42). Shear thinning behaviour was also observed at 20^0C and 25^0C for all the slurries tested. At 30^0C, 35^0C, and 40^0C the viscosities of the slurries almost remained unchanged for the shear rates varying from $25s^{-1}$ to $500s^{-1}$ confirming that the slurry showed Newtonian flow behaviour. Best results are obtained at 35^0C and 40^0C for an additive concentration varying from 0.2% to 0.4%. In this case also the untreated fly ash slurry showed

turbulent flow behaviour without depicting any definite trend (Figure 4.37) as compared to treated fly ash slurries.
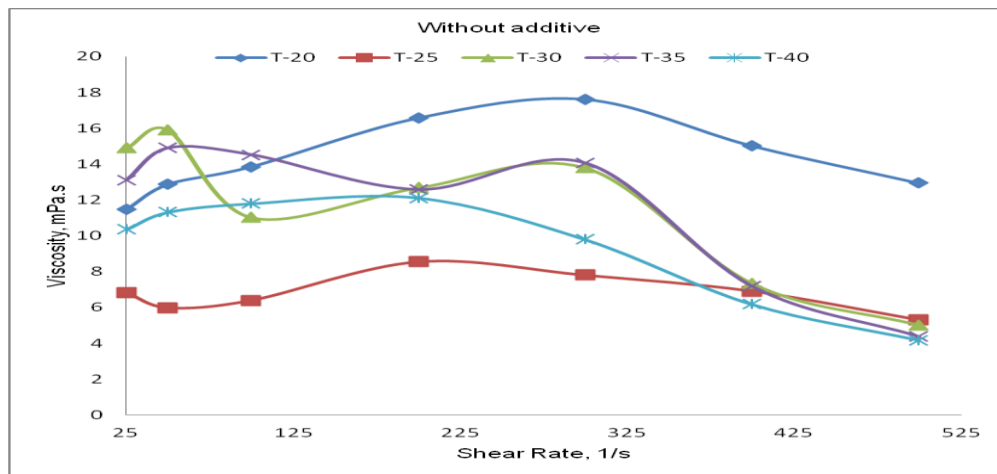

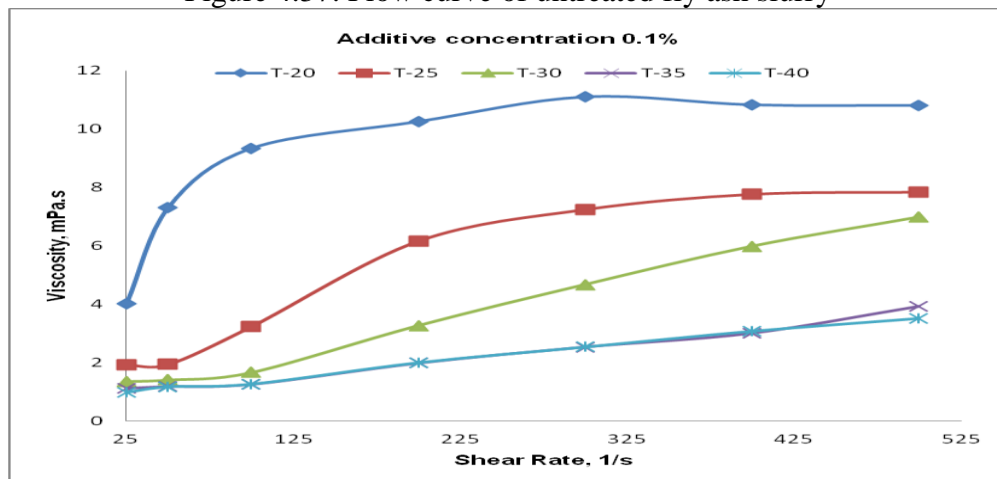Figure 4.37. Flow curve of untreated fly ash slurry

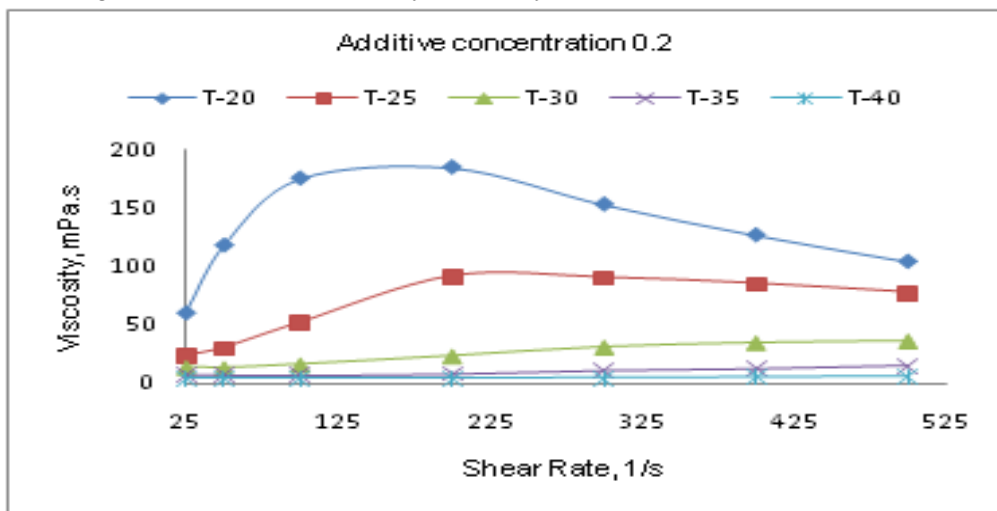Figure 4.38. Flow curve of fly ash slurry with additive concentration 0.1%

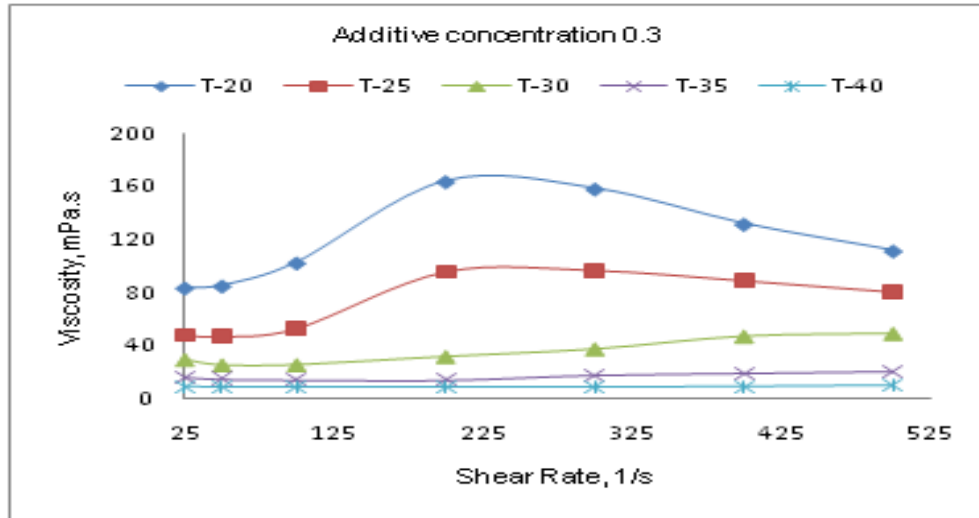Figure 4.39. Flow curve of fly ash slurry with additive concentration 0.2%

Figure 4.40. Flow curve of fly ash slurry with additive concentration 0.3%
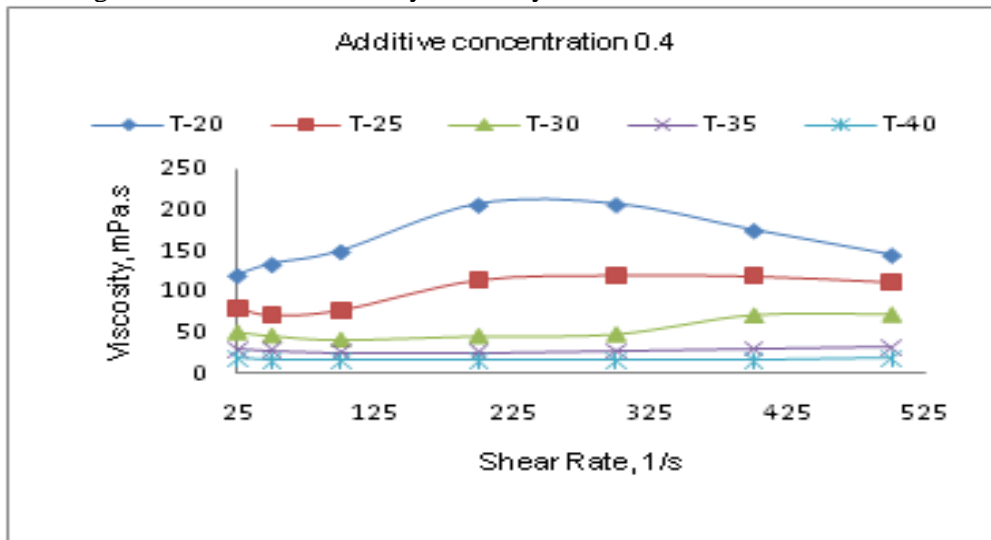

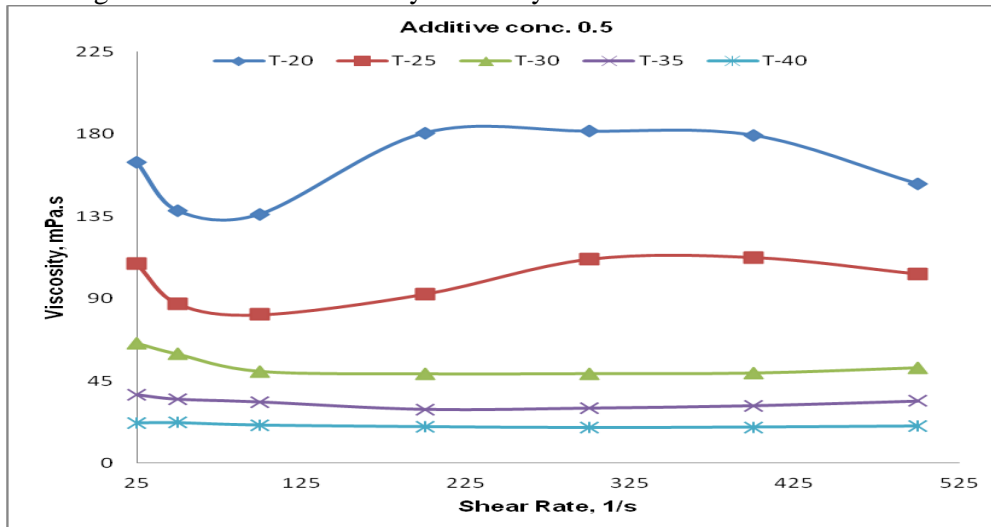Figure 4.41. Flow curve of fly ash slurry with additive concentration 0.4%

Figure 4.42. Flow curve of fly ash slurry with additive concentration 0.5%

4.3.2.1.3. Effect of temperature on fly ash slurry rheology

In this sub-section the results are analyzed with respect to viscosity variation with varying temperatures. It is observed that the values of both shear stress and viscosity decreased with increase in temperature (Figures 4.44 - 4.48) which confirms to fundamental properties of any viscous material as for all normal liquids (Topallar and Bayrak, 1998). This is due to the enhanced dissolving activity of the surfactant at higher temperatures. This result also compares favourably with the observations made by Shenoy (1976). This is due to decrease in number of particles and the surface area of the solids per unit volume of the slurry with reduction in solid concentration.

Figure 4.43. Viscosity vs. temperature plot of untreated fly ash slurry without additive

Figure 4.44. Viscosity vs. temperature plot of fly ash slurry with additive concentration 0.1%

Figure 4.45. Viscosity vs. temperature plot of fly ash slurry with additive concentration 0.2%

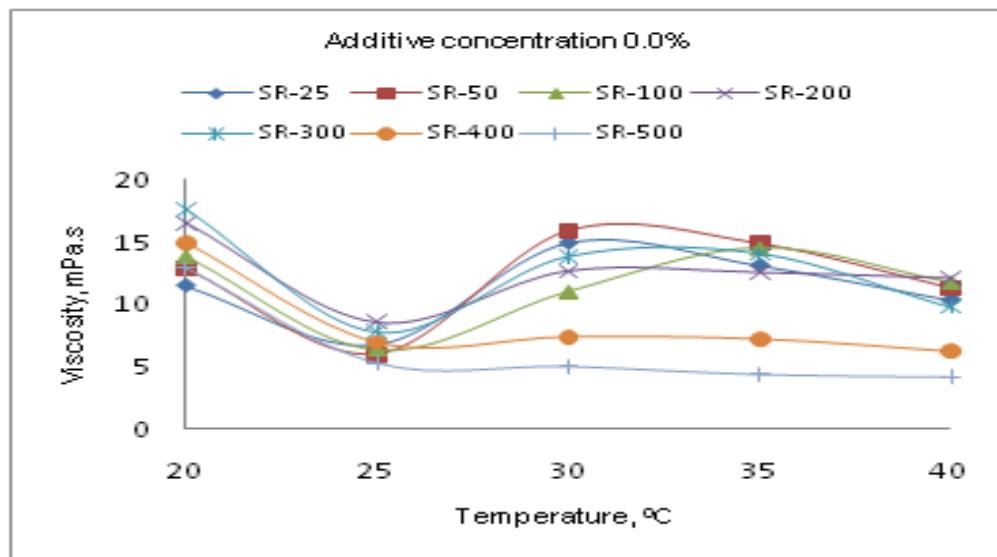Figure 4.46. Viscosity vs. temperature plot of fly ash slurry additive concentration 0.3%
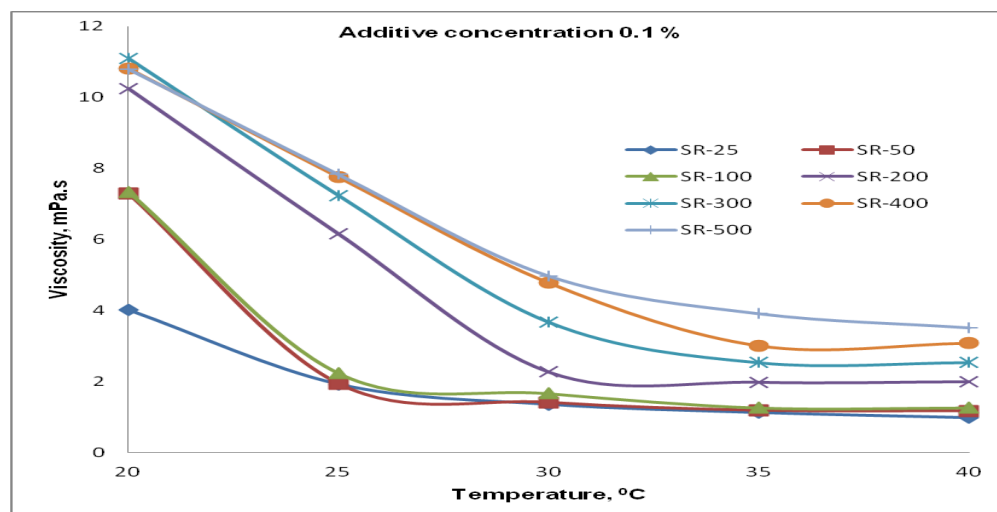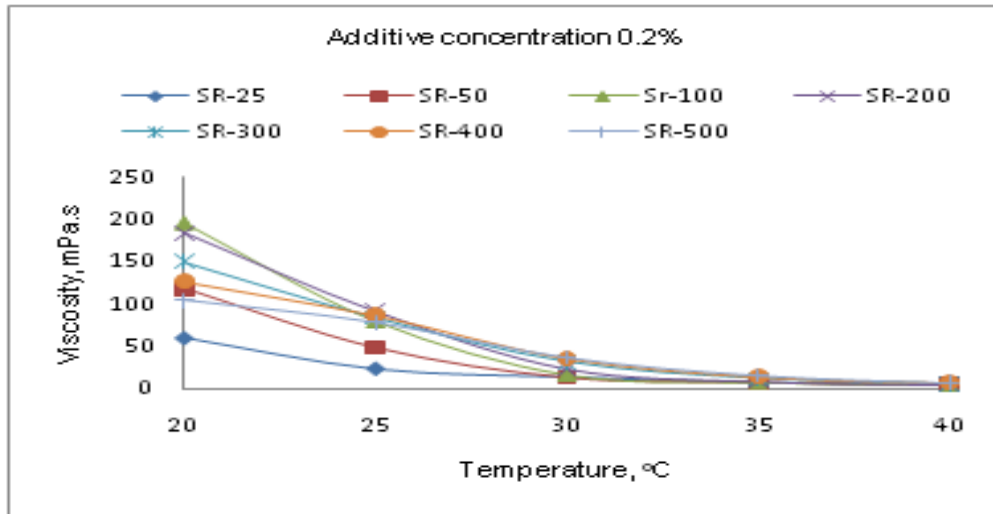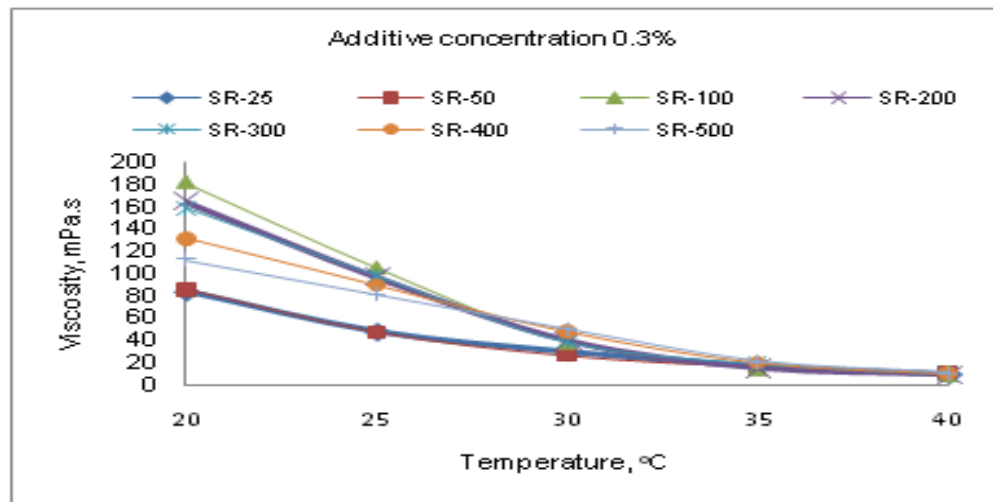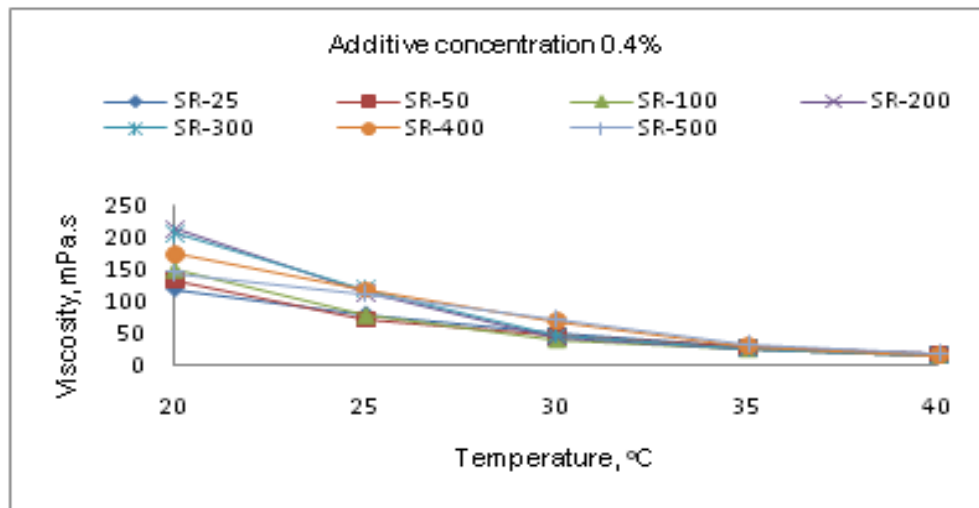

Figure 4.47. Viscosity vs. temperature plot of fly ash slurry with additive concentration 0.4%
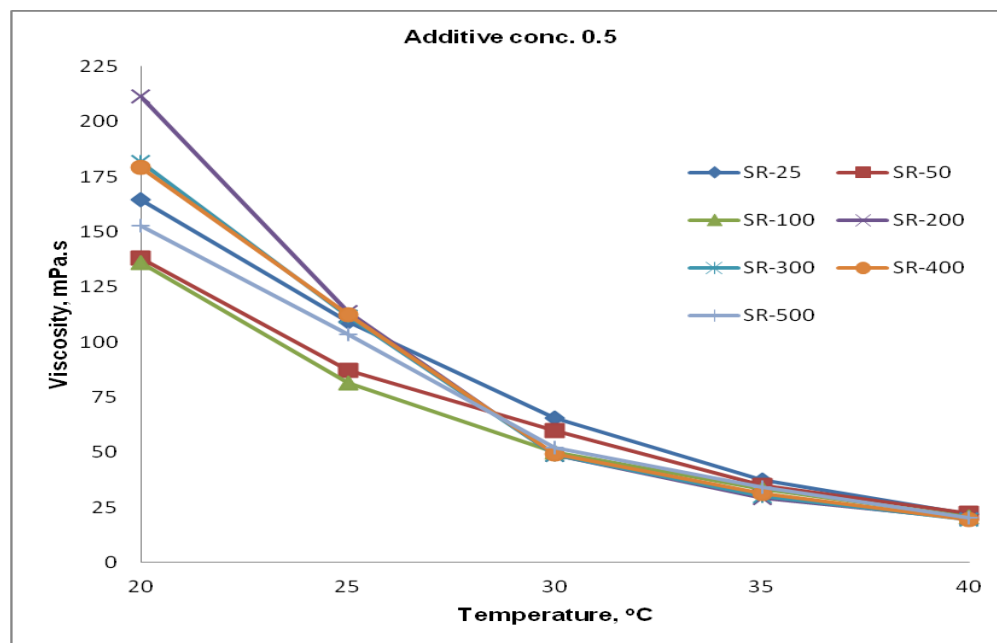
Figure 4.48. Viscosity vs. temperature plot of fly ash slurry with additive concentration 0.5%

Addition of surfactant caused a considerable decrease in viscosity. The decrease in viscosity with increasing temperature was steep from 20^0C to 30^0C and after that the viscosity decrease was marginal till 40^0C for all the shear rates studied. This is due to the formation of spherical micelles which grow continually in size with the increase of temperature until at the cloud point when they can no longer grow and phase separation occurs and it exists only in relatively dilute surfactant solutions (Shenoy, 1976). However, from Figure 4.43 (untreated fly ash slurry) it is observed that the flow behaviour did not show any definite trend compared to the treated fly ash slurries. In this case the flow behaviour is erratic and irregular compared to chemically treated fly ash slurries. At 0.1% additive concentration (Figure 4.44) the slurry behaviour was better at low shear rates i.e., $25s^{-1}$, $50s^{-1}$, and $100s^{-1}$ compared to higher shear rates.

4.3.2.2. Surface Tension (ST)

Surface tensions of the six fly ash slurries with and without an additive are presented in Table 3.8. Because of the addition of surfactant to the slurries, ST reduced by 43% to 46% compared to that of untreated slurries, and reduced by 51% to 54% as compared to ST of tap water (68.9mN/m). The surfactants facilitated easier spreading leading to lower the interfacial tension between solid particles and the liquid. This phenomenon is due to the hydrophobic group which is a long chain hydrocarbon with 12 carbons in the structure of surfactant, is

attached to the fly ash particle, converting it from hydrophilic to hydrophobic property (Xiao and Zho, 2002).

4.3.2.3. Zeta potential (ζ)

The zeta potential values of all the slurries are reported in Table 3.8. It was observed that the ζ value of the untreated fly ash slurry was -25mV at pH 7.30. However, in the presence of surfactants, the zeta potentials are dramatically shifted towards more positive values (>+31mV). This is an important observation since at ζ values exceeding +30 mV adequate dispersion of the fly ash particles seems to be sustained (He *et al*., 2004). This is due to electrostatic bonding between the negative sites of fly ash particles and the cationic head groups of the surfactants. This mechanism was expected to result in higher positive zeta potentials. As a result, negatively charged fly ash particles would repel each other and, therefore flocculation was prevented and dispersion achieved.

4.3.2.4. Summary of observations at 30% solid concentration

The following conclusions are made with respect to 30% solid concentration:

➢ All the treated fly ash slurries exhibited shear-thinning and/ or Newtonian flow properties with zero yield stress.

➢ Minimum viscosity and shear stress at 4.8mPa.s and 2Pa respectively were obtained with 0.2% additive concentration at 40^0 C.

➢ The surfactant additive has also modified the surface properties of the fly ash particles from negative ζ values to positive values and suspension stability of the slurry was improved.

➢ Surface tension of the fly ash slurries is reduced by 43% to 46% compared to that of untreated slurries, and it is reduced by 51% to 54% as compared to ST of tap water (68.9mN/m). It exhibits the positive characteristics of fly ash slurry for pipeline transportation with the addition of a cationic surfactant (CTAB) and a counter-ion (NaSal) which would reduce specific energy consumption and water requirements.

4.3.3. Results of 40% solid concentration (medium slurry concentration)

4.3.3.1. Influence of surfactant on slurry rheology

Data from rheometer are presented as a linear plot of shear stress versus shear rate (Rheograms). This type of plot allows the viewer to see directly if there is Newtonian behavior because the plot will take the form of a straight line through the origin. A non-Newtonian response is non-linear and may or may not pass through the origin. If the sample has an apparent yield stress, then the line or curve will have some positive y-axis intercept. Fly ash slurries exhibited strong flocculation behaviour in absence of chemical additives (Struble and Sun, 1995; Bentz, 2007). A yield stress is needed to break down this flocculated structure into smaller flocs or individual particles to induce flow. The yield stress value of 0.3 Pa to 4 Pa was obtained for 40% solid concentration without any additive (Figure 4.49.b). This Figure clearly depicted Bingham plastic model as given below:

$$\tau = \tau_y + \eta\, \dot{\gamma} \tag{4.2}$$

This is a straight-line fit shifted up the y-axis to accommodate a yield stress (τ_y). Bingham plastic materials do not flow until a critical yield stress is exceeded; thereafter a linear relationship is shown between the shear stress and shear rate. Thus, Bingham plastic materials behave as solids below the yield stress and flow like a viscous liquid when the yield stress is exceeded. The rheological parameters, namely yield stress and plastic viscosity, were calculated from the measured shear stress- shear rate curves for each of the mixtures from the above model. To know the flow behaviour of the untreated fly ash slurry, experiments were carried out for a wide range of shear rates varying from as low as $25 s^{-1}$ to as high as $1000 s^{-1}$ at 40^0C for fly ash slurry at 40% solid concentration to draw a complete rheogram. The result of the study is presented in Figure 4.49(a) which shows the relationship between shear stress and shear rate rheogram. Maximum shear rate observed was $611\ s^{-1}$, confirming observations reported by Shah and Jeong (2003). Beyond the shear rate value of $600\ s^{-1}$ shear stress decreased almost linearly reaching to a minimum value of about 10 Pa. Figure 4.49(b) shows the shear stress-shear rate relationship without any additive at varying temperature environment (20^0C to 40^0C).
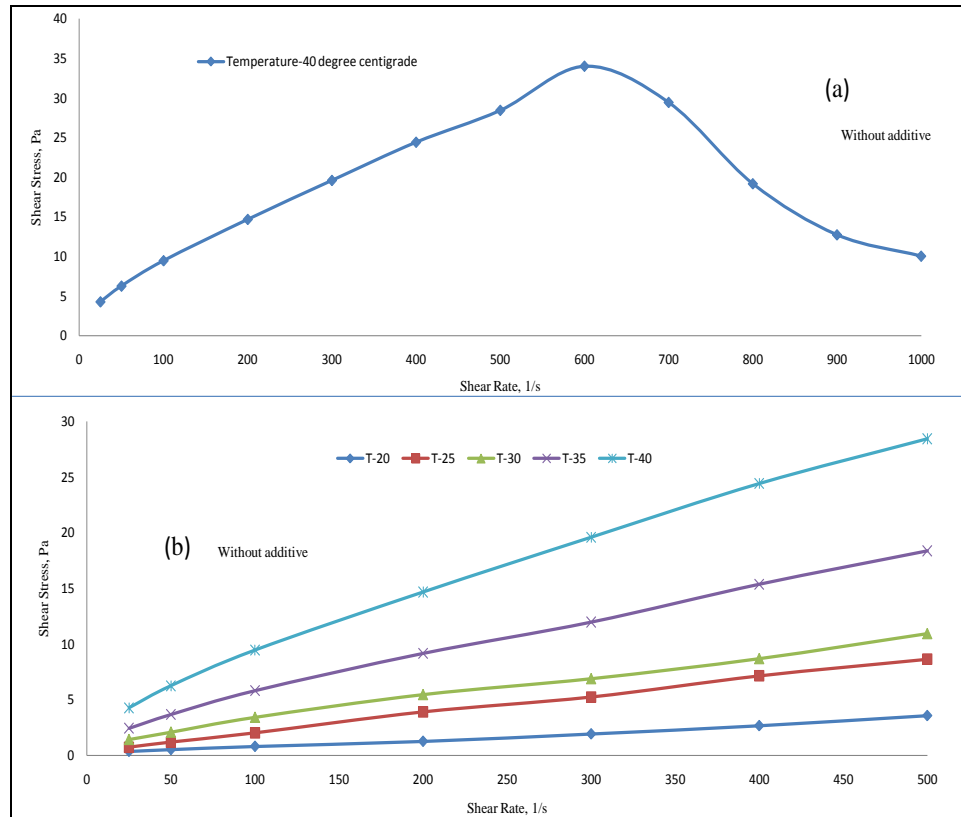
Figure 4.49. Rheogram of fly ash slurry without additive
(*Note: T-Temperature in degree centigrade*)

Slurry rheological parameters fitted well to Bingham plastic model with positive values of yield stress (0.3 Pa to 4 Pa). At 40^0C the yield stress value was maximum (4 Pa) and at 20^0C the yield stress value was minimum (0.3 Pa). However, addition of the surfactant to fly ash slurry completely eliminated the yield stress (Figures 4.50- 4.51 a, b, c, d). Therefore, the influence of the surfactant eliminated the yield stress of the slurries rather than the viscosity which compares favourably well with the results obtained by Jones & Chandler (1989). The yield stress increased almost exponentially as the temperature increased from 20^0C to 40^0C for the fly ash slurry without any additive (Figure 4.52). At 0.1% additive concentartion the slurry behaviour was shear thickening at 40^0C which is not a desirable property for pipeline transport systems (Figure 4.50). But the slurry behavour was shear thinning between 20^0C and 35^0C temperature range. Here again it is seen that the flow curves cross each other when the shear rate increased beyond 611 s^{-1} confirming to the results of Shah and Jeong (2003). It is established that shear rate beyond 600 s^{-1} would not facilitate reduced energy consumption.
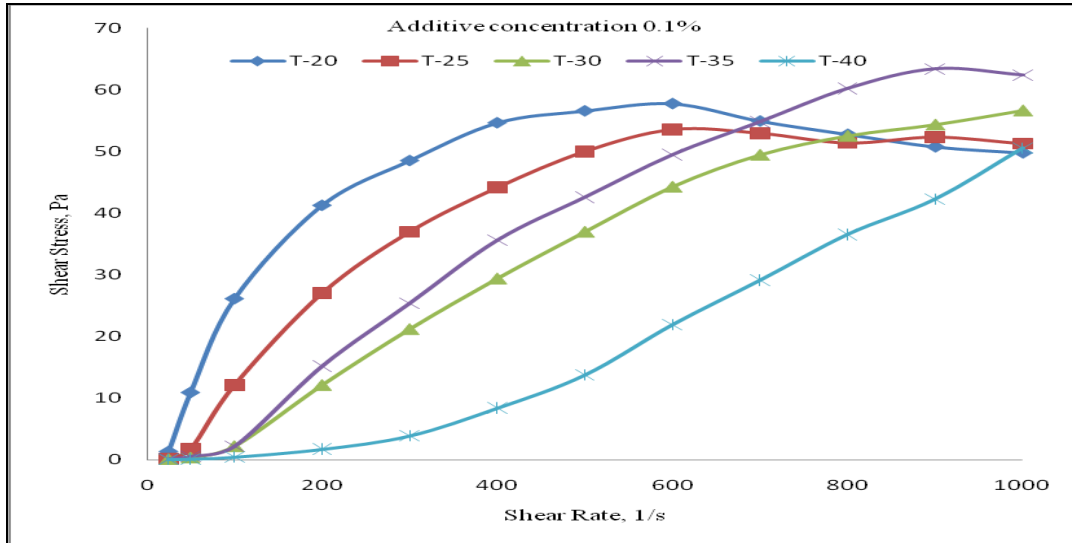
Figure 4.50. Rheogram of fly ash slurry with 0.1% additive
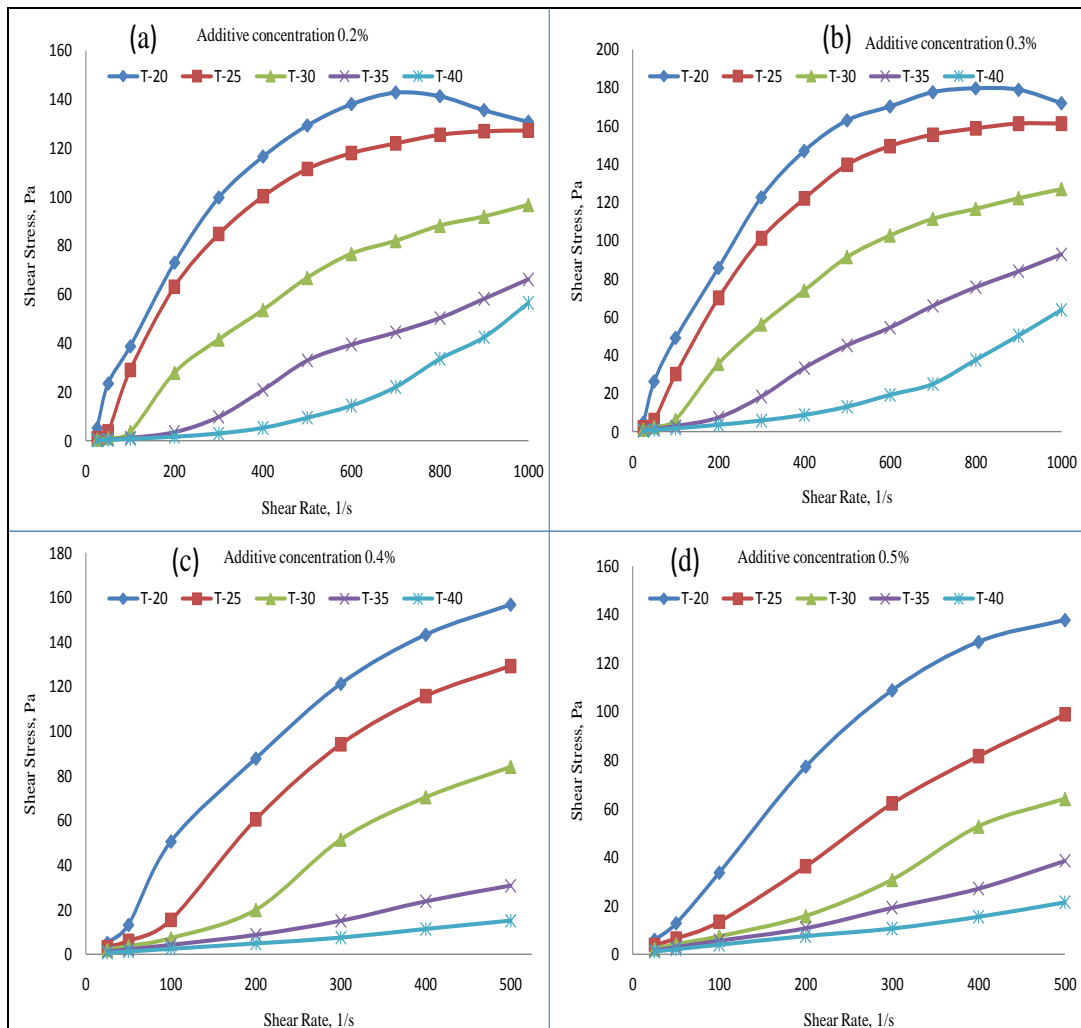(*Note: T-Temperature in degree centigrade*)

Figure 4.51. Rheogram of fly ash slurry with (a) 0.2%, (b) 0.3%, (c) 0.4%, and (d) 0.5% additive
(*Note: T-Temperature in degree centigrade*)

145
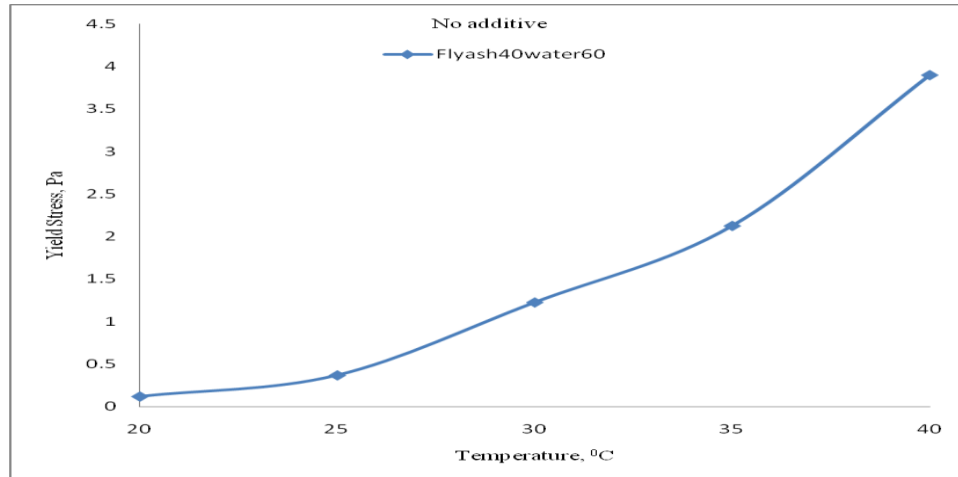
Figure 4.52. Yield stress vs. Temperature plot of fly ash slurry without additive

Figure 4.53(a) presents a complete flow curve for a time-independent non-Newtonian fluid. Region (1) corresponds to viscosities relative to low shear rates, region (2) corresponds to viscosities relative to the medium shear rates and region (3) corresponds to viscosities relative to high shear rates. Viscosity decreased as the shear rate increased for slurry without any additive as the shear rate is increased from 25 s^{-1} to 1000 s^{-1} (Figure 4.53.a). Lower temperature ranges (20^{0}C, 25^{0}C, and 30^{0}C) depicted good results (Figure 4.53.b) compared to higher temperature ranges (35^{0}C and 40^0).

Figure 4.53. Flow curve of fly ash slurry without additive
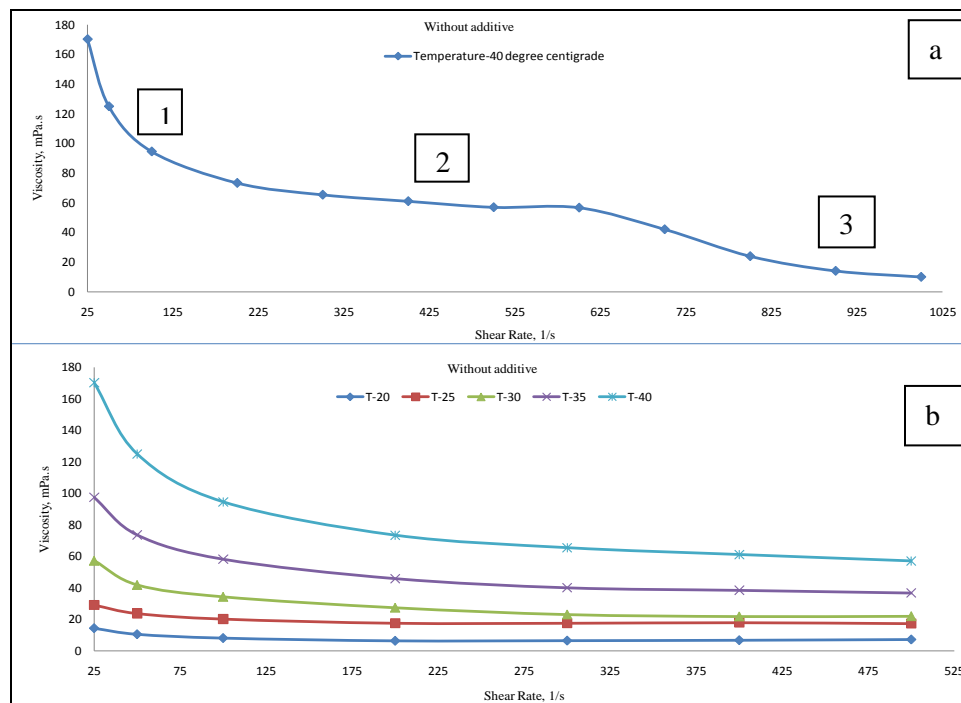(*Note: T-Temperature in degree centigrade*)

The viscosity increased as the temperature was increased from 20^0C to 40^0C for slurry without any additive (Figure 4.54). It showed shear thickening behavior.
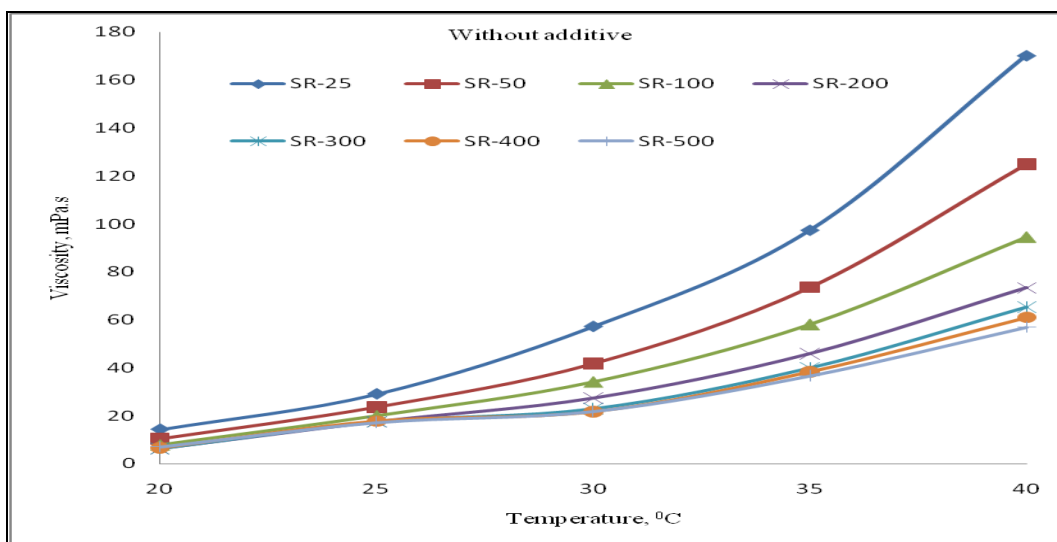
Figure 4.54. Viscosity vs. Temperature plot of fly ash slurry without additive
(*Note: SR-Shear Rate*)
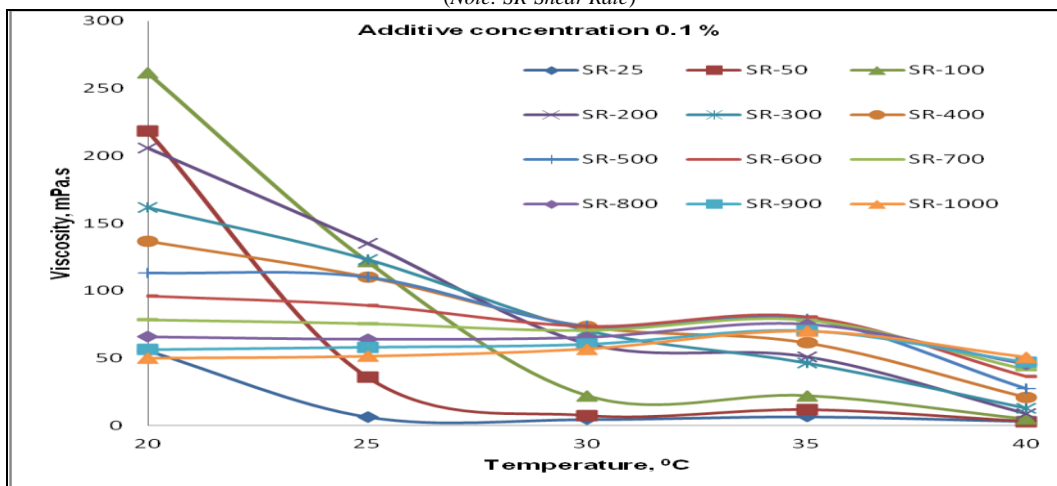
Figure 4.55. Viscosity vs. Temperature plot of fly ash slurry with 0.1% additive
(*Note: SR-Shear Rate*)

When surfactant was added to the slurry the rheological properties changed drastically (Figure 4.55). The viscosity decreasing substantially as the temperature was increased from 20^0C to 40^0C. These results compare favourably well as with the observations made by Shenoy (1976). This phenomenon is due to the formation of spherical micelles which grow continually in size with the increase of temperature until at the cloud point when they can no longer grow and phase separation occurs; which occurs only in relatively dilute surfactant solutions (Shenoy, 1976). At 0.1% additive concentration the slurry behaviour depicted erratic

results at lower temperature ranges and behaved reasonably well beyond 30^0C range (Figure 4.55).
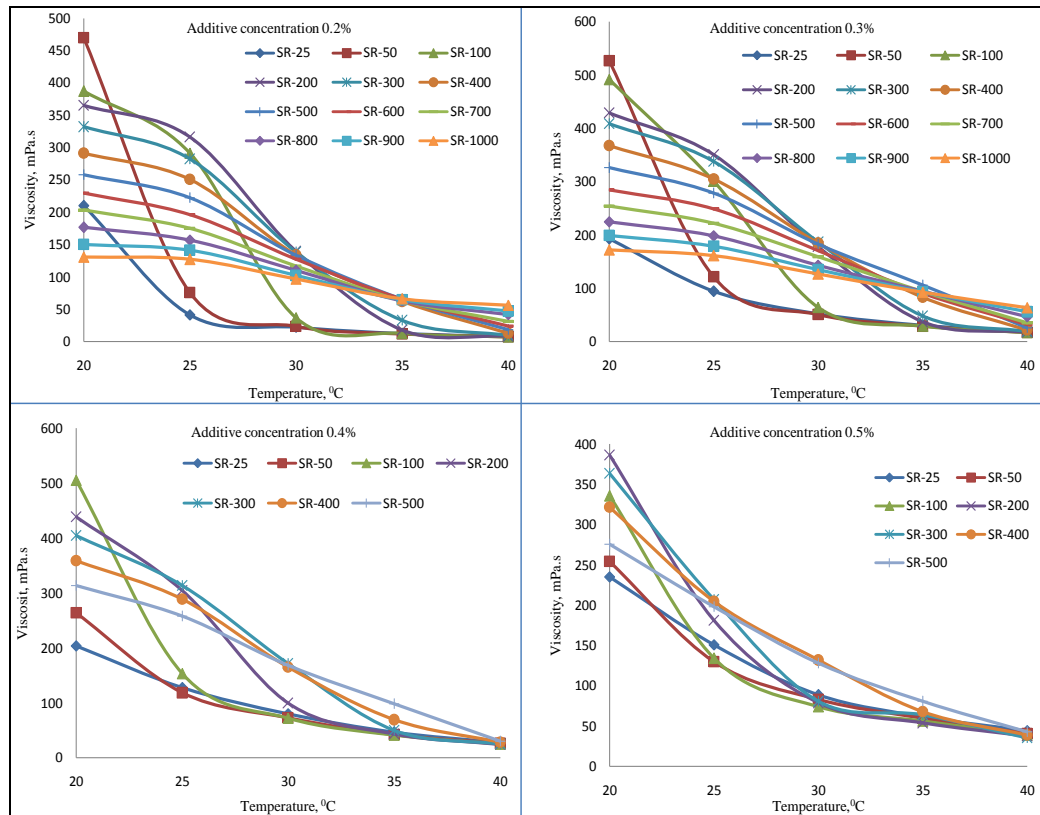
Figure 4.56. Viscosity vs. Temperature plot of fly ash slurry with additive
(*Note: SR-Shear Rate*)

4.3.3.2. Influence of surfactant on shear viscosity

At very low shear rates, from 25 - 50 s^{-1}, the slurry exhibited inconsistent results, because a minimum value of shear rate is required to start the flow to take place (Figure 4.57). Figure 4.58 shows the shear viscosity of fly ash slurries with additive concentration ranging from 0.2% to 0.5% (by weight) at varying temperatures. Shear viscosity decreased sharply from 20^0C to 40^0C, with the shear rates varying from 25 to 1000 s^{-1} for the entire additive ranges tested. Shear thinning behaviour, a favourable property for pipeline transport, was observed at 20^0C and 25^0C for all the slurries tested (Senapati and Mishra, 2012). The viscosity values of the slurries were nearly constant for the shear rates varying from 50 - 500 s^{-1} at 40^0C, confirming that the slurry showed Newtonian flow behavior i.e. the material would flow smoothly in pipelines. The results obtained at 35^0C and 40^0C with additive concentration of 0.4% and 0.5% (Figure 4.58) were favourable.
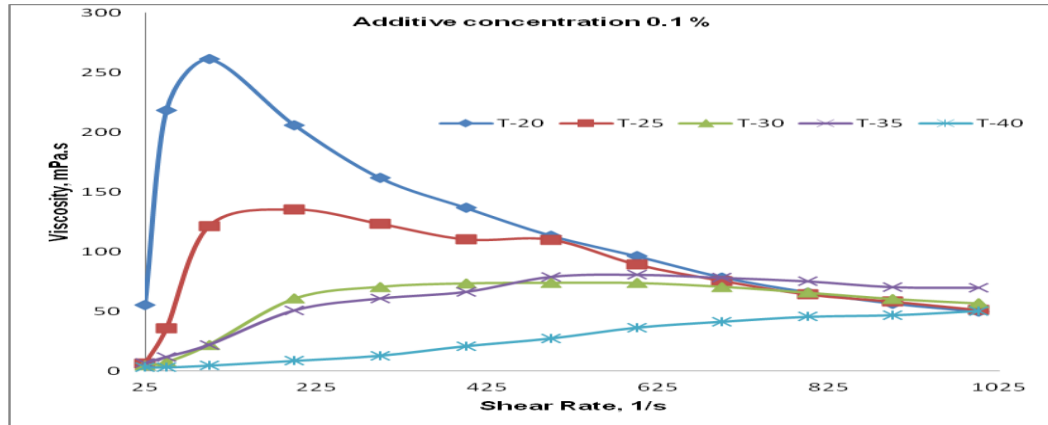
Figure 4.57. Flow curve of fly ash slurry with additive concentration 0.1%
(*Note: T-Temperature in degree centigrade*)
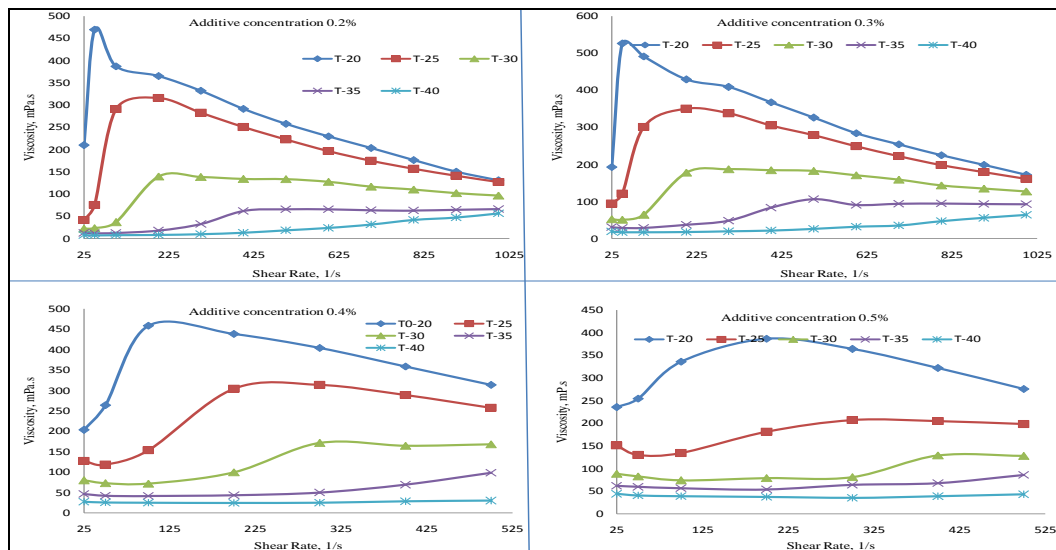
Figure 4.58. Flow curve of fly ash slurry with additive
(*Note: T-Temperature in degree centigrade*)

4.3.3.3. Surface Tension

The addition of surfactant reduced surface tension of fly ash slurries by 43% to 47% compared to untreated slurry and by 52% to 55% compared to plain tap water (Table 3.9). The surfactants facilitated easier spreading, leading to lower the interfacial tension between solid particles and the liquid.

4.3.3.4. Zeta potential (ζ)

Surfactants comprised of hydrophilic and hydrophobic groups, by which they act as a bond combining mineral particles and host polymers (Zana, 2002). It is advantageous to have a single chemical agent such as a surfactant that can accomplish both surface modification and stabilization of heavy metals. The ζ of the untreated fly ash slurry was -25 mV at pH 7.4,

increasing (> +31 mV) when the surfactant was added to the slurry (Table 3.9). From these results, it is confirmed that the fly ash slurry suspension is stable and the fly ash particles would repel each other and, therefore, flocculation would be prevented and dispersion achieved, facilitating smooth flow and reduced clogging of pipelines. Both yield stress and viscosity (apparent or plastic) strongly depends on the particle characteristics of the powders employed in preparing fly ash slurry with a constant volume fraction of water. As the yield stress is dominated by the characteristics of the fly ash particles, the additive acted as diluents, effectively decreasing the fly ash particle number density.

4.3.3.5. Summary of observations at 40% solid concentration

> ➢ The test results clearly indicated that the fly ash-water slurry rheology is strongly influenced by the chemical additives. The presence of elements such as iron oxide, aluminium oxide, and other alkaline earth materials in the fly ash slurry gave rise to adverse rheological properties, and these effects were negated by the addition of a surfactant (CTAB) that formed charged complexes with the fly ash particles.

> ➢ All the treated slurries exhibited shear-thinning and Newtonian properties. The surfactant modified the surface properties of the fly ash particles and improved its suspension stability.

> ➢ The surface tension of the treated fly ash slurry is reduced compared to untreated fly ash slurry and that of the suspending medium (water). This implies that this fly ash has greater potential to be transported in pipelines with the addition of a cationic surfactant and a counter-ion which will reduce specific energy consumption and water requirements.

> ➢ The flow properties and viscosity of the fly ash water suspensions were sensitive to the use of chemical additives.

4.3.4. Results of 50% solid concentration (medium slurry concentration)
4.3.4.1. Effect of surfactants on fly ash slurry rheology

Figure 4.59 shows the rheogram of fly ash-water slurries (at 20^0C to 40^0C) without any additive. The slurry without any additive exhibited shear thickening behavior with yield stress values of varying magnitude which is not a desirable feature for any slurry pipeline

transportation system. At 25^0C the behavior is closer to Bingham (yield-constant viscosity) non-Newtonian fluid. The value of the yield stress was found to be 2 Pa. At 35^0C and 40^0C also the slurry behaviour was same but the yield stress was reduced to 1.5 Pa. At 20^0C the flow behavior is shear thickening (i.e. dilatants). The rheological data suggests that shear thickening is occurring in the slurry at a shear rate of $300s^{-1}$ because of the increase in slope of the rheometric data beyond these shear rates. This is not the case however, as this increase in slope is actually an artifact that is caused by turbulent vortices forming at the bob surface, which occurs with low viscosity fluids being sheared at high shear rates (Chryss and Pullum, 2007). The governing relation for this behavior is given by Herschel-Bulkley model:

$$\tau = \tau_y + K\,\dot\gamma^n \qquad\qquad (4.3)$$
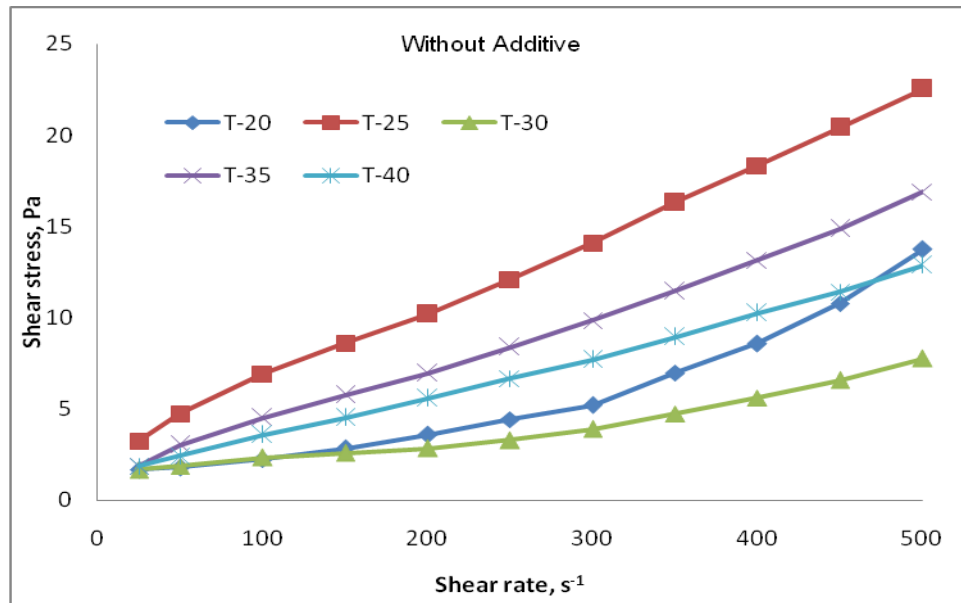
Figure 4.59.Rheogram of fly ash slurry without additive

At 50% solid concentration yield stress is completely or nearly eliminated in case of all surfactant treated slurries. Overall at 0.1% additive concentration the slurry depicted shear thinning behavior; this is a desirable feature for any hydraulic slurry pipeline transport system (Figure 4.60). Because, shear thinning materials display a decrease in viscosity with increasing shear rate, i.e. the material appears to flow more easily with increasing shear rate (Senapati and Mishra, 2012). Shear thickening materials, on the otherhand display an opposite behavior, i.e. the viscosity increases with increased shear rate. This behavior is seen in highly concentrated suspensions (Seshadri *et al*., 2005).
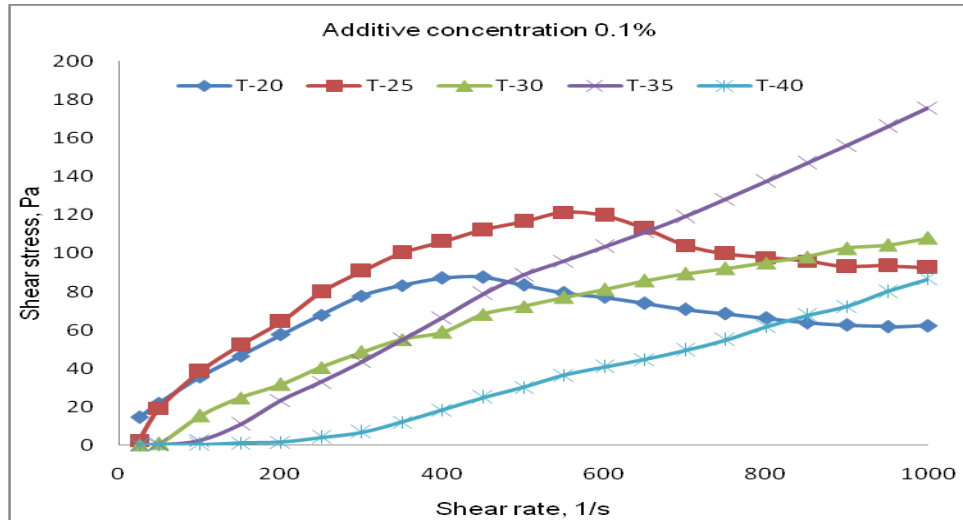
Figure 4.60.Rheogram of fly ash slurry with additive concentration 0.1%

When the additive concentration was 0.1% at the slurry temperature of 35^0C, Newtonian fluid behaviour without any yield stress was observed. When the additive concentration was increased to 0.2%, the slurry depicted shear thinning behaviour except at 40^0C which depicted shear thickening behaviour (Figure 4.61). Similar behaviour of coal water slurry was also obtained and attributed to the breaking of agglomerates at a higher shear rates (Swain and Panda, 1996).
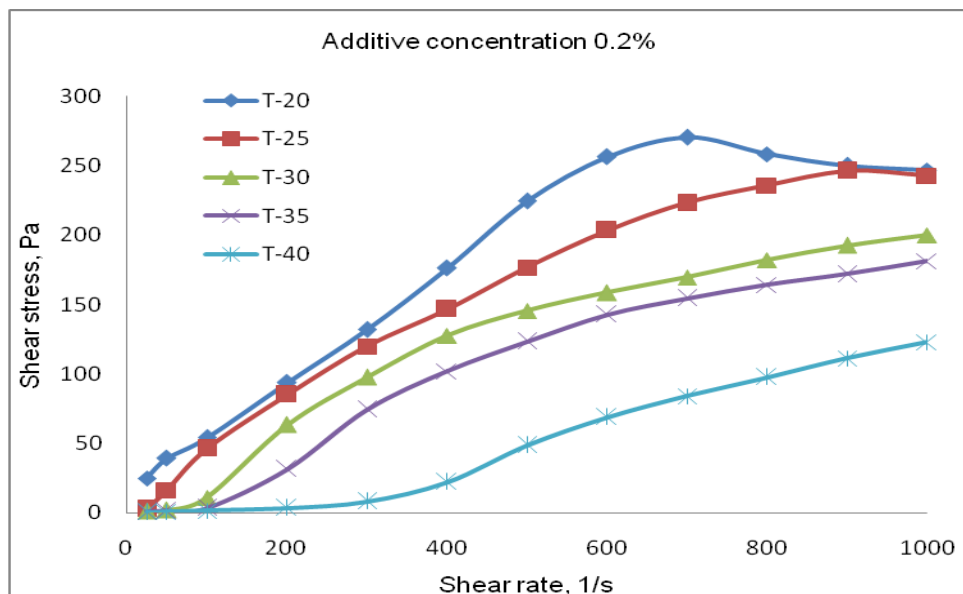
Figure 4.61.Rheogram of fly ash slurry with additive concentration 0.2%

At 0.3% additive concentration slurry behaviour was shear thinning except at 40^0C (Figure 4.62). Similar trend was observed at 0.4% and 0.5% additive concentration (Figures

4.63 and 4.64). However here also the slurry behaviour was shear thickening at 40^0C and 35^0C. Results obtained at 0.2% and 0.3% additive concentration between 30^0 C to 35^0C produced the most favourable flow properties. The flow curves of fly ash-water slurry presented in Figure 4.62 show pseudoplastic flow behaviour. As the shear rate increased the structure of the fluid became more ordered, which steadily reduced the apparent viscosity. The power law model also referred to as the Ostwald-de Waale model was used to fit the rheological data of pseudoplastic fluids.
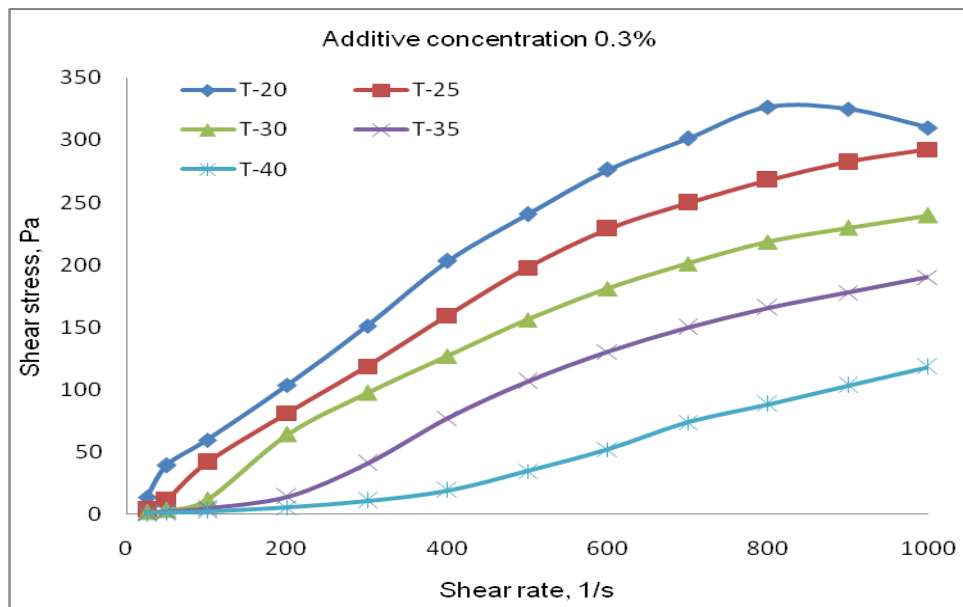
Figure 4.62.Rheogram of fly ash slurry with additive concentration 0.3%

Figure 4.63.Rheogram of fly ash slurry with additive concentration 0.4%

The flow properties of fly ash slurry at 50% solid concentration with surfactant exhibit minimum or near non-exist yield stress which is a favourable attribute for smooth flow. The primary purpose of adding surfactant to fly ash slurry was to disperse flocculated fly ash particles. Due to the dispersion effect, the fluidity of the slurry is increased, i.e. the yield stress and plastic viscosity reduced. The surfactant is believed to adsorb onto the fly ash particles and altered the degree of flocculation in one of these three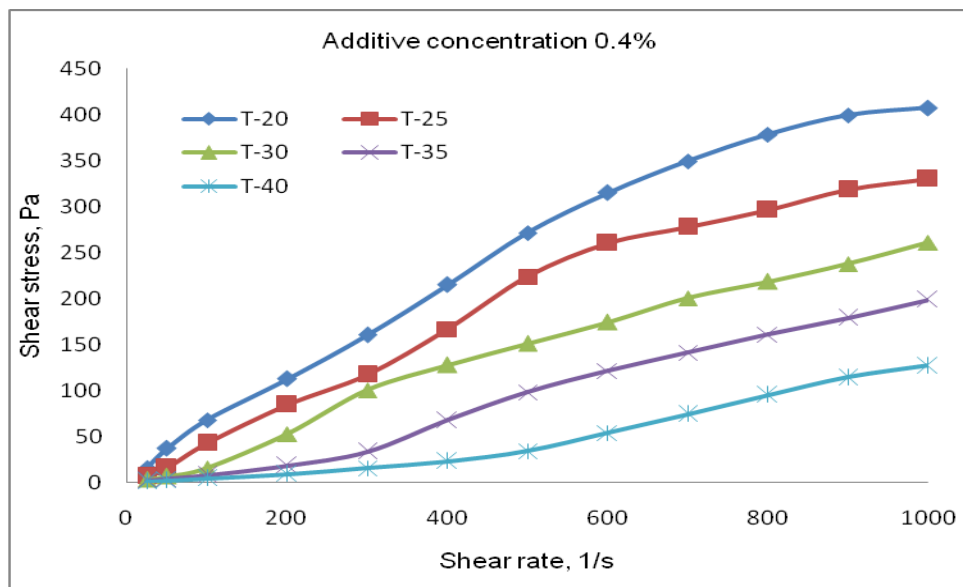 ways: (1) Increasing the zeta potential and, thus, the repulsive forces between the fly ash particles (electrostatic double layer repulsion), (2) Increasing solid-liquid affinity, (3) Introducing a physical barrier against flocculation, steric hindrance i.e., the importance of steric forces in dispersing fly ash suspensions through increasing the electrostatic double layer forces (Yoshioka *et al*. 1997).
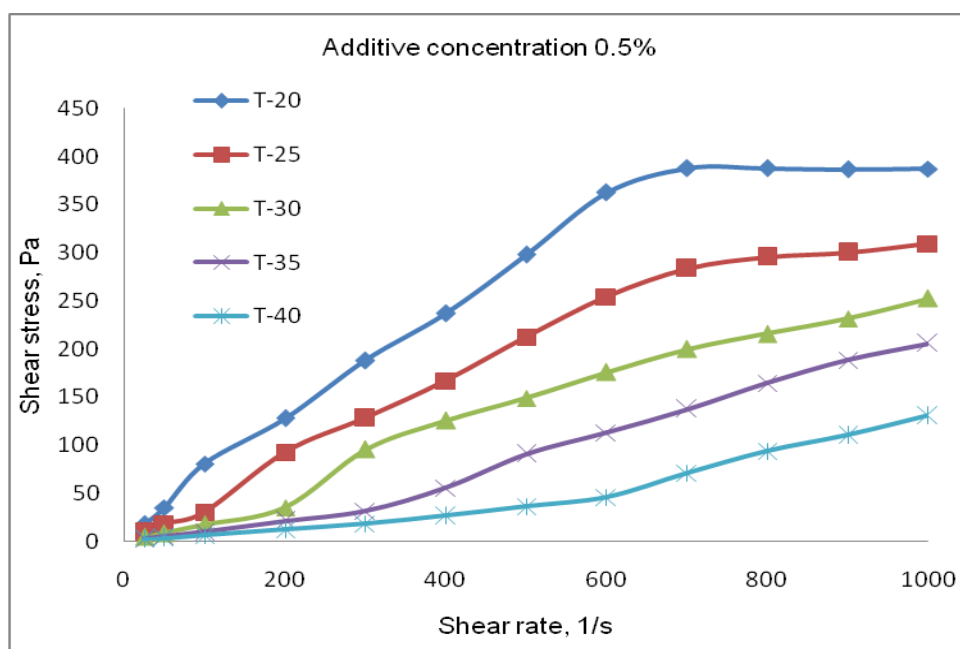
Figure 4.64.Rheogram of fly ash slurry with additive concentration 0.5%

4.3.4.2. Effect of surfactant on shear viscosity

The viscosity of untreated fly ash slurry was more than 60mPa.s at a shear rate value of $25s^{-1}$ that became asymptotic when shear rates increased to $200s^{-1}$ and beyond (Figure 4.65). But when the additive was added, the slurry behaved differently. At 0.1% additive concentration the slurry behaviour was Newtonian at 30^0C. At 20^0C and 25^0C the slurry behaviour was shear thinning and at 35^0C and 40^0C the behaviour was shear thickening (4.66). As the additive concentration was increased to 0.2%, 0.3%, 0.4%, and 0.5% (Figures 4.67-4.70) there was some noise in the data at low shear rates ($25s^{-1}$ to $50s^{-1}$). Beyond shear

rate values of $100s^{-1}$ the slurry behaviour was shear thinning except at 35^0C and 40^0C. At 50% fly ash concentration with 0.1% additive at 30^0 C the slurry exhibited Newtonian flow behavior even at lower shear rates. The behavior again became Newtonian for all concentration of surfactant irrespective of temperature ranges when the applied shear rate was $200s^{-1}$ or more. It confirms to that observed elsewhere (Seshadri *et al*., 2006).
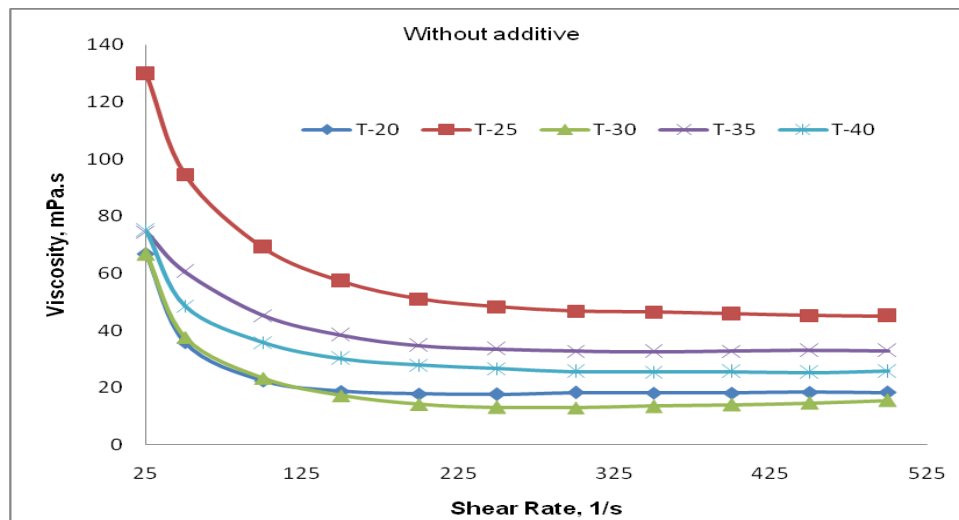
Figure 4.65.Flow curve of fly ash slurry without additive

Wide range of shear rate values varying from $25s^{-1}$ to $1000s^{-1}$ with additive concentration varying from 0.1% to 0.5% was investigated in order to draw a complete flow curve for this time-independent non-Newtonian fluid to clearly demarcate three flow regions i.e., region (1) corresponding to viscosities relative to low shear rates, region (2) corresponding to viscosities relative to the medium shear rates and region (3) corresponding to viscosities relative to higher shear rates (Whittingstall, 2001). This wide range of shear rates starting from $25s^{-1}$ to $1000s^{-1}$ was also investigated because for pumping of slurries common shear rate range varies from $1-10^3s^{-1}$ (Carrington and Langridge, 2005). With 50% solid concentration and additive presence from 0.2% to 0.5%, the viscosity values decreased with increasing shear rates upto $1000s^{-1}$ (Figures 4.67-4.70). Thus the additive (surfactant) influenced the rheological behavior of the treated slurries. Because the rheological behavior of a particle suspension is dependent on the balance between a range of different forces, i.e., van der Waals, electrical double layer forces, steric forces, acting between colloidal particles. If the summation of these forces results in an overall attractive inter-particle force, flocculation will be promoted. In concentrated suspensions these flocs create a continuous three-dimensional inter-particle

network which can display a considerable resistance to both flow and consolidation. On the otherhand, if the overall forces are repulsive the particles will be dispersed and suspension will flow readily (Marmy *et al.*, 2012).
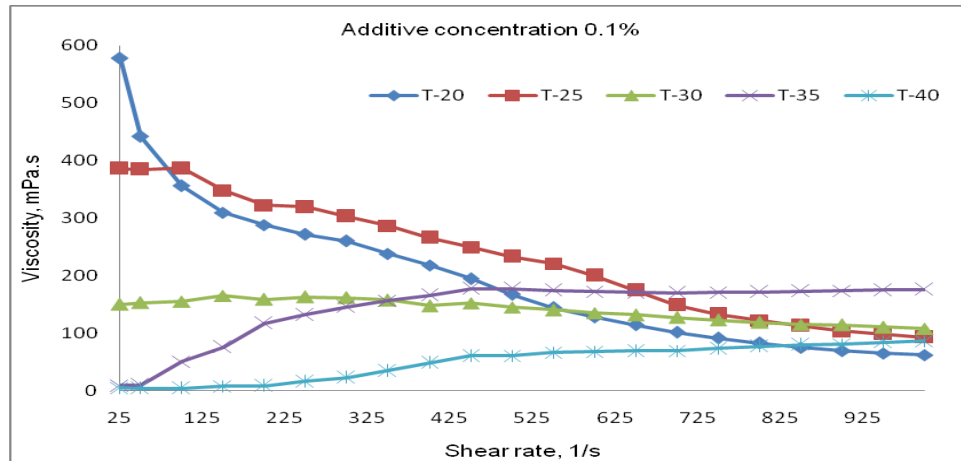
Figure 4.66.Flow curve of fly ash slurry with additive concentration 0.1%
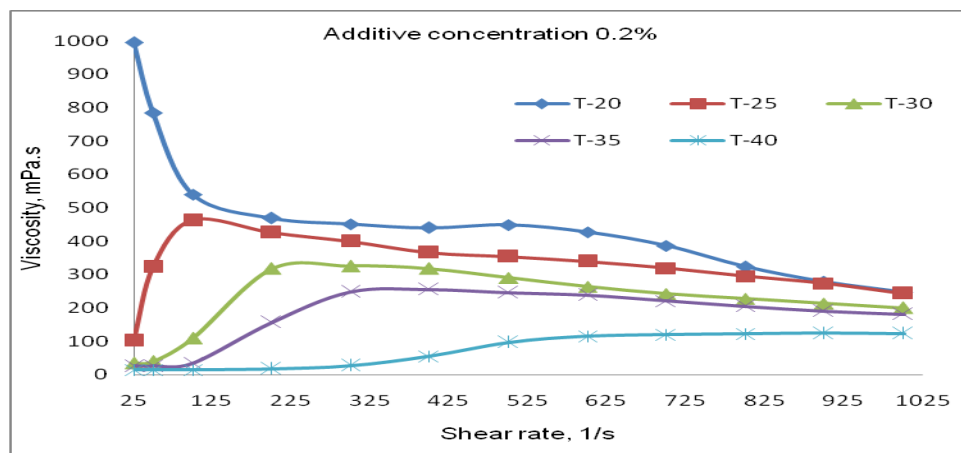
Figure 4.67.Flow curve of fly ash slurry with additive concentration 0.2%
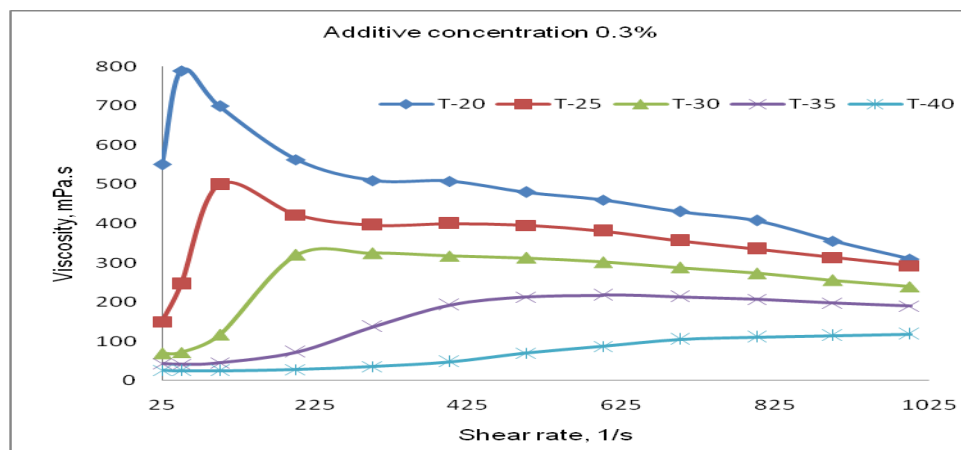
Figure 4.68.Flow curve of fly ash slurry with additive concentration 0.3%
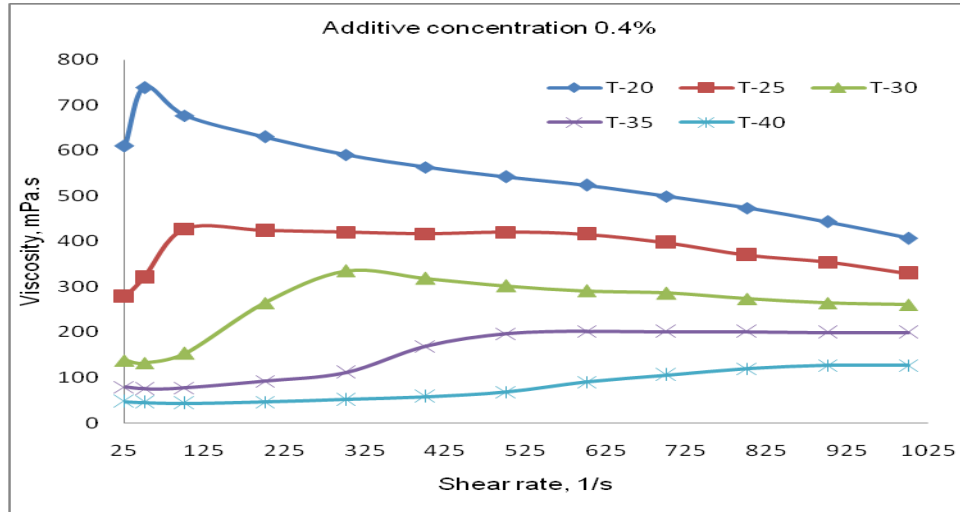
Figure 4.69.Flow curve of fly ash slurry with additive concentration 0.4%
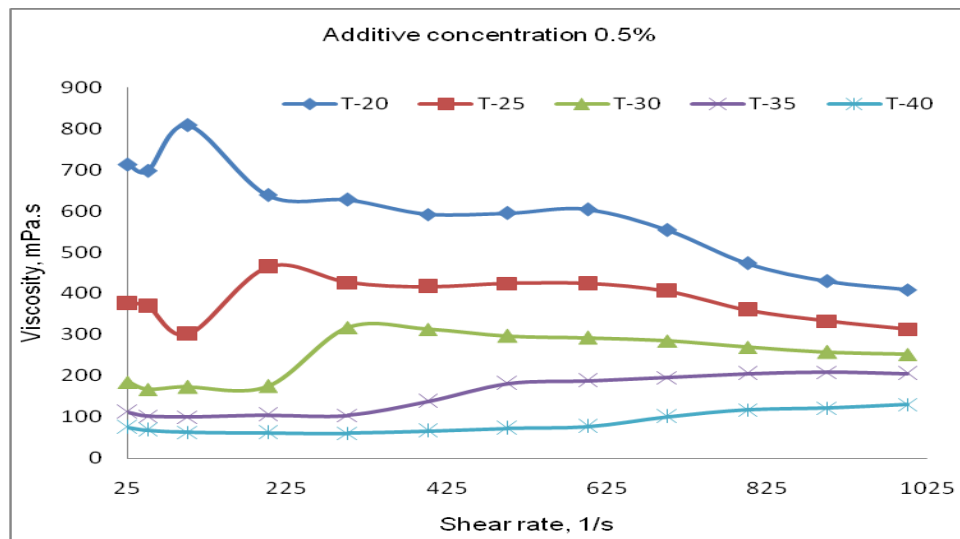
Figure 4.70.Flow curve of fly ash slurry with additive concentration 0.5%

4.3.4.3. Effect of temperature on fly ash-slurry viscosity

The untreated fly ash slurry depicted erratic and uneven flow behaviour as the temperature was increased from 20^0C to 40^0C and produced minimum visocity values at 30^0C (Figure 4.71). Addition of surfactant changed the behavior of fly ash slurry to smooth pattern though with varying viscosity values. At 20^0C the viscosity values were between 60 mPa.s to 1000 mPa.s which reduced to about 2 to 100 mPa.s at 40^0C at different shear rates though the rate of decrease beyond 30^0C is minimum (Figures 4.72 - 4.76). When the additive concentration was 0.1% at 30^0C there is culmination of all the curves at varying shear rates demarketing two viscosity regions (Figure 4.72). When the additive concentration was

increased to 0.2% best results are obtained at 30^0C, 35^0C, and 40^0C at low shear rate values i.e., at $25s^{-1}$, $50s^{-1}$, and $100s^{-1}$ (Figure 4.73). Minimum viscosity values obtained at 0.2% additive concentration at above shear rates at 40^0C due to the enhanced dissolving activity of the surfactant at higher temperatures. Similar trend was observed when the additive concentration was increased to 0.3%, 0.4%, and 0.5% (Figures 4.74 - 4.76).
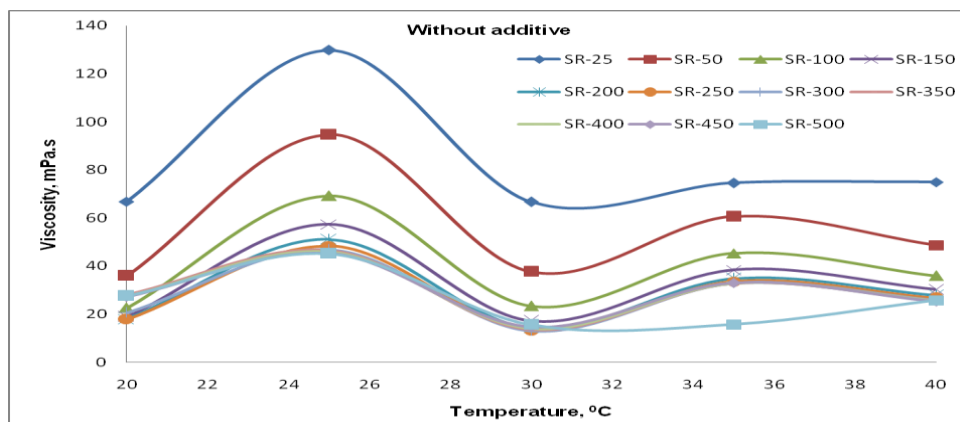
Figure 4.71. Viscosity vs. temperature plot of fly ash slurry without additive
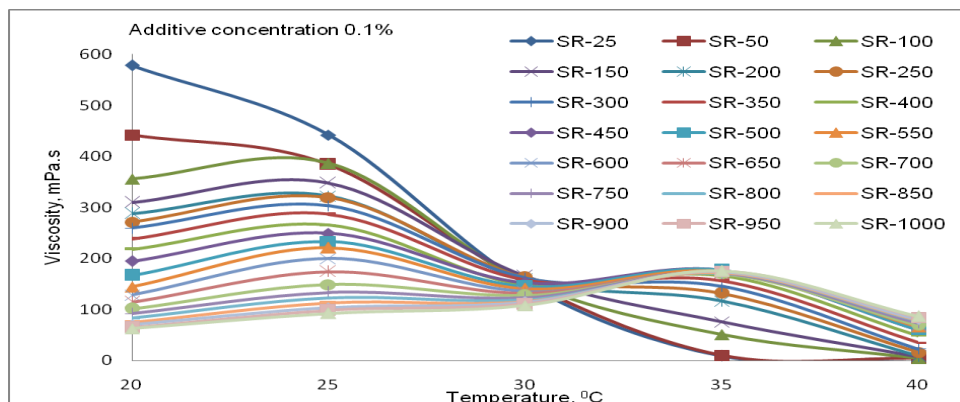
Figure 4.72. Viscosity vs. temperature plot of fly ash slurry with additive conc. 0.1%
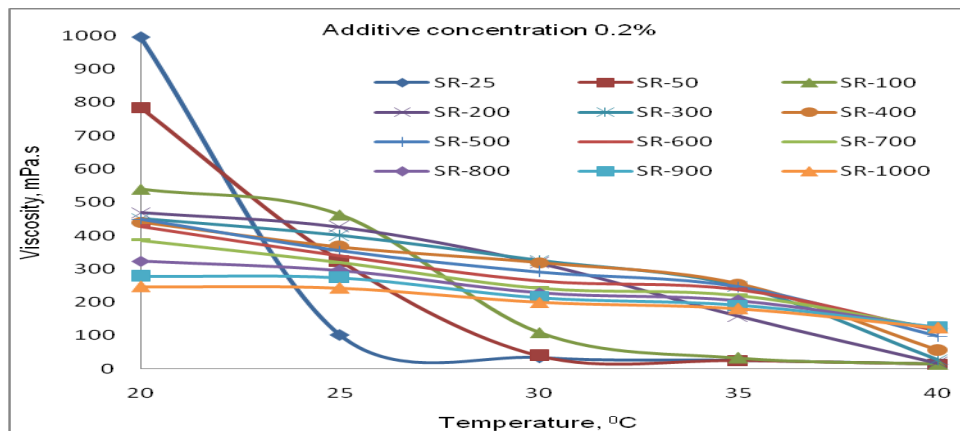
Figure 4.73. Viscosity vs. temperature plot of fly ash slurry with additive conc. 0.2%
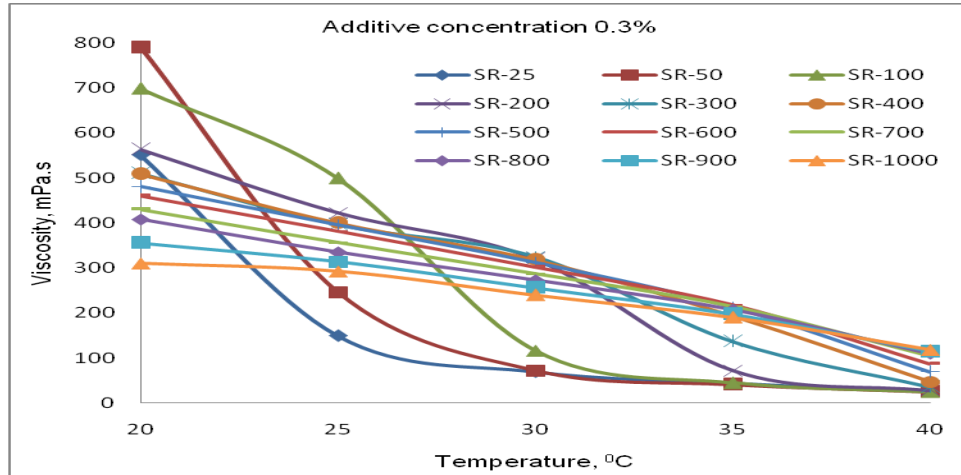
Figure 4.74.Viscosity vs. temperature plot of fly ash slurry with additive conc. 0.3%
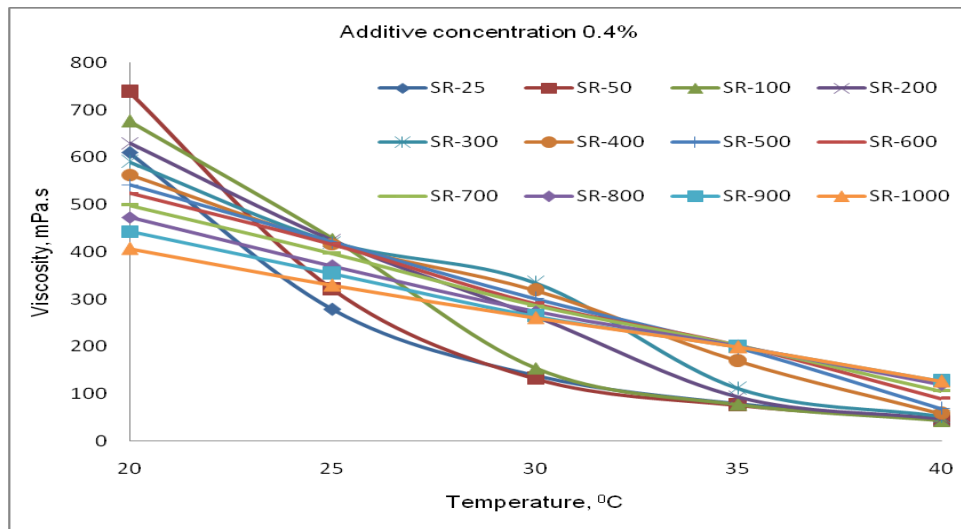
Figure 4.75.Viscosity vs. temperature plot of fly ash slurry with additive conc. 0.4%
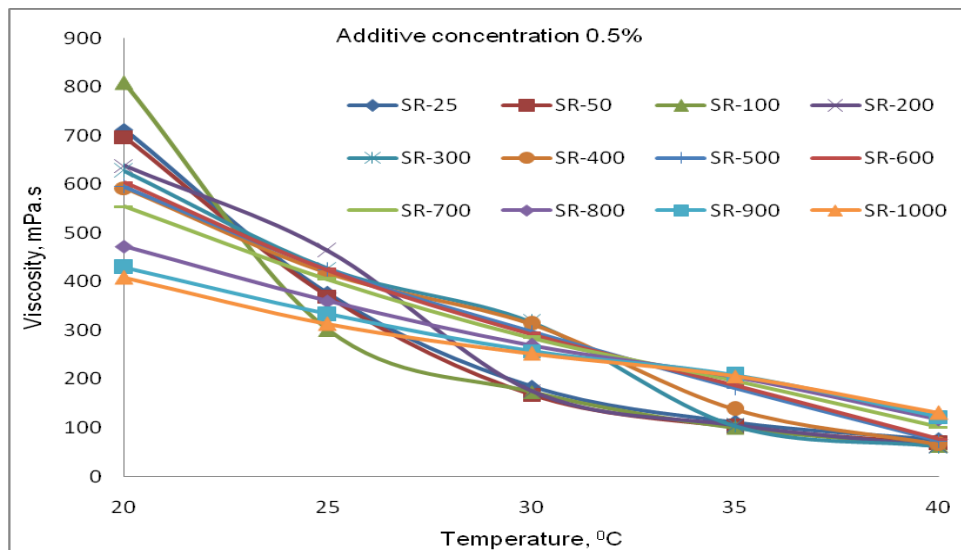
Figure 4.76.Viscosity vs. temperature plot of fly ash slurry with additive conc. 0.5%

4.3.4.4. Yield stress

The untreated 50% solid concentration fly ash slurry showed high yield stress values at varying temperatures. The minimum value obtained was at 30^0C (Figure 4.77). This phenomenon is due to the formation of spherical micelles which grow continually in size with the increase of temperature until at the cloud point when they can no longer grow and phase separation occurs (Shenoy, 1976). The optimum temperature was found to be 30^0C when no additive was added to the slurry. When surfactant of different concentration was added there was no yield stress value and hence not produced here.
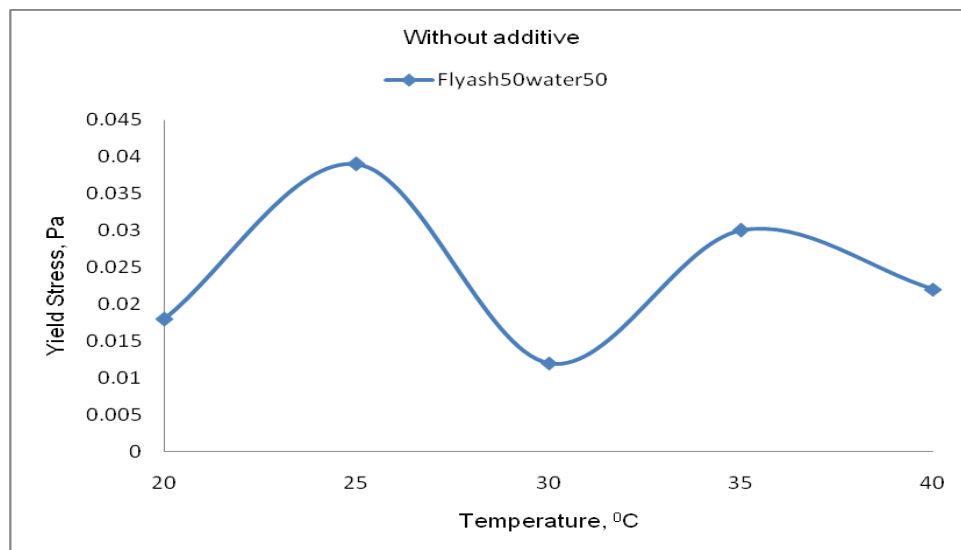
Figure 4.77.Yield stress vs. temperature plot of fly ash slurry without additive

4.3.4.5. Summary of observations at 50% solid concentration

➢ The test results clearly indicated that the fly ash-water slurry rheology depended on chemical additives. It was found that the flow properties and the apparent viscosity of the fly ash-water slurries are very sensitive to these reagents. Yield stress was completely eliminated in the presence of these reagents.

➢ The decrease in viscosity with increasing temperature is attributed to the increase of the kinetic energy of the fly ash particle and rapid movement of the dangled chains of the surfactant units at the fly ash – water interface.

➢ It is found that the optimum temperature is 30^0C and optimum surfactant concentration is found to be 0.2% taking into all the observations together.

4.3.5. Results of 60% solid concentration (high concentration slurry)

4.3.5.1. Influence of surfactant on fly ash-slurry rheology

The flow curve for fly ash slurry has been reported to fit several different mathematical forms (Mishra *et al*., 2002). The common denominator of all these functions is that all of them indicate the existence of a yield stress, i.e. flocculated fly ash slurry is a viscoplastic material. Rheograms were drawn for 60% solid concentration with and without an additive in the temperature range of 20^0C-40^0C. The untreated fly ash slurry (Figure 4.78) behaviour was Bingham yield plastic. The yield stress observed varied between 0.2 - 0.5 Pa. But when the slurry was treated with the additive the slurry depicted Newtonian flow behaviour without yield stress at 0.1% additive concentration except at 25^0C where shear thinning behavior was observed (Figure 4.79). Fly ash slurry at 60% solid concentration was evaluated for shear stress values at higher shear rates i.e. upto $1000s^{-1}$. But the shear stress values obtained were very random for shear rates of more than $200s^{-1}$ and hence those data were not reported here. This observation confirms to that published elsewhere (Seshadri *et al*. 2006). Since 60% solid concentration is high density slurry, so the shear rates varied from $25s^{-1}$ to $200s^{-1}$ only.

Figure 4.78.Rheogram of fly ash slurry without additive
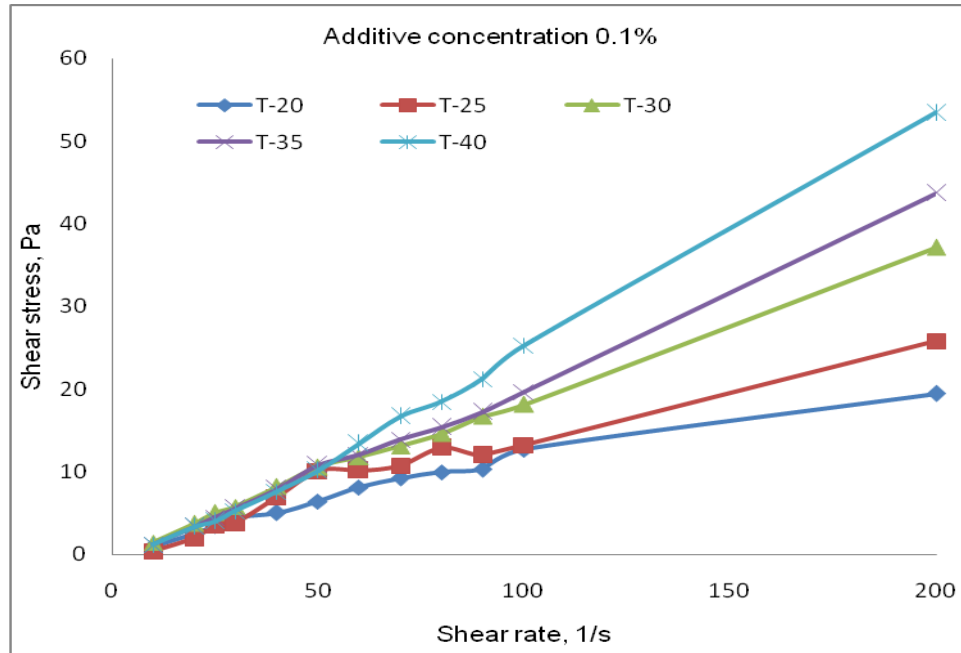
Figure 4.79.Rheogram of fly ash slurry with additive concentration 0.1%

From Figures 4.80 and 4.81 at 0.2% and 0.3% additive concentrations, best results were observed at 30^0 C and 40^0 C clearly depicting Newtonian flow behavior. All the 60% fly ash slurry types with varying additive concentration produced almost zero yield stress except at 20^0C and 25^0C. For high concentration slurry disposal system, 20^0 C temperatures with an additive concentration of 0.2% is found to be ineffective which may be due to the temperature is too low to start the reactions to take place. Here also, best results were obtained at 30^0 C which is the optimum temperature value for complete reaction to take place. No yield stress values were obtained at 0.1% additive concentration. Best results were again obtained at 0.4% additive concentration except at 20^0 C which depicted little amount of higher shear stress values compared to other temperature ranges investigated. Here the slurry behaved like a Newtonian fluid without any yield stress. The results were very much encouraging which confirms to the results obtained by Seshadri and co-workers (2006) where they concluded that as the solid concentration increases the specific energy consumption decreases which is true for this set of observations also. Compared to 0.4% additive concentration 0.5% additive concentration is found to be having some noise in the observational data. This is because of the high dose of additive concentration which produced some noise in the flow curves and rheograms. At 0.2% additive concentration and at 40^0C temperature produced best results. Again at 0.3% additive concentration best results are obtained at 40^0C.
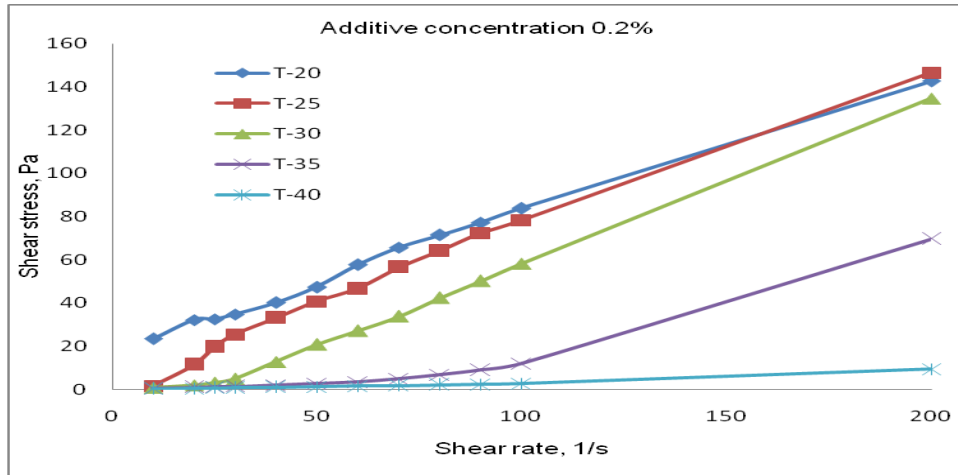
Figure 4.80.Rheogram of fly ash slurry with additive concentration 0.2%
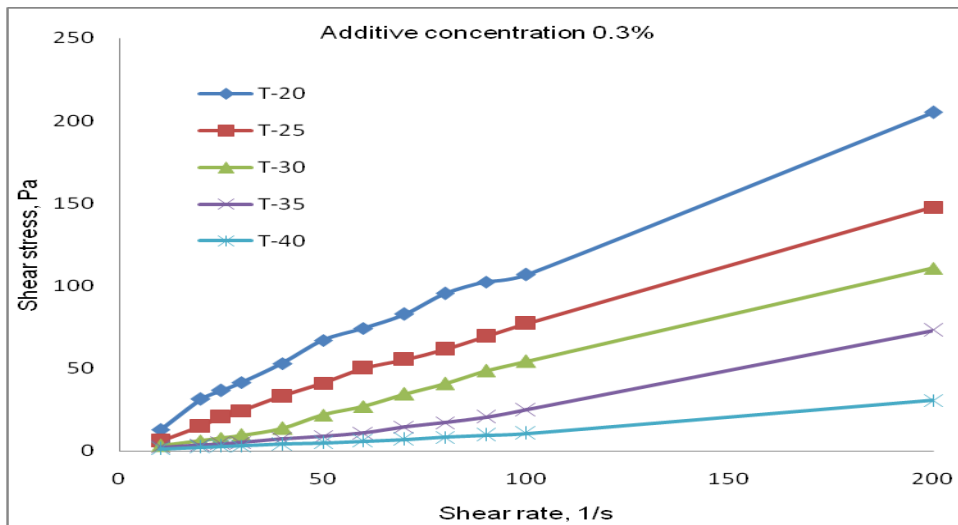
Figure 4.81.Rheogram of fly ash slurry with additive concentration 0.3%
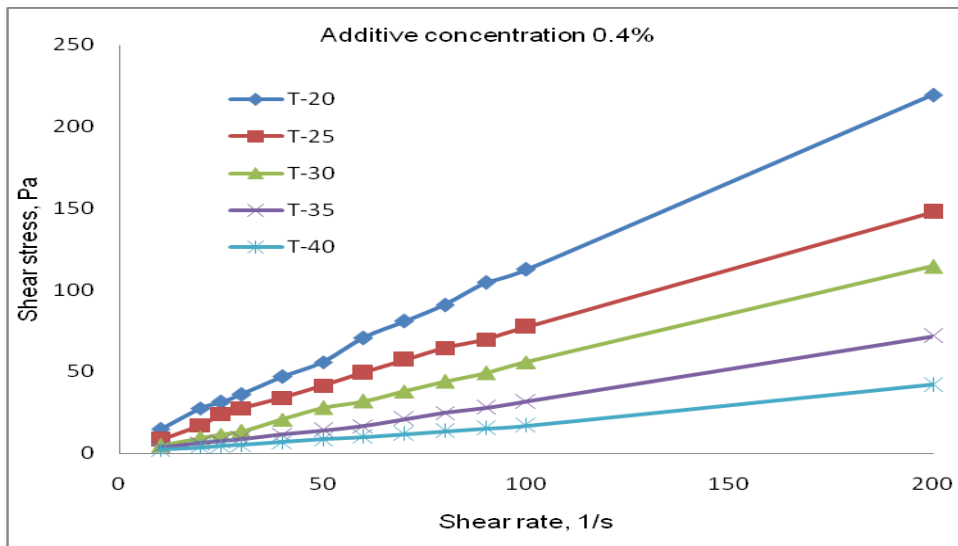
Figure 4.82.Rheogram of fly ash slurry with additive concentration 0.4%
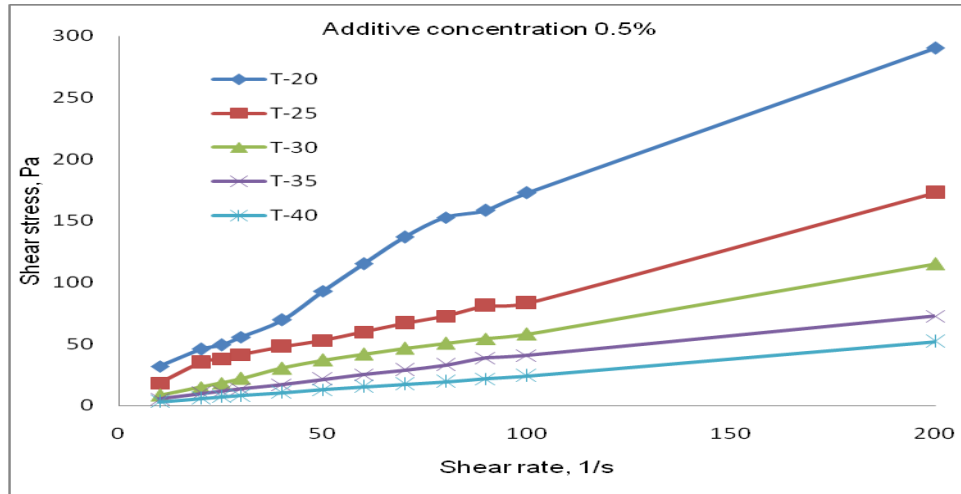
Figure 4.83.Rheogram of fly ash slurry with additive concentration 0.5%

4.3.5.2. *Effect of surfactant on shear viscosity*

Viscosity was found to be more in case of fly ash slurry without any additive (maximum 0.8 Pa.s) at 20^0 C that reduced to 0.3Pa.s at $200s^{-1}$ shear rate (Figure 4.84). When the additive was added, the viscosity values reduced to as low as 0.04 Pa.s. Reduction in viscosity was due to reduction in interparticle friction in the turbulent flow regime. In the laminar flow regime, this effect can be attributed to the reduction of surface tension and zeta potential of the fine particles due to the presence of additive (Chandel *et al.,* 2009). At 0.1% additive concentration maximum viscosity observed was 0.25 Pa.s at 40^0 C (Figure 4.85). Best results were obtained when additive concentration was increased to 0.2% and 0.3% at 40^0 C (Figures 4.86 and 4.87).
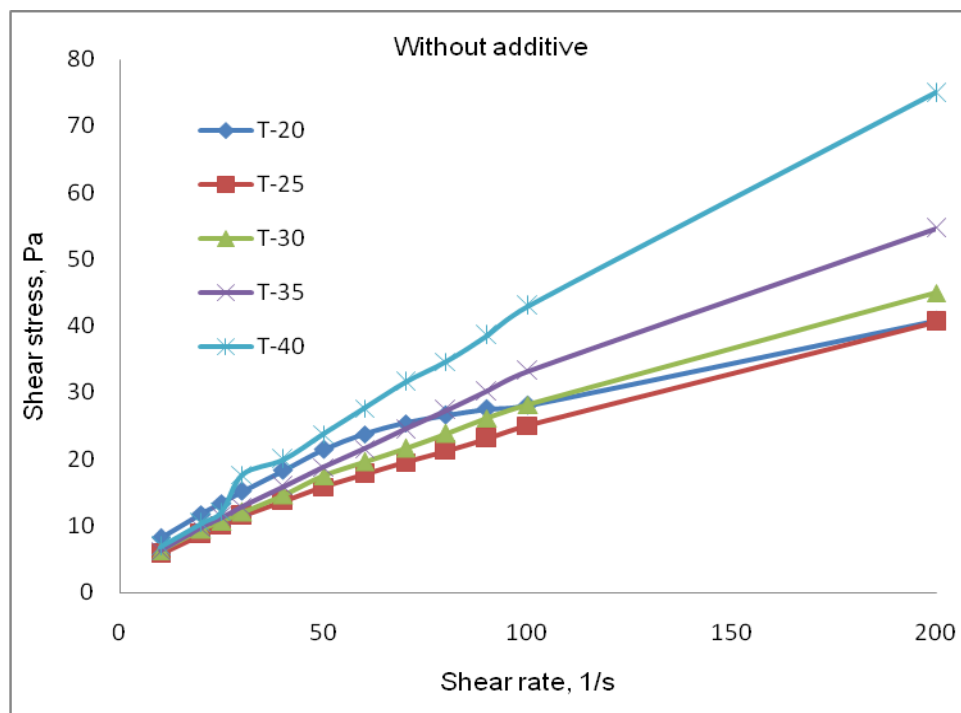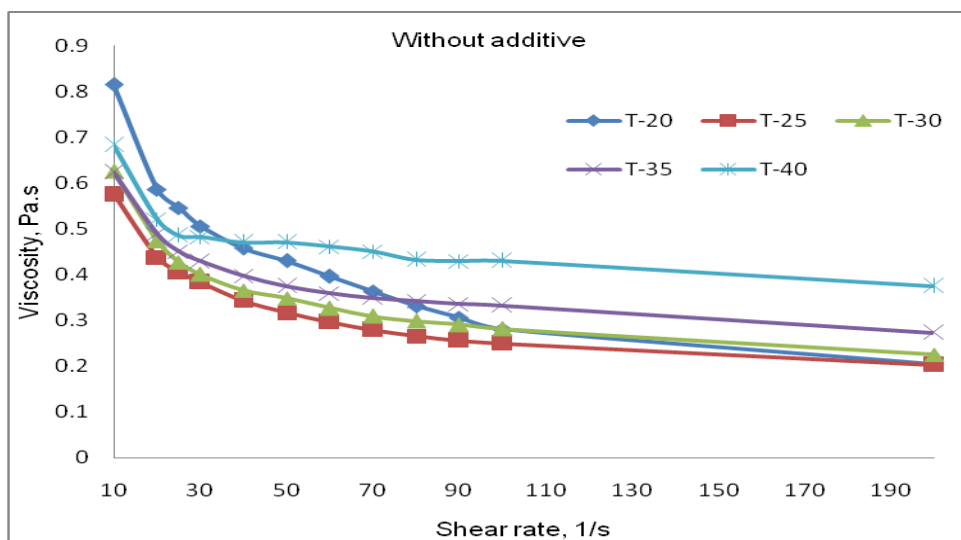

Figure 4.84.Flow curve of fly ash slurry without additive
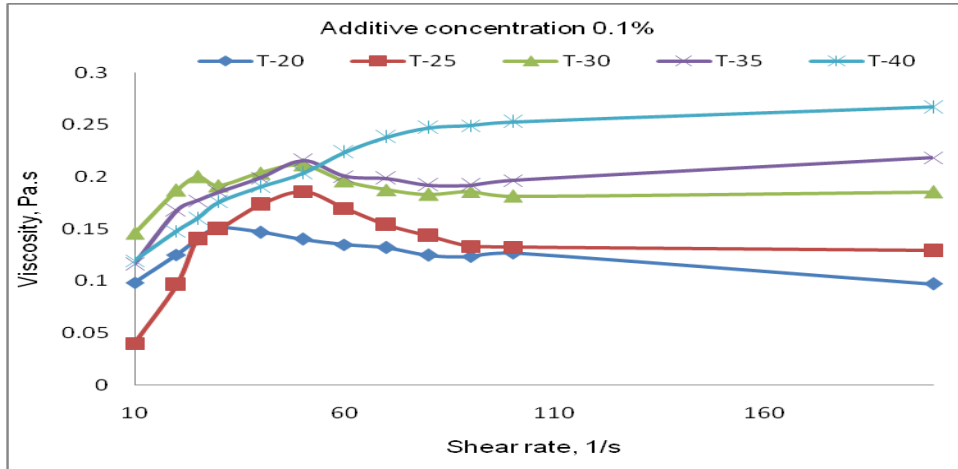
Figure 4.85.Flow curve of fly ash slurry with additive concentration 0.1%
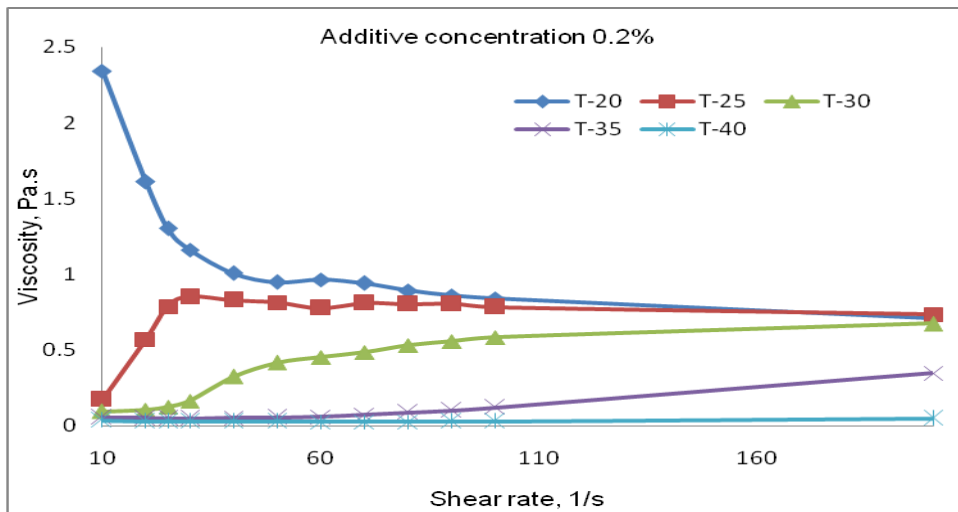
Figure 4.86.Flow curve of fly ash slurry with additive concentration 0.2%
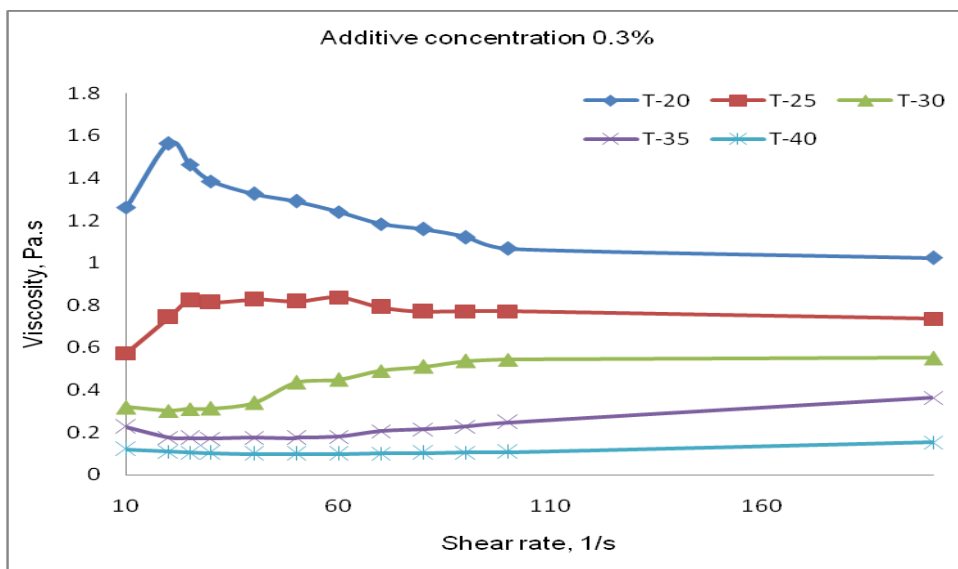
Figure 4.87.Flow curve of fly ash slurry with additive concentration 0.3%
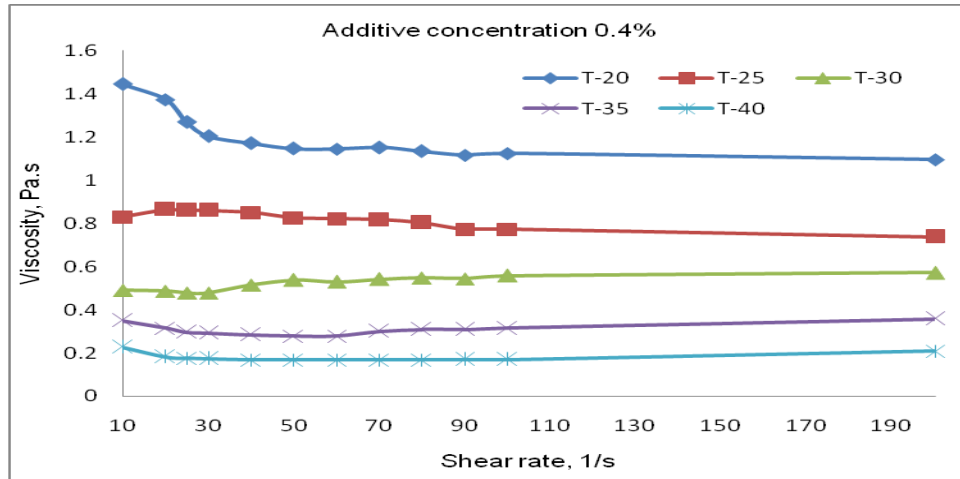
Figure 4.88.Flow curve of fly ash slurry with additive concentration 0.4%
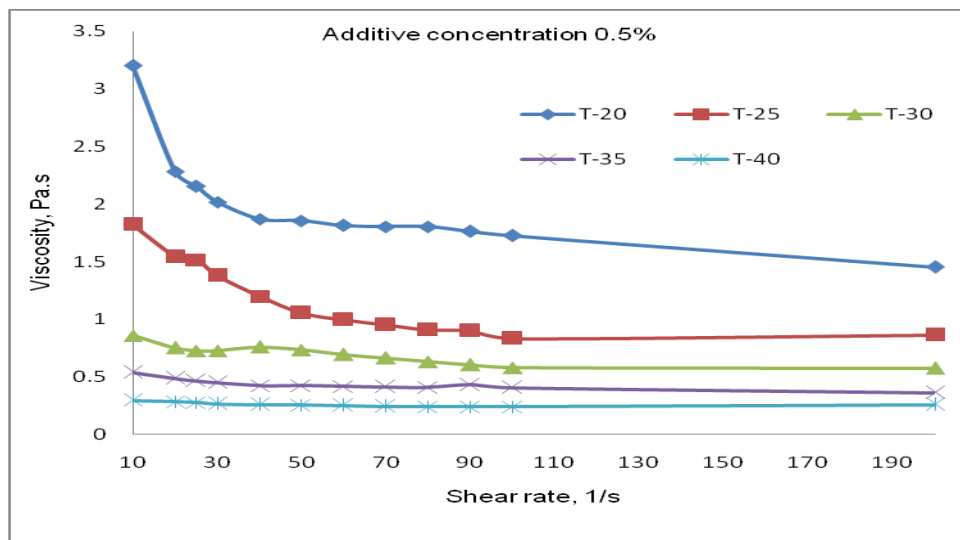
Figure 4.89.Flow curve of fly ash slurry with additive concentration 0.5%

At 0.2% additive concentration slurry behaved like a Newtonian fluid with viscosity values as low as 0.05 Pa.s and viscosity values remained constant in the shear rate range of $10s^{-1}$ to $200s^{-1}$ depicting laminar flow behaviour. Again at 0.3% additive concentration at 40^0 C temperature viscosity values were as low as 0.1 Pa.s (4.87). At 0.4% additive concentration at 40^0 C the viscosity values were more than 0.2 Pa.s (Figure 4.88). At 0.5% additive concentration at 40^0 C, viscosity values were more than 0.25 Pa.s (Figure 4.89).The variation in the rheological behaviour due to the changes in colloid interactions among fly ash particles is clearly seen in the plots of apparent viscosity against shear rate curves in Figure 4.87.The optimum condition obtained was at 0.2% additive concentration when the slurry temperature was maintained at 40^0C (Figure 4.86). Therefore, this slurry combination was selected for

studying the strength characteristics of the composite material by adding another reagent which can impart some strength to sustain the filled mass.

4.3.5.3. Effect of temperature on fly ash-slurry viscosity

An increase in the temperature of the system leads to an increase in the kinetic energy of the particles, which results in a decrease in the viscosity of the fly ash-water slurry. The slurry without any additive did not exhibit any established flow pattern and depicted irregular flow behaviours and shear thickening trends were observed (Figure 4.90). At additive concentration 0.1% also the slurry behaved erratically which was due to insufficient surfactant concentration to fully modify the fly ash surface properties (Figure 4.91). But as the surfactant concentration increased to 0.2% the slurry flow behavior improved (Figure 4.92) and at 0.3% additive concentration the slurry flow parameters further smoothened (Figure 4.93). The Slurry viscosities reduced from 1.6 Pa.s to 0.2 Pa.s when the temperature increased from 20^0C to 40^0C.
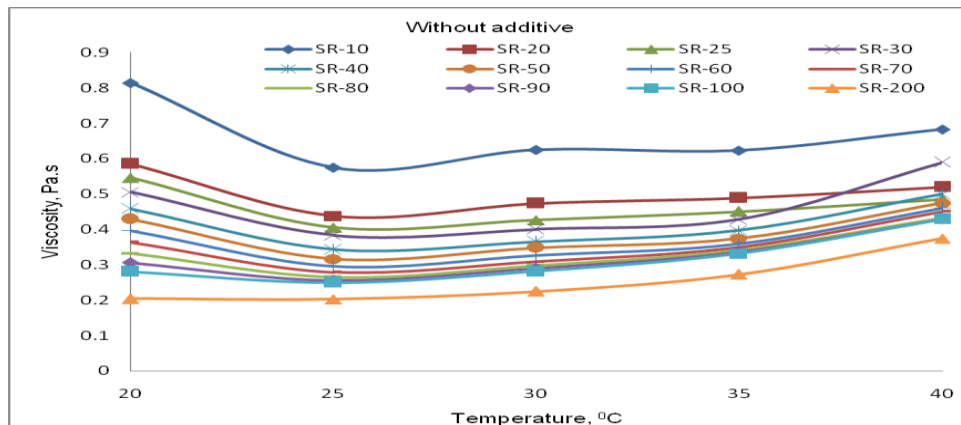
Figure 4.90.Viscosity vs. temperature plot of fly ash slurry without additive
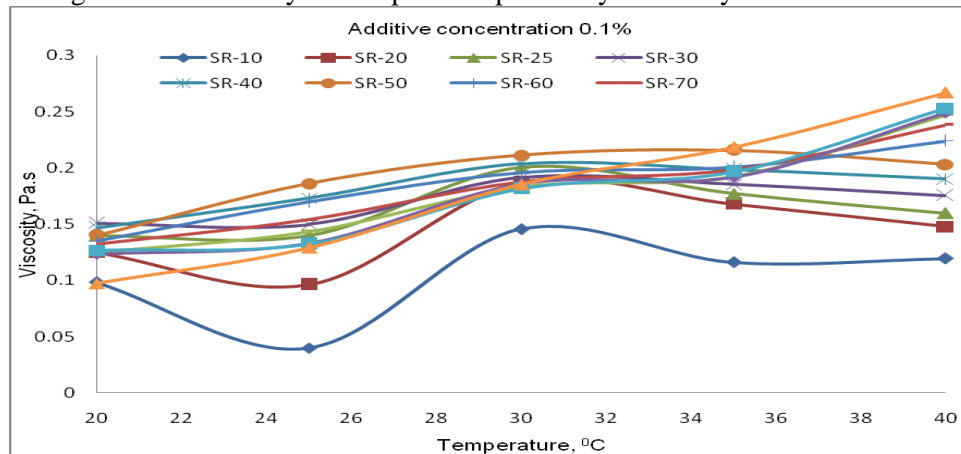
Figure 4.91.Viscosity vs. temperature plot of fly ash slurry with additive concentration 0.1%

Best results were obtained at 0.2% and 0.3% additive concentration as there was less noise in the data as depicted in Figure (4.92 and 4.93).
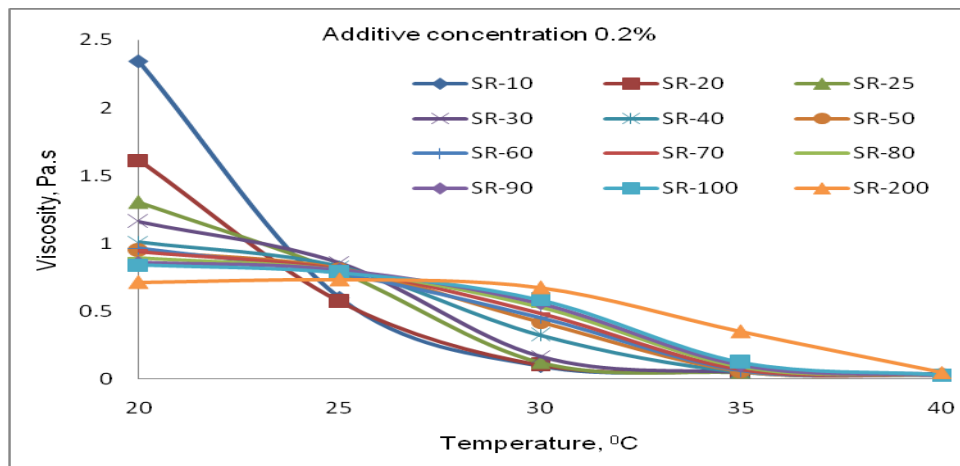
Figure 4.92.Viscosity vs. temperature plot of fly ash slurry with additive concentration 0.2%
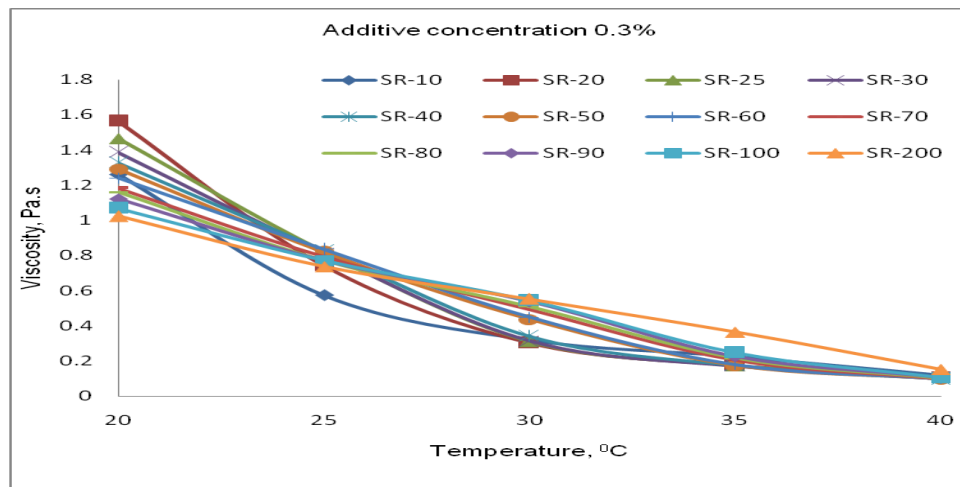
Figure 4.93.Viscosity vs. temperature plot of fly ash slurry with additive concentration 0.3%
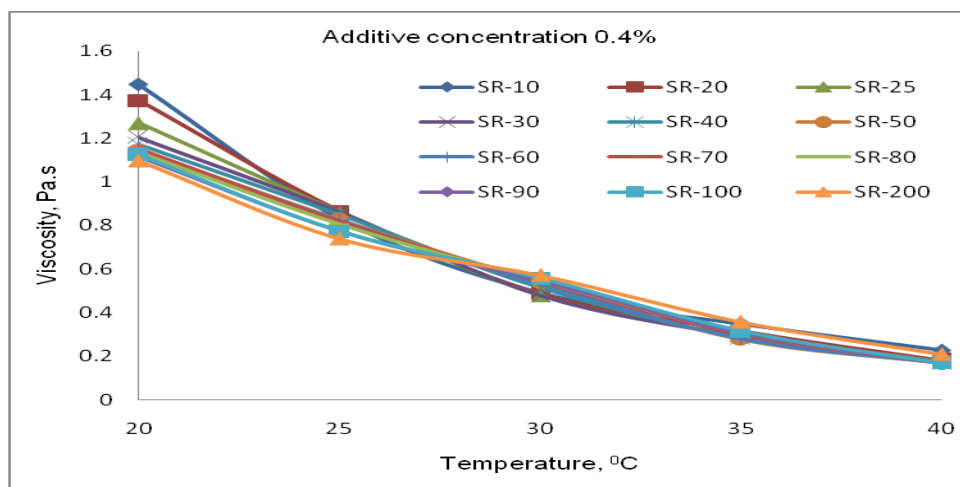
Figure 4.94.Viscosity vs. temperature plot of fly ash slurry with additive concentration 0.4%
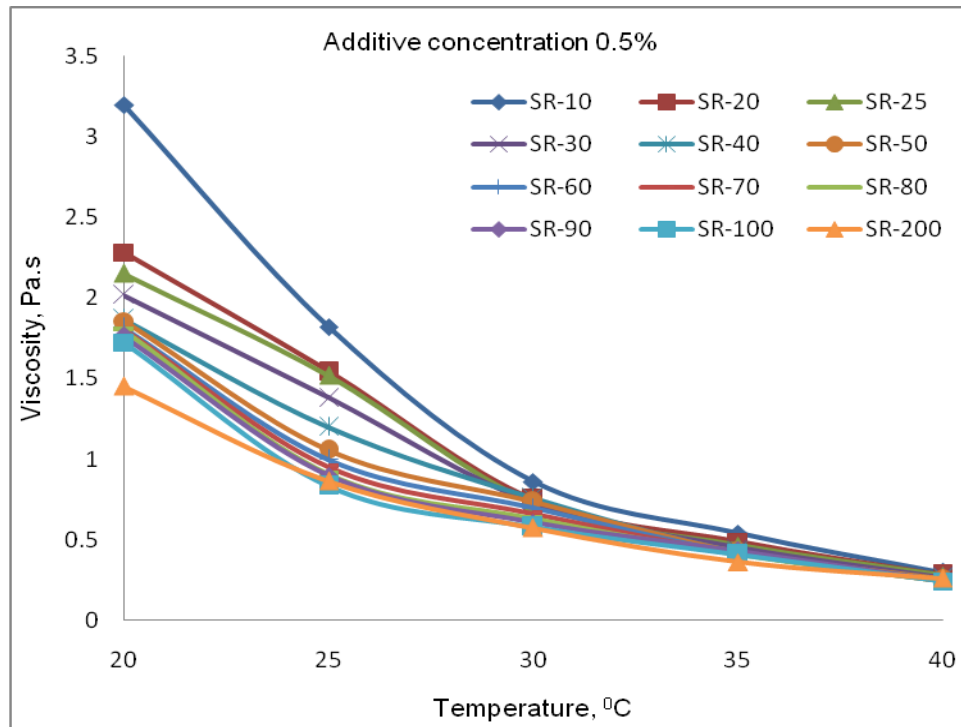
Figure 4.95.Viscosity vs. temperature plot of fly ash slurry with additive concentration 0.5%

4.3.5.4. Yield stress behavior

Maximum value of yield stress was observed (11 Pa) when the fly ash slurry was not treated with any additive which reduced to 6Pa at 40^0 C (Figure 4.96). The yield stress reduced drastically with addition of additive (Figures 4.97 to 4.101). When the additive concentration was 0.1% maximum yield stress observed was 1.43 Pa at 20^0 C and zero at 35^0C and 40^0C. Similarly at 0.2% additive concentration maximum yield stress was observed at 20^0 C which reduced to zero value at 30^0 C, 35^0 C, and 40^0 C. Similar observations were also made with 0.3% and 0.4% additive concentration (Figures 4.99 and 4.100). When the additive concentration was 0.5% maximum value of yield stress observed was 23 Pa which reduced to zero value at 40^0 C only (Figure 4.101). Similar observation was made with 0.5% additive concentrations at 40^0 C. Surfactant solutions form spherical micelles above a certain concentration called the critical micelle concentration (CMC). At appropriate conditions such as by addition of counterions, spherical micelles transform and rod-like micelles or even threadlike micelles are formed in the surfactant solutions (Qi *et al*., 2003). These rod-like or thread-like micelles can align along the flow direction in a pipeline like polymer chains and are the cause of the drag reduction ability of surfactant solutions.
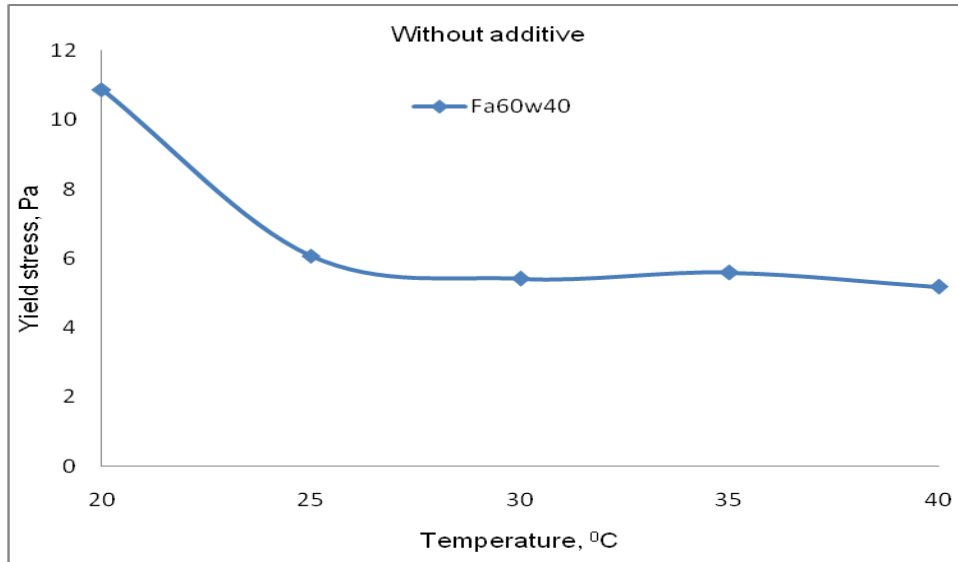
Figure 4.96.Yield stress vs. temperature plot of fly ash slurry without additive
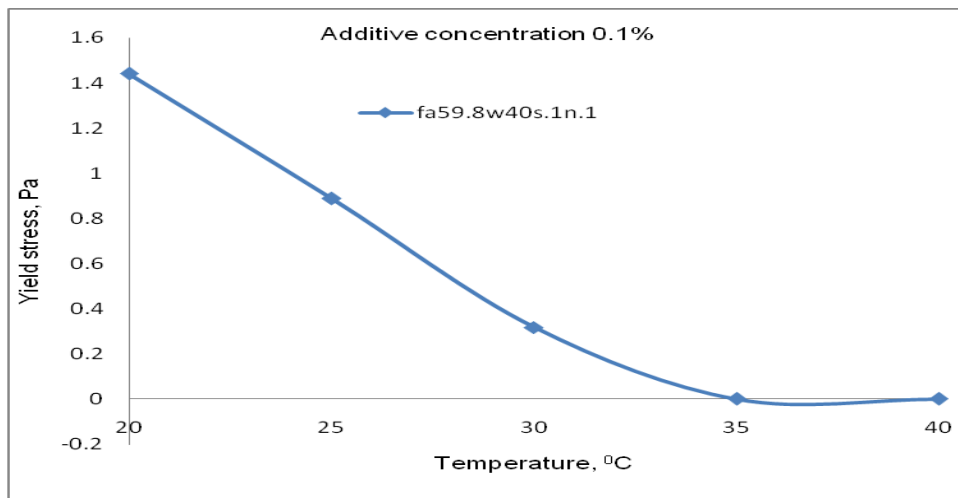
Figure 4.97.Yield stress vs. temperature plot of fly ash slurry with additive concentration 0.1%
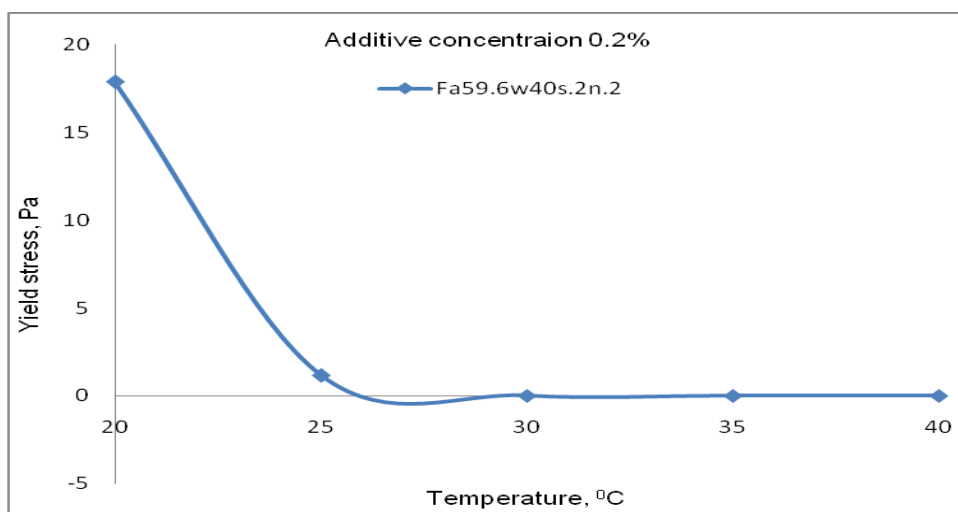
Figure 4.98.Yield stress vs. temperature plot of fly ash slurry with additive concentration 0.2%
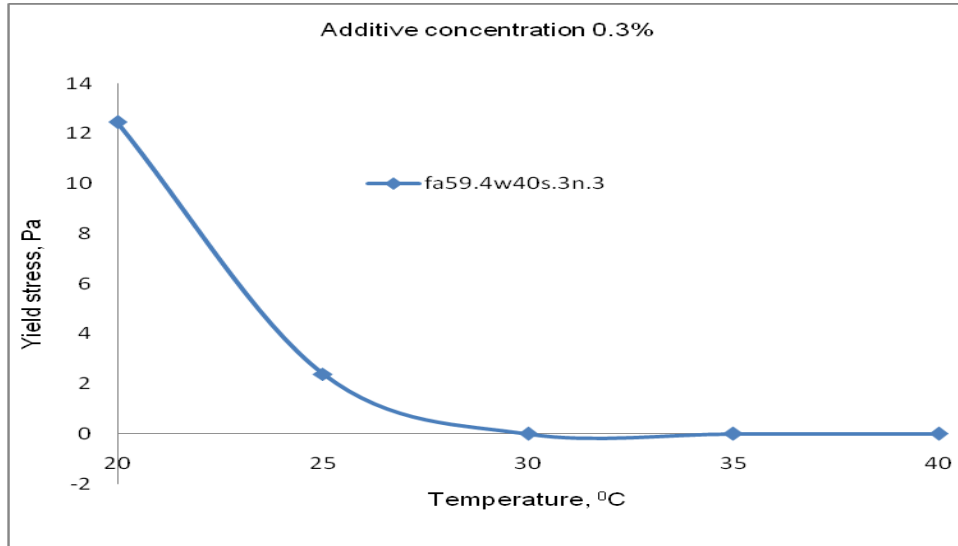
Figure 4.99.Yield stress vs. temperature plot of fly ash slurry with additive concentration 0.3%
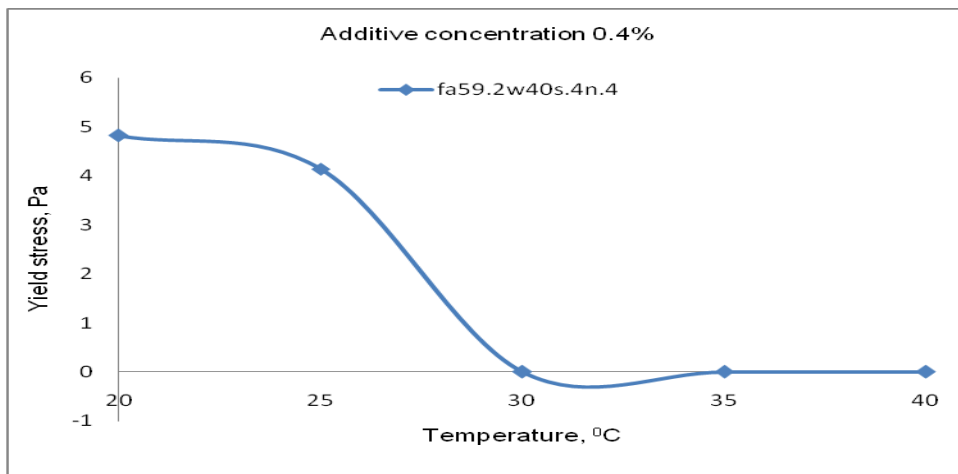
Figure 4.100.Yield stress vs. temperature plot of fly ash slurry with additive concentration 0.4%
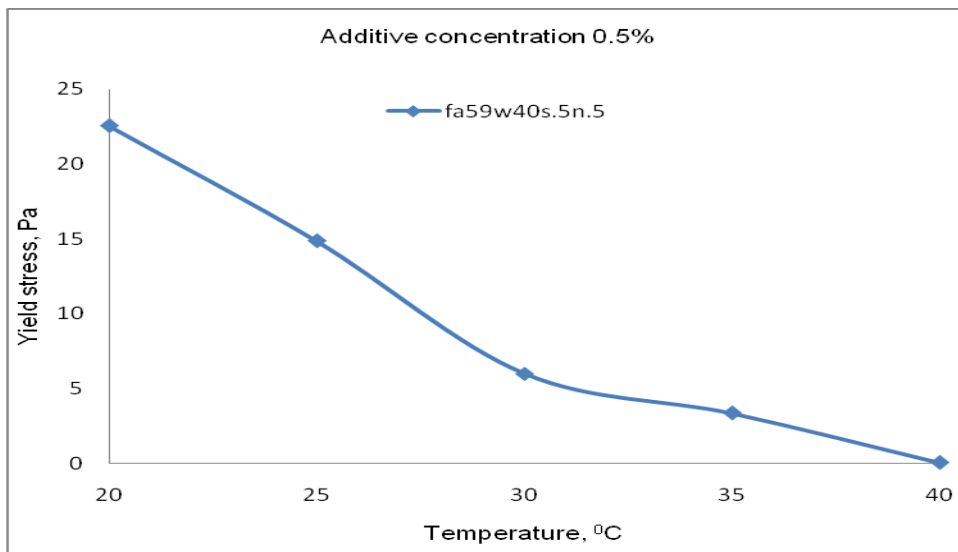
Figure 4.101.Yield stress vs. temperature plot of fly ash slurry with additive concentration 0.5%

4.3.5.5. **Summary of observations at 60% solid concentration**

The conclusions made here are:

➢ With 60% fly ash concentration at 40^0C with 0.2% surfactant the viscosity and shear stress values were minimum.

➢ The slurries prepared exhibited pseudoplastic behaviour. The slurry became more viscous with increases in solid content.

➢ 0.2% additive concentration produced best results. Therefore, 0.2% additive concentration was chosen for further study with respect to its in-place strength characteristics.

➢ The composite followed the Newtonian behavior and the relation obtained is approximately $\tau = 0.045 \; \dot{\gamma}$. The corresponding value of viscosity is found to be 0.045 Pa.s.

➢ Untreated 60% concentration fly ash slurry exhibited high yield stress values from 11 Pa to 6 Pa at different temperature environment.

➢ The rheological properties of fly ash-water slurry depend significantly on the solid concentration and temperature of the slurry.

4.3.6. Effect of pH on fly ash-slurry rheology

The surface properties of fly ash particles and the ionic strength of the supernatant solution strongly influence the rheology of fly ash-water slurry. Supernatant composition and ionic strength can vary with pH since comparatively large amounts of metal ions are dissolved at low pH and at pH greater than about 8 the dissolution of the same decreases to trace amounts (Kaji *et al.*, 1985). The resulting ionic strength has a significant effect on the stability of fly ash-water slurry stabilized by electric charge on the particles against flocculation (Heimenz, 1986). The oxygen-containing functional groups along with the inorganic minerals contribute to particle surface charge. The oxygen-containing functional groups with exchangeable cations play a very crucial role in influencing changes in yield stress and apparent viscosity (Boger *et al.*, 1987). The surface charge is low at low pH, as the functional

groups are hydrogen exchanged. The net attractive interaction between the particles results in flocculation. Hence at low pH the apparent viscosity of fly ash slurry is high. Kaji *et al.,* (1987) reported the influence of pH on the apparent viscosity of coal-water slurry in the pH range of 7 to 8.5 only. According to them, viscosity of coal-water slurry increases with decreasing pH, i.e., with increasing hydrogen ion concentration in the supernatant solution. Keeping the above theory in mind the pH was measured for fly ash slurries and the results are reported below. The pH test carried out with the selected fly ash slurry concentration (i.e. 20% to 40%) with varying surfactant and counter-ion exhibited favourable attributes (Tables 4.5 - 4.9). pH values of all the fly ash-additive slurry varied between 7.14 to 7.63 at room temperature i.e. $27^0 \pm 3^0$C. The pH of ordinary tap water is 7. Hence the additive used for this study has no influence on pH of the slurry. All the tested slurries were alkaline in nature which is a favourable trait without any adverse environmental impact.

Table 4.5.pH value of fly ash slurry at 20% solid concentration

Sample No.	Fly ash (gram)	Surfactant (gm)	Counter-ion (gm)	Water (ml)	Solid Conc. C_w (by wt.)	pH at 27 ± 1^0C temp.
20.1	19.0	0.5	0.5	80	20	7.30
20.2	19.2	0.4	0.4	80	20	7.59
20.3	19.4	0.3	0.3	80	20	7.47
20.4	19.6	0.2	0.2	80	20	7.57
20.5	19.8	0.1	0.1	80	20	7.25
20.6	20.0	0.0	0.0	80	20	7.74

Table 4.6.pH value of fly ash slurry at 30% solid concentration

Sample No.	Fly ash (gm)	Surfactant (gm)	Counter-ion (gm)	Water (ml)	Solid Conc. C_w (by wt.)	pH at 25^0C
30.1	29.0	0.5	0.5	70	30	7.73
30.2	29.2	0.4	0.4	70	30	7.63
30.3	29.4	0.3	0.3	70	30	7.24
30.4	29.6	0.2	0.2	70	30	7.64
30.5	29.8	0.1	0.1	70	30	7.66
30.6	30.0	0.0	0.0	70	30	7.30

Table 4.7.pH value of fly ash slurry at 40% solid concentration

Sample No.	Fly ash (gm)	Surfactant (gm)	Counter-ion (gm)	Water (ml)	Solid Conc. C_w (by wt.)	pH at 25^0C
40.1	39.0	0.5	0.5	60	40	7.23
40.2	39.2	0.4	0.4	60	40	7.33
40.3	39.4	0.3	0.3	60	40	7.14
40.4	39.6	0.2	0.2	60	40	7.34
40.5	39.8	0.1	0.1	60	40	7.56
40.6	40.0	0.0	0.0	60	40	7.40

Table 4.8.pH value of fly ash slurry at 50% solid concentration

Sample No.	Fly ash (gram)	Surfactant (gm)	Counter-ion (gm)	Water (ml)	Solid Conc. C_w (by wt.)	pH at 27 ± 1^0C
50.1	49.0	0.5	0.5	50	50	7.20
50.2	49.2	0.4	0.4	50	50	7.39
50.3	49.4	0.3	0.3	50	50	7.27
50.4	49.6	0.2	0.2	50	50	7.37
50.5	49.8	0.1	0.1	50	50	7.25
50.6	50.0	0.0	0.0	50	50	7.24

Table 4.9.pH value of fly ash slurry at 60% solid concentration

Sample No.	Fly ash (gm)	Surfactant (gm)	Counter-ion (gm)	Water (ml)	Solid Conc. C_w (by wt.)	pH at 25^0C
60.1	59.0	0.5	0.5	40	60	7.23
60.2	59.2	0.4	0.4	40	60	7.23
60.3	59.4	0.3	0.3	40	60	7.24
60.4	59.6	0.2	0.2	40	60	7.25
60.5	59.8	0.1	0.1	40	60	7.26
60.6	60.0	0.0	0.0	40	60	7.30

4.3.7. Effect of solids concentration on fly ash slurry rheology

The rheological properties of particle suspensions are controlled by factors of both physical and chemical origin. Some general factors are: Concentration of particles, specific surface of the particles, particle shape, and state of flocculation. In fly ash-water suspensions the hydration is also a contributing factor.
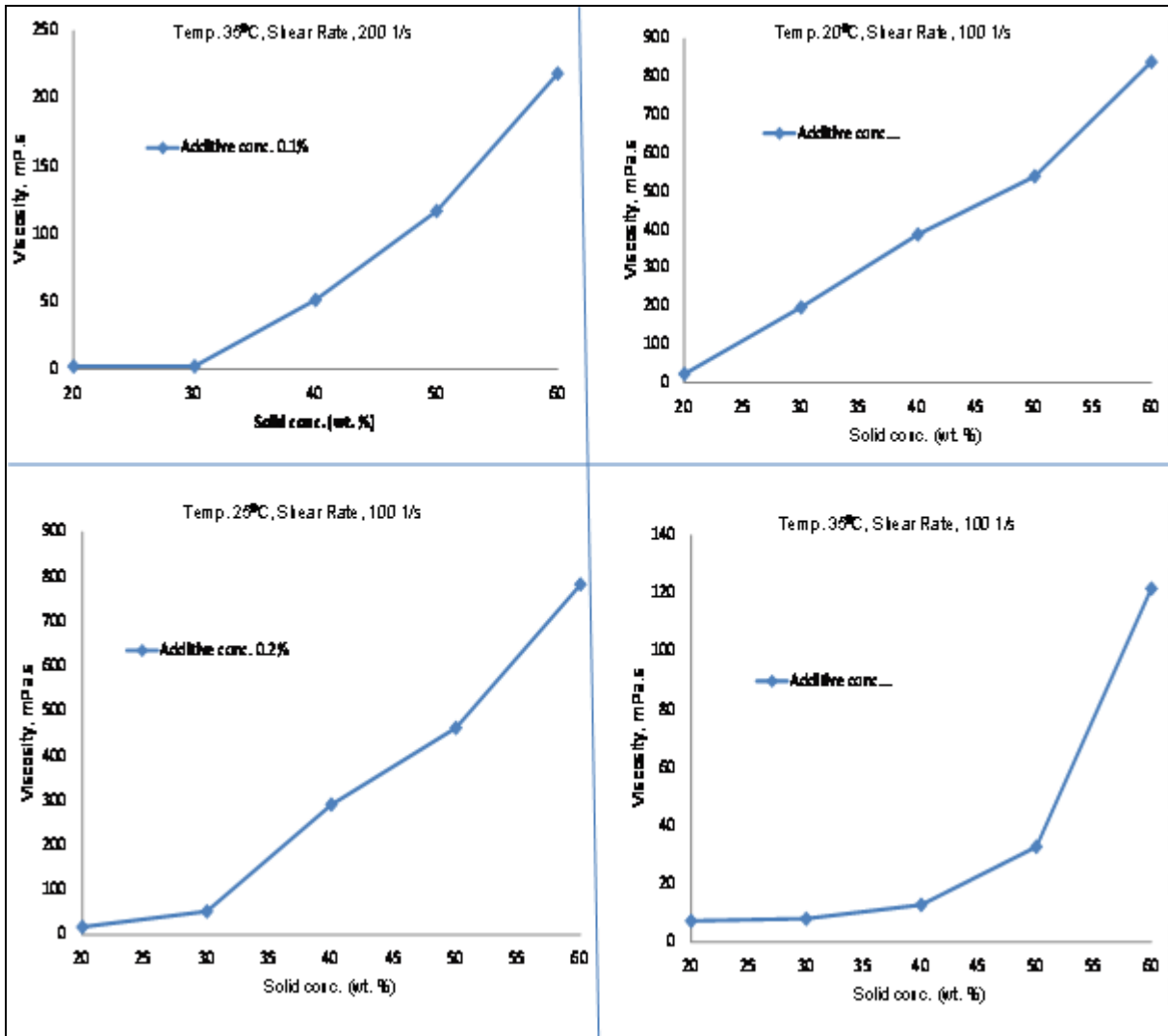
Figure 4.102. Viscosity vs. solid concentration at shear rate 100 and 200 s^{-1}

The effect of concentration on the viscosity of a suspension is described by the Krieger-Dougherty equation as given below (Struble and Sun, 1995):

$$\eta = \eta_s \, (1-\Phi/\Phi_m)^{-[\eta]\Phi m} \qquad (4.4)$$

Where η_s is the viscosity of the suspending medium (the liquid phase), Φ is the volume fraction of particles, Φ_m is the maximum volume fraction of particles, and $[\eta]$ is the intrinsic viscosity. The maximum concentration is very sensitive to the particle size distribution and particle shape. Furthermore, the flocculation of particles may lower Φ_m since the flocs themselves are not closely packed. The intrinsic viscosity is a measure of the effect of individual particles on the viscosity. Figure 4.102 illustrates the effect of concentration and

shape of particles, according to the Krieger-Dougherty equation, on the viscosity of a suspension. Apparent viscosity of the fly ash slurry increased with increase in solid concentration (Figures 4.102 and 4.103). This is due to the fact that hydrophilicity of fly ash surface increases with increase in solid concentration and the frictional forces between the particles become significant with corresponding increase in resistance. The inner surface of hydrophilic fly ash is not penetrated by water and hence more of it is available in the interparticular spaces. Availability of less water outside the hydrophilic fly ash particles decreases the fluidity or increases the viscosity of the slurry (Liang and Jiang, 1986; Liang and Jiang, 1987; Chong *et al*., 1971; Ting and Luebbers, 1957).
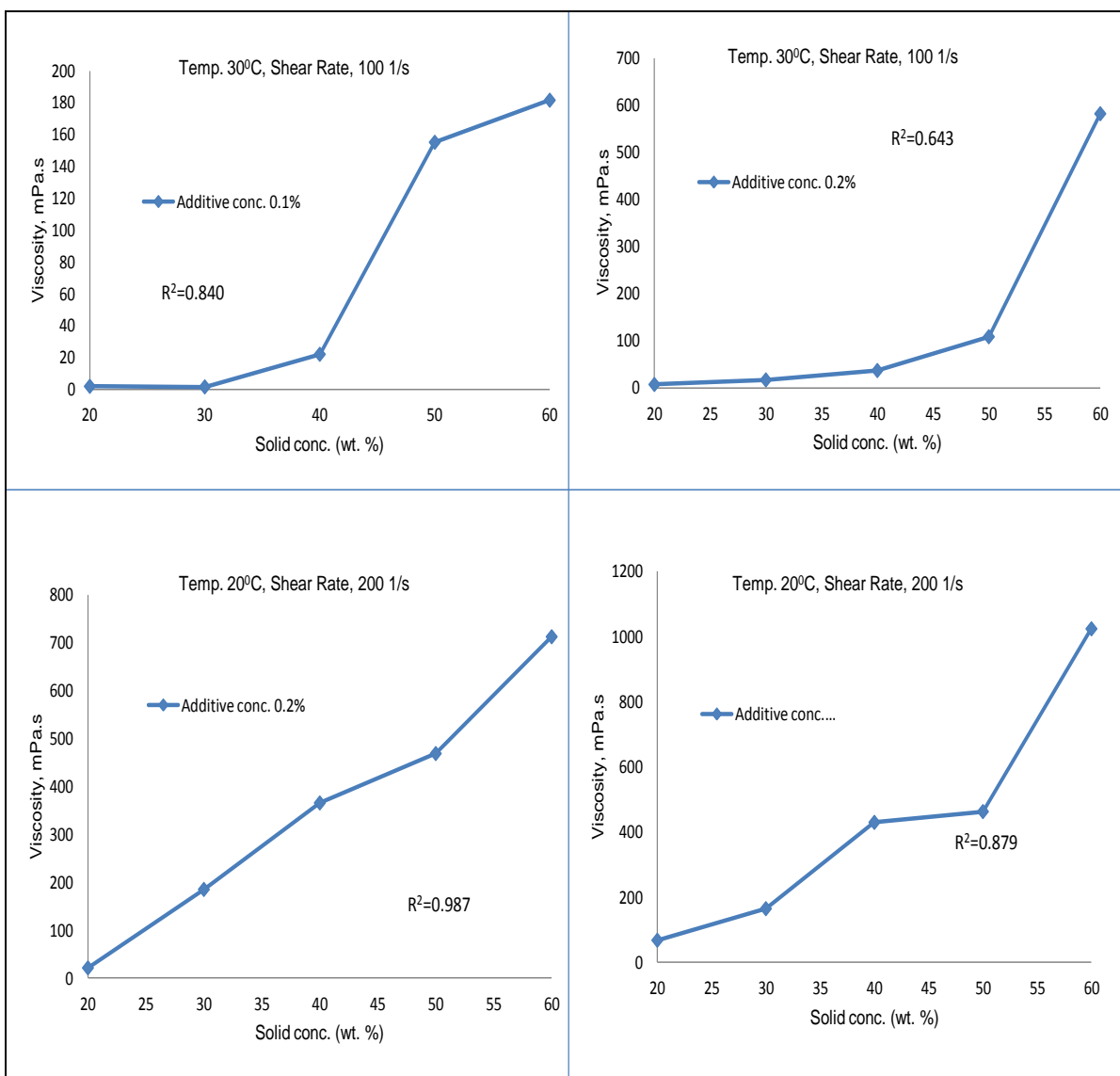
Figure 4.103.Viscosity vs. solid concentration at 20^0C and 30^0C

4.3.8. Settling rate of fly ash slurry

The settling rates of particles in the fly ash slurries used in this study were determined using a 100ml glass measuring cylinder (Figure 4.104-105). A quantity of 75ml of the slurry was placed in the measuring cylinder (where the solid volume fraction was the same as that used in the rheological tests) and thoroughly mixed by up-turning the cylinder multiple times. The settling velocity of the clear zone interface was then observed.

Figure 4.104: Settling study cylinder set up

Figure 4.105: Settling study cylinders at varying doses of additives

The settling rate varied dramatically between different additive concentrations, usually due to the existence of inter-particle forces and the fastest settling rate is observed without any additive (Figures 4.106 and 4.107). The fly ash particles settle down very quickly without any additive but with the use of the additive the particles remain floated during test experiments. Similar observations were also made with flocculant elsewhere (Jain, 2004). Therefore the shear stress- shear rate plots give a clear picture of the rheological behaviour of the fly ash water slurry under consideration.
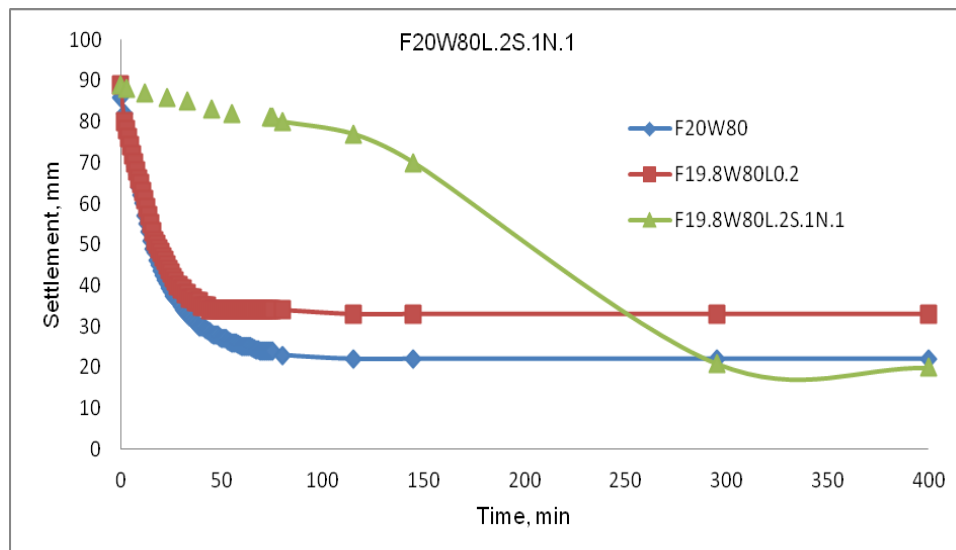
Figure 4.106: Settlement vs. time plot at 20% solid concentration
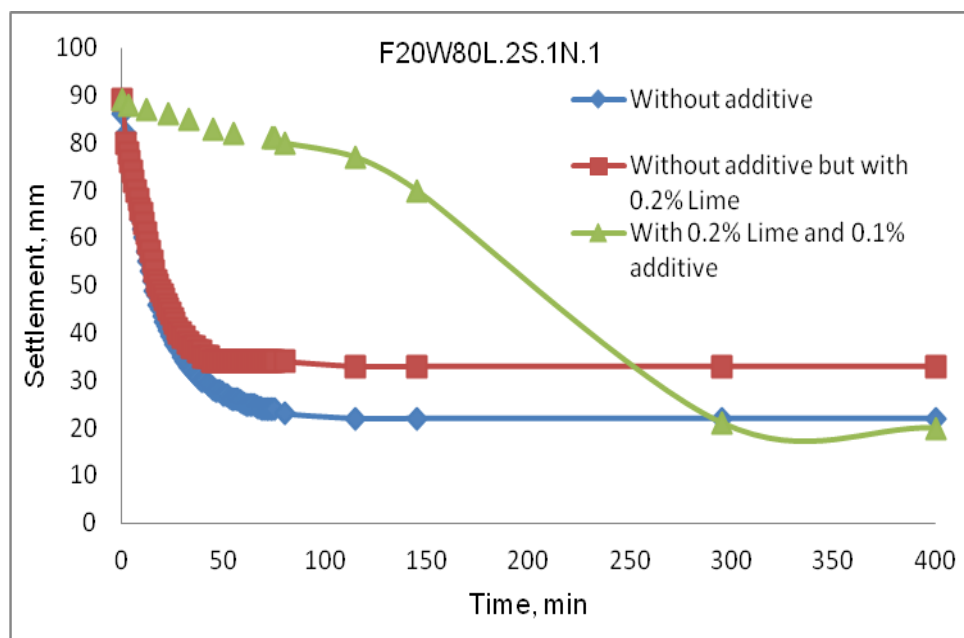
Figure 4.107: Settlement vs. time plot at 0.1% additive concentration

4.4. Section III

4.4.1. Results of geotechnical investigation of the selected material

The engineering properties of a material depend largely on the composition of the material. There exists wide variation in the composition of fly ash depending on coal types, types of furnace, temperature, collection technique adopted, etc. (Pandian *et al.,* 1995). The geotechnical properties of the developed composite materials were determined as per established methods. All the results of the current investigation and their corresponding analyses have been presented in different sections as mentioned below. The engineering properties of a material such as unconfined compressive strength, Brazilian tensile strength etc. is dependent on the moisture content and dry density. Typically the higher the compaction the better is its geotechnical characteristics. Hence it is necessary to achieve the desired degree of compaction to meet the expected properties (Nicholson *et al.,* 1994). Compaction is the process of increasing the density of material by the application of mechanical energy such as tamping, rolling, and vibration. It is achieved by forcing the particles closer with a reduction in air voids. Optimum moisture content (OMC) is the moisture content at which compacted material reaches the maximum dry density of solid particles.

4.4.1.1. Geotechnical properties of developed fly ash composite materials (FCMs)

The developed composite materials were subjected to various engineering tests such as Compaction behaviours, Unconfined Compressive Strength Test, Brazilian Tensile Strength Test, Ultrasonic Pulse Velocity Test, Micro Structural Analyses, and X-Ray Diffraction (XRD) Analysis, the results of which are presented in the following sub-sections.

4.4.1.1.1. Compaction Characteristics

The compaction characteristics of the developed fly ash composite materials were carried out to determine the optimum moisture content and maximum dry density the results of which are presented in Figure 4.108. As the water content was increased, the dry density of the specimen increased. The optimum MDD of the developed composite materials was found to be 1443 Kg/m^3 (Table 4.10) and the corresponding value for OMC was 12.51%.

Table 4.10 Engineering properties of FCM

Moisture Content (%)	Dry Density (Kg/m^3)
7.37	1260
9.97	1346
12.51	1443
16.11	1341
20.85	1254
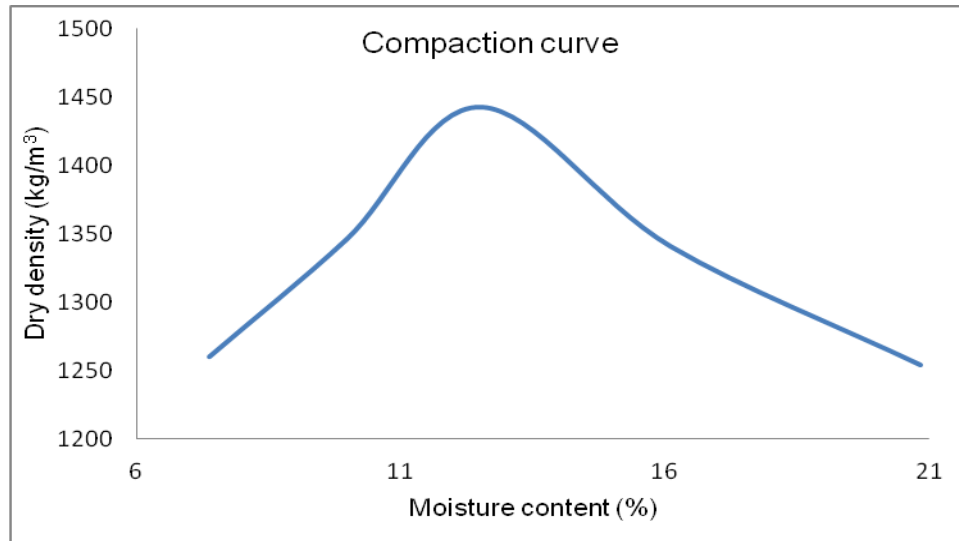
Figure 4.108: Compaction curve of fly ash composite material

4.4.1.1.2. Unconfined compressive strength

The unconfined compressive strength (UCS) of a material is its resistance to any externally applied load. It reflects inter granular cohesion as well as strength of cementing material holding those grains. The samples were tested both with and without lime addition. The sample without lime addition did not exhibit any significant strength value. It was only 297 kPa. There was no appreciable change in the strength value at different curing periods as well and hence those data are not reported here. However lime addition changed the strength behavior significantly. At 7 days of curing period the uniaxial compressive strength of the composite increased manifold. It failed at 1.215 MPa thus achieved a 305% increase (Table 4.11). Then the increase rate reduced to 10% exhibiting 1.330 MPa at 14 days. But the rate of increase increased to 54% at 28 days curing to exhibit 2.85 MPa. The specimen continued exhibiting increased strength value at 56 days though with much reduced rate (Figure 4.109). All the samples exhibited shear type of failures thus confirming to the development of cohesion between particles (Figure 4.110).

Table 4.11: UCS values of FCM at different curing periods

Curing Period (days)	Compressive Strength (MPa)
0	0.297
7	1.215
14	1.450
28	2.850
56	2.950
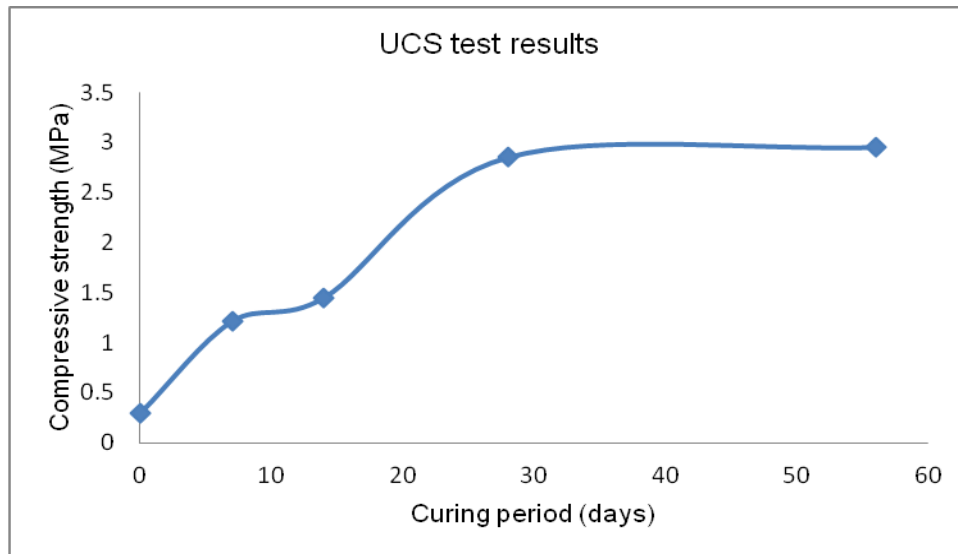
Figure 4.109.UCS values of fly ash composite material at different curing periods

Figure 4.110: Post failure profiles of UCS samples

4.4.1.1.3. Brazilian tensile strength characteristics

Tensile strength is an important property to predict the cracking behaviour of the filled mass and is a vital parameter to evaluate the suitability of fly ash as a filling material in mine voids. In the present study tensile test was conducted on developed composites to evaluate the tensile strength as well as the cracking behaviour of the material. The tensile strength of the fly ash composite material showed significant improvement with curing periods. At 28 days curing the tensile strength values increased at 100% and 200% to that of at 7 and 14 days respectively (Table 4.12). Marginal increase was also observed at 56 days curing period (Figure 4.112). All the specimens failed more or less at the middle through an induced force which is tensile in nature (Figure 4.111). The failure occurred within 70 to 110 seconds thus confirming to that suggested in ASTM D3967.
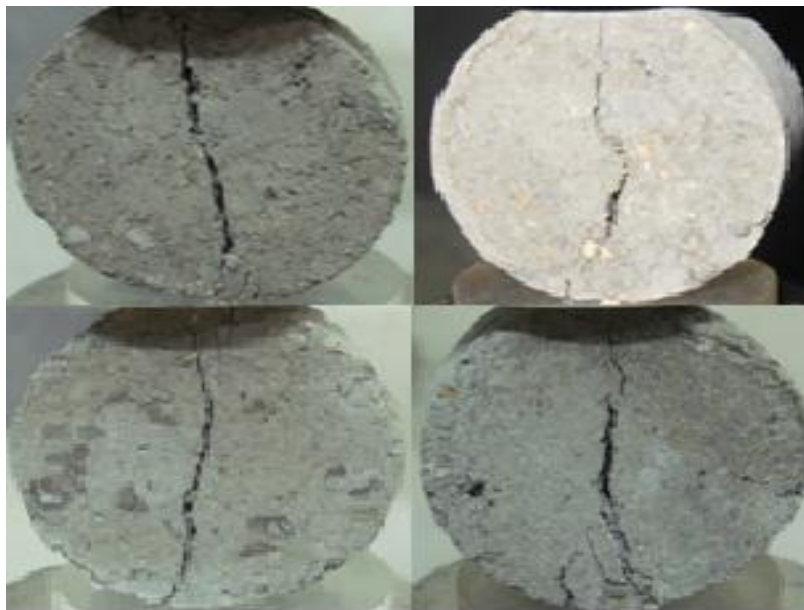
Figure 4.111.Post failure profiles of Brazilian tensile test samples

Table 4.12: Relationship between curing period and Brazilian tensile strength

Curing period (days)	Brazilian tensile strength (kPa)
0	057
7	150
14	180
28	300
56	335
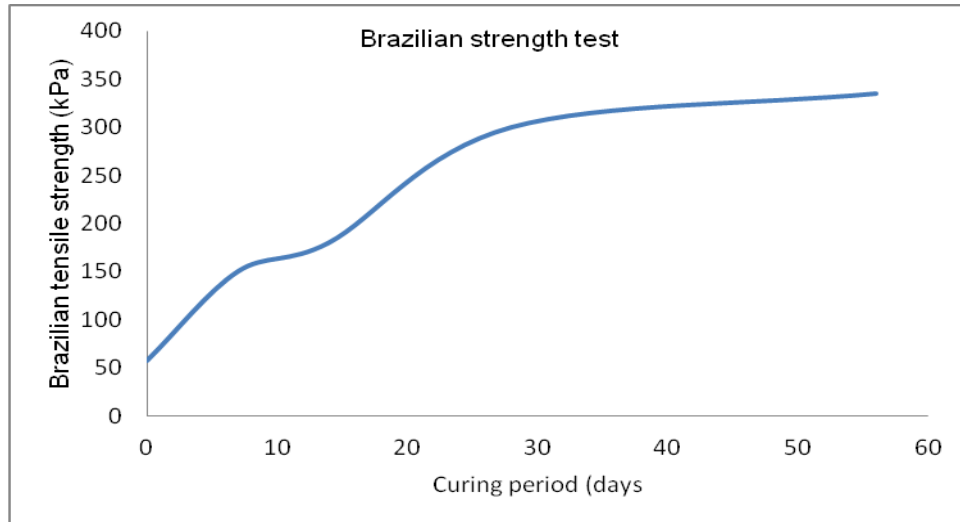
Figure 4.112: Tensile strength values of developed composites at different curing periods

4.4.1.1.4. Shear strength parameters

The post failure profile of a triaxial test specimen is presented in Figure 4.114. The shear strength parameters of compacted fly ash composite materials are presented in Table 4.13. There is little change in cohesion and angle of internal friction values at 7 and 14 days curing (Figure 4.113 and 4.115). Both cohesion and angle of internal friction increased with curing period. At 28 days curing the friction angle is about 35^0 which are typical of any medium hard rock (Vutukuri *et al*., 1978). This confirms that the developed composite material would be suitable to support roof load and would also resist putting pressure on barricades.

4.4.1.1.5 Ultrasonic Pulse velocity

The P-wave velocity depends on the quality of transmission, cohesiveness of constituent materials, dampness, presence of weaknesses such as cracks, voids, etc. Its accuracy also depends on the homogeneity of the specimen. The ultrasonic pulse velocities varied between 1410 m/s to 2158 m/s at varying curing periods from 7 days to 56 days (Table 4.15). Maximum values were obtained at 56 days curing period, thus confirming the increased conductivity in the sample. But it increased by 12% at 28 days thus reflecting improved transmissivity of the wave due to enhanced pozzolanic activity. The rise is marginal between 7 and 14 days of curing.

Table 4.13: Shear strength parameters of fly ash composite materials

Curing period	Cohesion (kPa)	Angle of internal friction (degrees)
7	53	27.85
14	54	28.35
28	71	34.60
56	78	36.52
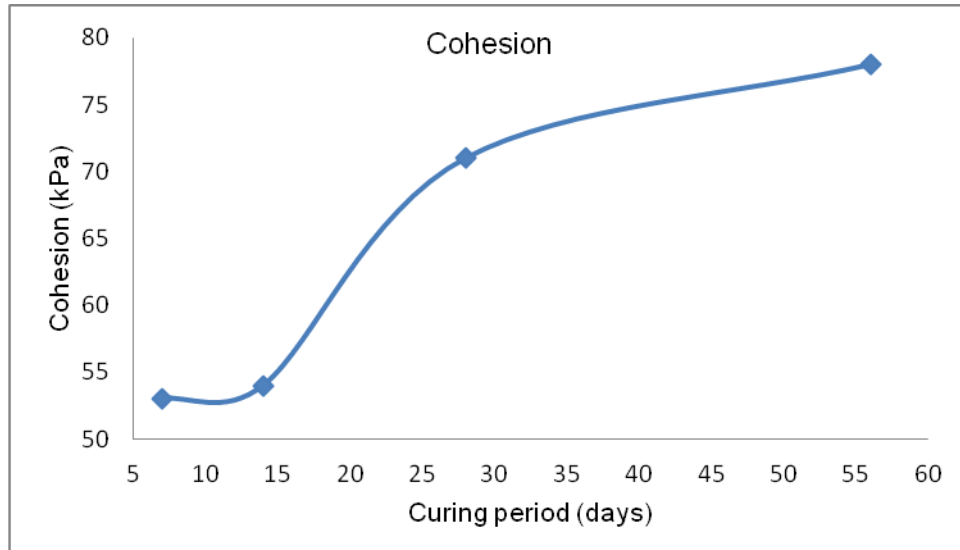
Figure 4.113: Relationship between curing period and cohesion

Figure 4.114: Post failure profile of a triaxial test specimen
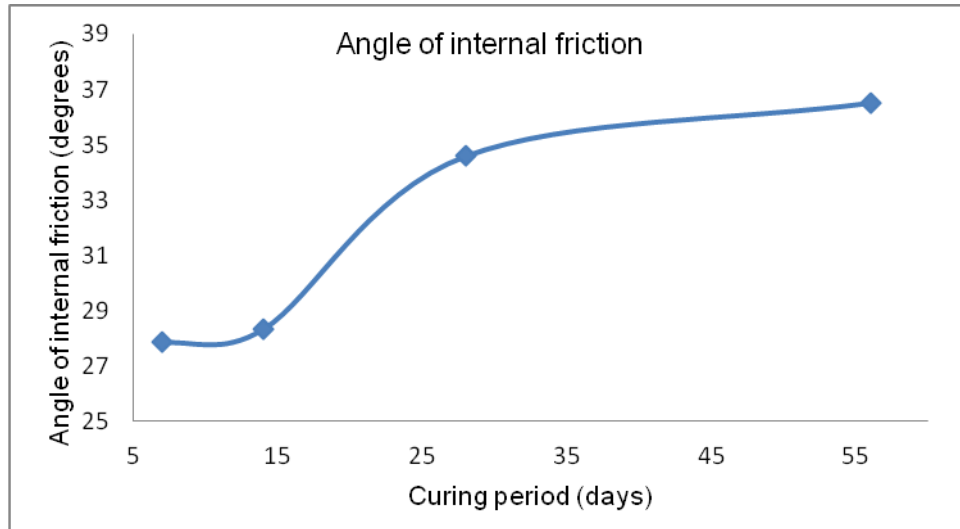
Figure 4.115: Relationship between curing period and angle of internal friction

The P-wave velocity at 56 days of curing period was 2158 kPa and least values were obtained for 7 days of curing period which confirms to the results obtained in UCS and BTS tests. The Poisson's ratio is also an important parameter of a material under loading. The Poisson's ratio values were obtained from ultrasonic pulse velocity test as well. The Poisson's ratio values of each composite decreased with increase in curing period. The Poisson's ratio values varied between 0.28 and 0.44 of all developed composites cured at 7, 14, 28 and 56 days (Table 4.14). The Poisson's ratio values of each composite did not change significantly with longer curing periods which are the typical characteristics of any material. Young's modulus (E) values were also obtained from nondestructive testing (Table 4.17). The Young's modulus (E) values increased with curing period confirming to enhance pozzolanic activities resulting in higher stiffness of the composites. The velocity of propagation increases with increased stiffness of the material (Yesiller *et al*., 2000). The density of the material also increased with curing period (Table 4.16) confirming to strength gain.

Table 4.14: Relationship between curing period and Poisson's ratio

No. of days cured	Poisson's ratio
07	0.44
14	0.41
28	0.40
56	0.22
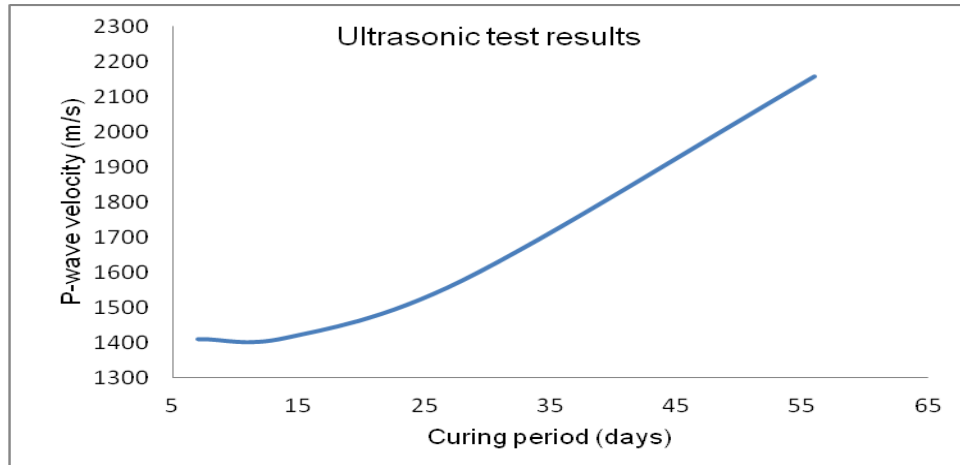
Figure 4.116: P-wave velocities of developed composites at different curing periods

Table 4.15: P-wave velocities of developed composites at different curing periods

Curing period (days)	P-wave velocities (m/s)	Poisson's Ratio
7	1410	0.44
14	1414	0.41
28	1577	0.40
56	2158	0.28

Table 4.16: Relationship between curing period and density

Curing period (days)	Density (Kg/m^3)
7	1460
14	1470
28	1520
56	1700
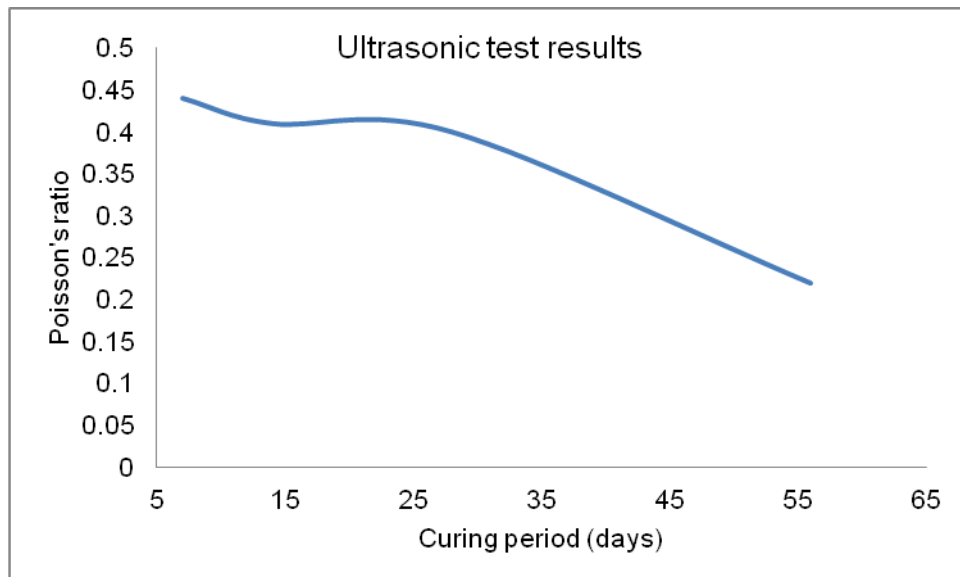
Figure 4.117: Relationship between curing period and Poisson's ratio
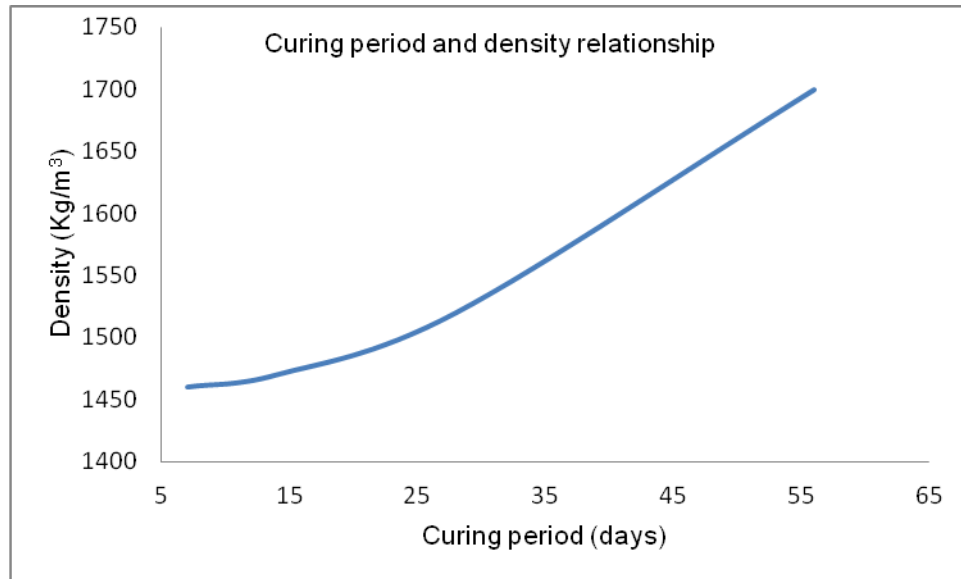
Figure 4.118: Relationship between curing period and density

Table 4.17: Ultrasonic test parameters

Ultrasonic test parameters	Curing Period (days)			
	7	14	28	56
Young's modulus (kPa)	950337	1196933	1764446	5750525
Bulk modulus (kPa)	1038263	2146938	3377293	4795166
Shear (Rigidity) modulus (kPa)	133268	425325	661389	2211523
S-wave velocity (m/s)	235	560	580	697

4.4.2. Micro-structural analysis

The SEM images show development of gel at different stages of pozzolanic reaction. It confirms to the observation that during early stages, the reactive particles in the fly ash composite served as nucleation sites for hydration and pozzolanic reaction products as (C-S-H,C-A-H,C-A-S-H) [Lav *et al*., 2000]. Cementitious compounds are formed around fly ash particles (Figures 4.119-4.123). The composite at 56 days of curing period exhibited dense-gel-like mass covering all reactive particles completely and filling up the inter-particle space with blurred grain boundaries (Figures 4.123). It appears like a massive unit compared to the other composites. The dense gel acted as a binding substance and appears to be evenly distributed to form compact structure, thus creating more contact and higher cohesion that in turn reflects in greater strength values. It was observed from static laboratory tests that all samples exhibited maximum strength values at 56 days. So its SEM analysis was carried out to understand the micro-structural aspects. The strength values of the developed fly ash

composites increased with increasing curing period due to the formation of calcium silicate hydrate (CSH) and calcium aluminate silicate hydrate gels (CASH) around fly ash particles (Cetin *et al*., 2010).
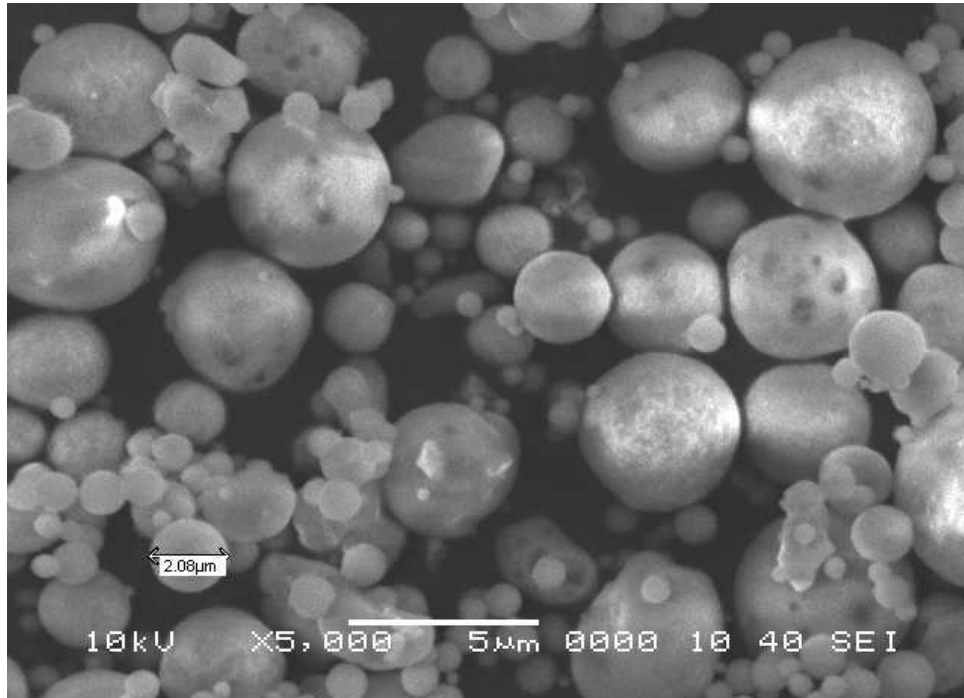
Figure 4.119: SEM image of untreated fly ash at 5000x
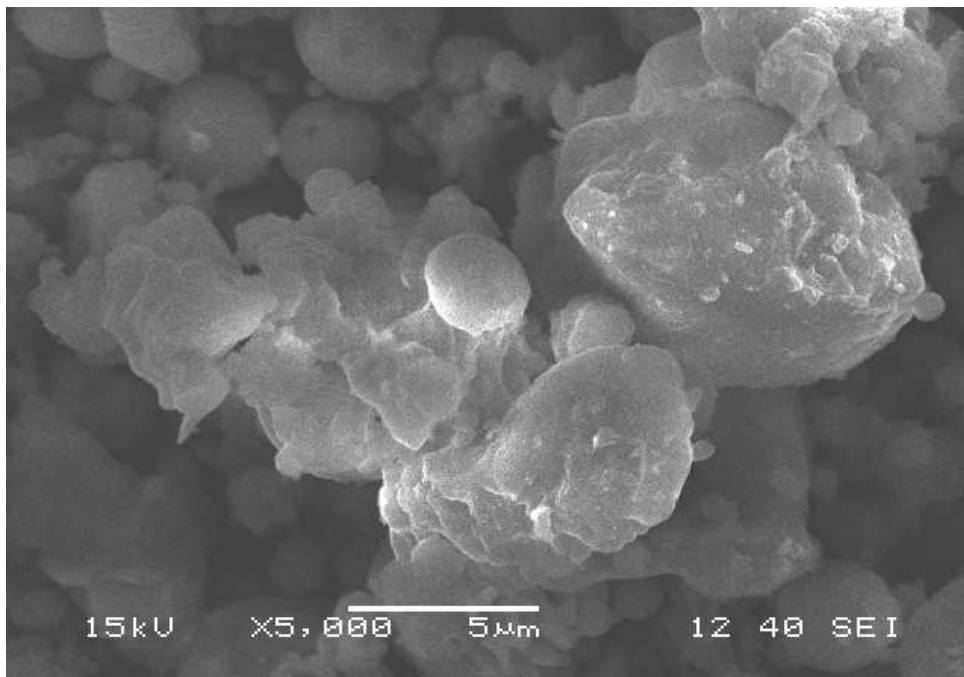
Figure 4.120.SEM image of 7 days curing at 5000 x
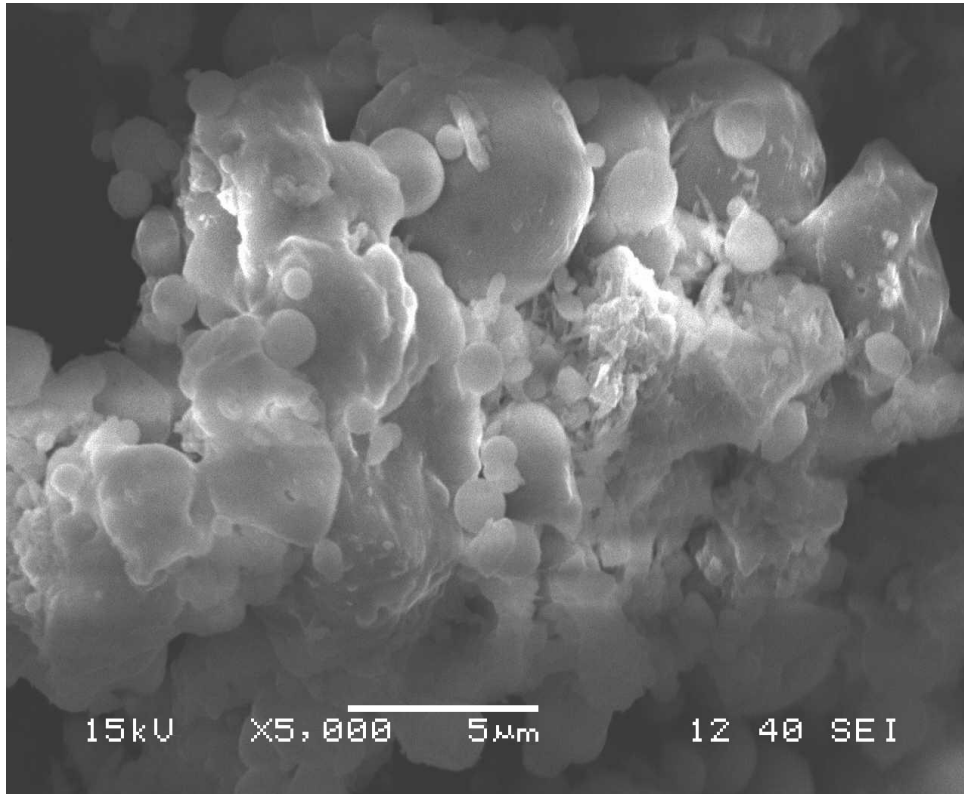
Figure 4.121.SEM image of 14 days curing at 5000 x
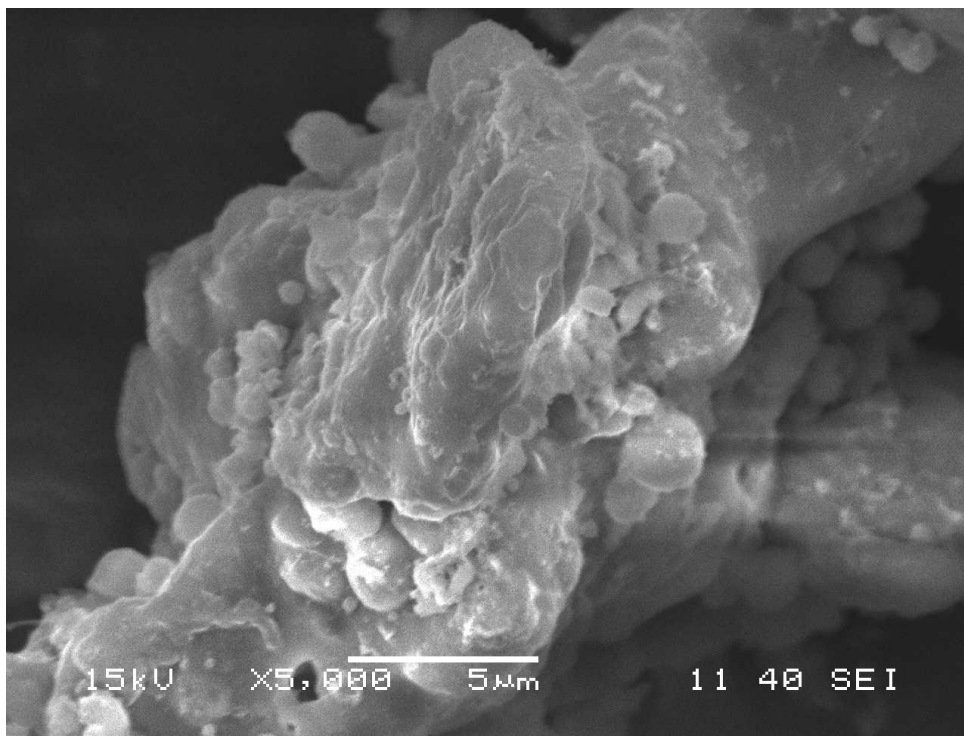
Figure 4.122.SEM image of 28 days curing at 5000 x
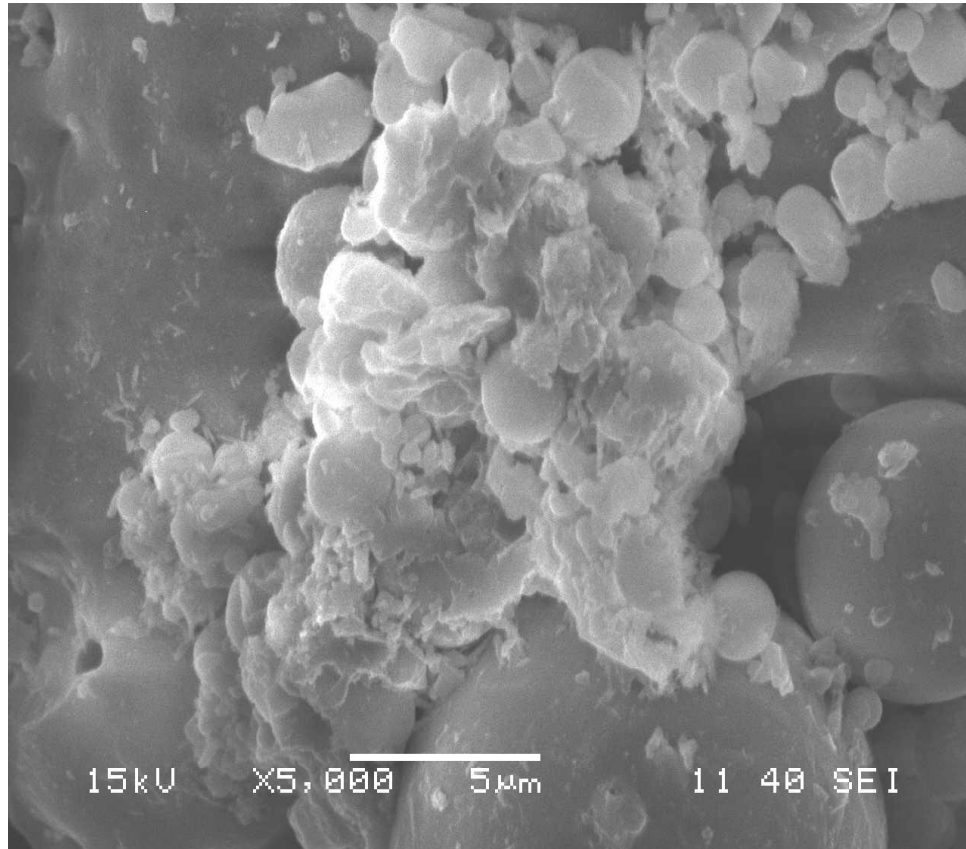
Figure 4.123.SEM image of 56 days curing at 5000 x

4.4.3. X-ray diffraction analysis of FCM

The mineralogical analyses of the composites are very important to determine the changes in the mineralogical phases due to pozzolanic reactions. Cementing compounds such as CSH, CAH and CASH were indentified in 3% cement stabilized fly ash only and fly ash – black cotton soil mixes at 28 days curing by XRD analysis (Krishna, 2001). The strength development is also dependent on the amount of hydration products as well as their interlocking mechanisms (Lav and Lav, 2000). The formation of reaction products such as calcium silicate hydrates CSH; Calcium aluminates hydrates (CAH) and Calcium aluminates silicate hydrates (CASH) were confirmed from x-ray diffraction analysis (Figures 4.124- 4.127). These new cementitious compounds induce aggregation effect in fly ash and bind the particles together to form fly ash clusters and resulted in overall enhanced strength behaviours of composites. Quartz the primary mineral present in fly ash indicated by sharp peaks at 27^0 (approximately).
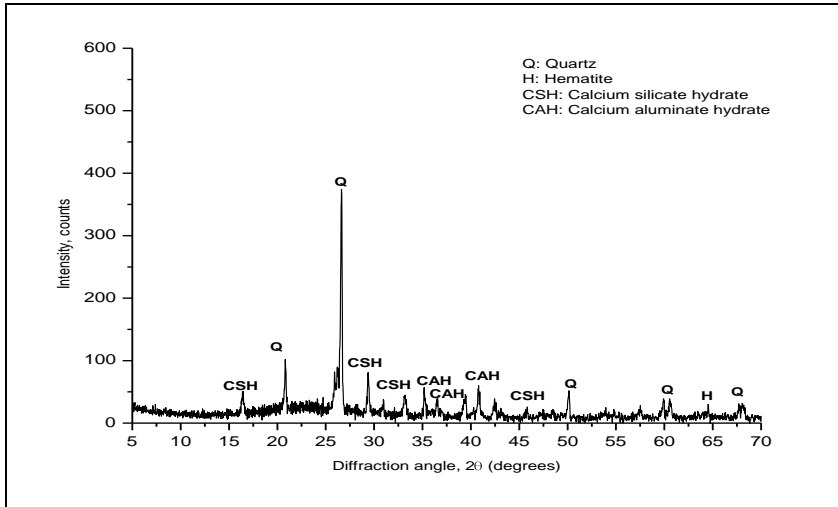
Figure 4.124.XRD peak of fly ash composite material at 7 days curing
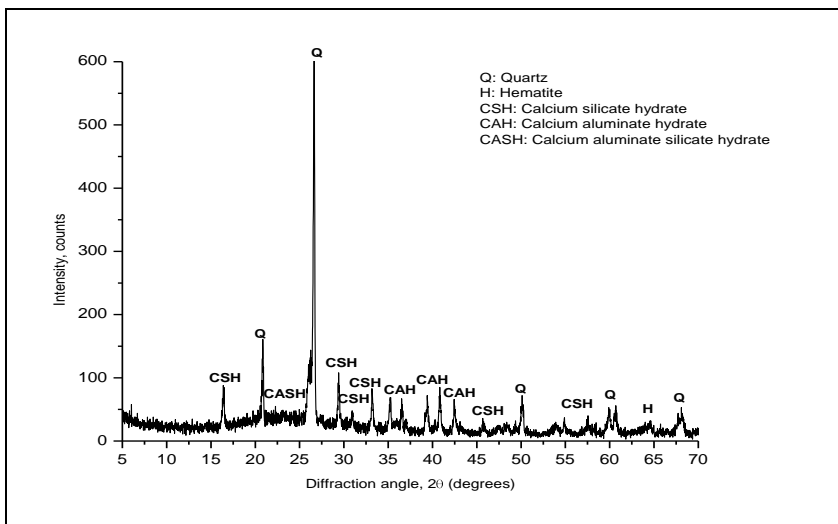
Figure 4.125.XRD peak of fly ash composite material at 14 days curing
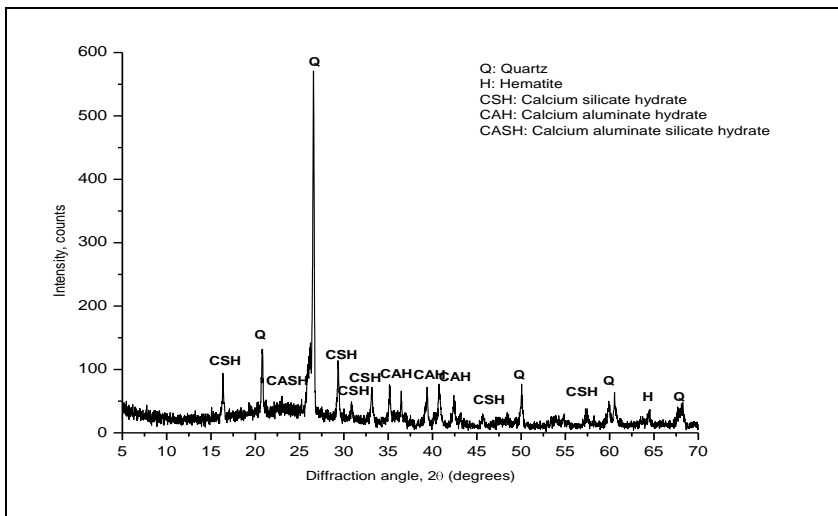
Figure 4.126.XRD peak of fly ash composite material at 28 days curing
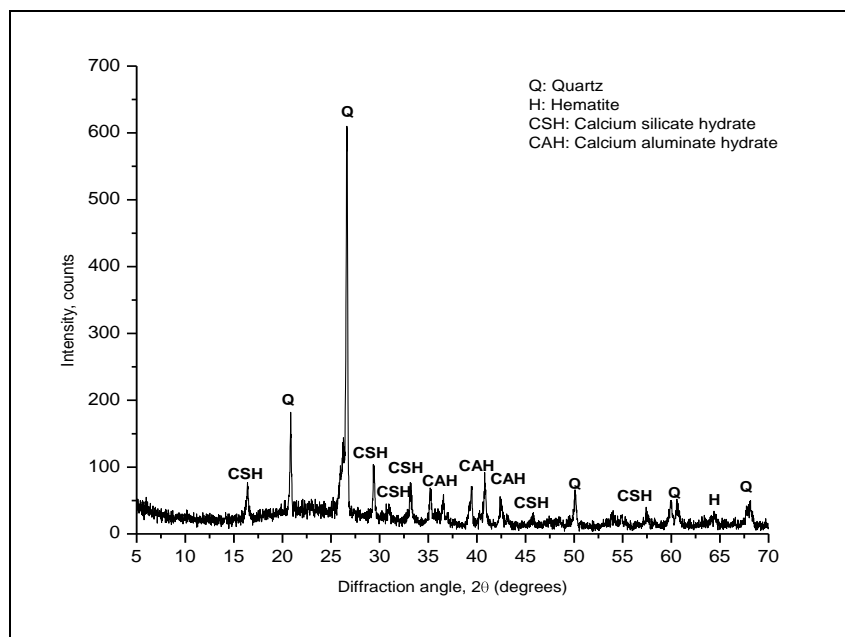
Figure 4.127.XRD peak of fly ash composite material at 56 days curing

4.4.4. FTIR Analysis

FTIR (Fourier Transform Infrared Spectrometry) investigation has been carried out to obtain information regarding functional groups of materials/compounds. The quality or consistencies of the fly ash-additive mixture after treatement have been significantly depicted. The FTIR monograph in Figure 4.128 shows that the untreated fly ash has peaks at 1089.78 cm^{-1}, 796.60 cm^{-1}, and 462.92 cm^{-1}. These peaks attribute to T-O-Si (internal linkage; T = Si or Al); Si-O-Si (external linkage); Si-O-Si or O-Si-O groups of fly ash that are mainly responsible for strength behavior of the material. When the fly ash was mixed with lime, surfactant and NaSal, a doublet (two peaks) was observed at ~ 790 cm^{-1} and a peak at ~ 1400 cm^{-1} region that reflects the presence of O-C-O group (Figures 4.129 - 4.130) i.e. no geolitesation even in presence of surfactant and counter-ion (Ojha *et al*., 2004). As the curing period progressed to 7 and 14 days the peaks were observed at ~ 3400 cm^{-1}, 1400 cm^{-1}, 1600-1650 cm^{-1}. The peaks depict OH stretching to OH bonding (Figures 4.132 – 4.134). These peaks depict the presence of O-C-O, H-O-H groups. At 28 days curing period 3300 – 3600, 1350 – 1450, 1600-1650 and ~ 950 cm^{-1} peaks with OH, O-C-O, H-O-H and O-C-O stretching and H-O-H and H-O-H internal Ti-O-Si group bonding were observed (Figure 4.135). This reflects higher bonding i.e. effective goelitesation (Park & Kang, 2008). The peaks were broader after 56 days of curing (Fig 4.136).
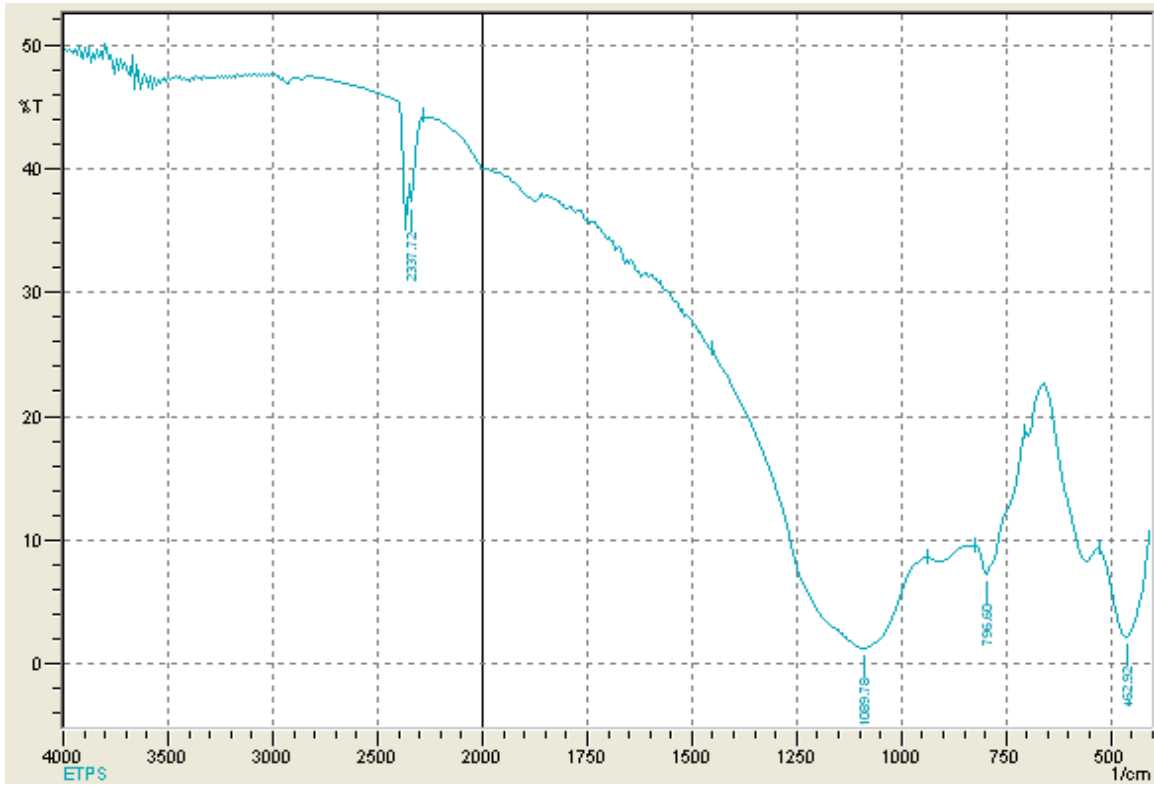
Figure 4.128: FTIR results of untreated fly ash
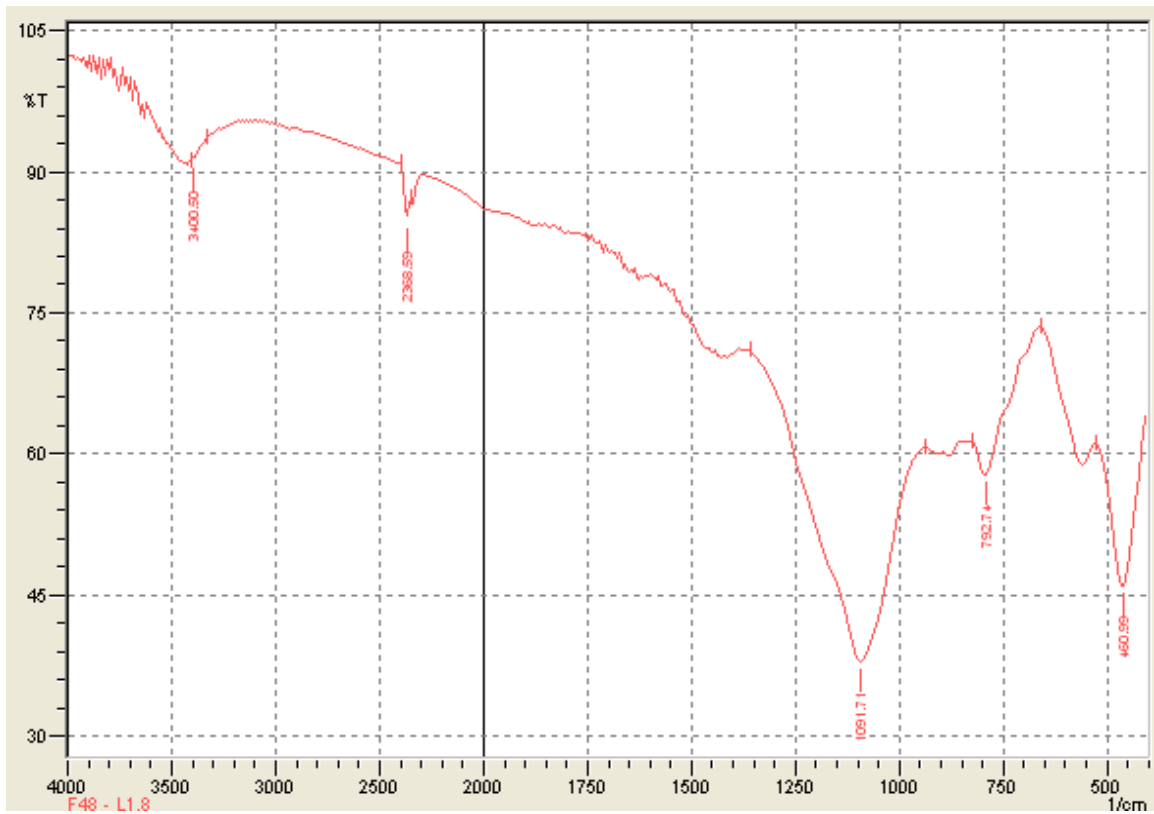
Figure 4.129.FTIR spectra of treated fly ash (FA 48w50S.1N.1L1.8)
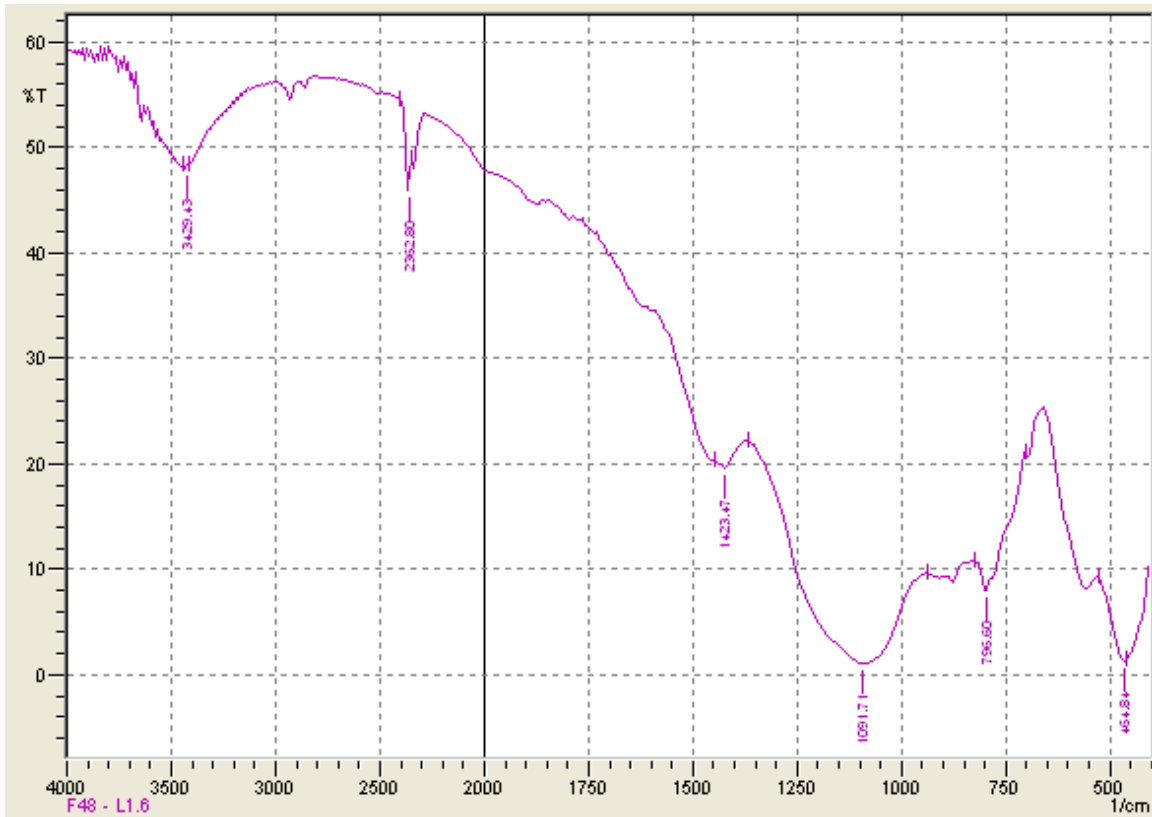
Figure 4.130: FTIR spectra of treated fly ash (FA 48w50S.2N.2L1.6)
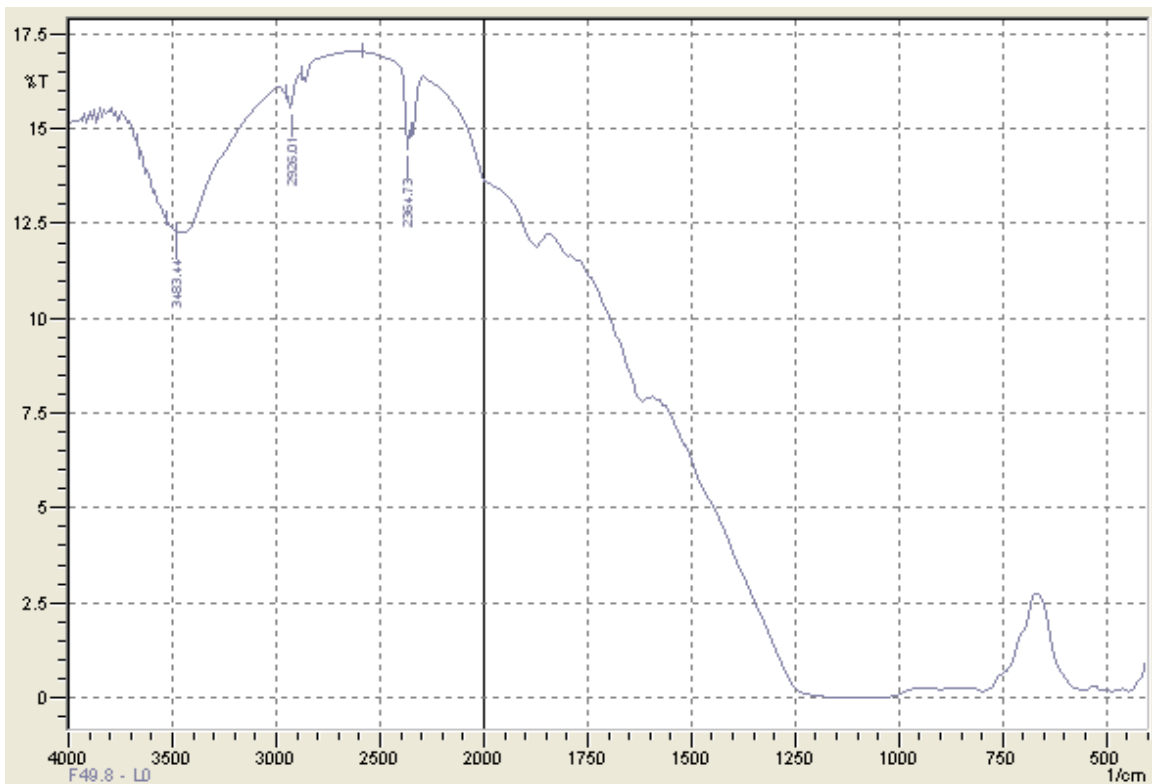
Figure 4.131: FTIR spectra of treated fly ash (FA 49.8w50S.1N.1L0)
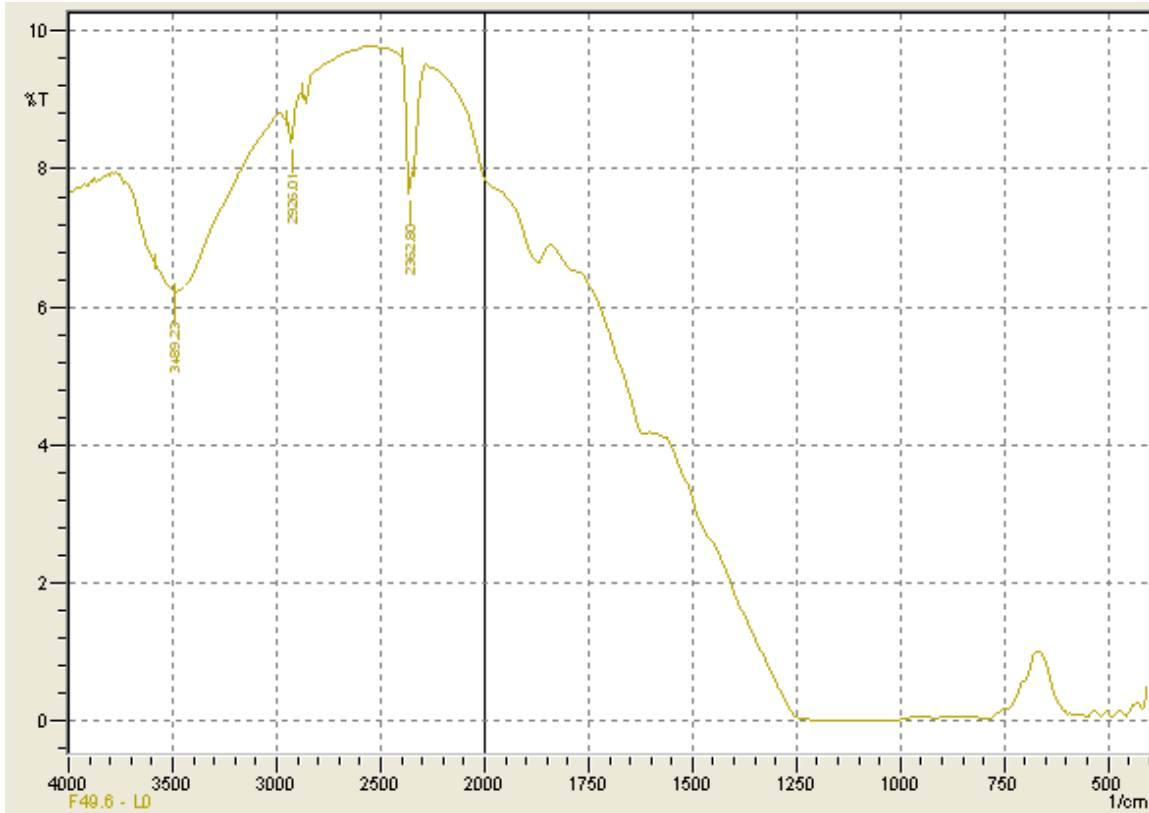
Figure 4.132: FTIR spectra of treated fly ash (FA 49.6w50S.2N.2L0)
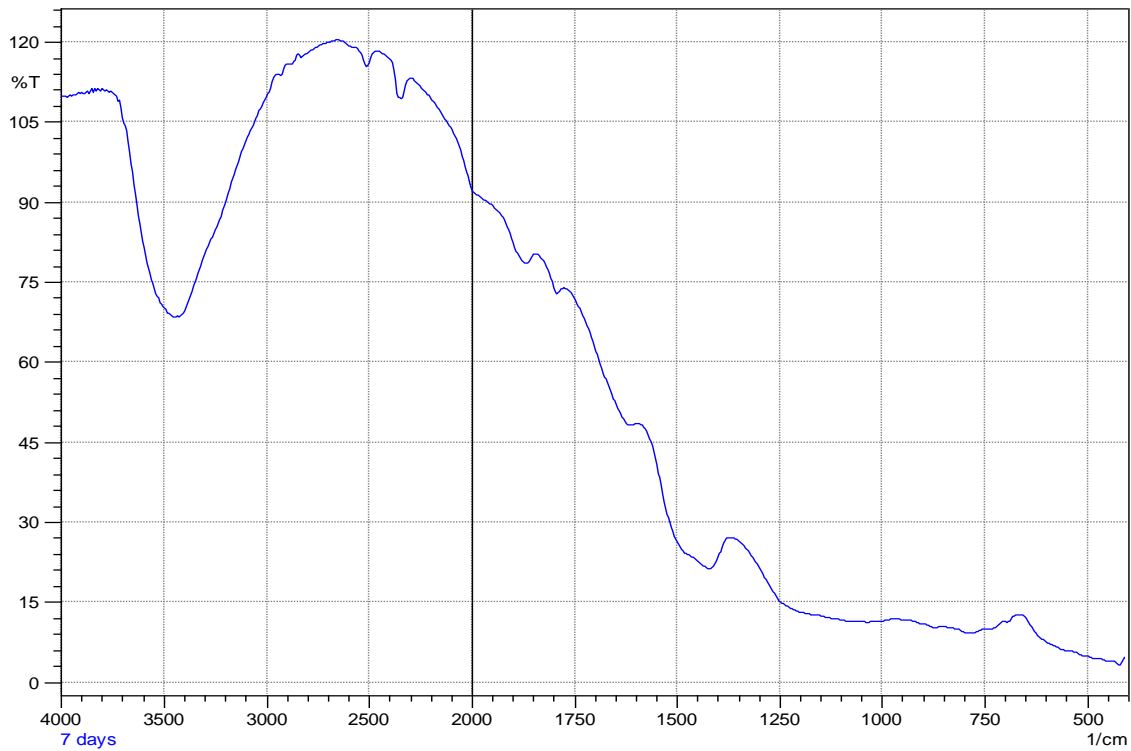
Figure 4.133.FTIR results of treated fly ash composites at 7 days curing period
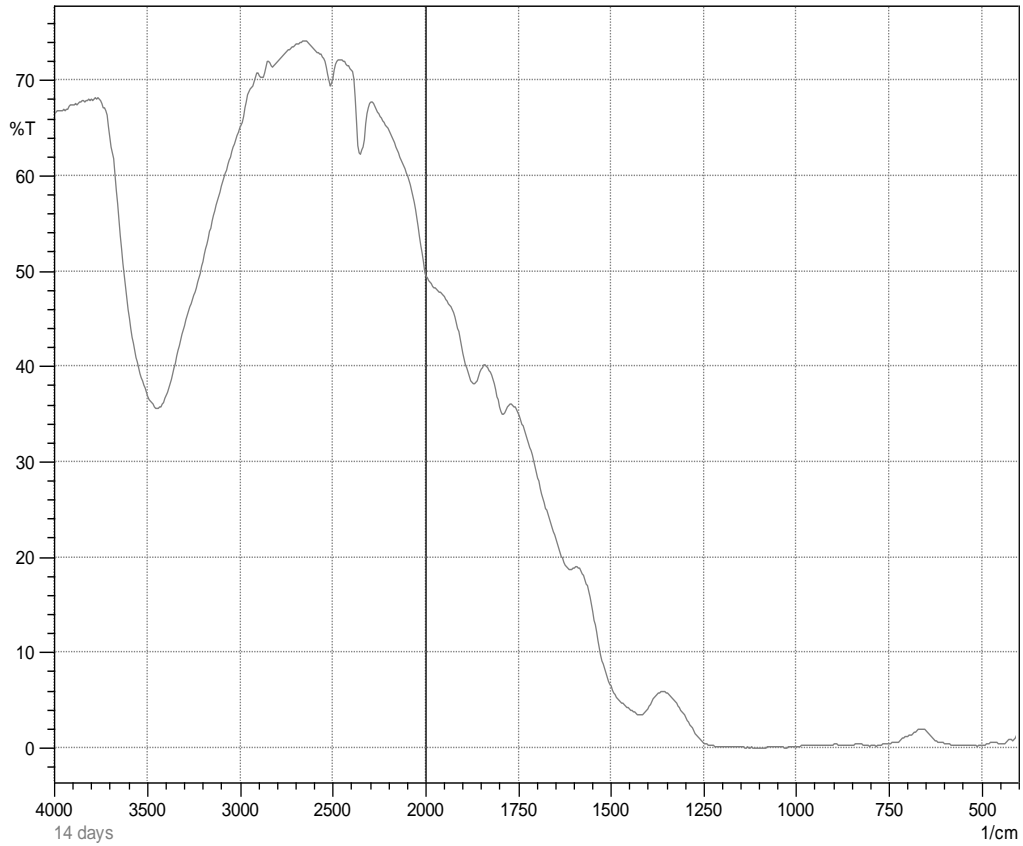
Figure 4.134: FTIR results of treated fly ash composites at 14 days curing period
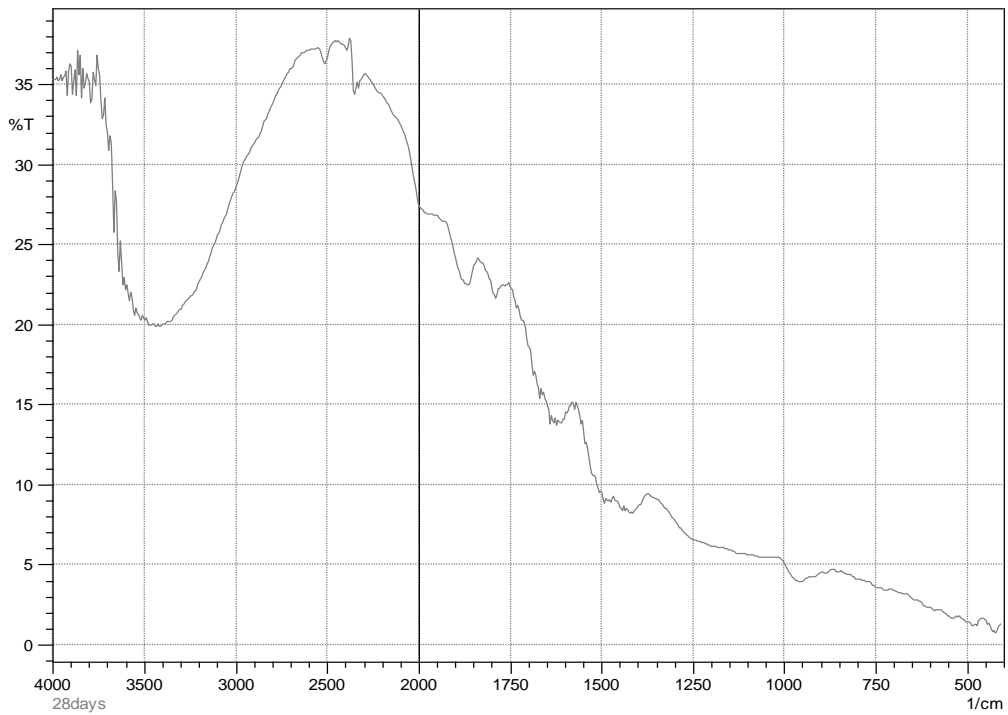
Figure 4.135: FTIR results of treated fly ash composites at 28 days curing period
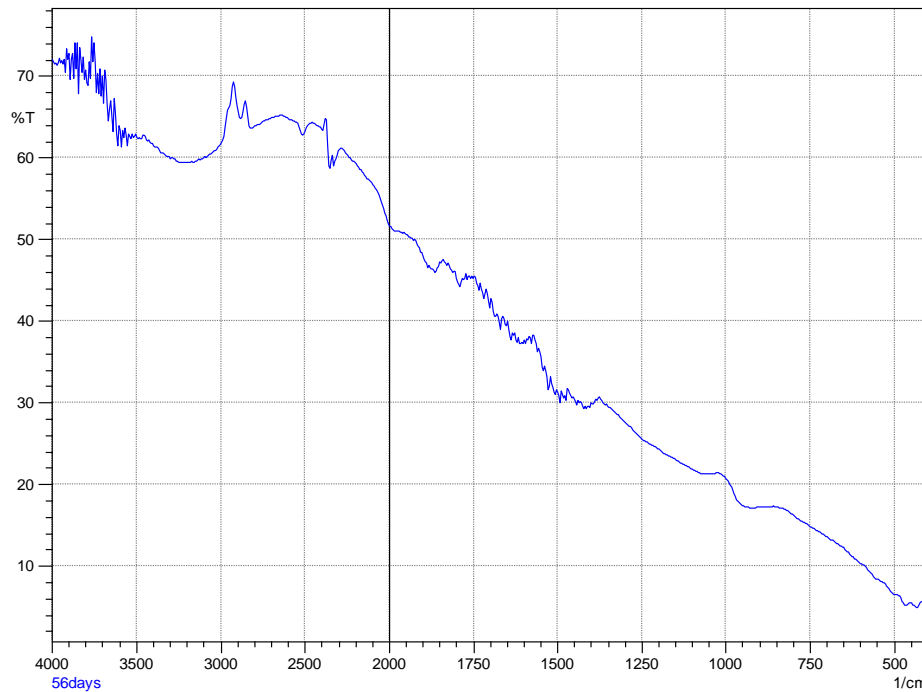
Figure 4.136: FTIR results of treated fly ash composites at 56 days curing period

4.4.5. Development of Empirical models

A part of the objectives was to develop model equations for the investigation with the parameters like UCS, BTS, and P-wave velocity. Those are reported here for the best fit coefficient of determination.

4.4.5.1. Relationship between UCS, BTS and P-wave velocity

The investigation involved samples for various parametric determinations. Each parameter has been discussed separately earlier. A few empirical models have been developed to establish mutual coefficient of determination between UCS and P-wave velocity, BTS and P-wave velocity etc. The data are analyzed using multiple regression models by the method of least squares (Figures 4.137-143). There exists relation between compressive strength of fly ash-lime and fly ash-lime-gypsum mixes with chemical composition, loss on ignition, CBR and tensile strength using power model (Ghosh and Dey, 2009). It confirms that the relationship between compressive strength and P-wave velocity become stronger with increasing curing period. The results of regression model between unconfined compressive strength, Brazilian tensile strength and P-wave velocity at different curing period are reported (Table 4.18).

Table 4.18: The developed correlation among various parameters of fly ash composite materials

Parameters	Best fit relation	R^2 value
UCS - BTS	y = 94.599x + 43.892	0.9790
Cohesion and angle of internal friction	y = 0.3511x + 9.3572	0.9972
Density and curing period	y = 5.0559x + 1404.8	0.9661
Density and P-wave velocity	y = 0.3146x + 1021.7	0.9988
P-wave velocity and poisson's ratio	y = -0.0002x + 0.7034	0.9688
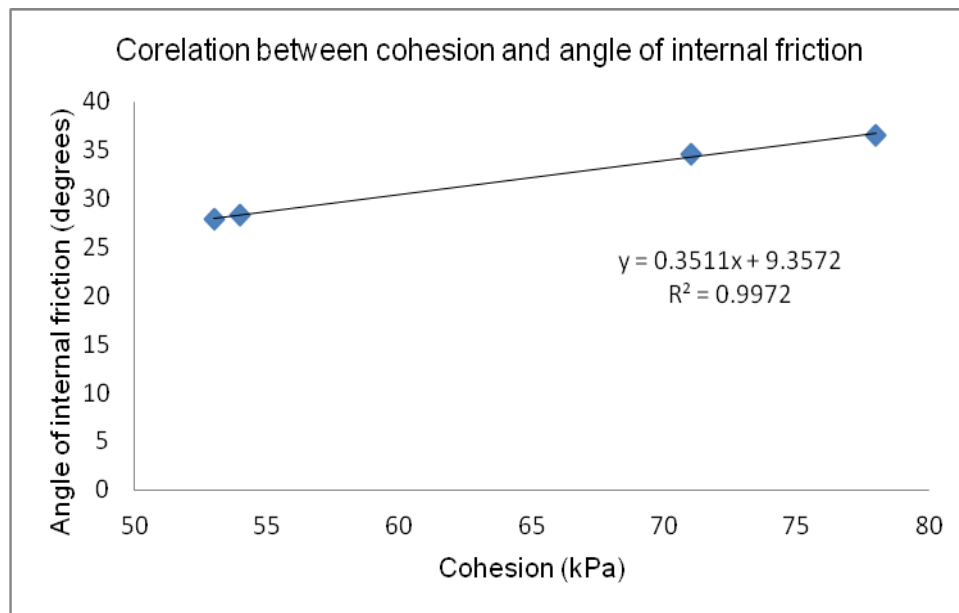
Figure 4.137: Correlation between cohesion and angle of internal friction
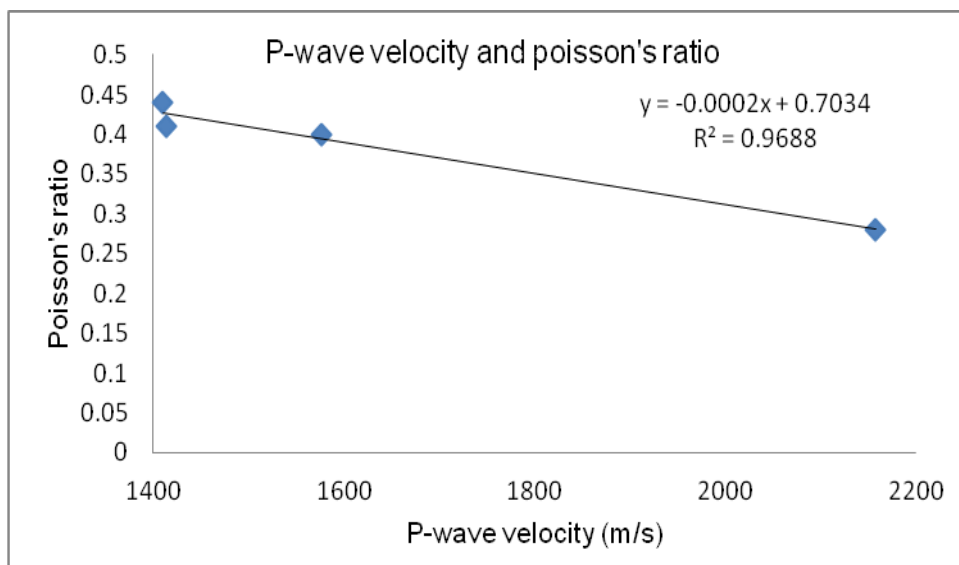
Figure 4.138: Correlation between P-wave velocity and Poisson's ratio
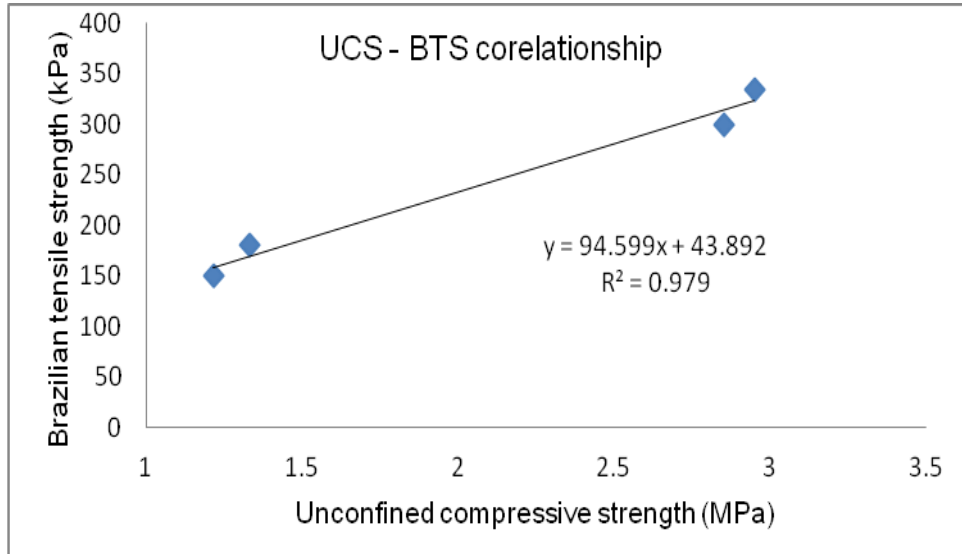
Figure 4.139: Relationship between BTS and UCS
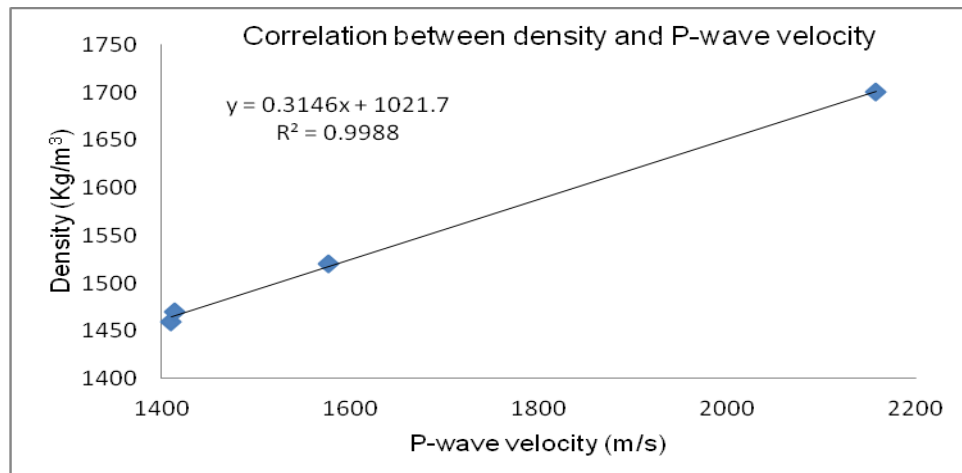
Figure 4.140.Correlation between density and P-wave velocity
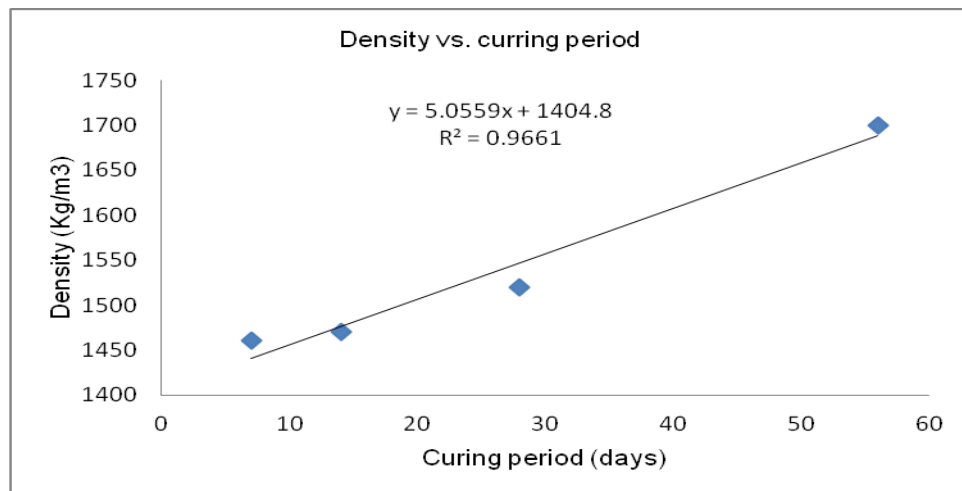
Figure 4.141.Correlation between density and curing period

4.4.6. Development of empirical equations from rheology study

Model equations for the investigation with the parameters like Shear Stress (SS), Shear Rate (SR), Viscosity (V), Yield Stress (YS), and Temperature (T). Those are reported here for some of the best fit correlations (Table 4.19).

Table 4.19.The developed correlation among various parameters of FCM

Sl.No.	Correlation between	Additive conc. (%)	Solid conc. (%)	Equation	R^2 Value
1.	SS-SR	0.2	20	y=0.0088x-0.1626	0.9939
2.	SS-SR	0.3	20	y=0.0282x+0.1048	0.9996
3.	SS-SR	0.2	30	y=0.0387x-1.4852	0.9926
4.	SS-SR	0.3	30	y=0.0106x-0.1304	0.9927
5.	SS-SR	0.5	40	y=0.2097x-3.9578	0.9935
6.	SS-SR	0.2	60	y=0.7299x-14.529	0.9932
7.	SS-SR	0.2	60	y=0.0456x-0.8206	0.9307
8.	SS-SR	0.3	60	y=0.588x-6.5426	0.9957
9.	SS-SR	0.4	60	y=0.5824x-2.5752	0.9992

4.5. Summary

In this study, the prime objective was to select an alternate backfill material to fill mine voids. To achive the objectives seven number of fly ash samples were collected from seven different sources. The seven number of fly ash samples were tested in the laboratory to study their suitability for mine filling purposes. Out of the seven fly ashes studied the best suitable one was selected for further study with respect to its flow and in-place strength characteristics. A surface active agent (surfactant) was added to the selected fly ash to modify the flow behaviour of the slurry in pipelines during its transportation to fill mine voids. Flow study was conducted at different additive concentration to optimize the same. The secondary objective was to measure the in-place strength characteristics of developed fly ash composite materials. The in-place strength characteristics of developed composite materials were measured by using another reagent called lime. The results of all the investigation were reported in this section.

CHAPTER 5

CONCLUSIONS

5.1. CONCLUSIONS

The primary objective of this study was to develop a suitable mine filling material and to evaluate its flow and in-place strength characteristics for the selected material. The reported results reflect some of the characteristics of fly ash samples from seven numbers of thermal power plants situated in various parts of the country. The potential of surfactant modified fly ash slurry was evaluated for its smooth flow in pipelines to be transported to mine sites for filling purposes. The modified slurry improved the flow properties by reducing drag friction in hydraulic pipelines. Besides flow, strength characteristics of any backfill material are vital parameters to judge its suitability for underground applications. Strength characteristics of the fly ash composites were studied through different methods such as unconfined compressive strength, Brazilian tensile strength, cohesion, angle of internal friction, Young's modulus, Poisson's ratio, bulk modulus, shear modulus, and ultrasonic pulse velocity useful for mine filling applications and to understand the engineering behavior of composite materials. Micro-structural analysis was carried out to gain better understanding of the mechanism of lime, fly ash, and surfactant interaction. The change in surface morphology and variation in chemical composition due to formation of hydration products were also analyzed through scanning electron micrographs and energy dispersive X-ray results. X-ray diffraction analyses were also carried out to identify the hydration production phases.

The results are concluded in three different sections i.e. I, II, and III. The investigation focused on analyzing and evaluating fly ash from seven different sources of India for their suitability for flowing in hydraulic pipelines (Section-I). The fly ash with most favorable flow properties has been further analyzed with respect to the surface behavior and its modification attributes (Section-II). The modified fly ash has been developed with strength enhancing agent and evaluated (Section-III).

5.1.1. Section-I (**Material characterization**)

From the material characterization study the following conclusions are made.

1. The coefficient of uniformity (C_u) of the seven fly ash samples varied from 0.70 to 6.3. The maximum value 6.3 was exhibited by ETPS (F_1) fly ash. This value is more than 6, thus this fly ash sample can be regarded as well graded compared with the other fly ash samples as per the classification and gradation of soils. Other fly ash specimens show C_u value less than 6.

2. The F_1 fly ash sample depicted bi-modal particle size distribution thought to be the sum total of two normal distributions. These materials are known to favor high densities of the consolidated mass because of their enhanced packing characteristics.

3. The specific surface area of the fly ash samples tested varied between 0.187 m^2/g and 1.24 m^2/g and the bulk density ranged between 1.60 g/cm^3 and 1.99 g/cm^3. Though there is little difference in values, comparatively, the average specific gravity and bulk density of fly ashes were found to be less than that of river bed sand.

4. The F_1 fly ash has low specific gravity (2.20) and more specific surface area (1.24 m^2/g) as compared to that of others which would facilitate improved surface modification by chemical additives for smooth flow in pipelines.

5. The fly ash particles in F_1 sample are similar in shape and form- distinctly spherical in shape and have much superior particle morphology that would create a lubricating effect resulting in a frictionless flow.

6. The F_1 fly ash sample has relatively high CaO content to assist in strength enhancement without sacrificing its flow attributes.

7. The porosity of the bulk fly ash samples varied between 9.135% and 34.2% and the moisture content varied between 0.15 % - 0.8%.

8. Overall results have indicated that the F_1 fly ash has several superior desirable properties that would make it attractive to fill mine voids. Therefore, F_1 fly ash sample was selected to undertake further study with respect to its flow and in-place strength characteristics.

5.1.2. Section-II (**Rheology study**)

This section gives the flow parameters results of both untreated fly ash slurry as well as surfactant modified fly ash slurry (treated) in two parts i.e. Part-A and Part-B.

5.1.2.1. Part-A (Untreated fly ash slurry)

1. The slurry without any additive exhibited shear thickening behavior with yield stress values of varying magnitude. Maximum value of yield stress observed was 11 Pa.

2. The untreated suspensions of fly ash slurries exhibited heterogeneous flow behavior.

3. The viscosity increased as the temperature was increased from 20^0C to 40^0C.

4. Fly ash slurries exhibited strong flocculation behavior in absence of chemical additives and the yield stress value of 0.3 Pa to 4 Pa was obtained for 40% solid concentration.

5. The untreated fly ash slurry showed turbulent flow behavior without depicting any definite trend. The ζ value of the fly ash slurry was negative (-27mV) without any additive, but changed to positive value (> +30mV) when surfactant was added to the slurry.

6. The addition of surfactant resulted in reduced surface tension by 53% to 56% as compared to that without any additive.

7. The shear viscosity increased sharply from 1mPas to 3mPas with the shear rates varying from 100 to 500 per second for all the temperature ranges tested.

5.1.2.2. Part-B (Treated fly ash slurry)

The conclusions derived from the treated fly ash slurry are the following.

1. Rheological behavior improved significantly when surfactant at 0.2% and 0.3% concentration were added to the fly ash slurry.

2. The surface tension (ST) of the treated fly ash slurry is reduced compared to untreated fly ash slurry and that of the suspending medium (water). The surfactants reduced the ST of the liquid significantly from a value of 71 mNm^{-1} to 31 mNm^{-1} confirming better wetting properties. It reduced by 51% to 54% as compared to that of tap water (68.9mN/m).

3. The zeta potential value (ζ) for the fly ash slurry with addition of surfactant exceeded +30 mV. It is a favorable attribute for the particles to remain floated that in the suspending medium so that no pipe jam takes place and hence requirement of water will be minimized.

4. The decrease in viscosity with increasing temperature is spectacular from 20^0C to 30^0C and after that the viscosity decrease is marginal till 40^0C for all the shear rates studied.

5. Minimum viscosity and shear stress at 4.8mPa.s and 2Pa respectively were obtained with 0.2% additive concentration at 40^0 C i.e. the slurry followed the fundamental properties of viscous materials.

6. At 0.1% additive concentration the flow behavior was erratic and uneven which is attributed to insufficient availability of additive concentration to modify the flow properties.

7. At 0.2% additive concentration, the shear stress value was minimum at 30^0 C at each shear rate.

8. It is found that the optimum temperature is 30^0C and optimum surfactant concentration is found to be 0.2% taking into all the observations together.

9. With 60% fly ash concentration at 40^0C with 0.2% surfactant the viscosity and shear stress values were minimum.

10. It is observed that the shear viscosity decreased sharply from 20^0C to 40^0C reaching a minimum value (4.8mPa.s) at 40^0C with shear rates varying from $25s^{-1}$ to $500s^{-1}$ for all the additive ranges tested.

11. 0.2% surfactant concentration produced best results. Therefore, 0.2% surfactant concentration was chosen for further study with respect to its in-place strength characteristics. The composite followed the Newtonian behavior and the relation obtained is approximately $\tau = 0.045 \ \dot{\gamma}$. The corresponding value of viscosity is found to be 0.045 Pa.s.

5.1.3. Section-III (Strength characterization)

The strength behavior of selected fly ash samples were also investigated with and without additives. The following conclusions are drawn with respect to strength behavior.

1. The fly ash sample used has less than 1% moisture content.

2. The sample without lime addition did not exhibit any significant strength value. It was only 297 kPa. There was no appreciable change in the strength value at different curing periods as well. Therefore, fly ash alone is not amenable to be used as a backfill material without any additive.

3. Addition of lime changed the strength behavior significantly. At 7 days of curing period the uniaxial compressive strength of the composite increased manifold. It failed at 1.215 MPa thus achieved a 305% increase. Then the increase rate reduced to 10% exhibiting 1.330 MPa at 14 days. But the rate of increase increased to 54% at 28 days curing to exhibit 2.85 MPa. The specimen continued exhibiting increased strength value at 56 days though with much reduced rate. All the samples exhibited shear type of failures thus confirming to the development of cohesion between particles.

4. The optimum MDD of the developed composite materials was found to be 1443 Kg/m^3 and the corresponding value for OMC was 12.51%.

5. Unconfined compressive strengths increased from 0.71 to 3.14 MPa with curing period. The FCM exhibited maximum compressive strength value of 3.14 MPa at 56 days curing.

6. Brazilian tensile strengths increased from 55.7 to 357 kPa with curing period.

7. The ultrasonic pulse velocities varied in the range of 797 m/s to 1699 m/s for varying curing periods, reaching a maximum value at 56 days curing.

8. The morphology of all the mixes showed the formation of hydrated gel at 56 days curing. The voids between the particles were filled by growing hydrates with curing time.

9. Microanalysis and compositional analysis confirmed the formation of new cementitious compounds such as calcium silicate hydrate (CSH), calcium aluminate hydrate (CAH), and calcium aluminate silicate hydrate (CASH) which leads to increase in strength of the material over time.

10. XRD patterns indicate CAH is the most dominant formation followed by CSH and CASH.

11. As the fly ash was mixed with lime, surfactant and NaSal, doublet (two peaks) were observed at 792.74 cm^{-1} with another at 1400 cm^{-1} region in FTIR monographs. It

reflects the presence of calcium, hence attribute of a good geolite. Without lime no geolitesation even in presence of surfactant and counter-ion was observed.

12. As the curing period progressed to 7 and 14 days the peaks went up to 3400 cm^{-1}, 1400 cm^{-1}, 1600-1650 cm^{-1}. The peaks depict OH stretching to OH bonding. At 28 days curing period broader peaks with O-C-O stretching and H-O-H bonding were observed. These reflect higher capacity of adsorption. The peaks were broader at 56 days of curing with silica-alumina bonding with extra at 950 cm^{-1}. These peaks with curing periods reflect that good geolite has been formed.

13. The tensile strength of the fly ash composite material showed significant improvement with curing periods. At 28 days curing the tensile strength values increased at 100% and 200% to that of at 7 and 14 days respectively. Marginal increase was also observed at 56 days curing period.

14. Both cohesion and angle of internal friction increased with curing period. At 28 days curing period the friction angle was about 35^0 which are typical of any medium hard rock. This confirms that the developed composite material would be suitable to support roof load and would also resist putting pressure on barricades.

15. The ultrasonic pulse velocities varied between 1410 m/s to 2158 m/s at varying curing periods from 7 days to 56 days. Maximum values were obtained at 56 days curing period, thus confirming the increased conductivity in the sample. But it increased by 12% at 28 days thus reflecting improved transmissivity of the wave due to enhanced pozzolanic activity. The rise is marginal between 7 and 14 days of curing.

16. The P-wave velocity at 56 days of curing period was 2158 kPa and least values were obtained for 7 days of curing period which confirms to the results obtained in UCS and BTS tests.

17. The Poisson's ratio values of each composite decreased with increase in curing period. The Poisson's ratio values varied between 0.28 and 0.44 of all developed composites cured at 7, 14, 28, and 56 days. The Poisson's ratio values of each composite did not change significantly with longer curing periods which are the typical characteristics of any material.

18. The Young's modulus (E) values increased with curing period confirming to enhance pozzolanic activities resulting in higher stiffness of the composites. The velocity of propagation increases with increased stiffness of the material.

19. The density of the material also increased with curing period confirming to strength gain.

20. The SEM images show development of gel at different stages of pozzolanic reaction. It confirms to the observation that during early stages, the reactive particles in the fly ash composite served as nucleation sites for hydration and pozzolanic reaction products as (C-S-H, C-A-H, C-A-S-H). Cementitious compounds are formed around fly ash particles.

21. The composite at 56 days of curing period exhibited dense-gel-like mass covering all reactive particles completely and filling up the inter-particle space with blurred grain boundaries. It appears like a massive unit compared to the other composites. The dense gel acted as a binding substance and appears to be evenly distributed to form compact structure, thus creating more contact and higher cohesion that in turn reflects in greater strength values.

22. The formation of reaction products such as calcium silicate hydrates CSH; Calcium aluminate hydrates (CAH), and Calcium aluminates silicate hydrates (CASH) were confirmed from X-ray diffraction analysis. These new cementitious compounds induce aggregation effect in fly ash and bind the particles together to form fly ash clusters and resulted in overall enhanced strength behaviors of composites.

23. The model equations governing the relationship between Brazilian tensile strength and unconfined compressive strength and unconfined compressive strength and ultrasonic pulse velocity values were developed having correlation coefficient (R^2) values varying from 70% to 90%.

5.2. Scope for future work

The investigation has certain limitations and hence all the factors that contribute to the smooth flow in pipelines could not be addressed in time. So the future research work should incorporate the following aspects in detail.

i. A study of the surface chemistry of the slurry by X-ray photoelectron spectroscopy (XPS) under considered chemical treatments is recommended in future work to describe the observed changes in the rheological properties.

ii. Drag reduction experiments can be conducted with laboratory scale pipe loop setups to verify the percentage drag reduction by surfactant modified fly ash slurries and that with untreated slurries.

iii. Pipe loop tests can be carried out to measure the pressure loss and head loss parameters both in horizontal pipelines and vertical pipelines.

iv. Numerical modeling can be carried out to verify the experimental data and predict the flow behaviors and pressure loss parameters.

v. Performance of developed composites was evaluated experimentally. Same should be carried out in field conditions and correlated.

5.3. Strength and weaknesses of thesis

5.3.1. Strengths

(a) The research work undertaken involved a very extensive laboratory experiments in three phases, viz. the determination of material characteristics and particle size analysis, geo-technical characteristics and enhancement of strength properties and lastly the experiments related to flow parameters such as viscosity, shear stress, shear rate and solid-water concentrations. Further the flow behavior was also determined with additives.

(b) Substantial literature survey was undertaken

(c) The thesis is made in greater detail and meticulously prepared.

(d) A good number of publications, both in international and national journals as well as conferences from the work undertaken.

(e) The influence of surfactants on fly ash flow parameters explained.

5.3.2. Weaknesses

Investigation was limited to seven numbers of samples. The same should be carried out for more number of samples with more variations not limited by time.

REFERENCES

Aguilar, G., Gasljevic, K., Matthys, E.F., 2006. Reduction of friction in fluid transport-experimental investigation, Revista Mexicana De FISICA, 52(5), 444-452.

Ahmaruzzaman, M., 2010. A review on the utilization of fly ash, Journal of Progress in Energy Combust. Sci., 36, pp. 327-363.

Arora, S., Aydilek, A.H., 2005. Class F fly-ash-amended soils as highway base materials, Journal of Materials in Civil Engg. ASCE 17 (2005): pp. 640-649.

ASTM C 204 84, 1984.Standard test method for fineness of Portland cement by air permeability apparatus Annual Book of ASTM Standards, American Society for Testing and Materials, Philadelphia Vol.04.01, 56-162.

ASTM C 618 94, 1995.Standard specification for coal fly ash and raw or calcined natural pozzolana for use: as a mineral admixture in Portland cement concrete. Annual Book of ASTM Standards, American Society for Testing and Materials, Philadelphia, Vol.04.08, 304-306.

ASTM D 2487 06, 2006.Standard Practices for Classification of Soils for Engineering Purposes (Unified Soil Classification System), Annual Book of ASTM Standards, American Society for Testing and Materials, Philadelphia, Vol.04.08, 1-12.

ASTM D 854 92, 1995.Standard test methods for specific gravity of soils, Annual Book of ASTM Standards, American Society for Testing and Materials, Philadelphia, Vol. 04.08, 80-83.

ASTM D-2487, 1998. Standard classification of soils for engineering purposes (Unified soil classification system).

ASTM D422 63, 1994. Standard test method for particle size analysis of soils. Annual Book of ASTM Standards, 04.08, 10-6.

Baker, M.D., Laguros, J.G., 1984. Reaction products in concrete, MRS Proceedings, 43, 73, doi: 10.1557/PROC-43-73.

Bandyopadhyay, D., 2000. The role of fly ash management in combating the global environmental pollution, Proc. of the 2nd International Conference on fly ash disposal and utilization, vol.-I, IV-6, pp: 39-45.

Barnes, H.A., Hutton, J.F., Walters, K., 1989. An introduction to rheology, Elsevier, New York.

_____

Barret, J.F., Appell, J., Porte, G., 1993. Linear rheology of entangled wormlike micelles, Langmuir, 9, 2851-2854.

Beaty, W.R., Johnston, R.L., Kramer, R.L., Warnock, L.G., Wheeler, G.R., 1984. Offshore crude oil production increased by drag reducers. Sellin, R.H.R., and Moses, R.T. (eds), Drag Reduction, F.1-1.

Behera, B., Mishra, M.K., 2011. Strength behavior of surface coal mine overburden-fly ash mixes stabilized with quick lime. International Journal of Mining, Reclamation and Environment, DOI: 10.1080/17480930.2011.552285, 1-17.

Bentz, D.P., 2007. Cement hydration: Building bridges and dams at the microstructure level, Mater. Struct. 40, 397-404.

Bewersdorff, H.W., Ohlendorf, D., 1988. The Behavior of Drag-Reducing Cationic Surfactant solutions. J. Colloid and Polymer Science, 226(10), pp. 941-953.

Bilgen, E., Boulos, R., 1972. Transaction of the CSME, 1, 25.

Bingham, E.C., Green, H., 1919. Proceedings of American Society of Testing and Materials, 20(11), 640.

Biswas, A., Gandhi, B.K., Singh, S.N., Seshadri, V., 2000. Characteristics of coal ash and their role in hydraulic design of ash disposal pipelines. Indian Journal of Engineering and Material Science 7, 1-7.

Blissett, R.S., Rowson, N.A., 2013. An empirical model for the prediction of the viscosity of slurries of coal fly ash with varying concentration and shear rate at room temperature, Fuel 111, 555-563.

Boger, D.V., Leong, Y.K., Mainwaring, D.E., Christine, G.B., 1987. Proc. 3rd Eur. Conf. on coal liquid mixtures, Malmo, Sweden, 1.

Boger, D.V., Nguyen, Q.D., 1985. Yield stress determination, J. Rheology, 29, 335.

Boltenhagen, P., Hu, Y., Matthys, E.F., Pine, D.J., 1997. Observation of bulk phase separation and co-existence in a sheared micellar solution, Phys Rev Lett, 79(12), 2359-2362.

Bournonville, A., Nzihou, A., 2002. Rheology of non-Newtonian suspensions of fly ash: Effect of conc, yield stress, and hydrodynamic interactions, Powder Tech. 128, 148-158.

Boylu, F., Atesok, G., Dincer, H., 2005. The effect of carboxymethyl cellulose (CMC) on the stability of coal-water slurries. Fuel 84, 315-319.

Bulusu, S., Aydilek, A.H., Petzrick, P., Guynn, R., 2005. Remediation of abandoned mines using coal combustion by-products, J. Geotech. Geoenviron. Eng. 131, 958-969.

_____

Bulusu, S., Aydilek, A.H., Rustagi, N., 2007. CCB-based encapsulation of pyrite for remedial of acid mine drainage, J. Hazard. Materials, doi: 10.1016/j.jhazmat.2007.01.035.

Bunn, T.F., 1989. Dense phase hydraulic conveying of power station fly ash and bottom ash. Third International Conference on Bulk Materials, Storage, Handling and Transportation, Newcastle, 27-29 June, 250-255.

Bunn, T.F., Chambers, A.J., 1991. Characterization of fly ash slurries, Intl. Mech. Engg. Cong., Sidney, NSW, Australia, 8-12 July, pp. 50-61.

Bunn, T.F., Chambers, A.J., 1993. Experiences with Dense Phase Hydraulic Conveying of Vales Point Fly Ash. Intl. Journal of Powder Handling and Processing, 5(1), pp. 35-45.

Bunn, T.F., Chambers, A.J., Goh, C.M., 1990. Rheology of some fly ash slurries, Intl. Coal Engg. Conf., Sidney, pp. 7-14.

Burger, E.D., Chorn, L.G., Perkins, T.K., 1980. Studies of drag reduction conducted over a broad range of pipeline conditions when flowing Pudhoe Bay crude oil. Journal of Rheology 24, 603-626.

Candau, S.J., Hebraud, P., Schmitt, V., Lequeux, F., Kern, F., Zana, R., 1994. International Nuovo Cimento, 16(9), 1401-1410

Canty, G.A., Everett, J.W., 2001. Physical and chemical evaluation of CCBs for alternative uses, J. Energy Engg., 127(3), 41-58.

Carrington, S., Langridge, J., 2005. Flow characterization: selecting appropriate technology, American Laboratory News.

Casassa, E.Z., Parffit, G.D., Rao, A.S., Toor, E.W., 1984. Effect of surface active additives on coal/water slurry rheology. American Society of Mechanical Engineers (paper), ASME, New York, NY, USA, 10p 84, WA/HT-96.

Cates, M.E., 1993. Isotropic phases of self-assembled amphiphilic aggregates, Philos. Trans. R. Soc. London A, 344, 339-356.

Cates, M.E., Candau, S.J., 1990. Statics and dynamics of wormlike surfactant micelles, J. Phys. Condens. Matter, 2, 6869-6892.

Cetin, B., Aydilek, A.H., Guney, Y., 2010. Stabilization of recycled base materials with high carbon fly ash, Journal of Resources, Conservation Recycling, 54, pp. 878-892.

Chandel, S., Seshadri, V., Singh, S.N., 2009. Effect of additive on pressure drop and rheological characteristics of fly ash slurry at high concentration, Particulate Sc and Tech. 27(3), 271-284.

Chandel, S., Singh, S.N., Seshadri, V., 2009. Deposition Characteristics of coal ash slurries at higher concentrations, Advanced Powder Technology, 20, 383-389.

Chandel, S., Singh, S.N., Seshadri, V., 2009. Effect of additive on the rheological characteristics of fly ash and bottom ash mixture at high concentrations, Intl J. Fluid Mech & Res, 36(6), 538-551.

Chandel, S., Singh, S.N., Seshadri, V., 2010. Transportation of high conc. coal ash slurries through pipelines, Intl Archive of Applied Sciences and Tech., 1(1), 1-9.

Chandel, S., Singh, S.N., Seshadri, V., 2011. A comparative study on the performance characteristics of centrifugal and progressive cavity slurry pumps with high conc. fly ash slurries, Particulate Sc and Tech., 29: 4, 378-396.

Chandel, S., Singh, S.N., Seshadri, V., 2011. Effect of additive on the performance characteristics of centrifugal and progressive cavity pumps, with high conc. fly ash slurries, Coal Combustion and Gasification Products, 3, 67-74.

Chen, Liangyong., Duan, Y., Zhao, C., Yang, L., 2009. Rheological behavior and wall slip of concentrated coal water slurry in pipe flows, Chemical Engg. & Processing: Process Intensification, 48, 1241-1248.

Chhabra, R.P., Richardson, J.F., 1999. Non-Newtonian flow in the process industries, fundamentals and engineering applications. Butterworth Heinemann, Oxford.

Choi, H.J., John, M.S., 1996. Industrial Engineering Chemistry Research, 35, 2993.

Choi, H.J., Kim, C.A., Sung, J.H., Kim, C.B., Chun, W., John, M.S., 2000. Universal drag reduction characteristics of saline water-soluble poly (ethylene oxide) in a rotating disk apparatus. Colloid Polymer Science 278, 701-705.

Chou, L.C., 1991. Drag reducing cationic surfactant solutions for district heating and cooling systems, Ph.D. dissertation, The Ohio State University, Columbus, OH.

Chu, T.Y., Davidson, D.T., Goecker, W.L., Moh, Z.C., 1955. Soil stabilization with lime-fly ash mixtures: preliminary studies with silty and clayey soils. Highway Research Board Bulletin, 108, pp. 102 – 112.

Chugh, Y.P., Biswas, D., Deb, D., Deaton, G., 1999. Underground placement of coal processing waste and CCBs based paste backfill for enhanced mining economics, Technical Report of the Department of Mining and Mineral Resources Engineering, Southern Illinois University, Carbondale, USA, pp: 143-153.

_____

Chugh, Y.P., Biswas, D., Deb, D., Deaton, G., 2001. Underground placement of coal processing waste and CCBs based paste backfill to enhance mining economics, ICC No. 97 US1, pp: 52.

Connors, C., 2001. Methods to reduce Portland cement consumption in backfill at Jerritt Canyon's u/g mines, Proc. 7th Intl. Symposium on Mining with backfill, Mine fill 2001, ed David Stone, P.E. pp. 301-309.

Craig, H., 2003. Ash Utilization-an Australian Perspective, Proc. of the International Ash Utilization Symposium, Center for Applied Energy Research, University of Kentucky, pp: 1-13.

Das, S.K., Yudhbir, 2006. Geotechnical properties of low calcium and high calcium fly ash, Journal of Geotechnical and Geological Engineering, 24, pp. 249-263.

Davis, R.E., 1949. A review of pozzolanic materials and their use in cement concrete, Special Technical Publication, ASTM, 99, pp. 3-15.

Deb, D., Chugh, Y.P., 2005. Development and underground placement of paste backfill material based on CCBs and coal processing waste, Proc. of the International Congress on Fly Ash Utilization, Vol.-IX, pp. 5.1-5.11.

Dhir, R.K., 2005. Emerging trends in fly ash utilization: World Scenario, Proc. of International Conference on fly ash utilization, pp: 1.1-1.10.

DiGioia, A.M., Nuzzo, W.L., 1997.Fly ash as structural fill. Journal of Power Division, ASCE; Vol. 98(1), 77-92.

DIN EN ISO 3219, 1993. Determination of viscosity of polymers and resins in the liquid state or as emulsions or dispersions using a rotational viscometer with defined shear rate.

Dodge, D.W., Metzner, A.B., 1959. Turbulent flow of non-Newtonian systems, AIChE Journal 5, 189-204.

Duangprasert, T., Sirivat, A., Siemanod, K., Wilkes, J.O., 2008. Vertical two-phase flow regimes and pressure gradients under the influence of SDS surfactant, Experimental Thermal and Fluid Science, 32, 808-817.

Durand, R., 1951. Transport hydraulique de graviers et galets en conduit, Houille Blanche No. Special B: 609-619.

Dutta, B.K., Khanra, S., Mallick, D., 2009. Leaching of elements from coal fly ash-assessment of its potential for use in filling abandoned coal mines. Fuel 88, 1314-1323.

_____

Elizabet, M.V., Linda, C.P., Richard, A.K., Lethabo, C.M., 2011. Characterization of coal fly ash modified by sodium lauryl sulphate, World of Coal Ash Conf. (WOCA), Denver, USA.

Erol, M., Genc A., Ovecoglu, M.L., Yucelen, E., Kucukbayrak, S., Taptik Y., 2000. Characterization of a glass-ceramic produced from thermal power plant fly ashes, Journal of European Ceramic Society, 20, pp. 2209- 2214.

Eromoto, T., Tatsuoka, F., Shishime, M., Kawabe, S., Benedetto, H.D., 2006. In: Springer (Eds), Solid stress behaviour: Measurement, Modelling and Analysis, Geotechnical Symposium, Rome.

Fabula, A.G., 1971. Fire-fighting benefits of polymeric friction reduction. Transactions of the ASME Journal of Basic Engineering 93, 453-455.

Fawconnier, C.J., Korsten, R.W.O., 1982. Ash fill in pillar design-Increased u/g extraction of coal, the SAIMM Monograph Series 4, 277-361.

Feng-Chen L., Kawaguchi, Y., Bo Y., Jin-Jia W., Hishida, K., 2008. Experimental study of drag reduction mechanism for a dilute surfactant solution flow. International Journal of Heat and Mass Transfer, 51, 835-843.

Fisher, G.L., Prentice, B.A., Silberman, D., Ondov, J.M., Ragaini, R.C., McFarland, A.R., 1978. Physical and morphological studies of size-classified coal fly ash, Environmental Science and Technology. American Chemical Society 12, 447-451.

Fontaine, A.A., Deutsch, S., Brungart, T.A., Petrie, H.L., Fenstermacker, M., 1999. Drag Reduction by Coupled Systems: Micro-bubble Injection with Homogeneous Polymer and Surfactant Solutions. Springer-Verlag, Experiments in Fluids, Vol.26, pp. 397-403.

Gadd, G.E., 1966. Reduction of turbulent friction in liquids by dissolved additives, Nature 212, 874-877.

Gahlot, V.K., Seshadri, V., Malhotra, R.C., 1992. Effect of density, size distribution and conc. Of solids on the characteristics of centrifugal pumps, J of Fluid Engg., 3(114): 386-389.

Galvin, J.M., Wagner, H., 1982. Use of ash to improve strata control in bord and pillar working, Proc. Symp. On strata mechanics, Univ. of New Castle upon Tyne, 264-269.

Gandhi, B.K. et al. 2005. Performance characteristics of the centrifugal slurry pump handling ash slurries at high concentrations, Proc. of the International Congress on fly ash utilization, Vol.-V, pp: 8.1-8.11.

_____

George, R.G., Darley, H.C., Walter, F.R., 1984. Composition and properties of oil well drilling fluids. Fourth Edition, Gulf Publishing Company, Houston, Texas, 3-239.

Ghosh, A., 1996. Environmental and engineering characteristics of stabilized low lime fly ash, Unpublished Ph.D thesis, Indian Institute of Technology, Kharagpur, India.

Ghosh, A., Dey, U., 2009. Bearing ratio of reinforced fly ash overlying soft soil and deformation modulus of fly ash, Journal of Geotextiles and Geomembranes, 27, pp. 313-320.

Ghosh, A., Subbarao C., 2001. Microstructural development in fly ash modified with lime and gypsum, Journal of Mater, in Civil Eng, 13, pp. 65-70.

Ghosh, C.N. et al. 2005. Hydraulic ash stowing in underground coal mines − a case study, Proc. of Fly Ash India-International Congress on Fly Ash Utilization, 9, pp. 1.1-1.11.

Ghosh, C.N., 2005. Pond ash: A substitute of sand for mine stowing, Proc. of National Seminar cum business meets on use of fly ash in Mining sector, pp. 6-16.

Ghosh, C.N., Mondal, P.K., Prashant, 2006. Suitability of Fly Ash as a stowing material for underground coal mines-some studies, Proc. of 1st Asian mining congress, pp. 113–123.

Golda, J., 1986. Hydraulic transport of coal in pipes with drag reducing additives. Chemical Engineering Communications 43, 53-67.

Goodrich, W.G., Daniel E. Charhut. 2003. High concentrated slurry system for fluidized bed boiler ash disposal, pp: 1-10.

Gopalan, M.K., Haque, M.N., 1986. Strength development of clinically cured plain and fly ash concretes, Proc. Of Australian Road Research Board, 13(5), 27-33.

Granville, P., 1977. Paper B1 in Proc of 2nd Intl Conf on drag reduction, BHRA Fluid Engg., (Cranfield, England), pp. B1-1.

Gray, D.H., Lin, Y.K., 1972. Engineering properties of compacted fly ash, Journal of Soil Mech. Foundation Engg., ASCE, 98, pp. 361-380.

Greenwood, R., Kendall, K., 1999. Selection of Suitable Dispersants for Aqueous Suspensions of Zirconia and Titania Powders using Acoustophoresis, Journal of the European Ceramic Society, Vol. 19 (4), pp. 479-488.

Guo, R.Q., Rohatgi, P.K., Nath, D., 1996. Compacting characteristics of aluminium-fly ash powder mixtures. Journal of Material Science, 31, 5513-5519.

Gyr, A., Bewersdorff, H.W., 1995. Drag reduction of turbulent flows by additives, Kluwer Academic Publishers, The Netherlands.

Hackley, V.A., Ferraris, C.F., 2001. The use of nomenclature in dispersion science and technology. NIST Recommended Practice Guide, SP 960-3.

Hanks, R.W., Hanks, K.W., 1982. A new viscometer for determining the effect of particle size distributions and concentrations on slurry rheology, Proc 7th Intl Conf on slurry rheology and transportation, Washington DC, pp. 151-161.

Hansen, L.D., Fisher, G.L., 1980. Elemental distribution in coal fly ash particles, Environmental Sci. & Tech., American Chemical Society 14, 1111-1117.

He, M., Wang, Y., Forssberg, E., 2004. Slurry rheology in wet ultrafine grinding of industrial minerals: a review. Powder Technology 147, 94-112.

He, W., Park, C.S., Norbeck, J.M., 2009. Rheological study of comingled biomass and coal slurries with hydrothermal pretreatment, Energy and Fuels, American Chemical Society, A-D.

Heimenz, P.C., 1986. Principles of colloids and surface chemistry, New York, Dekker.

Hellsten and Harwigsson, 1999. Use of a betaine surfactant together with an anionic surfactant as a drag-reducing agent, US patent issued on May 11, 1999.

Herscheel, H., Bulkley, R., 1926. Proceedings of American Society of Testing and Materials, 26(II), 621.

Horiuchi, S., Kawaguchi, M., Yasuhara, K., 2000. Effective use of fly ash slurry as fill material, Journal of hazardous Materials, 76(2-3), pp: 301-337.

Horsley, R.R., 1962. Viscometers and pipe loop test on gold slime slurry at very high concentration (by weight) with and without additive, Proc. of Hydro-transport 8, BHRA Fluid Engg., Cranfield, Bedford, U.K. pp. 122-133.

Horsley, R.R., 1982. Viscometer and pipe loop tests on gold slurries at very high concentration (by weight), Hydro-transport (BHRA) 8, pp. 367-382.

Hoyt, J.W., 1986. Drag Reduction, in Encyclopedia of Polymer Science and Engineering, Vol. 5.

Hoyt, J.W., Fabula, A.G., 1963. Proc 10th Intl Towing Tank Conf., Teddington.

Hu, Y., Matthys, E.F., 1997. Rheological and Rheo-optical characterization of shear-induced structure formation in a non-ionic drag reduction surfactant solution, J. of Rheology, 41, 151-165.

Hunter, R.J., Nicol, S.K., 1968. The dependence of plastic flow behavior of clay suspensions on surface properties, Journal of Colloid and Interface Science, 28, 250-259.

_____

Huynh, L., Jenkins, P., Ralston, J., 2000. Modification of the rheological properties of concentrated slurries by control of mineral solution interfacial chemistry. Int. Journal Miner. Process 59, 305-325.

Hwang, S., Lattore, I., 2011. Impact of manufactured coal ash aggregates on water quality during, open pit restoration: 1. a statistical screening test, Coal Combustion and Gasification Products, 3, 1-7.

Ihle, C.F., Tamburrino, A., Variables affecting energy efficiency in turbulent ore concentrate pipeline transport, Minerals Engineering 39, 62-70.

IS Codes. 1987. Compendium of Indian Standards on Soil Engineering, Part-1. Bureau of Indian Standards, November, New Delhi, India.

Jackson, M.L., 1958. Soil Chemical Analysis. Prentice-Hall International, London.

Jain, M.K., Sastry, B.S., 2001. Fly Ash status in India and its utilization in mining, Proc. of National Seminar on Environmental Issues and Waste Management in Mining and Allied Industries, pp: 74-85.

Jain, M.K., Sastry, B.S., 2003. Settling characteristics of some Indian Fly Ash, Proc. of the 3rd International Conference on Fly Ash Utilization & Disposal, Vol. II, pp. 34-41.

Jain, M.K., Sastry, B.S., 2004. Slurry flow behavior of Fly Ash, Proc. of the Conference on Technology and Management for Sustainable Exploitation of Minerals and Natural Resources, pp: 149-160.

Jain, S.K. et al. 2005. Leaching characteristics of Fly Ash, Proc. of the International Congress on Fly Ash utilization, Vol.-IV, pp: IV 4.1-4.9.

Jirina, T., Jan, S., 2010, Reduction of surface subsidence risks by fly ash exploitation as filling material in deep mining areas, Natural Hazards 53, 251-258.

Jones, R.L., Chandler, H.D., 1989. The effect of drag-reducing additives on the rheological properties of silica-water suspensions containing iron (III) oxide and of typical gold-mine slurry. Journal of South Afr. Inst. Min. Metall. 89, 187-191.

Jorgenson, and Crooke, 2001. Fly ash paste utilization for placement as mine and landfill at Great River Energy's Coal Creek Station, Proc. 7th Intl. Symposium on Mining with backfill, Mine fill 2001, ed. David stone, P.E. pp. 187-194.

Joshi, R.C., Duncan, D.M., McMaster, H.M., 1975.New and conventional Engineering uses of Fly Ash. Journal of Transport Engineering, ASCE; Vol. (101), 791-806.

Joshi, R.C., Marsh, B.K., 1987. Some physical, chemical, and mineralogical properties of some Canadian fly ashes, Mater Res Soc Symposium Proc. 86, 113-125.

_____

Kaji, R., Muranaka, M., Otsuka, K., Hishinuma, Y., Kawamura, T., Murata, M., Takahasi, Y., Arikawa, Y., Kikkawa, H., Igarshi, A., Higushi, H., 1983. Rheology of coal slurries, Proc. 5th Intl. Symp. On coal slurry combustion and technology, Tampa, FL, P-151.

Kaji, R., Muranaka, Y., Otsuka, K., Hishinuma, Y., 1986. Water absorption by coal: Effects of pore structure and surface oxygen, Fuel 65, 288.

Karmakar, N.C., Goyal, A., Sethi, R., Gupta, S., Treatment of coal mine effluent using noionic, anionic and cationic flocculants, Proc. Intl. Conf. on technological challenges and management issues for sustainability of mining industries, 77-86.

Kaushal, G.K., Kaushal, D.R., 2005. Effect on CBR value and other geotechnical properties of fly ash reinforced with non-woven geo-fibres and treated with lime and $C_{19}H_{42}BrN$, Proc of fly ash India 2005, New Delhi, VIII, 15.1-15.8.

Kawaguchi, Y., Daisaka, H., Yabe, A., Hishida, K., Maeda, M., 1997. Turbulence Characteristics in Transition Region of Dilute Surfactant Drag Reducing Flows. Proc. 11th Intl. Symposium, Turbulent Shear Flows, Sep. Grenoble, France, pp. PI49-PI54.

Kim, K., Sirviente, A.I., 2007. Wall versus centreline polymer injection in turbulent channel flows, Flow, Turbulence and Combustion, 78(1), 69-89.

Kim, S.S., Chun, B.S., 1994. The study on a practical use of wasted coal fly ash for coastal reclamation, XIII, ICSMFE, 1607-1612.

Knezevic, D., Kolonja, B., 2008. The influence of ash conc. on change of flow and pressure in slurry transportation, Int. J. Mining and Mineral Engg., 1(1), 104-112.

Krishna, K.C., 2001. CBR behaviour of fly ash-soil-cement mixes, Unpublished Ph.D thesis, Indian Institute of Science, Bangalore, India.

Kuganathan, K., 2001. A method to design optimum pastefill mixes through flow cone and mini slump cone testing, Proc 7th Intl Symposium on mining with backfill, Mine fill 2001, Ed David Stone, P.E. pp. 163-177.

Kumar, 2003. Key note address, Proc. of 3rd International Conference on Fly Ash Utilization & Disposal, pp: 1-4.

Kumar, 2010. A comprehensive model for fly ash handling and transportation for mining sector. Fly ash an opportunity for mining sector, New Delhi, India.

Kumar, H., Mishra, D.P., Das, S.K., 2006. Settling characteristics of Fly Ash of Talcher Thermal Power Station, Proc. of 1st Asian Mining Congress, pp: 135 – 139.

_____

Kumar, S., 2000. Leaching study of trace elements from fly ashes: a case study of Chandrapur thermal power station, Proc. of the 2nd International Conference on fly ash disposal and utilization, vol.-I, IV-2, pp: 11-15.

Kumar, V., 2006. Fly ash: A Resource for Sustainable Development. Proc. of the International Coal Congress & Expo, pp. 191-199.

Kumar, V., Ahuja, B.P., Dattatreyulu, J.V., Rao, B.B., Ghosh, C.N., Sharma, A.K., 2003. Hydraulic stowing of pond ash in underground mines of Manuguru, India, Proc. of the International Conference on Fly Ash Utilization & Disposal, Vol. VI, pp. 1–10.

Kumar, V., Mathur, M., 2005. Use of Fly Ash in mining sector-an overview, Proc. of National Seminar cum business meet on use of fly ash in Mining sector, pp: 1-5.

Landriault, D., Welch, D., John, F., 2001. Bulyan Hulu Mine: Blended paste backfill and surface paste deposition/ the state of the art in paste Technology, Proc. of the 7th Intl. Symposium on Mining with Backfill, Mine Fill 2001, pp 403-416.

Landriault, D.A., Brown, R.E., 2000. Paste Backfill study for deep mining at Kidd Creek, CIM/ICM Bulletin, Volume 93, pp 156-160, January.

Lav, A.H., Lav, M.A., 2000. Microstructural development of stabilized fly ash as pavement base material, J of Materials in Civil Engg., ASCE, 12(2), 157-163.

Lav, A.H., Lav, M.A., Goktepe, A.B., 2006. Analysis and design of a stabilized fly ash as pavement base material, Fuel, 85, 2359-2370.

Lee, S.H., Kim, H.J., Sakai, E., Diamon, M., 2003. Effect of particle size distribution of fly ash-cement system on the fluidity of cement pastes, Cement and Concrete Res, 33, 763-768.

Lei, L., Usui, H., Suzuki, H., 2002. Study of pipeline transportation of dense fly ash-water slurry. Coal Preparation, 22(2), pp. 65-80.

Leonards, G.A., Bailey, B., 1982. Pulverized coal ash as structural fill, Journal of Geotech. Engg. Div., ASCE, 108, pp. 517-531.

Lester, C. B., 1994. Hydraulics for pipelines, Vol.1, Fundamentals. Second Edition, Gulf Publishing Company, Houston, Texas, London, Paris, Tokyo.

Li, F.C., Kawaguchi, Y., Yu, B., Wei, J., Hishida, K., 2008. Experimental study of drag reduction mechanism for a dilute surfactant solution flow. International Journal of Heat and Mass Transfer 51, 835-843.

_____

_____

Liang, W., Jiang, L., 1986. Effect of wettability and adsorpability of coal on the slurryability of coal, Proc 8th Int. Symp. On coal slurry fuels prep. util., U.S. Dept. of energy, Pittsburgh energy Tech. Cent., Pittsburgh, PA, pp. 19-24.

Liang, W., Jiang, L., 1987. Effect of wettability and adsorpability of coal on its slurryability: Factors affecting the prep. Of highly concentrated coal-water slurry (HCCWS). J. Coal Qual. 6(2): 448.

Link, J.M., Faddick, R.R., Lavingia, N.J., 1974. Slurry pipeline economics, paper presented at the Society of Mining Engineers, AIME Annual Meeting Dallas Texas.

Lu, B., Li, X., Scriven, L.E., Davis, H.T., Talmon, Y., Zakin, J.L., 1998. Effect of chemical structure on viscoelasticity and extensional viscosity of drag reduction cationic surfactant solution, Langmuir, 14, 8-16.

Lumley, J.L., 1969. Drag reduction by additives, Ann Review Fluid Mech VI: 367-384.

Mahlaba, J.S., Kearsley, E.P., Kruger, R.A., 2011. Effect of fly ash characteristics on the behavior of pastes prepared under varied brine conditions, Minerals Engg., doi: 0.1016/j.mineng.2011.04.009.

Marmy, R.M.S., Hayder, A.B., Rosli, M.Y., 2012, Improving the flow in pipelines by Cocos nucifera fiber waste, International Journal of Physical Sciences 7(26), 4073-4080.

Maser, K.R., Wallhagen, Dieckman, J., 1975. Development of fly ash cement mine sealing system, USBM, open file report, NTIS-PB-250611, 26-76.

Matras, Z., Malcher, T., Gzyl-Malcher, B., 2008. The influence of polymer-surfactant aggregates on drag reduction. Thin Solid Films, 516, pp. 8848-8851.

Matthys, E.F., 1991. Journal of Non-Newtonian Fluid Mechanics, 38, 313.

McCarthy, D.F., 2007.Essentials of Soil Mechanics and Foundations, 7th edition, New Jersey, Pearson.

McCormick, C.L., Block, J., Schulz, D.N., 1986. Water soluble polymers, in Encyclopedia of polymer Science and Engineering, Vol. 17.

McLoren, H., Bayer, D., Peppin, C., 2001. Effects of admixtures on strength and flowability characteristics of cemented backfill, Proc. 7th Intl. Symp. On Mining with Backfill, Stone, D. (ed). Society for Mining, Metallurgy, and Exploration, pp. 73-80.

Meyers, J.F., Pichumani, R., Kapples, B.S., 1976. Fly ash as a construction material for Highways, Report No. FHWA-FP-76-16, US Department of Transportation, Washington D.C. USA.

Minnick, L.J., 1959. Fundamental characteristics of pulverized coal fly ashes, in: Proc. of ASTM, 59, pp. 1155-1177.

Mishra, D., Das, S.K., 2010. A study of physico-chemical and mineralogical properties of Talcher coal fly ash for stowing in underground coal mines. Materials Characterization 61, 1252-1259.

Mishra, M.K., Rao, K.U.M., 2006. Geotechnical characterization of fly ash composites for backfilling mine voids. Journal of Geotechnical and Geological Engineering 24, 1749-1765.

Mishra, S.R., Kumar, S., Park, A., Rho, J., Losby, J., Hoffmeister, B.K., 2003. Ultrasonic characterization of the curing process of PCC fly ash, Journal of Mats Char, 50, 317-323.

Morgan,J.R., Tucker, J.S., Mcinnes, D.B., 1994. A mechanistic design approach for unsealed mine haul roads, Pavement design and performance in road construction, 1412, 69-81.

Mosa, E.S., Saleh, A.M., Taha, T.A., EI-Molla, A.M., 2008. Effect of chemical additives on flow characteristics of coal slurries, Physico-chemical problems of Mineral Processing, 42, 107-118.

Munekata, M., Matsuzaki, K., Ohba, H., 2006. Vertex motion in a swirling flow of surfactant solution with drag reduction. Journal of Fluids Engineering 128, 101-106.

Myska, J., Chara, Z., 2001. The effect of a zwitterionic and cationic surfactant in turbuleny flows, Experimental Fluids, 30, 229-236.

Myska, J., Mik, V., 2003. Application of a drag reducing surfactant in the heating circuit, Energy and building, 35, 813-819.

Myska, J., Stern, P., 1998. Significance of shear induced structure in surfactants for drag reduction, Colloid Polymer Sc 276, 816-823.

Nagataki, S., Sakai, E., Takeuchi, T., 1984. The fluidity of fly ash-cement paste with superplasicizer, Cem. Concr. Res. 14(5), 631-638.

Narashimha, V.L., Sundararajan, T., Revati, V., 2003. High calcium fly ash gypsum slurry: A potential material for high volume utilization of fly ash, Proc. 3rd Intl. Conf. on fly ash utilization and disposal, Feb. 19-21, New Delhi, India, 64-70.

Nguyen, H., Ishihara, K., Suzuki, H., Usui, H., 2006. Structure Analysis of Drag-Reducing Surfactant Rod-like Micelles with Fluorescence Probe. Nihon Reoroji Gakkaishi, 34 (1), pp. 17-23.

_____

Nicholson, P., Kashyap, V., Fugi C., 1994. Lime and fly ash admixture improvement of tropical Hawaiian soils, Transportation Research Record, Washington, DC, Report No. 1440.

Nigel, I.H., Neil, J.A., 2003. Solid/Liquid handling. www.Cepmagazine.org, April 2003 CEP viewed on 19 January 2011.

Oberacker, R., Reinshagen, J., Both, H.V., Hoffmann, M.J., 2001. Ceramic slurries with bimodal particle size distributions: rheology, suspension structure and behaviour during pressure filtration. Ceramic Transactions 112, 179-184.

Ohlendorf, D., Inherthal, W., Hoffman, H., 1986. Surfactant systems for drag reduction, physico- chemical properties and rheological behavior. Rheol. Acta 26, 468-486.

Ojha, K., Pradhan, N.C., Samanta, A.N., 2004. Zeolite from fly ash: synthesis and characterization, Bull. Mater. Sci., Vol. 27, No. 6, pp. 555-564.

Oliver, D.R., Bakhtiyarov, S.I., 1983. Journal of Non-Newtonian Fluid Mechanics, 12, 113.

Ousterhout, R.S., Hall, C.D., 1961. Reduction of friction loss in fracturing operations. Journal of Petroleum Technology 13, 217.

Ozerskii, A.Y., Ozerskii, D.A., 2003. Disposal of ash and slag waste of the Berezovsk state regional power plant in the Berezovskii-1 mined-out space: a promising direction of environmental protection in the region. Powder Technology & Engineering 37, 248-251.

Palariski, J., 1993. The use of fly ash tailings, rock and binding agents as consolidated backfill for coal mines, In Proc. Of mine fill 1993, Edi. H.W. Gelen, SAIMM, 403-408.

Pandey, S.N., Kumar, A., 2005. An approach towards sustainable backfilling of open cast mines, Proc. of the Intl. Cong. on fly ash utilization, Vol.–II, pp: 6.1-6.6.

Pandian, N. S., Rajasekhar, C., Sridharan, A., 1995. Fly ash-lime systems for the retention of lead ions, in: Proc. of Indian Geotechnical conference, Bangalore, 1, pp. 219-222.

Pandian, N. S., Rajasekhar, C., Sridharan, A., 1998. Studies on the specific gravity of some Indian coal ashes, Journal of Testing and Evaluation, ASTM, 26, pp. 177-186.

Pandian, N.S., 2004. Fly ash characterization with reference to geotechnical applications, Journal of Indian Inst. of Sc., 84, pp. 189-216.

Pandian, N.S., Balasubramonian, S., 2000. Leaching studies on ASTM type F fly ashes by an accelerated process method, Journal of Testing Evaluation, ASTM, 28, pp. 44-51.

Parida, A., Panda, D., Mishra, R.N., Senapati, P.K., Murty, J.S., 1996. Hydraulic transport of fly ash at higher conc, Ash ponds and ash disposal systems, eds. Raju, V.S. et al. Naros Publ House, New Delhi, pp. 17-28.

_____

Parida, A., Panda, D., Senapati, P.K., Mishra, R.N., 2003. Pipeline design for hydraulic backfilling of coal mines with use of fly ash and fly ash-bottom ash mixture at high concentrations, Proc. of the 3rd International Conference on Fly Ash Utilization & Disposal, Vol. III, pp. 35-45.

Park, S.S., Kang, H.Y., 2008. Characterization of fly ash pastes synthesized at different activator conditions, Korean Journal of Chem. Eng., Vol. 25, No.1, pp. 78-83.

Paul, B.C., Chaturvedula, S., Paudel, H., Chatterjee, S., 1994. Use of shake tests as predictors of long term leaching of coal combustion residues in contact with ground water, in Manage High Sulfur Coal Combust Residues, Issues Pract Conf Proc ed. by Chugh, Y.P., and Bensley, G.A., National Technical Information Service, Springfield, VA. 58-79b.

Paul, F. Ziemikiewicz et al. 2005. FBC ash placement in coal mines for AMD control, Proc. of the Intl. Congress on Fly Ash Utilization, Vol.-IX, pp: 6.1-6.13.

Petulanas, G.M., 1988. High volume fly ash utilization projects in the US and Canada (2nd Ed), Final report CS-4446 to EPRI, Palo Alto, CA, 244.

Phukan, S., Kumar, P., Panda, J., Nayak, B.R., Tiwari, K.N., Singh, R.P., 2000. Application of drag reducing commercial and purified guargum for reduction of energy requirement of sprinkler irrigation and percolation rate of the soil, Agricultural Waer Management, 47, 101-118.

Piotrowski, Z., 2008. Gospodarka Surowcami Mineralnymi, Tom, 24, Zeszyt 4/1.

Prasad, B., Srivastava, A., Mondal, K.K., 2003. Leaching studies of Indian fly ashes for evaluation of their suitability as mine fill material, Proc. of the 3rd International Conference on Fly Ash Utilization & Disposal, Vol. III, 46-51.

Prashant, 2005. Use of coal ash in Open Cast mine filling, Proc. of National Seminar cum business meet on use of Fly Ash in mining sector, pp. 34 –39.

Prashant, et al. 2005. Paste fill the future of filling in underground coal mines, Proc. of Fly Ash India 2005, Vol.-IX, pp: 2.1 – 2.8.

Qi, Y., Weavers, L.K., Zakin, J.L., 2003. Enhancing heat-transfer ability of drag-reducing surfactant solutions with ultrasonic energy. Journal of Non-Newtonian Fluid Mechanic 116, 71-93.

Qi, Y., Zakin, J.L., 2002. Chemical and rheological characterization of drag- reducing cationic surfactant systems. Ind. Eng. Chem. Res. 41, 6326- 6336.

_____

Rahman, Z., 2005. Thermal Power Fly Ash/Pond Ash in mine stowing at Durgapur Rayatwari Colliery (W.C.L), Proc. of the International Congress on Fly Ash Utilization, Vol.-IX, pp: 3.1- 3.10.

Raju, V.S., Datta, M., Seshadri, V., Aggarwal, V.K., Kumar, V. (Eds.), 1996. Ash ponds and ash disposal systems, Narosa Publishing House, New Delhi.

Ram, L.C., Masto, R.E., 2010. An appraisal of the potential use of fly ash for reclaiming coal mine spoil. Journal of Environmental Management 91, 603-617.

Ram, L.C., Srivastava, K.N., Tripathy, C.R., Thakur, K.S., Sinha, A.K., Jha, A.K., Masto, E.R., Mitra, S., 2007. Leaching behavior of lignite fly ash with shake and column tests, Environ. Geology, 51: 1119-1132.

Ram, L.C., Srivastava, N.K., Jha, S.K., Sinha, A.K., Masto, R.E., Selvi, V.A., 2007. Management of lignite fly ash for improving soil fertility and crop productivity, Env. Mgt., 40, 438-452.

Ramamurthy, 2005. Key note address, Proc. of 3rd International Conference on Fly Ash Utilization & Disposal, New Delhi, India.

Ramesh, H.N., Sivamohan, M., Sivapullaiah, P.V., 1998. Geotechnical properties of Muddanur fly ash with lime, Proc. Indian Geotechnical Conf., New Delhi, 247-249.

Rao, B.B., Kumar, V., Rao, T.S., Hussain, M.F., 2005. On site field experiences of ash stowing in underground coal mines of Singareni Colllieries Company Limited, Proc. of National Seminar cum business meet on use of Fly Ash in mining sector, pp: 24–33.

Raymond, S., 1961. Pulverized fuel ash as embankment material, Proc. Of the Institution of Civil Engineers, 19, 515-536.

Rehage, H., Hoffmann, H., 1991. Viscoelastic surfactant solutions: model systems for rheological research. Molecular Physics, Vol.74, pp. 933-973.

Rehsi, S.S., Garg, S.K., 1988. Characteristics of Indian fly ashes, in: Proc. of National workshop on utilization of fly ash, Roorkee, pp. 131-135.

Revati, V., Narasimha, V.L., Jayanthi, S., 2009. Studies on the performance of quarry waste in flowable fly ash-gypsum slurry, Modern Applied Sci, 3(2), 147-153.

Roh, N.S., Shin, D.H., Kim, D.C., Jong-Duk, K., 1995. Rheological behavior of coal-water mixtures-effect of surfactants and temperature, Fuel, 74(9), 1313-1318.

Roi, G., Alex, L., Gad, H., 2004. Characterization of turbulent flow in a flume with surfactant. Transactions of the ASME, Journal of Fluid Mechanics 126, 1054-1057.

Roode, M.V. 1987. X-ray Diffraction Measurement of Glass Content in fly ashes and slag. Concrete Research 17, 183-197.

Roode, M.V., 1987. X-ray diffraction measurement of glass content in fly ashes and slag, Journal of Concr. Res., 17, pp. 183-197.

Rose, G.D., Foster, K.L., Slocum, V.L., Lenhart, J.G., 1984. In: Sellin and Moses (eds) Proc 3rd Intl Conf on drag reduction, Bristol, 2-5 July, University of Bristol.

Rout, D.K., Parida, P.K., Behera, G., 2005. Man-made disaster- a case study of NALCO ash-pond in the Angul district, Orissa using remote sensing and GIS technique, Journal of the Indian Society of Remote Sensing, 33(2), 291-295.

Roychowdhury, A., 2005. Ash Utilization of Damodar Valley Corporation's Thermal Power Stations for mine filling – a potential option", Proceedings of National Seminar cum business meet on use of fly ash in mining sector, pp. 40– 48.

Rozenblit, R., Gurevich, M., Lengel, Y., Hetsroni, G., 2006. Flow patterns and heat transfer in vertical upward air-water flow with surfactant. International Journal of Multiphase Flow 32, 889-901.

Rudzinski, L., 2005. The effect of fly ashes on the rheological behavior of cement pastes, BORDAS-GAUTHIER-VILLARS, 369-372.

Sadisun, I.A., Shimada, H., Ichinose, M., Matsui, K., 2006. Rheological and Mech. Properties of fly ash-rock-cement mixtures for erosion control of slake prone rocks, Proc Intl Symp on Geotechnical hazards prevention, mitigation, and Engg. Response, pp. 201-205.

Sahay, A.N., 2010. R&D initiatives in utilization of fly ash in coal sector, in: Proc. of Fly ash an opportunity for Mining Sector, New Delhi, India.

Sakai, et al. 2003. Coal ash utilization in Japan, Proc. of International Conference on Fly Ash Utilization, pp: I 2.1-2.10.

Sargeant, A.L., 2008. The application of post-consumer glass as a cementing agent in mine backfill, Master thesis, Queens University, Canada.

Sarkar, A., Rano, A., Udaybhanu, G., Basu, A.K., 2006.A comprehensive characterization of fly ash from a thermal power plant in Eastern India. Fuel Processing Technology 87, 259-277.

Sarkar, A., Rano, R., 2007. Water holding capacities of fly ashes: Effect of size fractionation, Energy Sources, Part A, 29, 471-482.

_____

Sarkar, A., Rano, R., Mishra, K.K., Sinha, I.N., 2005. Particle size distribution profile of some Indian fly ash- a comparative study to assess their possible uses, Fuel Processing Tech., 86, 1221-1238.

Savins, J.G., 1994. Society of Petroleum Engineering, 4, 203.

Schure, M.R., Soltys, P.A., Natusch, D.F.S., Mauney, T., 1985. Surface area and porosity of coal fly ash. Environmental Science and Technology. American Chemical Society 19, 82-86.

Sear, L.K.A., 2001. The use of PFA as a fill material and the environment, Geo-environmental impact management, Proc. 3rd Conf. by British Geo-technical Association and Cardiff School of Engg., 17-19 Sept., Edinburgh.

Sellin, R.H., Hoyt, J.W., Pollert, J., Scrivener, O., 1982. The effect of drag-reducing additives on fluid flows and their industrial applications Part 2: Present applications and future proposals. Journal of Hydraulic Research 20(3), 235-292.

Sellin, R.H., Hoyt, J.W., Scrivener, O., 1982. The effect of drag-reducing additives on fluid flows and their industrial applications 1: basic aspects. Journal of Hydraulic Research 20(1), 29-68.

Sellin, R.H., Ollis, M., 1980. Polymer drag reduction in large pipes and sewers: results of recent field trials. Journal of Rheology 24, 667-684.

Sen, S., Kumar, A., 1995. NTPC's experience in utilization of coal ash, Proc. of the Workshop on fly ash Utilization, pp: 103-121.

Senapati, P.K., Mishra, B.K., 2012. Design considerations for hydraulic backfilling with coal combustion products (CCPs) at high concentrations, Powder Technology 229, 119-125.

Senapati, P.K., Mishra, B.K., Parida, A., 2010. Modeling of viscosity for power plant ash slurry at higher concs: Effect of solids volume fraction, particle size, and hydrodynamic interactions, Powder Tech. 197, 1-8.

Senapati, P.K., Panda, D., Parida, A., 2005. Studies on the maximum settled concentration, mixing and rheological properties of high concentration fly ash-bottom ash mixture slurry. Proc. of the International Conference on Fly Ash Utilization, New Delhi, pp. 4.1-4.9.

Senapati, P.K., Panda, D., Parida, A., 2008. Studies on hydraulic transportation of sewage sludge-fly ash mixture slurry, J of Solid waste Tech. and Management.

_____

Sengupta, J., 1991. Characterization of Indian coal ash and its utilization as building material, in: Proc. Int. Conf. on Environmental Impact of Coal Utilization from Raw Materials to Waste Resources (K. C. Sahu, ed.), Indian Institute of Technology, Bombay, pp.165-184.

Senol, A., Bin-Shafique, M.S., Edil, T.B. and Benson, C.H., 2003. Use of class C fly ash for the stabilization of Soft soil as Sub-base, ARI, The Bulletin of the Istanbul Technical University, vol. 53, pp. 89-95.

Senol, A., Bin-Shafique, M.S., Edil, T.B., Benson, C.H., 2003. Uses of class C fly ash for the stabilization of soft soil as sub-base, ARI, The Bulletin of the Istanbul Technical University, 53, 89-95.

Senol, A., Edil, T.B., Bin-Shafique, M.S., Acosta, H.A., Benson C.H., 2006. Soft Sub grades stabilization by using various fly ashes, Journal of Resources, Conservation and Recycling, 46, pp. 365-376.

Seshadri, V., 1997. Design of pipelines for wet disposal of fly ash and bottom ash at higher concentrations, Management of ash ponds, collection of papers from National Seminar on Management of ash ponds held at IIT, Madras, Narosa Publishing House, pp 29-40, November.

Seshadri, V., Singh, S.N., 2000. Wet disposal of fly ash and bottom ash at higher concentrations, Proc. of the 2nd International Conference on fly ash disposal and utilization, CBIP, Vol.-1, pp: III 36-50.

Seshadri, V., Singh, S.N., Jain, K.K., Verma, A.K., 2005. Rheology of fly ash slurries at high concentrations and its application to the design of high concentration slurry disposal system. Proc. of the Int. Con. on Fly Ash Utilization, New Delhi, pp. V.1.1-10.

Seshadri, V., Singh, S.N., Jain, K.K., Verma, A.K., 2008. Effect of additive on head loss in the high conc slurry disposal of fly ash, IE (I) Journal-MC, 89, 3-10.

Shah, S.N., Jeong, Y.T., 2003. The flow characteristics of fly ash slurry for plugging abandoned wells using coiled tubing. Int. Ash Utilization Symposium, Centre for Applied Energy Research, University of Kentucky, Paper # 110.

Shaver, R.G., Merrill, E.W., 1959. Turbulent flow of pseudoplastic polymer solutions in straight cylindrical tubes, AIChE Journal, 5, 181.

Shenoy, A.V., 1976. Drag Reduction Surfactants at Elevated Temperatures. Rheol. Acta Vol. 15, pp. 658-664.

Shenoy, A.V., 1984. A review on drag reduction with special reference to micellar systems. Colloid & Polymer Science 262, 319-337.

_____

_____

Shikata, T., Hirata, H., Kotada, T., 1988. Structure analysis of drag-reducing surfactant rod-like micelles with fluorescence probe, Langmuir, 4, 345.

Shimada, H., Yoshida, Y., Oya, J., Sasaoka, T., Matsui, K., Nakagawa, H., Gottfried, J., 2010. Application of injection material for rehabilitation of u/g pipeline using fly ash surfactant mixtures, Intl. J. of Mining, Reclamation and Environment, 24(1), 5-17.

Shimada, H., Yoshida, Y., Sasaoka, T., Matsui, K., 2008. Characteristics and tasks of lubricant injected into over-cutting area for pipe jacking, J. of Japan Sewage works Association, 45(550), 141-153.

Singh, A.K., Goel, J.K., 2006. Thermal power ash as a replacement material of sand in the underground hydraulic stowing – an experiment, Proc. of International Symposium on Environmental Issues of mineral Industry, pp: 361 – 365.

Singh, D.N., Kolay, P.K., 2002. Simulation of ash-water interaction and its influence on ash characteristics, Progress in Energy and Combustion Science, 28, pp. 267-299.

Singh, T.N., Singh, V., 2003. Use of Fly Ash in filling of underground openings in mines, the Mining Engineer's Journal, pp. 24-27.

Sivapullaiah, P.V., Prashanth, J.P., Sridharan, A., 1995. Optimization of lime content for fly ash, Journal of Testing and Evalu., 23, pp. 222-227.

Sive, A.W., Lazarus, J.H., 1986. A comparison of some generalized correlations for the head loss gradient of mixed regime slurries, Proc. Hydro transport 10, BHRA Fluid Engineering, Cranfield, Bedford, England, Paper E2, pp. 149-175.

Slaczka, A., Piszczynski, Z., 2008. Effect of selected additives on the stability and rheology of coal-water slurry fuels, Gospodarka Surowcami Mineralnymi, Tom 24, 363-373.

Sridharan, A., Pandian, N.S., Kumar, V., 1999. Ed. Fly ash characterization and its geotechnical applications, Allied Publishers Ltd., India, p 266.

Sridharan, A., Prakash, K., 2007. Geotechnical Engineering Characterization of Coal Ashes, 1st ed., S.K. Jain for CBS Publishers, New Delhi.

Steve Carrington and Joanne Langridge, 2005: American Laboratory News, November, 2005.

Steward, N.R., Slatter, P., 2009. The transport of fly ash pastes through pipelines, Australian Bulk Handling Review, 561, 2-8.

Struble, L., Sun, G.K., 1995. Viscosity of Portland cement paste as a function of concentration. Adv. Cem. Bas. Mater. 2, 62-69.

_____

Suzuki, H., Nguyen, H.P., Nakayama, T., Usui, H., 2005. Development characteristics of fluctuating velocity field of drag-reducing surfactant solution flow in a duct. Rheologica Acta 44, 457-464.

Swain, P., Panda, D., 1996. Rheology of coal-water mixture, Fuel Sci and Tech. Intl. 14(9): 1237.

Tannant, D.D., Kumar V., 2000. Properties of fly ash stabilized haul road construction materials, Int. Journal of Mining, Reclamation Environ., 14, pp.121-135.

Thissen, P., Erik van der Kuy, 2005. Rheology of fly ash and bottom ash from Indian coal and pipeline pressure calculations for high concentration slurry land fill, Proc. of International Congress on fly ash utilization, Vol.-V, pp:2.1- 2.13.

Throne, D.J., Watt, J.D., 1965. Composition and pozzolanic properties of pulverized fuel ashes, II. Pozzolanic properties of fly ashes as determined by crushing strength tests on lime mortars, Journal of Appl. Chem., 15, pp. 595-604.

Tiederman, W.G., 1985. Wall layer structure and drag reduction, Journal of F. M., 156, 419-437.

Ting, A.P., Luebbers, R.H., 1957. Viscosity of suspensions of spherical and other isodimensional particles, AIChE J. 3(1): 111.

Topallar, H., Bayrak, Y., 1998. The effect of temperature on the dynamic viscosity of Acetone Suflower-seed oil mixtures, Turk J Chem, 22, 361-366.

Torrey, S., 1978. Coal ash utilization: Fly ash, bottom ash, and slag, Park Ridge, NJ: Noyes Data.

Trivedi, A., Singh, S., 2004. Geotechnical and geo-environmental properties of power plant ash. Journal of Institution of Engineers (India) 85, 93-99.

Tsai, S. C., Knell, E.W., 1986. Viscometry and rheology of coal water slurry, Fuel, 65, 566-571.

Tsutsumi, A., Yoshida, K., 1987. Effect of temperature on rheological properties of suspensions, J. of Non-Newtonian Fluid Mechanics, 26, 175-183.

Turkel, S., 2007. Strength properties of fly ash based controlled low strength materials, J Hazard Mater, 147(3), 1015-9.

Usui, H., Li, L., Suzuki, H., 2001. Rheology and Pipeline Transportation of Dense Fly Ash-water Slurry, Korea-Australia Rheology Journal, 13(1), pp. 47-54.

_____

_____

Verkerk, C.G., 1982. Transport of fly ash slurries, Proc 8th Intl Conf on the hydraulic transport of solids in pipes, Hydrotransport 8, Johannesburgh, South Africa, 25-27 August, pp. 307-316.

Verkerk, C.G., 1986. The transport of fly ash and bottom ash in slurry form, 2nd Intl. Conf. on Bulk Materials Storage, Handling, and Transport, Wallongong, N.S.W., 7-9 July.

Verma, A.K., Singh, S.N., Seshadri, V., 2006. Effect of particle size distribution on rheological properties of fly ash slurry at high concentration. Intl. Journal of Fluid Mechanics Research 33, 445-457.

Verwey, E.J.W., 1947. Theory of the stability of lyphobic colloids, J. Phys. Colloid Chem., 51: 631.

Vickery, J. D., Boldt, C. M. K., 1989. Total Tailings Backfill Properties and Pumping", Proc. of 4th Intl. Conf. on Mining with Backfill, Balkema, pp 369-378, October.

Virk, P.S., 1971. Drag reduction in rough pipes, J. Fluid Mech., 45, 225-246.

Vlasak, P., Chara, Z., 2004. Laminar and turbulent transition of fine-grained slurries. Particulate Science and Technology, Vol. *22*, No. 2, 189-200.

Vlasak, P., Chara, Z., 2007. Flow behavior and drag reduction of fluidic ash-water slurries. Hydro transport 17. The 17th International conf. on the Hydraulic Transport of solids, the southern African Institute of Mining and Metallurgy and the BHR Group, pp. 39-55.

Vlasak, P., Chara, Z., 2009. Conveying of solid particles in Newtonian and non-Newtonian carriers, Particulate Sc and Tech., 27(5), 428-443.

Vlasak, P., Chara, Z., Hrbek, J., Servera, M., Vatolik, K., 1993. Ash slurry behavior in process of hydraulic backfilling in u/g coal mine, Proc 12th Intl Conf on slurry handling and pipeline transport, Hydrotransport-12, Brugge, Belgium, pp. 473-483.

Vlasak, P., Chara, Z., Stern, P., 2010. Drag reduction of dense fine-grained slurries, J. Hydrol. Hydromech., 58(4), 261-270.

Vlasak, P., Chara, Z., Stern, P., Konfrst, J., El-Nahhas, K., 2002. Flow behavior and drag reduction of Kaolin suspensions, Hydrotransport 15, BHR group, Banff (Canada), pp. 345-360.

Vories, K.C., 2003. The Surface Mining Control and Reclamation Act: A response to concerns about placement of coal combustion by products at coal mines, Technical report of mid-continent regional coordinating center, U.S. DOI office of surface mining, Alton, Illinois, Vol.-VI, pp: 94-102.

Wang, S., Ma, Q., Zhu, Z.H., 2008. Characteristics of coal fly ash and adsorption application, Fuel 87, 3469-3473.

Wang, Y., Ren, D., Zhao, F., 1999.Comparative leaching experiments for trace elements in raw coal, laboratory ash, fly ash and bottom ash, International Journal of Coal Geolog, 40, pp. 103-108.

Ward, A., Bunn, T.F., Chambers, A.J., 1999. The Bayswater fly ash transportation system, Coal Prep J. 21, 125-147.

Wasp, E.J., Kenny, J.P., Gandhi, R.L., 1975. Solid liquid flow slurry pipeline transportation, Trans. Tech. Publ.

Wei H., Chan, S. P., Joseph, M. N., 2009. Rheological study of comingled biomass and coal slurries with hydrothermal pre-treatment, Energy and Fuels, American Chemical Society, DOI: 10.1021/ef9000852.

White, S.C., Case, E.D., 1990. Characterization of fly ash from coal-fired power plants. Journal of Material Science 25, 5215-5219.

Whittingstall, P., 2001. Overview of viscosity and its characterization, Current Protocols in Food Analytical Chemistry, Unit H1.1-H1.1.1.6.

Wood, D.J., Kao, T.Y., 1966. Unsteady flow of solid-liquid suspension. Procs ASCE, J. Eng. Mechs. Div. Vol. 92, No. EM6, 117–134.

Wood, D.J., Kao, T.Y., 1971. Transient flow of solid-liquid mixtures in pipes, in Advances in solid-liquid flow in pipes and its application, Pergamon Press, Oxford and New York, pp. 87–100.

Xu, A., Sarkar, S.L., 1994. Microstructural developments in high volume fly ash cement system, J of Materials in Civil Engineering, ASCE, 1, 117-136.

Yesiller, N., Hanson, J.L., Usmen, M.A., 2000. Ultrasonic Assessment of Stabilized Soils, in: Proc. Of the ASCE Geo-Institute Soft Ground Technology (GSP 112): pp. 170-181.

Ying, Z., Yunying, Q., Zakin, J.L., 2005. Head group effect on drag reduction and rheological properties of micellar solutions of quaternary ammonium surfactants. Rheol Acta, 45, 42-58.

Yoshioka, K., Sakai, E., Diamon, M., Kitahara, A., 1997. Role of steric hindrance in the performance of superplasticizers for concrete, J. Am. Ceram. Soc. 80, 2667-2671.

Yu, T.R., Counter, D.B., 1988. Use of fly ash as backfill at Kidd Greek Mines, CIM Bulletin, 44-50.

_____

Yu, T.R., Counter, D.B., 1998.Use of fly ash in Backfill at Kidd Creek Mines", CIM/ICM Bulletin, Volume 81, No.909, pp 44-50.

Zakin, J.L., Lu, B., Bewersdorff, H.W., 1998. Review in Chemical Engineering, 14(4-5), 253-320.

Zakin, J.L., Lu, B., Bewersdorff, H.W., 1998. Surfactant drag reduction, Reviews in Chemical Engineering, 14, 253-320.

Zakin, J.L., Lui, H.L., 1983. Variables affecting drag reduction by non-ionic surfactant additives. Chemical Engineering Communication, 23, 77-80.

Zhang, Y., Qi, Y., Zakin, J.L., 2005. Head group effect on drag reduction and rheological properties of micellar solutions of quaternary ammonium surfactants. Rheologica Acta 45, 42-58.

Ziemkiewicz, P.F., Black, D.C., 2002. Disposal and use of coal combustion product in mined environment, Short program in Assessment of Physical, Chemical, Mineralogical and Geotechnical characteristics of coal ashes for the use in different applications, Sept. 19-20, NTPC, Noida, India, pp 1-11.

_____

LIST OF PUBLICATIONS

A. *Journal Articles*

1. **Naik, H.K., Mishra, M.K., Rao, K.U.M., and Dey, D., 2009**, Evaluation of the role of a cationic surfactant on the flow characteristics of fly ash slurry, Elsevier Journal of Hazardous Materials, Vol. 169, pp. 1134-1140.

2. **Naik, H.K., Mishra, M.K., and Rao, K.U.M., 2009**, The effect of drag-reducing additives on the rheological properties of fly ash-water suspensions at varying temperature environment, International Peer-reviewed on-line Journal of Coal Combustion and Gasification Products, Vol. 1, pp. 25-31.

3. **Naik, H.K., Mishra, M.K., and Rao, K.U.M., 2011**, Influence of chemical reagents on rheological properties of fly ash slurry at varying temperature environment, International Peer-reviewed on-line Journal of Coal Combustion and Gasification Products*,* Vol. 3, pp. 83-93.

4. **Naik, H.K., Mishra, M.K., and Rao, K.U.M., 2011**, Parametric Evaluation of Some Indian Fly ashes for Filling Underground Coal Mine Voids, International Peer-reviewed on-line Journal of Coal Combustion and Gasification Products, Allen Press Publ., USA*,* CCGP-D-12-00002.1, Vol. 4, pp. 28-36..

5. **Naik, H.K., Mishra, M.K., and Rao, K.U.M., 2011,** Potential of fly ash utilization in mining sector-a review, Indian Mining and Engineering Journal, Vol. 50, No. 03, pp. 07-22.

6. **Naik, H.K., 2006**, Environment friendly large volume utilization of coal combustion by-products by the mining and other Industries- the present scenario, The Indian Mineral Industry Journal, pp. 126-131.

B. *Conference Presentations (International)*

7. **Naik, H.K., Mishra, M.K., and Rao, K.U.M.,** (**2009**), Rheological characteristics of fly ash slurry at varying temperature environment with and without an additive, Proceedings of the International Conference on "World of Coal Ash (WOCA) 2009" held at the University of Kentucky, Lexington, USA, can be viewed online at http://www.flyash.info/, pp.1-12.

8. **Naik, H.K., Mishra, M.K., and Rao, K.U.M.,** (**2011**), Evaluation of Flow Characteristics of Fly Ash Slurry at 40% Solid Concentration with and without an Additive, Proceedings of the International Conference on "World of Coal Ash (WOCA) 2011" held at Denver, Colorado, USA, can be viewed online at http://www.flyash.info/, pp.1-15.

9. **Naik, H.K., Mishra, M.K., and Behera, B. (2007): "**Laboratory Investigation and Characterization of Some Coal Combustion Byproducts for their Effective Utilization", Proc. of the 1st International Conference on Managing the Social and Environmental

_____

Consequences of Coal Mining in India, 19-21 Nov. 2007, jointly organized by the I.S.M. University, University of New South Wales and Australian National University. pp: 763-770.

10. **Naik, H.K., Mishra, M.K., Das, M.P.S., and Sahu, V. (2007): "**Large volume coal combustion by-product (CCB) utilization in mine void filling: a preliminary laboratory study", Proceedings of the Indian Mining Congress on "Emerging Trends in Mineral Industry", Udaipur, Rajasthan, India, pp: 257-264.

11. **Naik, H.K., Mishra, M.K., Nayak, P.K., and Srikrishnan, V. (2007): "**Strength Development of Fly Ash by Lime and Gypsum Addition for its Effective Utilization-a Laboratory Investigation", Proc. of the Indian Chemical Engineering Congress, Chemcon-2007, organized by Indian Institute of Chemical Engineers, Kolkata, West Bengal, pp. 402.

C. Conference Presentations (National)

12. **Naik, H.K., and Mishra, M.K. (2007): "**Environmental Issues Concerning to Thermal Power Plants – A Critical Review", Proceedings of the National Seminar on "Energy, Environment and Economics", Electrical Engineering Department, N.I.T. Rourkela, Odisha, pp: TP12 (1-7).

13. **Naik, H.K., Mishra, M.K., Das, M.P.S., and Sahu, V. (2007): "**Flow characteristics study of fly ash slurry for underground mine void filling by Fluent-a Computational Fluid Dynamics Software", Proc. of the National Seminar on "Mining Technology-Present and Future", Bhubaneswar, Odisha, pp: 27-34.

14. **H.K.Naik, M.K.Mishra, and K.U.M. Rao, (2011),** Evaluation of Some Indian Fly ashes for Filling Underground Coal Mine Voids, *National conference on Fly Ash, Hotel ITC Kakatiya, Hyderabad, conducted by Centre for fly Ash Research and Management (C-FARM), New Delhi during 5th to 7th Dec. 2011.*

15. **Naik, H.K. and Mishra, M.K. (2007): "**Fly ash: A resource material for multifarious utilization", Proceedings of the National Environment Awareness Campaign-2006, Rourkela, Odisha, pp: 01-14.

16. Behera, B., **Mishra, M.K., and Naik, H.K.,** (**2008**), Critical review of Fly Ash Utilization in Mines, Proc. of National Conference on "Emerging Trends in the Mining and Allied Industries", Department if Mining engineering, NIT, Rourkela, pp. 277-283.

17. **Naik, H.K. (2007): "**Environmental Impact of power plant coal combustion by-products", Proc. of the National Seminar on Industrial Waste Management, NIT, Rourkela, pp: 38-43.

18. **Naik, H.K. (2007): "**Coal Combustion By-products utilization and management- The Current Scenario", Proc. of the All India Seminar on Catalyzing Vision 2020: Challenges of Indian Chemical Engineers, NIT Rourkela, Odisha, pp. 146-153.

_____

19. **Naik, H.K. (2007): "**Environmental and Ecological Concerns of Thermal Power Plants vis-à-vis non-conventional energy sources", Proc. of the National Conference on Technological Advances and Emerging Societal Implications, N.I.T. Rourkela, pp: 266-277.

20. **Naik, H.K. (2007): "**Environment friendly utilization of fly ash – a review of recent practices**",** Proc. of the National seminar on Environmental Management, Asansol, West Bengal, pp: 18

21. **Naik, H.K. (2007):** "Environmental impact of fly ash and its utilization trends in India – a review of current practices", Proc. of the National Conference on Technology for Sustainable Utilization of Natural Resources 'TechSUNR 2007', Paralakhemundi, Odisha, pp: 39

22. **Naik, H.K. (2006): "**Possible Areas of Large Volume Utilization of Thermal Power Wastes in Mines – an overview" Proc. of all India Seminar on Minerals & Metallurgical Industries Wastes & By- Products, Bhubaneswar, Odisha, pp: 22-32.

23. **Naik, H.K. (2006): "**Fly ash: Its Material Characteristics, Environmental Implications and Utilization Strategies in India – A Review", Proc. of the 3rd Annual workshop on fly ash and its application, Paralakhemundi, Odisha, pp: 34-37.

24. **Naik, H.K. (2006): "**Fly ash: A resource Material for large volume Utilization in mines – A Review", Proceedings of the National Seminar on "Mining Technology and Environmental Issues", Udaipur, Rajasthan, pp: 81-87.

25. **Naik, H.K. (2006): "**The Origin and Multifarious Utilization of Coal ash-An overview", Proc. of the National Workshop on Modern Management on Mine Production, Safety and Environment, Bengal Engineering and Science University, Shibpur, Howrah, West Bengal, pp: 123-129.

5. Details of completed sponsored research projects during Ph.D. study period

Title of the Project	Funding agency/client	Total financial outlay (Lakhs)	Year of start & total period
Evaluation of flow and in place strength characteristics of fly ash composite materials	Department of Science and Technology, GOI	Rs.14.25 lakhs	2009, 2 years

_____

Curriculum Vitae

1. Name	**HRUSHIKESH NAIK**
2. Father's Name	Birabara Naik
3. Mother's Name	Bachana Naik
4. Date of birth	19th February, 1959
5. Designation	Associate Professor and Head, Mining Engineering Dept.

6. Professional Degrees Obtained

UNIVERSITY	DEGREE	YEAR	FIELD OF SPECIALISATION
Regional Engineering College, Rourkela (Presently N.I.T, Rourkela)	*B. Sc. Engg. (Mining)*	1984	Mining Engineering
Indian School of Mines University, Dhanbad	*M. Tech.*	1990	Opencast Mining

7. **Employment Record**

UNIVERSITY/ INSTITUTION	DESIGNATION	PERIOD
National Institute of Technology, Rourkela, Odisha	Associate Professor (Mining Engineering Department)	01.01.2006 - Till Date
National Institute of Technology, Rourkela, Odisha	Assistant Professor (Mining Engineering Department)	09.12.1995 - 31.12.2005
Regional Engineering College, Rourkela, Odisha	Project officer and Head of the Nodal Centre for Odisha (NTMIS)	30.12.1991- 08.12.1995
Regional Engineering College, Rourkela, Odisha	Lecturer (Senior Scale)	19.08.1991- 29.12.1991
Regional Engineering College, Rourkela, Odisha	Lecturer	19.08.1985 - 18.08.1991

8. Other Related Experience- Research/ Industrial

Industry	Designation	PERIOD
Coal India Limited	Junior Executive Trainee	05.09.1984-17.08.1985

_____

9. Professional Development Courses Completed during the Ph.D. Study Period relating to the chosen field of research

a	Two weeks training program on "**Advanced Mining Research Laboratory Equipments**"	Sponsored by Technical Education Quality Improvement Program (TEQIP), NIT Rourkela	16th to 27th July 2006 (two weeks)	Department of Mining and Mineral Resources Engg., Southern Illinois University, Carbondale, **USA**
b	Short term course on "**The Science of Coal Ash Utilization**"	Organized by: University of Kentucky, Centre for Applied Energy Research, USA, in collaboration with American Coal Ash Association	4th to 7th May, 2009	Lexington Convention Centre, Kentucky, **USA**
c	Short term course on "**The Science of Coal Ash Utilization**"	Organized by: University of Kentucky, Centre for Applied Energy Research, USA, in collaboration with American Coal Ash Association	9th to 10th May, 2011	Marrion Tech Centre, Denver, Colorado, **USA**
d	Short term course on "**Transportation and Storage of Fly Ash**"	Industrial Tribology, Machine Dynamics and Maintenance Engineering Centre	3rd to 5th December 2008	Indian Institute of Technology, New Delhi
e	Advanced short term course with extended program on "**ASH DYKE MANAGEMENT AND ITS DESIGN**"	Dept. of Civil Engineering, National Institute of Technology, Rourkela	8th February to 12th February 2007	Civil Engg. Dept. N.I.T, Rourkela
f	One week short term course on " MATLAB, SIMULINK AND LABVIEW FOR ENGINEERING APPLICATIONS"	Department of Electrical Engineering, National Institute of Technology, Rourkela	19th February to 23rd February 2007	Electrical Engg. Dept. N.I.T., Rourkela
g	Short term course on "Advanced Ceramics Processing & Characterization"	Department of Ceramic Engineering, National Institute of Technology, Rourkela	1st July to 4th July 2008	Ceramic Engg. Dept. NIT Rourkela

_____

h	Conference on "Open Access to Science Publications: Policy Perspective, Opportunities and Challenges"	Council of Scientific & Industrial Research, PUSA, New Delhi-110012	24th March 2009	India Habitat Centre, New Delhi
i	Short term course on "Materials Technology: Advanced Processes and Characterizations"	Department of Metallurgical and Materials Engineering, National Institute of Technology, Rourkela	7th -11th December 2009	Metallurgical and Materials Engg. Dept., NIT Rourkela

11. Fellowship of Academic bodies and Professional Societies: Fellow of Institution of Engineers (India) awarded in the year 2009

10. Membership of Scientific and Professional Societies

Sl.No.	Name of the Institution / Society/Forum	Membership No.
i	Mining, Geological and Metallurgical Institute of India	MMGI-6115
ii	Mining Engineers Association of India	LMMEA-2756
iii	Institution of Engineers (India)	Life membership No.115538/5
iv	Mining and Engineering Journal Readers Forum	LMJRF-416
v	Indian Society for Technical Education (ISTE)	Life membership No. 7895
vi	Indian Institute of Chemical Engineers (IIChE)	Life membership

Residential Address: **Hrushikesh Naik**
                       Q. No. B-11, Third Street,
                      N.I.T, Campus, Rourkela-769 008
                       Dist- Sundargarh, Odisha, India
                       Email: hknaik@nitrkl.ac.in,
                      hrushi1920033@gmail.com
                      Phone: 09937115419 (M)